PROBABILISTIC SEISMIC HAZARD ASSESSMENT AND SITE CHARACTERISATION OF SOUTHWEST INDIA

Thesis

submitted in partial fulfillment of the requirements for the degree of

DOCTOR OF PHILOSOPHY

by

SHREYASVI C.

(**158010CV15F16**)

DEPARTMENT OF CIVIL ENGINEERING

NATIONAL INSTITUTE OF TECHNOLOGY KARNATAKA

SURATHKAL, MANGALORE - 575 025

August 2019

D E C L A R A T I O N

I hereby declare that the Research Thesis entitled **PROBABILISTIC SEISMIC HAZARD ASSESSMENT AND SITE CHARACTERISATION OF SOUTHWEST INDIA** which is being submitted to the National Institute of Technology Karnataka, Surathkal in partial fulfillment of the requirements for the award of the Degree of Doctor of Philosophy in **Civil Engineering** is a *bonafide report of the research work carried out by me*. The material contained in this *Research Thesis* has not been submitted to any University or Institution for the award of any degree.

………………………………………………………

(158010CV15F16, Shreyasvi C)

Department of Civil Engineering

Place: NITK Surathkal

Date: 12/08/2019

C E R T I F I C A T E

This is to *certify* that the Research Thesis entitled **PROBABILISTIC SEISMIC HAZARD ASSESSMENT AND SITE CHARACTERISATION OF SOUTHWEST INDIA** submitted by **Ms. SHREYASVI C. (Register Number: 158010CV15F16)**, as the record of the research work carried out by her, is *accepted* as the *Research Thesis submission* in partial fulfillment of the requirements for the award of degree of Doctor of Philosophy.

…………………………………………

Dr. Katta Venkataramana
Professor
Department of Civil Engineering
National Institute of Technology Karnataka, Surathkal

………………………………………

Chairman – DRPC
Department of Civil Engineering
National Institute of Technology Karnataka, Surathkal

ACKNOWLEDGMENT

ABSTRACT

The present study is an attempt to perform region-specific seismic hazards assessment for the southwest part of India. The area of interest belongs to seismic zone III i.e susceptible to moderately sized earthquakes up to magnitude (M_W) 6.0. The overall study area includes Goa, a major portion of Karnataka and North Kerala. The closely located epicenters of the past earthquakes along the western coastal stretch intrigued this investigation. The study houses a whole bunch of petrochemical industries and infrastructures of commercial and religious interest, making seismic preparedness inevitable. The local site effects are incorporated into PSHA, thereby, making the outcome of the study applicable to current seismic design practices. A regional seismic catalog spanning over 190 years with a few prehistoric events from the early 16th century has been compiled. The seismic hazard has been computed by for a reference site condition ($V_S > 1500ms^{-1}$). The investigation suspects mining-induced seismicity in Bellary and Raichur districts though there is no mention of this in the prior literature. The local site effect has been captured by performing 1D equivalent linear analysis using SHAKE 2000. The amplification models as a function of input ground motion for 'sand', 'clay' and 'other soil' have been developed for different periods. The 'sand' amplifies 33% more than 'other soil' and 29% more than the 'clay' for lower input acceleration. 'Sand' exhibits nonlinear behavior whereas 'clay' demonstrates sustained amplifications at longer periods with increasing plasticity index. These amplification models are incorporated into PSHA by transforming the GMPEs. The resulting uniform hazard spectrum (UHS) for all the three soil types was compared with the elastic spectrum of various codes. The codal provision underestimates the spectral values at smaller periods (T<0.5s) and overestimates at higher values. The local soil data was unavailable for the whole of the study region and hence, the digital elevation maps have been used to determine the site topography. The slope calculated from topography is correlated to shear velocity in the top 30m ($V_{S\,(30)}$) and the ground motion parameters are estimated. A maximum of 60% to 80% amplification has been observed in the study area.

Keywords: Regional earthquake catalog, Seismic Source Zones, Sensitivity analysis, topographic slope, host-to-target adjustment, local site effects, Elastic design spectrum.

CONTENTS

i

LIST OF FIGURES

LIST OF TABLES

NOTATIONS

AF (f)	Amplification factor as a function of frequency
ASC	Amateur Science Centre
ASCE	American Society of Civil Engineers
BIS	Bureau of Indian Standards
D	Damping ratio (%)
DBE	Design Basis Earthquake
DEM	Digital Elevation Map
EC	Euro Code
ENA	Eastern North America
EQL	Equivalent Linear Method
g	Acceleration due to gravity
G	Secant shear modulus
G/G$_{max}$	Shear modulus reduction coefficient
GMPE	Ground Motion Prediction Equation
G-R	Gutenberg – Richter recurrence parameter
GSI	Geological Survey of India
H$_M$	Median Hazard Level
H$_L$	Lower Hazard Level
H$_H$	Higher Hazard Level
HTTA	Host To Target Adjustment
IM	Intensity Measure
IMD	Indian Meteorological Department
IRIS	Incorporated Research Institutions for Seismology
ISC	International Seismological Centre
M$_C$	Magnitude of Completeness
MCE	Maximum Considered Earthquake
M - R	Modulus Reduction curve
MSK	Medvedev–Sponheuer–Karnik scale
MMI	Modified Mercalli Intensity Scale
M$_{max}$	Maximum magnitude of the earthquake

$M_{max(obs)}$	Maximum observed earthquake
M_W	Moment Magnitude
M_L	Local Magnitude
m_B	Body wave magnitude
M_S	Surface wave magnitude
MZ	Microseismic zones delineated in the study
N	Standard Penetration Resistance
NEHRP	National Earthquake Hazards Reduction Program
PGA	Peak Ground Acceleration (g)
PI	Peninsular India
POE	Probability of Exceedance
PSA	Pseudo-Spectral Acceleration (g)
PSHA	Probabilistic Seismic Hazard Analysis
R_{epi}	Epicentral distance (km)
R_{hyp}	Hypocentral distance (km)
R_{JB}	Joyner-Boore Distance (km)
R_P	Return period
R_{rup}	Closest distance to rupture (km)
S_a	Spectral Acceleration (g)
S_a^r	Rock Spectral acceleration (g)
$S_a^s(f)$	Surface spectral acceleration (g)
SCR	Stable Continental Region
SHA	Seismic Hazard Analysis
SPT	Standard Penetration Test
SPT	Standard Penetration Test
SRA	Site Response Analysis
UHS	Uniform Hazard Spectrum
USGS	United States Geological Survey
V_S	Shear wave velocity (ms^{-1})
γ	Shear Strain
ρ	Unit weight (kN/m^3)

$\boldsymbol{\tau}$	Shear Stress (N/mm^2)
$\boldsymbol{\varepsilon}$	Epsilon
h	Thickness of the soil strata (m)
$\bar{\mathbf{Y}}$	median amplification between the reference site condition and the base of the soil profile
d	Depth of the soil column from the surface (m)

CHAPTER 1

INTRODUCTION

1.1   General

Earthquakes are the signatures of Earth's crustal movements and are known to have shaken mankind from time immemorial. In recent years, earthquakes of both tectonic and man-made nature have become a routine. Earthquakes on their own are not lethal but the poor performance of the built environment against seismic actions lead to casualties. A thorough understanding of the earthquakes aids in accurate estimation of the seismic forces and design of various structural components to these forces. The interpretation of earthquakes demands sound knowledge of Geology, Geophysics, and Geotechnics. The entire discipline of earthquake engineering has been developed based on observations and experiences.

The concept of earthquake-proof buildings is the dream for the future, however, the attempts so far have been successful in building earthquake resistant structures. The principle behind these structures can be generally stated as scaling down of the intensity of ground shaking on a structure and enhancing its deformation capability. In order to estimate the seismic force acting on a building during an earthquake, various factors such as natural period, geographical location, deformation capability of the building as well the local site condition needs to be considered. Usually, an elastic design response spectrum provides peak values of the response quantity (Displacement, velocity, and acceleration) for a range of buildings with natural period varying between o and 4s. Conventionally, the response spectra representing peak acceleration values (PGA or PSA) are used in earthquake resistant design of structures. A site-specific response spectra account for the observed local seismicity and site conditions. In other words, to generate a site-specific response spectrum, the observed seismicity and the local site response need to be assessed.

The macroseismic activity witnessed in a study area of interest is compiled together in the form of an earthquake catalog. Usually, these catalogs span over many decades starting from prehistoric events till the latest instrumental records. The seismic potential

of a study area is assessed through the catalogs in order to make future predictions with marginal uncertainty. In spite of careful evaluation of local seismicity, the soil site conditions usually govern the extent of seismic damage observed in surface and subsurface structures. This phenomenon is known as local site effects. Apart from evaluating the seismic characteristics of the source, the local site conditions and its dynamic response to the propagating seismic waves need to be analyzed. In other words, the seismic waves originating from the source located at a depth undergoes significant modification on its way towards the surface as illustrated in Figure 1.1. The geological strata underneath the surface can be divided into three main categories viz., seismic bedrock, engineering bedrock, and sediment layers. This classification simplifies the complexity in understanding the subterranean deposits and is classified based on the Shear-wave Velocity (V_S) of the constituting material.
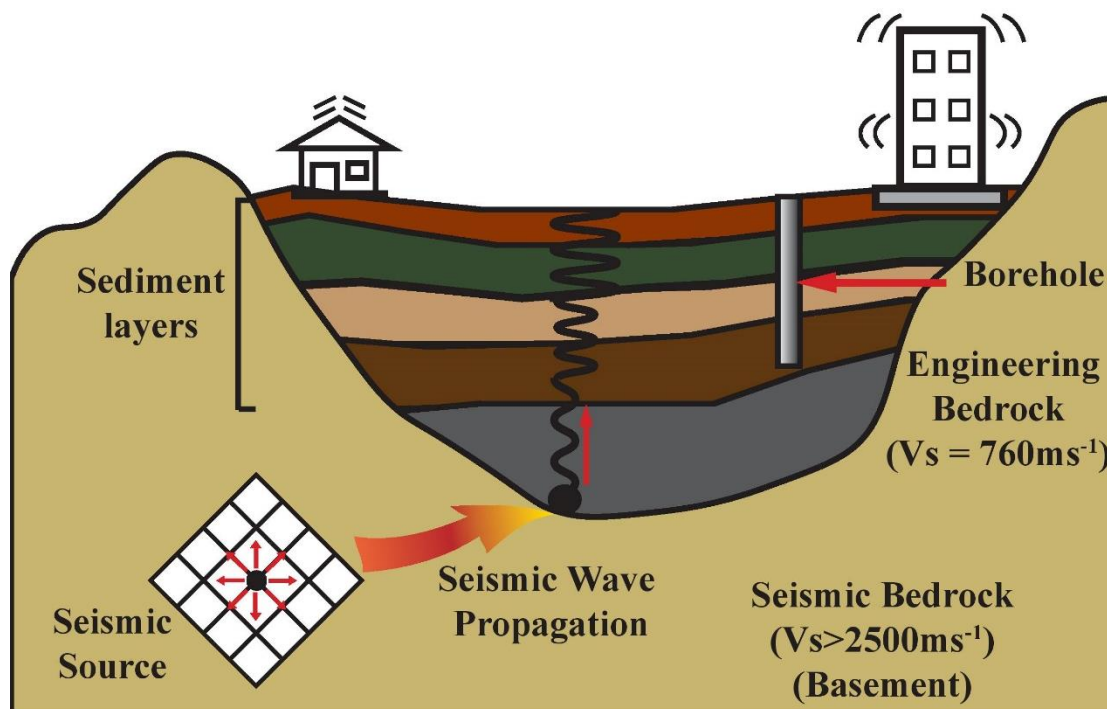
Figure 1.1 Illustration representing the key components of SHA and SRA.

In order to produce a site-specific design spectrum, both seismic hazard analysis and geotechnical site characterization is necessary. In Seismic Hazard Analysis (SHA), all the possible seismic sources with the potential to cause ground shaking at a chosen site of interest are identified and assessed. The seismic site characterization refers to the evaluation of the dynamic behavior of the subsurface material to the ground motion.

Site Response Analysis (SRA) is a commonly adopted technique to characterize and estimate local site effects. The elastic design response spectrum is a combined output of both SHA and SRA useful for analysis and design of surface and subsurface structures. Both the analytical methods i.e. SHA and SRA are explained in detail in the subsequent sections.

In the present study, the regional seismic hazard has been evaluated in a probabilistic manner and the local site effect has been captured by two conceptually distinctive indirect methods. The outcome of the adopted method is expected to enumerate the Probability of Exceedance (POE) of a ground motion parameter (PGA, PSA or S_a at 5% damping) with respect to a certain intensity level in a given time frame. The present study is an attempt to integrate the observed seismicity with the local site conditions in order to produce outcomes useful in building a seismic resilient community.

1.2   Seismic Hazard Analysis

Seismic hazard is a threat arising due to potential earthquakes in a given area of interest. This seismic hazard varies geographically and is represented in the form of seismic hazard maps obtained from the SHA. As a matter of fact, SHA is a fundamental step in performance-based seismic assessment. A seismic hazard map is the culmination of tectonic features and its associated seismicity in a region, wave propagation characteristics, and near-surface local site conditions. These maps serve as an aid for planning land-use, disaster mitigation, and emergency response.

The framework for SHA involves explicit evaluation of all possible seismic sources in a study region and their potential to generate earthquakes in the future. Further, the ground motion that can be expected at a site located at a certain distance from the already identified seismic sources in the region is computed. The former is known as seismic source modeling and the latter is known as ground motion modeling. The SHA combines the seismic source models and the ground motion models to produce hazard curves as shown in Figure 1.2. The seismic hazard of a region can be computed deterministically, probabilistically or neo-deterministically. In the study, a probabilistic approach has been adopted to determine the hazard using CRISIS 2015. In probabilistic seismic hazard analysis (PSHA), the uncertainty in the size and location of the

earthquake along with the path and site effects are assessed individually and combined to express ground motion parameters for a defined POE. The methodology estimates the hazard level for various return periods (R_P) by exploring all the possible combinations of magnitude (M) and distances (R) of seismic activity with due consideration to local site effects. The return periods used for design consideration are 475 years and 2475 years which is equivalent to 10% and 2% probability of exceedance in 50 years.
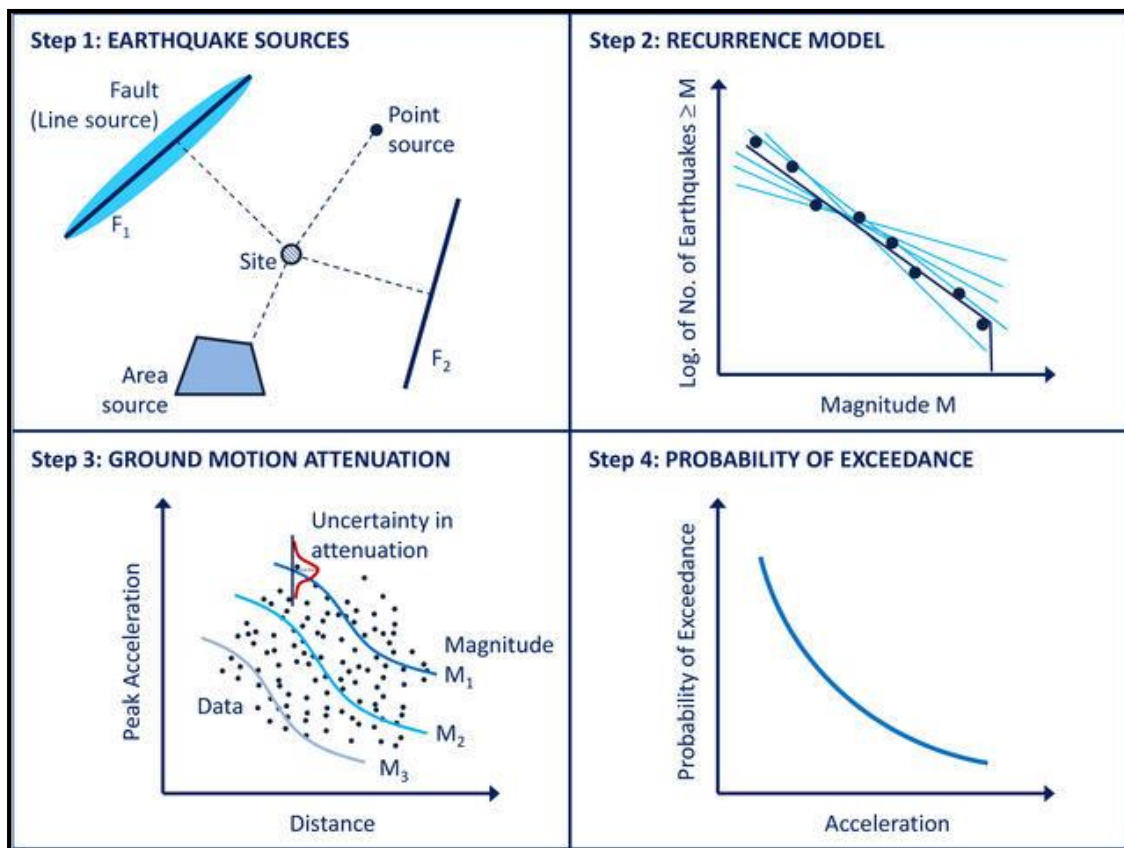
Figure 1.2 Schematic of the framework of PSHA (https://www.norsar.no/r-d/safe-society/earthquake-hazard-risk/earthquake-hazard-assessment/)

The outcome of PSHA is presented in the form of hazard curves and uniform hazard spectrum in addition to hazard maps. The hazard curves represent the POE of a specific value of the intensity measure (such as PGA, PSA or S_a) in a given time frame (usually 50 years). The Uniform Hazard Spectrum (UHS) represents the peak value of a chosen Intensity Measure (IM) for a wide range of periods between 0 to 5s. UHS is similar to

a response spectrum generated from different combinations of M and R for a given site, whereas the response spectrum is a result of an individual earthquake.

The SHA deals with the geological and geophysical aspects of an earthquake. However, the methodology is incomplete without the incorporation of the near site conditions. In this regard, the role of the local site in modifying a seismic wave being propagated through its medium needs to be identified and appraised.

1.3   Seismic Site characterization

The seismic site characterization is necessary for the outcome of seismic hazard analysis to be relevant for built environment applications. This involves laboratory and field investigations, compilation of the experimental data, numerical analysis and interpretation of the results to explain the physical phenomena. The data from laboratory investigation consists of index and engineering properties of the soil. The dynamic characteristics of the underlying material beneath the surface is usually captured by the shear wave velocity in the top 30m ($V_{S(30)}$). There are various geophysical methods available for in-situ measurement of the V_S for a given soil deposit. A few of them are seismic refraction survey, seismic reflection survey, surface wave methods, cross hole method, downhole method, and suspension logging. The compiled data is used as an input to compute the site response to the wave propagation using Site Response Analysis (SRA). The amplification and/or attenuation characteristics of the local soil deposits can be assessed through this numerical investigation. The outcome from SRA can be further used for generating synthetic ground motions and design spectra. The elastic design response spectra generated from SRA is a result of a wide range of M and R of various earthquakes relevant to the study region. In the present study, SRA has been carried out on SHAKE 2000.

The in-situ methods are expensive and demand skilled labor. Additionally, determining the site characteristics in hilly terrains and other inaccessible places is highly impractical. Hence, alternate methods using the topographic slope as a proxy to the seismic site condition can be adopted. This method utilizes the globally available Digital Elevation Model (DEM) to calculate the topographic slope, which is further correlated to $V_{S(30)}$. The amplification factor or the soil factor determined based on the

$V_{S(30)}$ is further combined with the initial computation of PSHA. The method was developed based on field observations and has the ability to provide first-order estimates of the local site characteristics.

The estimated site response is further integrated into the initial results of PSHA in a deterministic or probabilistic manner based on the prescribed level of complexity. The outcome of the site-specific (from SRA) / region specific (from Topographic slope) PSHA represents the local seismicity as well the site conditions.

1.4   Motivation and Scope of the study

Peninsular India was considered to be a stable continental landmass until stricken by a few major intraplate earthquakes such as Latur (1993), Jabalpur (1997), and Bhuj (2001). These events inspired further research into understanding the seismotectonics of intraplate regions. The Western continental margin of peninsular India is a trailing passive margin and researchers have observed significant seismic activity along the coastal stretch. Additionally, this part of India houses port structures, petrochemical industries, ancient architecture depicting religious beliefs and other infrastructures of socio-economic importance. However, no micro-level seismic hazard studies have been conducted exclusively for this region. The study aims to create benchmark regional seismic hazard model based on up to date homogenous data sets and well-established tectonic features. The outcome of the investigation produces seismic hazard maps that are beneficial for policymakers and engineers in improving earthquake preparedness. The widely available field data has been used to develop simple site amplification models to encourage practitioners in adopting site-specific methods. The adopted methodology in the present investigation serves as a guide for conducting a site-specific investigation for important infrastructures such as bridges, nuclear power plants, and dam sites. Additionally, the study highlights the use of widely practiced soil testing methods to characterize the dynamic behavior of soils.

1.5   Objectives of the study

The aim of the present investigation is to highlight the seismic potential of an intraplate region and provide region-specific guidelines useful for practical applications. In this direction, the following objectives were formulated.

- Identification of potential seismic sources contributing to the seismicity of South West India. Formulation of seismic source and ground motion prediction models by considering the uncertainty in the input parameters.

- Performing probabilistic seismic hazard analysis for a reference site condition (i.e NEHRP 'A', $V_S > 1500 ms^{-1}$). De-aggregation of the seismic hazard.

- Compilation of regional borehole data to characterize the local soil deposits. Selection of hazard consistent ground motion records and simulation of site response.

- Generation of amplification models as a function of natural period and input motion for various soil types. Derivation of elastic design response spectrum for different soil conditions.

- Transformation of a ground motion prediction model (GMPM) to incorporate the developed site amplification model and produce site-specific seismic hazard maps and uniform hazard spectrum.

- To develop shear wave velocity ($V_{S (30)}$) map and surface level seismic hazard map for the entire study region from topographic data.

1.6   Organization of the thesis

The probabilistic seismic hazard analysis with the integration of local site effects has been performed and the same has been detailed in the thesis. Seismic hazard estimation and site characterization are the two fundamental components of the study. Both the components involve step by step procedures with the output of each step leading as an input to its succeeding step. Hence, a separate chapter has been dedicated to each component. The entire study has been presented systematically in six chapters and data supplements are arranged in the appendix.

- The brief introduction about the topic of the thesis has been presented in **Chapter 1**. Additionally, the motivation, scope, and objectives of the study have been elucidated.

- A detailed literature review on regional seismicity and seismotectonics, seismic source and ground motion modeling, seismic hazard analysis, site response analysis has been presented chronologically in **Chapter 2.**

- The geology and geomorphology of the study area have been outlined in **Chapter 3.** The methodology adopted for probabilistic seismic hazard analysis and site characterization has been explained.

- **Chapter 4** presents the step by step findings of PSHA. The evaluation of seismicity parameters and computation of seismic hazard has been discussed. De-aggregation of the computed seismic hazard has been performed.

- **Chapter 5** explains the findings of different Seismic Site characterization techniques adopted in the study. The site-specific outcomes such as hazard maps and hazard spectra are presented.

- The conclusions drawn from Seismic hazard analysis and local site characterization studies have been enumerated in **Chapter 6**. Also, recommendations for future work has been listed in the chapter.

- **Appendix I** lists the earthquake catalog compiled for the study in the chronological order.

CHAPTER 2

LITERATURE REVIEW

2.1   Introduction

Earthquakes are known to have an enormous impact on human life. The unpredictable nature of the earthquakes has provoked interest among researchers for a few decades now and continue to challenge mankind in finding a sustainable solution. A decent understanding of earthquakes and the progress made so far in combating them has been possible only through careful review of the past experiences. The main focus of any research is to prevent loss of life and ensure adequate operability of the building stock post an earthquake. In this regard, understanding the seismic potential of a region and planning the infrastructure growth accordingly is the key.

Seismic hazard estimation and microzonation studies are the common approaches in assessing the seismic potential of any region/study area. Seismic hazard involves assessing the hazard at a given study area due to earthquakes and microzonation maps the hazard parameters at a local scale by incorporating local site conditions. These techniques demand inputs from a diverse range of disciplines such as geology, geophysics, seismology, and geotechnical engineering. The genesis of an earthquake and the seismic wave propagation characteristics can be understood from seismology. The geological formations and the geophysical properties of the earth convenient for the manifestation of the tectonic processes are the elements of geology and geophysics. Geotechnical engineering emphasizes the impact of local site conditions in ground shaking and the resulting geotechnical damages such as landslides and liquefaction.

Considering the interdisciplinary nature of the present study, the literature review has been presented categorically. The articles referred during the course of the study have been arranged in the chronological order in each section. The chapter begins with the seismicity and seismotectonics of Peninsular India, explaining the tectonic activity in the Intraplate region also known as a Stable Continental Region (SCR). The statistical analysis and interpretation of the observed seismic activity have been explained. The previous seismic hazard studies and site characterization methods carried out for various regions within India have been presented under their respective sections.

2.2   Overview of Tectonic setting of India

The geological formations and their associated seismic activity must be identified and examined to understand the susceptibility of any given area to earthquakes. The geological features responsible for seismic activity also known as tectonic features have to be studied from its creation. One of the earliest attempts in understanding the tectonic movements and its associated seismic activity was by Alfred Wegener in 1912 through Continental drift theory. The theory states that, approximately 4.6 billion years ago, the earth was formed consisting of one super ocean 'Panthalassa' surrounding one supercontinent 'Pangea'. Later Pangaea was split into different plates which drifted apart gradually and the present continents were formed as shown in Figure 2.1. However, this theory failed to explain the reason for the drift of different landmasses and was later overshadowed by other plausible theories such as "Sea Floor Spreading" and "Plate Tectonic Theory".
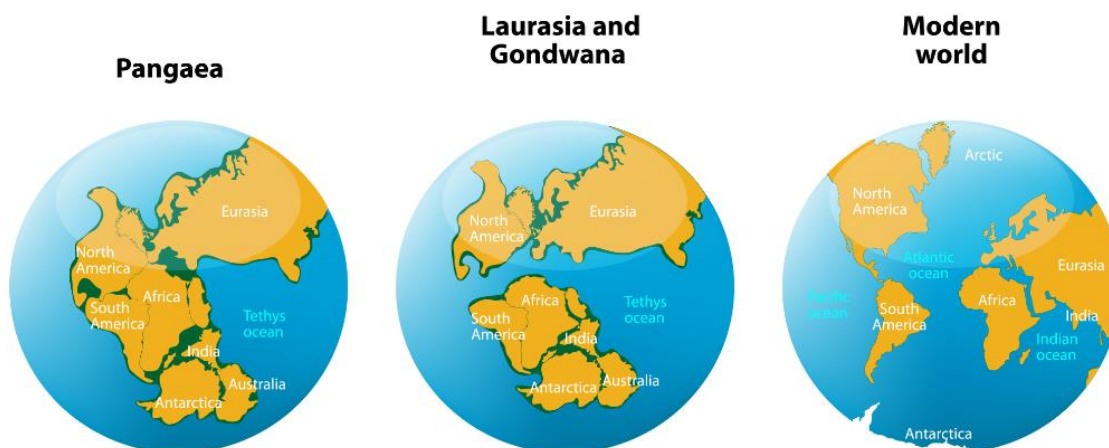
Figure 2.1 Continental drift witnessed over the last few millions of years (https://www.xearththeory.com/supercontinents/expanding-earth-7/)

During the Precambrian Era, Pangea split into Laurasia (Northern Part) and Gondwana (Southern Part). These two huge landmasses were separated by the Tethys Sea. India along with present Africa, South America, Australia, and Antarctica formed part of the Gondwana supercontinent. The volcanic activity in the Gondwana land lead to the formation of cracks and the landmasses separated along these cracks. The continents started drifting apart with different velocities, paving way for the present Indian Ocean. In the late Cretaceous, approximately around 100 million years ago, India split from Madagascar and started its Northward journey. During this movement, the Indian plate

passed over an active reunion hot spot in the Indian Ocean. The basaltic lava from the hot spots cracked and overflowed on the landmass creating sedimentary layers of basaltic rock also known as Deccan traps. Many scientists claim that around 55 million years ago i.e., in Eocene epoch of Cenozoic era Indian plate collided with Eurasia. When the Indian plate collided with the Eurasian plate, the latter was partly crumpled and buckled up above the Indian plate but due to their low density/high buoyancy, neither of the continental plates subducted. This caused the continental crust to thicken due to folding and faulting by compressional forces pushing up the Himalaya and the Tibetan Plateau. The continental crust here is twice the average thickness at around 75 km. The Himalayas are still rising by more than 1 cm/year as India continues to move northwards. The drift of the Indian plate from the south to the equator is considered as one of the fastest plate movements so far which reduced its rate of drift around 50 to 40 million years ago to 4 – 6 cm/year ((Molnar and Tapponnier, 1975) as shown in Figure 2.2. The relative positions of Indian and Eurasian plates in the geological past have been estimated from the history of sea-floor spreading in the Indian Ocean. The study on magnetic reversals in the floors of the Indian and Atlantic oceans found that Indian subcontinent has traveled about 5000km northward over a period of about 20–30 million years before its collision with Eurasia (Molnar and Tapponnier, 1979).

2.3   Seismotectonics of Peninsular India

The peninsular India which was once considered to be stable land mass has been exhibiting seismic activity at an interesting rate and many researchers have proposed various theories for tectonic stress accumulation and its release over the period. The tectonic stress developed in peninsular India can be attributed to various reasons such as the effect of

- Continental margin
- Differential crustal movement
- Hotspots
- Continental collision

According to Sykes (1970), the high stresses generated by the continental collision between the Indian and Eurasian plate may have a broader spatial extent owing to the seismic activity throughout the Peninsular. Bott & Dean (1972), suggested that the

gradient in thickness and density of the oceanic and continental crust at the continental margin may provoke a stress system responsible for the evolution of normal faults in the continental crust and thrust faults in the oceanic crust.
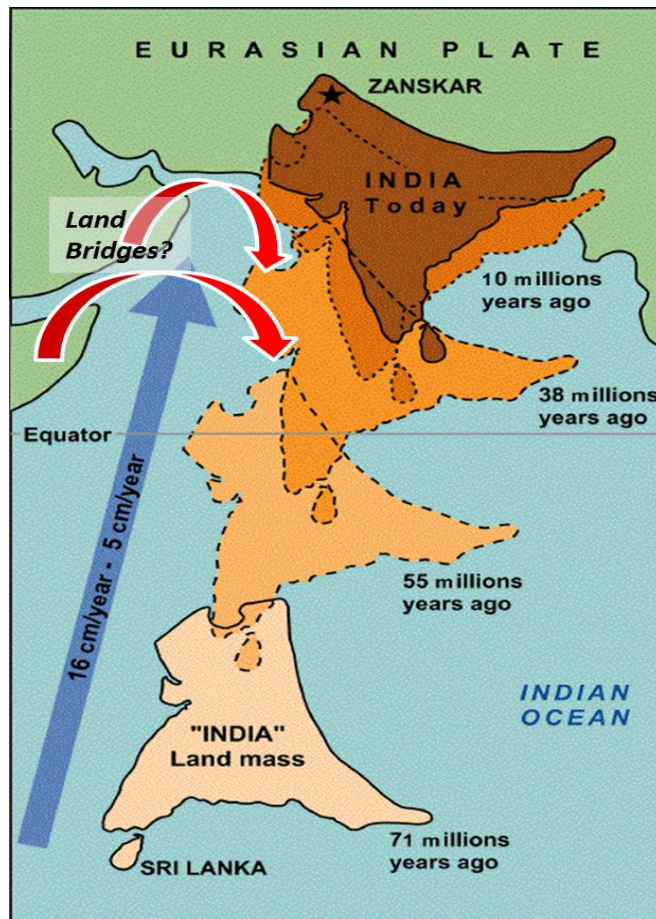
Figure 2.2 Northward movement of the Indian plate
(https://en.wikipedia.org/wiki/Indian_Plate)

The Indian landmass is composed of three main proto continents namely, Aravalli, Dharwar, and Singhbum which are demarcated by rifts as shown in Figure 2.3. The joint or the junction between each of these protocontinents engendered lineaments which are at present known as Narmada, Son, and Godavari Lineaments. These lineaments were reactivated during Gondwana times leading to the development of tensile forces owing to the formation of Damodar and Mahanadi rift valley. Simultaneously cracks were developed along the western coast of Indian plate which was reactivated when the Indian plate collided with the Eurasian plate.

Figure 2.3 Cratonic division of Peninsular India (Burke et al, 1978)

The study area stretches along the west coast of India encompassing Goa, Karnataka, and Kerala. The studies conducted by Kaila et al (1972) for the preparation of quantitative seismicity maps suggest that the west coast is more seismically active than the east coast. While reviewing the seismic status of Peninsular India, Guha et al (1974) postulated that the marginal areas of the Peninsular shield such as the Coastal fringes of the west and east coasts could be considered seismically active with the potential to generate moderate-sized earthquakes. Studies have revealed that the Western continental margin is similar to that of the Eastern margin of the African continent in terms of tectonic and its associated magmatic evolution (Chandrasekharam, 1985). Rao (1992) suggested that the southern part of the Karnataka coast is transitional in character and seismically active with frequent earthquakes of low magnitude.

There are two prominent trends of the faults existing in the area. First set of faults run parallel to the coasts in NNW-SSE direction and the second set of faults run perpendicular to the coastal line NNE – SSW direction. According to Rastogi (1992), the northward movement of the Indian plate induced compression in Peninsular and led to the formation of NE trending faults. The accumulated compressive stresses give rise to occasional slip along these faults. However, the slip being small in dimension results in minor earthquakes except for a few major intraplate earthquakes such as Bhuj (2001).

13

The older NW trending faults are also triggered by this compression. The Western Ghat seismic zone striking parallel to the west coast of India was formed by major faulting and uplifting of blocks in the Jurassic period and is suspected to be undergoing adjustments (Radhakrishna, 1993). Subrahmanya (1996) identified an east-west trending ridge passing from Mulki on the west coast to Pulicat Lake on the east coast characterized by thinner crust and microseismicity (Figure 2.4). This ridge separates northeast flowing rivers from the southeast-flowing rivers. Bansal & Gupta (1998) established the fact that the western ghat zone extending between 15°N to 21°N and striking NNW parallel to the western coast is one of the most active zones. Mandal (1999) suggests that the regions near the western end of Dharwar as well as the south granulite terrain (SGT) are the potential locales for future earthquakes. The regional strain rates in the stable continental region (SCR) is low of order of 10^{-10} to 10^{-12}/yr. Despite the lower strain rates, the SCR has witnessed damaging earthquakes owing to the presence of numerous critically loaded spatially distributed tectonic features (Seeber et al, 1999). The crustal velocity of the upper layers is a key to understanding regional tectonics and evolution of the present day crustal configuration. Reddy & Rao (2000) studied the subsurface velocity heterogeneities in the Indian Shield. Their findings point out that the Dharwar craton has an average velocity of $5.9 - 6.4$kms^{-1} and $6.8 - 7.0$kms^{-1} corresponding to upper and lower crusts extending to a depth of 22 to 38km respectively. The velocity in the upper mantle is around 8.1kms^{-1}. Southern Peninsular is composed of three major tectonic domains namely, Dharwar craton, Eastern Ghat mobile belt and Southern Granulites Terrain (SGT). The study area is classified as Gneissic complex/Gneissic Granulites with major inoculation of green stone and allied supracrustal belt as shown in Figure 2.5.

Dharwar craton is divided into two parts by an N − S shear zone and the Closepet Granite. Studies have revealed the existence of the low-velocity layer in the entire Moyar-Bhavani Shear zone and the region covering these shear zones are interpreted as a collision zone (Reddy and Rao, 2000). The Moyar − Bhavani Shear zone, approximately 200km long trending in E-W direction is believed to be releasing the stresses accumulated due to the Northward collision of the Indian plate (Valdiya, 2001). Singh et al, (2003) in their study established the fact that earlier the Dharwar granite-greenstone terrain and the Southern Granulite terrain (SGT) formed a singular crustal

block, namely the Dharwar Crustal Province (DCP). Due to the northward tilt of the crustal block and differential erosion, regional metamorphism from north to south has increased. Jade (2004) measured the velocity of Southern Peninsular India using GPS and recommended that the entire Southern part moves as a rigid plate at a rate of 20mm/yr.
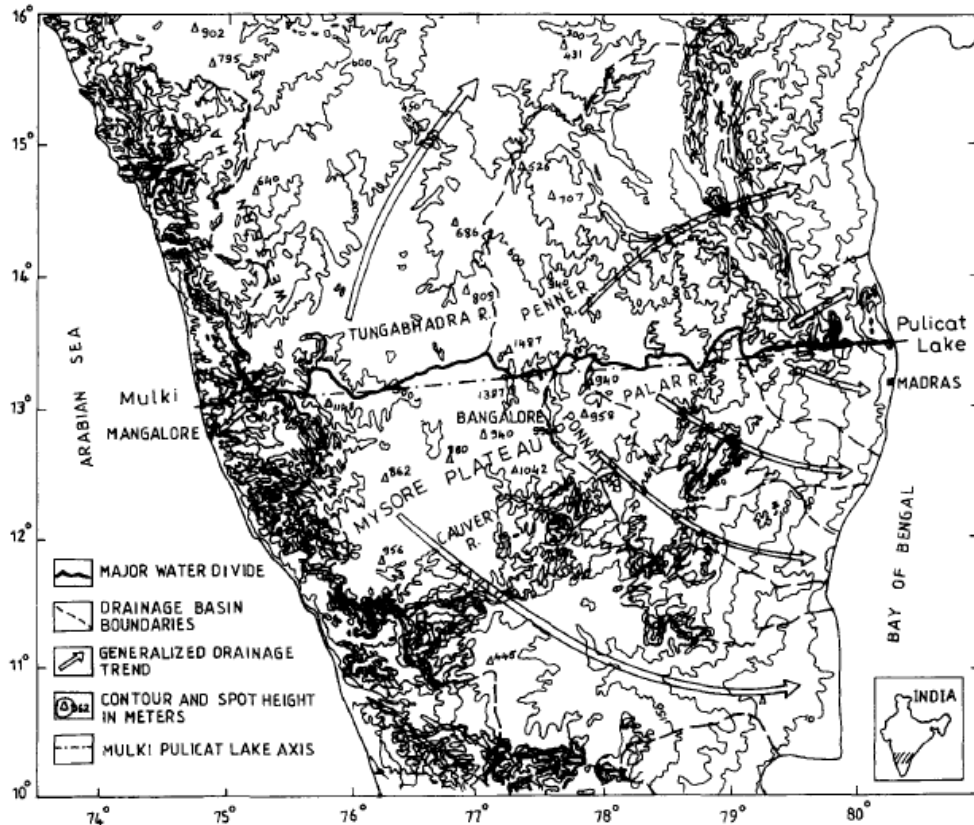
Figure 2.4 A major water divide close to Mulki-Pulicat Lake Axis (Subrahmanya, 1996)

The western continental margin consists of a number of horsts, grabens, and faults having developed in inshore and offshore areas (Sukhtankar et al, 2004). During the Gondwana period (Upper Carboniferous to Lower Cretaceous), intense block movement took place in the platform, resulting in the formation of several grabens, probably along major basement lineaments (Gupta, 2006). The major geo-fracture of this terrain is the west coast fault (WCF), which trend NNW, and is considered to be related to the breaking away of the Indian plate from the Gondwanaland (Kayal, 2008). Verma & Bansal (2013) measured the average crustal thickness in the Dharwar craton to be 35km with gradual thinning towards the coastal region due to the transition from continental to oceanic crust.
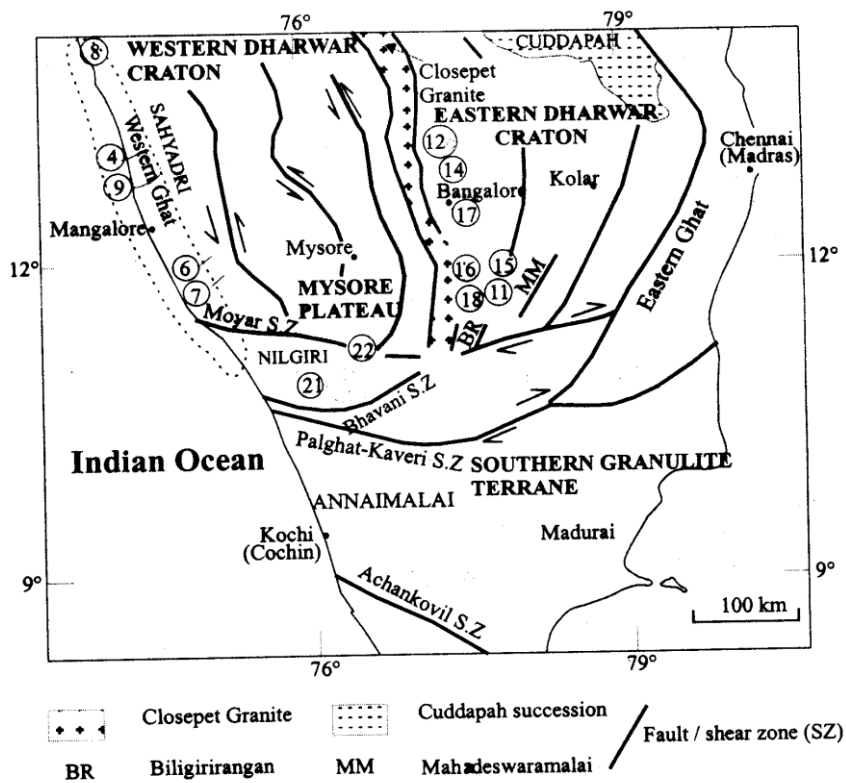
Figure 2.5 Tectonic domain of South Indian Shield (Valdiya, 2001).

2.4 Seismicity of Peninsular India

India has witnessed both interplate as well as intraplate earthquakes. The frequency of occurrence of interplate earthquakes is high than intraplate earthquakes. However, the latter can be devastating due to higher population density in the intraplate regions when compared to the interplate regions. The earliest record on earthquakes reveals seismic activity in Dholavira (Khadir islet of Kachchh, India) in the year 2200BC supported by the evidence of ground displacement and the collapse of walls. The intraplate region of India i.e. the Southern Peninsular has witnessed major earthquakes such as Koyna (M_W 6.6) in 1967, Latur (M_W 6.2) in 1993, Jabalpur (M_W 5.8) in 1997, Bhuj (M_W 7.7) in 2001. The seismic potential of intraplate regions in India was underestimated before the Bhuj earthquake. However, post-2001, seismic microzonation studies were initiated for major cities and severe earthquake-prone areas. In 2017, the National Centre for Seismology, Ministry of Earth Sciences (Govt. of India) initiated Geotechnical and Geophysical investigations for the seismic microzonation of 30 cities in India.

2.4.1 Regional earthquake catalogs

The absence of detailed tectonic information for a region can be balanced with the aid of epicenter of past earthquakes. The observed seismicity in the past serves as an index for the seismic potential of the region. In this regard, various researchers have investigated to collect information about the earthquakes from a period when seismic recording instruments were not so popular. With the advancement of the instrumentation in seismic recording, many local and global agencies are maintaining the accurate records of earthquakes post-1960. The earthquakes from the pre-instrumental era were mainly reported on the Intensity scale. One of the earliest catalogs compiled for India was by T Oldham (1883) and John Milne (1911). The former concentrated on Indian earthquakes whereas the latter covered earthquake data for a larger spatial extent. Chandra (1977) compiled an earthquake catalog from the earliest times till 1974 with the spatial extent varying between 5°N-28°N and 67.5°E-90°E. Rao and Rao (1984) listed historical earthquakes of India spanning between 1340 to 1983. The events were reported on Richter and MMI scale. The study highlighted the occurrence of Shimoga earthquake in 1975. This event was intriguing as there was no evidence of past earthquakes in this region. Rao (1992) observed that a large number of micro to moderate earthquakes ranging from M2 to M5 occur close to 13°N. Reddy (2003) highlighted that the south Indian seismicity is neither understood properly nor given importance since it is of micro-dimensions. There are no notable detailed hazard studies carried out in southern India except Mumbai region. The Epicentral locations of the major intraplate earthquakes were major deciding factors in preparing a seismic zonation map (Walling and Mohanty, 2009). In recent years, the compilation of regional earthquake catalog is one of the prerequisites for hazard assessment. One such attempt was by Iyengar et al (2010), wherein an earthquake catalog consisting of events of magnitude greater than 4 was compiled from the earliest time till 2008. Martin and Szeliga (2010) collected 8339 intensity observations in India and its surrounding region from the 17th century to 2010. These events were reported on EMS scale. A recent study suggested that the spatial and temporal pattern of these two categories of earthquakes are substantially different and Intraplate earthquakes can occur in regions with no previous seismicity and no surface evidence (Calais et al., 2016).

2.4.2 Homogenization of earthquake events

The earthquake events have been reported on the various magnitude and intensity scales. Hence, these events need to be homogenized to a common scale for further assessments. The moment magnitude (M_W) has been widely adopted as a standard for reporting earthquake. In this regard, many researchers have attempted to propose correlations in homogenizing the earthquake events reported on different scales. Anderson (1986) proposed correlations between different magnitude and intensity scale to Seismic moment. The seismic moment is further used in calculation M_W. Johnston (1996) proposed a correlation between different magnitude scales for the stable continental region. Scordilis (2006) collected data on earthquakes from all over the world through various international agencies and proposed correlation with a standard error in the estimation. However, the correlations based on regional data must be used in order to obtain reasonably accurate estimates. In this regards, many attempts such as Kolathayar et al, (2012) for Peninsular India, Baruah et al, (2012) for Shillong plateau and its adjoining regions, Das et al, (2012) for Northeast India have been made by considering the earthquake data from various parts of India.

The compiled earthquake catalog from various sources is associated with a higher level of uncertainty which needs to be addressed. Additionally, fake events and duplication of the same events are also a possibility when the earthquake data is collected from a wide range of sources. Grünthal and Wahlström (2012) demonstrated the procedure for compiling an artifact-free catalog with the uncertainty in the data source accounted for the European and Mediterranean region. Stucchi et al (2013) developed a set of guidelines for formulating a homogenous earthquake catalog and methodology to derive seismicity parameters.

2.4.3 Declustering of the compiled earthquake data

The earthquake data consists of a series of mainshocks and its associated foreshocks and aftershocks. The basic assumption in hazard estimation is that the earthquake follows the Poissonian distribution. In order to hold this assumption, it is necessary to remove the dependent events i.e foreshocks and aftershocks from the catalog. This process is known as Declustering and various researchers have suggested algorithms in

terms of distance from the epicenter and duration from the mainshock. The declustering can be both static as well as dynamic. Static windowing method involves a definite number with respect to duration and distance. In dynamic windowing methods, the duration and distance is a function of the magnitude of the event. Gardener and Knopoff (1974) proposed a declustering algorithm assuming a circular spatial window. The duration of the aftershock sequence, as well as its spatial extent, has been derived as a function of the mainshock in the sequence. The algorithm was further modified by Urhammer (1986).

2.5   Seismic Source Zones

The seismic activity observed in Peninsular India cannot be attributed to a particular fault or lineament. In other words, the observed seismic activity is distributed and diffused in nature, as a result, direct fault modeling cannot be adopted for the present study. In order to bridge the gap between the potential seismotectonic features and the observed seismicity, seismically active zones are identified. Active zones are characterized by numerous earthquake events with few tectonic features such as faults and lineaments in the vicinity. These active zones are geometrically modeled as areal sources with an assumption that the seismicity is uniform within the zone. Additionally, area source zones accommodate the possibility of the existence of unidentified faults in a study region. The segregation of the study area into a number of potential seismogenic sources (area sources) is accomplished with the aid of seismological, geological, tectonic and geodetic information. Earlier seismic hazard studies have identified and delineated seismogenic sources based on historical seismicity, geology and tectonic features (Khattri et al, 1984). Bhatia et al (1999) highlighted that the seismic activity is intense along the plate margins of the Indian peninsula and diffused in other regions except for some spots such as Koyna. They demarcated the region around Bellary as source zone 75, as the region had experienced moderate-sized earthquakes in the past. Seeber et al (1999) identified 9 potential seismic zones based on observed seismicity and tectonic trends in South India. Mandya, Bangalore, and Kolar have been the epicenter for many earthquakes recorded in this region and Raj and Nijagunappa (2004) recommends upgrading these areas from seismic zone 2 to 3 (IS 1893, 2016) based on the remote sensing studies. Gupta (2006) attempted to correlate the tectonic features

19

with the available data on past seismicity and identified 81 potential seismic sources for the whole of India. An area of low finite strain exists near North of Bangalore between eastern and western supracrustal belts (Balasubrahmanyan, 2006). Studies suggest a reverse/normal fault with dominant strike-slip movement rupturing at close intervals to be the main reason behind low to moderate-sized earthquakes in Bangalore. The maximum reported earthquake event is of magnitude Mw 5.6 and studies have suggested that the Killari earthquake (1993) and Sumatra Earthquake (2004) has triggered few investigations of intensity IV in this zone (Sitharam and Anbazhagan, 2007). Seismic sources are defined as the defined volumes of earth's crust with the earthquake potential the same as the size of the earthquake events that can be generated (B C Hydro, 2008). Nath & Thingbaijam (2012) has recommended areal source zones for India delineated on the basis of seismicity, fault patterns and similarity in fault plane solutions. Kolathayar and Sitharam (2012) identified 104 regional seismic sources based on the pattern of seismic event distribution. The common observation made from all the available literature on seismic source delineation is that the coastal region is considered as a separate seismic zone and in other regions zones are identified based on the fault alignment and spatially distributed seismic events. Areal source zones are a simplification over a continuously observed seismicity but on the contrary, this method checks the overinterpretation of an earthquake catalog covering a short time window compared to the return period of larger earthquakes (Ashish et al, 2016). They delineated the entire Southern Peninsular India into 11 zones out of which Gujarat was modeled as a separate tectonic region i.e active crust within the stable continental region.

2.6   Ground motion modeling

The seismic potential of any region can be realized by estimating the seismicity parameters. In order to understand the susceptibility of any region/site to an earthquake of certain magnitude occurring at a given distance predictive/ attenuation relationships are necessary. These are referred to as Ground Motion Prediction Equations (GMPEs) and incorporating them into PSHA needs thorough assessment. GMPEs are mostly derived from a limited number of datasets on real-time ground motion recordings or by simulating the geophysical properties. The limitations arising from the datasets lead to

larger epistemic uncertainty. In order to capture the epistemic uncertainty more than one GMPE must be used in hazard estimation and various GMPEs must be combined together using a logic tree. Bommer et al, (2005) presented a procedure for assigning a weight to different branches of the logic tree with each branch representing a GMPE. The criteria for selecting and adjusting the GMPEs developed for a host region to match the characteristics of the target region was recommended by Cotton et al (2006). They suggested that the combined estimation of ground motion parameter from multiple candidate GMPEs must reflect the expected ground motion at a target region. The criteria for selecting GMPEs involves quality, derivation, and applicability. They suggested the procedure for adjusting the GMPEs to target region by demonstrating a case study in West-Central Europe. The selection criteria for GMPEs was further improvised by Bommer et al (2010). They suggested a workflow for modeling GMPEs for the state of the art seismic hazard assessment. The ground motion prediction in Indian scenario was investigated by Nath and Thingbaijam (2011). They recommended that the GMPEs must be subjected to qualitative and quantitative tests. Additionally, they proposed statistical tests involving a log-likelihood method for ranking the GMPEs applicable for a target region. Delavaud et al (2012) demonstrated the assessment of GMPEs to be used in logic tree combination for a seismic hazard assessment project for Europe. Stewart et al (2013) presented a selection procedure for GMPEs based on trellis plots, evaluation of their functional forms and quantitative tests. Their recommendations included a separate set of models for different tectonic regimes such as stable continental regions (SCRs), interface and in-slab subduction zone and active shallow crustal regions (ACRs). Anbazaghan et al (2016) provided a set of guidelines for selecting, testing and ranking of GMPEs applicable for peninsular India. They suggested efficacy tests in the context of major intraplate earthquakes in India.

2.7   Probabilistic Seismic Hazard Analysis (PSHA)

The analytical framework for evaluating the seismic hazard in a probabilistic manner was first introduced by Cornell (1968). In recent years, many researchers have focused on quantifying the seismic hazard for the whole of peninsular India as well as for smaller regions taken as independent studies. The probabilistic seismic hazard map for India and the adjoining regions was generated by Khattri et al (1984) by dividing the

entire study region into 24 seismic zones and adopting distance attenuation laws developed for Eastern North America. Similar work was carried out by Bhatia et al (1999) for the same region under Global Seismic Hazard Assessment Program (GSHAP) and peak ground acceleration was determined at the center of each grid of size 0.5°X0.5°. Peninsular India was considered to be a stable continental landmass until it was hit by few major intraplate earthquakes such as Latur (Mw - 6.2, 1993), Jabalpur (Mw – 5.8, 1997) and Bhuj (Mw – 7.7, 2001) in recent times. These events inspired further research into understanding the seismotectonics of intraplate regions. Jaiswal & Sinha (2007) combined observed seismicity and known geological characteristics in identifying 9 seismogenic source zones in peninsular India. Additionally, they adopted a zone free method to estimate the seismic hazard. Ashish et al (2016) distinguished Gujarat region from the rest of peninsular India by characterizing it as an active crustal region and adopted multiple seismicity models in estimating the seismic hazard. Apart from the studies carried out for the entire Indian subcontinent, hazard quantification has been performed for important cities such as Delhi (Iyengar & Ghosh, 2004), Bangalore (Anbazaghan et al, 2009), Gujarat (Chopra et al, 2013), Mumbai (Desai & Choudhary, 2014), North East India (Das et al, 2016), West Bengal (Maiti et al, 2017), Himalayan region (Rout et al, 2018).

2.8   De-aggregation of Seismic Hazard

The seismic hazard is a combination of multiple earthquake scenarios representing the ground motion parameter for a chosen probability of exceedance. In performance-based design, it is vital to determine the influential earthquake scenarios for a given site of interest. This will aid further in determining the ground motions for SRA. The de-aggregation of the computed seismic hazard provides better insights into the significance of various influential parameters contributing to hazard (Bazzurro & Cornell, 1999).   A scenario earthquake can be identified in terms of Magnitude (M), distance (R) and Epsilon (ε). The ε value is calculated as the number of standard deviations by which the target ground motion deviated from the median value predicted from a GMPE for a given M and R. De-aggregation can be carried out for a range of probabilities of different spectral periods. However, the procedure must reflect the aleatory and epistemic uncertainty (Hong and Goda, 2006). The numerical results from

the study suggested that the uncertainty in GMPEs can contribute significantly to the de-aggregation. De-aggregation was carried out for two largest urban centers of Canada for a range of spectral periods between 0.2s to 2.0s (Halchuk er al, 2007). They suggested that the contribution of larger magnitude earthquakes is predominant at longer periods than shorter periods. The scenarios leading to negative epsilon values was investigated by Burks and Baker (2011). The negative values of epsilon are of importance as they influence the conditional mean spectrum. This spectrum is an alternative to the conventional UHS to be used as a target spectrum for selection and scaling of ground motion records.

2.9   Site characterization

The local geology and soil characteristics influence the intensity of ground shaking at any given site of interest. In this regard, the dynamic behavior of the subsurface material need to be assessed and suitable design measures should be undertaken to prevent extensive seismic damage. Seismic Site characterization mainly involves measurement and interpretation of the dynamic characteristics of the subsurface material and generation of outputs relevant for seismic design practices. Field tests are conducted to determine the index and the engineering properties of the soil. The data on the local soil deposits are processed further to deliver meaningful outcomes. The local site amplification, acceleration time history, and surface response spectrum are some of the useful outcomes of site characterization. Shear velocity in the top 30m ($V_{S(30)}$) is used as a common index for estimating the amplification.

Several researchers have proposed amplification equations for site amplification considering $V_{S(30)}$ as an independent variable. One such effort was by Choi and Stewart (2005) in developing empirical relations for estimating nonlinear amplification factors. The proposed relationship was developed by considering 1828 strong ground motion data from 154 earthquakes. The study suggested that the amplification factors depended on $V_{S(30)}$ and the input acceleration value. A similar attempt was made by Raghukanth and Iyengar (2007) by using the instrumental recordings of Peninsular India. The study developed coefficients for each NEHRP site class to be used in the computation of amplification also known as soil factor.

Certain GMPEs such as Abrahamson et al (2014), Boore et al (2014), and Campbell and Bozorgnia (2014) modeled site conditions in their relationships by incorporating a site term. Usually, the site term is a function of $V_{S(30)}$ and is developed from global data sets which would yield a generic estimation. Also, Stewart and Afshari (2015) pointed out that such GMPEs are based on incomplete datasets and their predictions are ergodic. The site-specific applications demand site-specific investigations which involve field tests and interpretation of the dynamic behavior by performing numerical studies such as site response analysis. The Site response analysis is one of the commonly used methods to estimate amplification and surface-level ground motion parameters. An alternate cost-effective method using topographical features can also be employed in seismic site characterization. Both methods are explained in the subsequent sections.

2.9.1   Site Response Analysis (SRA)

The dynamic simulation of the shear wave propagation through a series of horizontal soil layers laid parallel to each other is known as site response analysis. The propagation of the shear wave can be realized in 1, 2 or 3 dimension based on the available information and expected level of sophistication in the outcome. The 1D site response analysis can capture impedance, nonlinear behavior of soils and resonance effects. Both linear and nonlinear behavior of the soil material can be captured in the time or frequency domain. The major inputs required for SRA are the soil profiles and ground motion records. The index properties and shear strength parameters are the key elements in soil modeling. The dynamic behavior of the soil is modeled through modulus reduction curves and damping curves. The modeled soil profile is subjected to a recorded ground motion to evaluate its dynamic behavior. However, the outcome from SRA must account for uncertainties in the estimation. The estimated shear velocity profile possess some amount of variability irrespective of the method through which it has been generated. Similarly, a single ground motion cannot capture the overall nonlinear behavior of the soil under dynamic conditions. Therefore, the major variability lies in soil modeling, selection, and scaling of ground motions and method of site response analysis. The uncertainty and bias in the estimates from SRA were evaluated by Baturay and Stewart, (2003) by comparing the ground motion parameters obtained from recordings and that of SRA for same site conditions. The results

consisted of 134 motions from 68 sites and revealed that SRA is unbiased up to T≤ 1s but underestimates for a longer period. They further recommended that SRA is ideal for soft soil deposits with no additional benefits for stiff / rock sites. Bazzurro and Cornel (2004a) conducted statistical tests on uncertainty in the soil properties of two soil sites viz., saturate sand and soft clay and their impact on results from SRA. The uncertainty in the surface ground motion was studied by applying multiple ground motions. They recommended that a minimum of 10 ground motion records may be sufficient to accurately estimate the amplification factor without any due consideration to regional seismic hazard. They concluded that the uncertainty in the soil parameters is of secondary importance when compared to the same in ground motion records. SRA has multiple sources of uncertainty and Rathje et al, (2010) attempted a numerical study by varying the input parameters. They observed a reduction in the predicted median ground motion parameters and increased standard deviation of the amplification factors due to variability in the soil properties. Papaspiliou and Kontoe (2013) investigated the sensitivity of SRA to ground motion records. Their study concluded that 10 number of ground motions are sufficient for nonlinear and 20 for equivalent linear analysis to obtain stable estimates. The influence of uncertainty in soil modeling on the soil amplification and fundamental frequency was investigated by Barani et al, (2013). The soil thickness was found to be influential, particularly when the depth to bedrock is unknown or largely uncertain. Prasad et al, (2019) focussed on the issues of site characterization. They recommended that the stratification of the soil layers must be continuous and not abrupt. Additionally, they highlighted that the present provisions of Indian code do not accommodate the site effects effectively.

2.9.2   Integration of SRA with PSHA

The amplification of the seismic waves passing through various geological stratum needs to be quantified. In this regard, various approaches are available to predict the seismic hazard at the surface for a given hazard value at the bedrock level. The site effects can be included in seismic hazard through deterministic, semi probabilistic and probabilistic methods. Each method has its own procedure characterized by different levels of sophistication, from the simpler one based on the use of standard ground motion predictive equations for specific ground types to the more complex one based

on the convolution of a site-specific amplification function (and its variability) with the hazard curve for reference rock. The deterministic method involves choosing a certain value of the amplification factor based on the recommendation from the code for a given site class. The amplification factor can be determined from the standard empirical GMPEs developed elsewhere as well. The seismic hazard estimation at the bedrock level is modified with the chosen amplification factor. However, these deterministic methods are unable to address the uncertainties associated with the soil properties and the model parameters.

A study by Bazzurro and Cornell (2004a) suggested that Sar (f) of the input record is the single most helpful parameter for the prediction of AF (f) at the same oscillator frequency, f. The site-specific amplification functions derived from the site response analysis was incorporated into the framework of probabilistic seismic hazard analysis (PSHA) (Bazzurro & Cornell (2004b). The hazard at the soil surface is computed by convolving the site-specific hazard curve at the bedrock level with the probability distribution of the amplification function. This approach provides more precise surface ground-motion-hazard estimates than those found by means of standard attenuation laws for generic soil conditions. The authors pointed out that the use of generic ground-motion predictive equations may, in fact, lead to inaccurate results especially for soft-clay-soil sites, where considerable amplification is expected at long periods, and for saturated sandy sites, where high-intensity ground shaking may cause loss of shear strength owing to liquefaction or to cyclic mobility. Goulet and Stewart (2007) compared the deterministic and probabilistic implementation of local site response with PSHA. The deterministic application assumes that the source and epsilon values controlling the hazard on the soil are the same as that of the rock. The deterministic and semi probabilistic approaches produce results that may not be suitable for new age performance-based design. Further, they recommended the incorporation of local site amplification into PSHA at the GMPE level. A fully stochastic procedure for estimating the site amplification of ground motion was proposed and applied to a case study in central Italy by Rota et al (2011). The methodology allows taking into account the record-to-record variability in the input ground motion and the uncertainty in dynamic soil properties and in the definition of the soil model. The target spectrum compatible

ground motions are chosen and scaled accordingly before performing 1D Stochastic site response analysis. The seismic hazard and site-specific ground motion were estimated for important ports in Gujarat by Shukla and Choudhury, (2012). The seismic hazard was estimated for three different hazard levels with return periods of 72, 475 and 2475 years and SRA was performed to obtain surface level spectral acceleration values. Papaspiliou et al. (2012) adopted a similar approach of incorporating the local amplification function into PSHA methodology by performing site response analysis for two sites namely clayey and sandy. They have modified the GMPE to accommodate the amplification function within the computation of the surface seismic hazard.

A technical report summarizing the existing methods to perform site-specific seismic hazard assessment was prepared by Ariztabal et al, (2015). The report presents a case study by applying various methods in estimating the hazard to EUROSEIST site in Greece. The study suggested that the reduced aleatory variability associated with site-specific approaches adds to the additional costa in geological, geophysical and geotechnical site investigations. A non-ergodic site response approach using the locally recorded ground motion and/or site-specific ground response analysis was proposed by Stewart et al (2017). Their study highlights the partitioning of ground motion variability and suggests procedures for computing non-ergodic standard deviation by removing site-to-site variability. A comparison of various approaches for incorporating SRA in PSHA has been discussed by highlighting the strengths and weaknesses of each of them by Barani and Spallarossa (2017). In addition, a fully non-ergodic approach that separates the epistemic contribution (i.e., the epistemic uncertainty affecting the soil properties) from the total variability in site amplification is presented.

The soil nonlinearity was quantified by defining empirical relationships between input ground motion and soil factors by Andreotti et al (2018). These soil factors were further suggested as a substitute for existing provisions in Eurocode 8. The soil factors are multiplied to rock level hazard values to obtain the surface level hazard values. A similar attempt was made by Sandikkaya et al (2018) to yield site factors for a predefined exceedance probability. The proposed method has an advantage of depicting the regional seismicity in the derived soil factors.

2.9.3 Site Characterization using Topography

The seismic hazard assessment with the inclusion of the local site effects is a complete representation of ground motion. However, characterizing the local site conditions using in-situ methods is not always feasible, especially, when the site is inaccessible. Additionally, in-situ methods require skilled laborers and expensive instruments. Hence, it is desirable to adopt cost-effective methods with outcomes of sufficient accuracy. Since $V_{S(30)}$ is the most commonly accepted parameter for site characterization, the topographic slope was correlated to $V_{S(30)}$. The correlation between topographic slope and surficial geology was first attempted in California by Wills et al (2000). A similar study was conducted in Japan by Matsuoka et al (2005) and Taiwan by Chiou and Youngs (2006) and confirmed the correlation between $V_{S(30)}$ and the slope. Wald and Allen (2007) proposed correlations for the stable region and active tectonic region by aggregating the findings from the United States, Italy, Taiwan, and Australia. They observed that the active region was characterized by higher topographic relief whereas stable region's topography was more subdued. Hence, two different sets of correlation were proposed based on the tectonic regime.

The data on local topography is widely available in the form of Digital Elevation Models (DEM) for the entire globe at different sampling intervals. Hence, a first-order site characterization map can be derived from topography. Initially, the correlation between the topographic slope and $V_{S(30)}$ was proposed for a DEM with a resolution of 30 arcseconds. The correlation was improvised by Allen and Wald (2009) with higher resolution data i.e 9 arcseconds. The higher resolution data was able to account for the minor differences in the gradient of higher topographic relief but based on the experience, amplification is not of much significance in higher relief. On the other hand, the higher resolution may not account for improved estimation in lower topographic relief. These correlations were verified by Lemoine et al (2012) and recommended that the method can be used for regional and national level hazard estimates alone and not for site-specific cases. In conclusion, site characterization based on topography is the most feasible option in the absence of information on local geology and its effects.

2.10　Summary of literature review

The studies on regional tectonics and observed seismicity reveal the seismic potential of Intraplate regions. The western coastal stretch of PI has witnessed numerous low to moderate earthquakes in the past. Previous seismic hazard studies have assessed the ground motion parameter such as PGA at a macro level for the whole of Southern Peninsular India. However, the western coastal margin has not received much attention in spite of being categorized as seismic zone III by IS 1893 (2016). Hence, a micro-level seismic hazard assessment in this region is necessary. The local site effects may be predominant than the seismic potential itself owing to a variety of soil strata. Site amplification is the most important parameter used in estimating surface level PGA. $Vs_{(30)}$ is used as a common predictor variable in estimating site amplification. However, a few studies on local site amplification reveal that the nonlinear behaviour of the soil is crucial in determining amplification. The code specified elastic design response spectrum accounts for the soil behavior and ground motion characteristics recorded elsewhere. Attempts on developing site-specific design spectra representing the seismic hazard and local site effects are scarce.

CHAPTER 3

STUDY AREA AND METHODOLOGY

3.1 Introduction

The seismic potential of intraplate regions has been receiving much attention in the last two decades after a major earthquake (M_W 7.7) struck Bhuj in 2001. The structural and geotechnical damage observed during this earthquake demonstrated the need for a seismic resilient built environment. The ground shaking experienced at the surface level is a culmination of multiple phenomena. Each of this phenomenon must be studied and quantified meticulously to produce relevant inputs for seismic design.

The size and duration of ground shaking, distance from the epicenter, local geology, regional tectonics, and soil characteristics are some of the factors influencing the intensity of ground shaking at a given site. Seismic hazard analysis aims to capture the geological, seismological and geotechnical aspects of earthquake ground motions. The unpredictable nature of earthquakes poses a serious problem in estimating definite hazard values. In this regard, a probabilistic approach is considered to be rational.

The study area belongs to an intraplate region susceptible to moderate level earthquakes. A major challenge in estimating seismic hazard for an intraplate region is the lack of data on past earthquakes, unidentified faults with the potential to reactivate in future and insufficient ground motion records. In such cases, Probabilistic Seismic Hazard Analysis (PSHA) relies on the previously compiled catalogs, well established tectonic features, and regionally applicable Ground Motion Prediction Equations (GMPEs). The local site amplification has to be numerically modeled and integrated with the seismological parameters to obtain site-specific hazard estimates.

The present chapter describes the geological, geomorphological and tectonic attributes of the study area. The chapter details the methodology adopted to estimate the seismic hazard, capture the local site effects and finally the integration of local site effects into PSHA. The overall methodology can be segregated into three phases viz., 1) estimation of seismic hazard for a reference site condition, 2) site characterization and site response analysis, 3) incorporation of local site effects into a seismic hazard to produce

surface level estimates. The output of the preceding phase serves as an input to the succeeding phase. The detailed procedure involved in each phase has been outlined.

3.2   Study Area

The Bellary earthquake (1843) of M_W 5.7 was felt over a radius of 300km while Coimbatore earthquake (1900) of M_W 6.0 was felt over major parts of South India. Additionally, the Latur earthquake (1993) of M_W 6.1 caused extensive damage in Bijapur and Gulbarga districts of Karnataka. Based on these observations, it was concluded that a moderate sized earthquake can be felt up to a radius of 300km depending on local geology. In other words, seismic sources located up to a distance of 300km from a given site can significantly influence its seismic hazard. Further, USNRC 1.208 (2007) suggests conducting regional geological and seismological investigations within a radius of 320km of the site to identify seismic sources. The focus of the study is to ascertain the seismic potential of Southwest India. Hence, a circular area within a radius of 350km (latitude 10.3° N to 16°N and longitude 73°E to 78° E) from Surathkal (near Mangalore) has been chosen. The western coastal stretch of the Indian Peninsular encompassing the southerly states such as Goa, Karnataka, Kerala is the geographical extent of the study area as shown in Figure 3.1.

As evident from the figure. 3.1, half of the study area is in the sea and hence, only the land area covering approximately 1,83,560 sq. km has been considered for the study. Bureau of Indian Standards (IS 1893, 2016) has identified the coastal stretch to be prone to moderate earthquakes, categorizing it under seismic zone III. This zone can be characterized as moderate damage risk zone liable to intensity of VII on the MSK scale with a zone factor of 0.16g (PGA). The rest of the study area belongs to a lower seismic zone with a zone factor of 0.10g.

Mangalore is one of the coastal cities located on the west coast of India and a major commercial hub for Karnataka. The city houses a whole bunch of petrochemical industries apart from being India's eighth largest port. Further, the study area consists of 13 dams out of which Supa, Krishnaraja Sagara, Linganamakki are a few prominent ones. There are a few mining areas such as Kudremukh, Raichur, and Bellary in the study region. Bangalore, Belgaum, Panaji, Calicut, Coimbatore are some of the cities

in the study area witnessing rapid urbanization. Ancient temples and shrines existing in the study area add to the religious sentiments of society. Hence, the study area is of socio-economic importance and its seismic potential needs to be identified and evaluated to build a seismic resilient community.
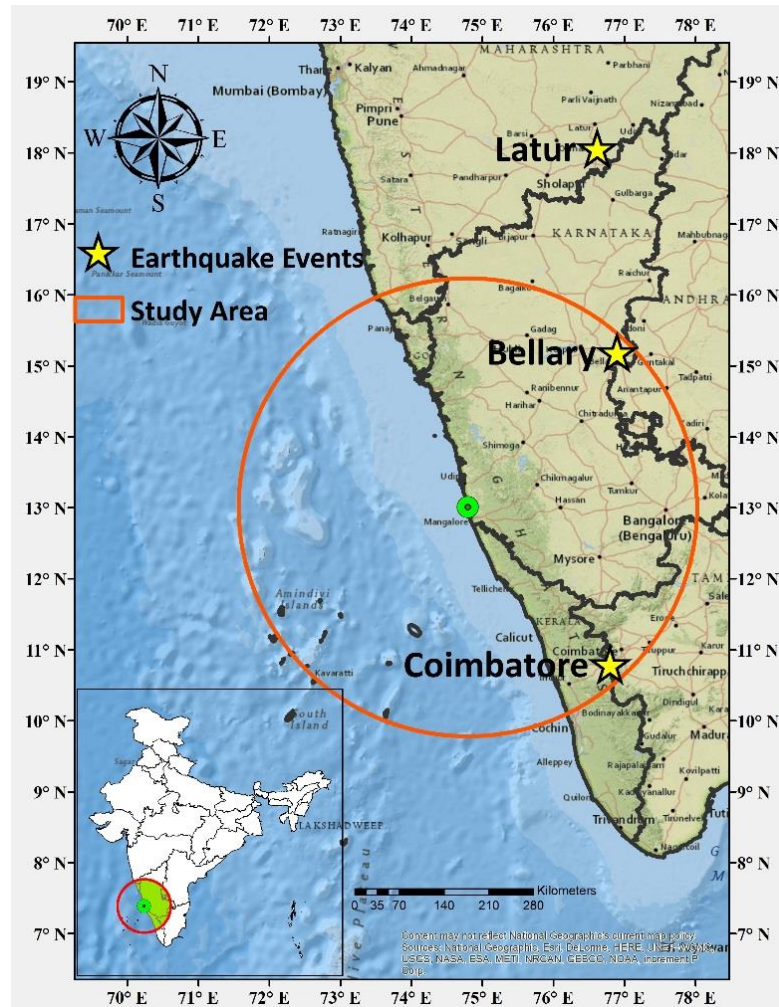
Figure 3.1 Geographical extent of the study area

3.2.1 Geology and Geomorphology

Peninsular India is one of the oldest landmasses of the earth's crust formed by the collision of three proto continents such as Singhbhum, Aravalli, and Dharwar. Peninsular India is mainly composed of Archaean rocks such as granites, gneisses and schists and Proterozoic rocks such as shales, slates, limestone, and quartzite. The later formations lie unconformably over the Archean basement which can be subdivided into four folded areas arranged in chronological order: Dharwar, Aravali, Eastern Ghat and

Satpura fold belts (Bansal and Gupta, 1998). The study area encompasses Goa, major parts of Karnataka and Kerala, limited parts of Maharashtra, Tamilnadu, and Telangana. The geological formations in Karnataka are dominated by Sargur group (about 3300 to 3000 million years ago), Peninsular gneissic complex, Dharwar Supra group (about 3000 to 2600-million-year-old), Closepet granite, Bhīma, Kaldgi (Proterozoic age) and Deccan Traps. These formations are overlaid by laterite and alluvium. The Dharwar supracrustal Supergroup comprises of older Bababudan Group (3000 to 2700 million years) and younger Chitradurga Group (2700 to 2500 million years) as shown in Figure 3.2. The soil formations typically vary from red fine loamy to clayey soils apart from red laterite with large variation in overburden thickness. The southern part of Karnataka and Tamilnadu are characterized by high-grade granulite terrain consisting of the expanse of gneisses spotted with rifts of supracrustal schist belts. The northern part of Karnataka, Goa, Telangana comprise of several greenstone (supracrustal) belts surrounded by gneisses and granitoids. The supracrustal constituting Goa is predominant with greenstones (metabasalts) and rests on a basement of the 3300-3400 million years old Anmode Ghat trondhjemite gneiss. These formations show lithological similarities with the lower part of the Bababudan Group (Dessai, 2011).

Deccan traps consisting of volcanic rocks (basaltic lava) is widely observed in Maharashtra. Owing to the volcanic origin of the igneous rocks, basalt and granite are the common rock formations in the Peninsular plateau. The basaltic Deccan traps are observed in the form of step-like weathered hills gradually reducing towards South. Laterite rich in iron and aluminum is found near to coastal plains. These laterites can be observed at higher elevations in the form of plateaus. The Deccan plateau is mainly composed of black cotton soil. Kerala comprises of Precambrian crystalline, acidic and ultra-basic intrusives (Archaean to Proterozoic age) of Tertiary (Mio-Pliocene) sedimentary rocks and Quaternary sediments of fluvial and marine origin. Both the crystalline and the Tertiary sediments have been extensively lateritised (GSI, 2005).

The geomorphological units observed in the study region are low land (coastal tracts), Midland (rolling hills), upland and flood plain of major rivers with higher vegetative cover. The western coastal stretch is alongside the Arabian Sea on the west and the Western Ghats (upland) on the east making its topography vary from plain on the

coastal side to a hilly terrain towards its east. Karnataka alone has a coastal stretch of 300km.
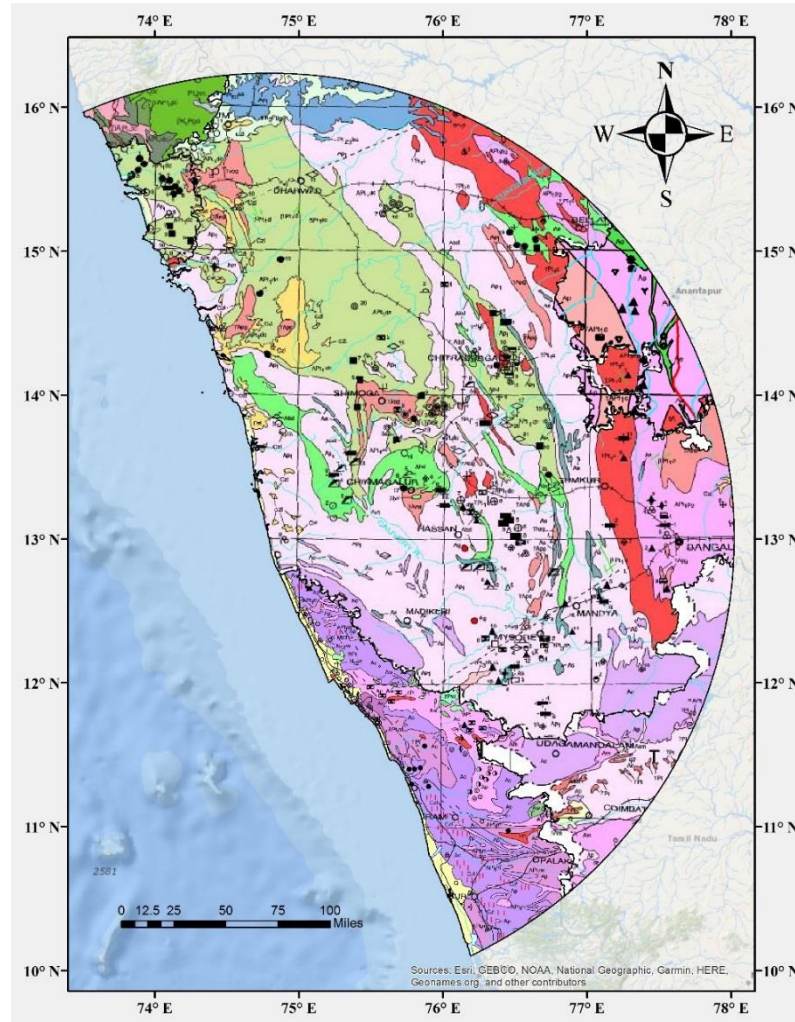
Symbol	Description	Symbol	Description	Symbol	Description
Czl	Laterite	Ap₁	Peninsular Gneiss 1	γPt₃ch	Potash rich granite
βK₃Pgd	Deccan Trap	γPt₁C	Alkali Granite	γApg	Granitoid and Gneiss
Apt₁M	Composite gneisses and schist	Ac	Charnockite Group	Apt₁dc	Chitradurga Group
Av	Quartz-mica schist and quartzite conglomerate	Ap	Peninsular Gneissic Complex (Older phase)	Ak	Khondalite Group
W	Warkalli Formation, Guillen Formation	βApt₁dc	Chitradurga Group (Metabasalt)	Q	Fluvial / coastal sediments and pebble beds.
γPt	Basic and acid intrusive: Granite and Granophyre	Pt₂₃ka	Dolomite, Limestone, Shale, breccia, and sandstone	Aw	Wayanad Schist Complex
βK₃Pg₂d	Basalt with intrappeans	Abd/Ae	Bababudan Group/ Eastern green stone	As	High-grade schists with metaultramafites.

Figure 3.2 Geological formations observed in the study area (after GSI,2006)

Midlands comprises of dense forests and rivers favorable for intensive cultivation of cash crops. Granitic outcrops and boulder-strewn hills are observed in the cratonic parts of the Peninsula. Deep lateritic weathering profiles are common in the northern part of Goa while the southern part presents a rugged topography with hills ranging in altitude up to 60 m, especially near the coast. The present coastal line emerged during the late Neogene and presumably before the onset of Pleistocene glaciation (Sriram and Prasad, 1979). The overall terrain is undulated with a generous number of perennial and non-perennial rivers.

3.3   Methodology

The causes for the structural damage during an earthquake can be classified into three categories namely, seismological, geotechnical, and structural. In the seismological category, the sources capable of causing ground shaking and the propagation path characteristics are addressed. The seismic wave originated at a depth undergoes modification as it passes through different layers of soil deposits to the surface. This modification can be amplification or attenuation in the amplitude of the seismic wave depending on the dynamic characteristics of the soil medium and is referred to as local site effect. The geometric configuration, natural period and load deformation capability of a building determines its earthquake resistance. The present study addresses the seismological aspect by performing Probabilistic Seismic Hazard Analysis (PSHA) and geotechnical aspect though topography and Site Response Analysis (SRA).

The overall methodology implemented in the study has been illustrated in the form of a flowchart in Figure3.3. PSHA combines the inputs from the seismic source model and ground motion model to estimate ground motion parameters for a reference site condition. Usually, the reference site condition is slightly idealistic and differ from the actual local soil condition achieved from in-situ tests. The estimated ground motion parameters need to be adjusted from the reference (host) site conditions to local (target) site condition. The adjusted ground motion parameters are used to scale the ground motions selected based on de-aggregation of the already computed seismic hazard. The scaled ground motions are used for performing SRA. The geological data and geotechnical data are combined to estimate the V_S profile and model the dynamic

characteristics of the soil deposit. The ground motion propagation through the modeled soil profile is simulated to obtain the local site response.

INPUT

- Local Geology
- Geomorphology
- Seismology
- Seismotectonics

Seismic Source Model

Ground motion model

SEISMIC HAZARD ANALYSIS

Host-to-target adjustment

Selection and scaling of hazard consistent ground motions

- Geological data
- Geotechnical data of North Kerala

Soil modelling

SITE RESPONSE ANALYSIS

Integration of local site response into seismic hazard analysis

Site characterization using topographic slope

OUTPUT

1. Maximum credible earthquake
2. Uniform hazard spectrum
3. Hazard maps at reference site conditions
4. De-aggregation (combination of M, R, ε)

1. Amplification spectrum
2. Surface response spectrum
3. Shear stress and strain characteristics
4. Amplification models as a function of input bedrock motion
5. Variation of input acceleration along the depth of the soil column
6. Site natural period

1. Hazard maps for North Kerala
2. Site – specific uniform hazard spectrum

1. Surface level seismic hazard maps for the whole study region
2. Uniform hazard spectrum

Figure 3.3 Flowchart of the methodology adopted in the study

The outcome of SRA in the form of spectral amplification is applied to PSHA to obtain hazard estimates relevant to site-specific conditions. Due to higher topographic relief in certain parts of the study region, in-situ tests to determine geotechnical characteristics of the local soil suffers from inaccessibility. Additionally, in-situ test for the entire study region is tedious and uneconomical. Hence, the topography determined from the digital elevation model (DEM) is used as an indirect measure of V_S and further integrated with the PSHA to obtain region-specific hazard estimates.

3.3.1   Probabilistic Seismic Hazard Analysis

Probabilistic seismic hazard analysis (PSHA) is a multidisciplinary approach integrating seismicity, tectonics, path characteristics, and local site effects to estimate ground motion parameters. There are uncertainties involved in the location, size, and rate of occurrence of earthquakes. PSHA provides a framework in which these uncertainties can be identified, quantified, and combined in a rational manner to give a complete picture of the seismic hazard (Kramer, 1996). The outcome of PSHA specifies the probability of exceedance of a specified intensity level in a given time frame for a chosen site.

The process of hazard estimation demands inputs from observations of seismic activity, regional tectonic features, local site characteristics, and regionally applicable GMPEs. The local seismicity and regional tectonics aids in the formulation of seismic source models and estimation of seismicity parameters. The seismic source can be modeled as a point, line, area or grid sources. In the case of SCR such as the present study area, the seismic activity cannot be definitively attributed to a specific tectonic feature. In other words, diffused seismicity is modeled using area or grid source. In the present study, area sources were adopted for modeling the observed seismicity. Delineation of the area seismic source zones has been explained in detail in Chapter 4. Characterization of seismic source involves consideration of spatial and temporal variability of seismicity within the geometrical bounds of the source. The seismicity parameters are estimated for each of the modeled seismic sources using Gutenberg – Richter (G-R) recurrence law. The temporal behavior of the seismic sources is characterized by a Poissonian model. The basic assumption of a Poissonian model is that each earthquake event is independent of the other or the occurrence of each event is purely random. The

Poissonian model evaluates the probability of a number of occurrences of a given event in a specific time frame. The probability of an event following Poisson process occurring 'N' number of times is represented as

$$P\ (N = n) = \frac{\mu^{n} * e^{-\mu}}{n!} \tag{3.1}$$

The term 'μ' represents the average number of occurrences of an event in a given time interval. The time between two consecutive occurrences of an event can be exponentially represented with the recurrence rate 'λ' in a period of interest 't'.

Hence, $$\mu = \lambda * t \tag{3.2}$$

$$P\ (N = n) = \frac{(\lambda t)^{n} * e^{-\mu}}{n!} \tag{3.3}$$

The hazard values are estimated by combining the Poissonian model with the G-R recurrence law. The probability of exceedance of a given event occurring more than once in a given period of 't' years is given as

$$P(N \geq 1) = 1 - e^{\lambda_m t} \tag{3.4}$$

The hazard values are the probability of exceedance of the ground motion parameter exceeding a specified intensity level in a given time frame. The ground motion parameter resulting from an earthquake event of magnitude 'M' for a site located at a distance 'R' from the source is estimated using GMPEs. GMPEs combine source, path, and site characteristics and provide a wide range of results resulting from various combinations of M and R. The hazard is presented as the probability of a ground motion parameter 'Y' exceeding a particular value 'y*' using total probability theorem.

$$P(Y > y^*) = \iint P[Y > y^*|M, R] f_M(m) f_R(r) dm\ dr \tag{3.5}$$

The term $\iint P[Y > y^*|M, R]$ is obtained from GMPE whereas $f_M(m) f_R(r)$ are the probability density functions of M and R respectively. The probabilistic approach used in estimating the seismic hazard needs to accommodate the uncertainty in each of the input parameters. The epistemic uncertainty involved in the estimation of G-R parameters and choice of GMPE is addressed using a logic tree. The aleatory uncertainties are accommodated by assigning a reasonable standard error in the estimation.

The procedure for performing PSHA for a given site can be prescribed in four steps (Reiter, 1991) as summarised below.

Step 1: Identification of the potential seismic sources contributing to the hazard at a given site. These sources can be point sources, linear/fault sources, and areal sources.

Step 2: Characterization of seismicity of each individual seismic source using Gutenberg – Richter recurrence relation. The recurrence rate of an earthquake of a certain magnitude is obtained for all the identified seismic sources.

Step 3: Estimation of ground motion parameters for an earthquake event of any given size occurring at any given distance using ground motion prediction models.

Step 4: Unifying the source and ground motion models to obtain the probability of exceedance of a certain intensity level in a given time frame.

3.3.2   De-aggregation of Seismic Hazard

De-aggregation of the computed seismic hazard is performed to identify critical earthquake scenarios in terms of Magnitude (M), Distance (R) and Epsilon (ε) for a chosen site of interest. De-aggregation varies with the period of interest (T = 0.01s, 0.5s, 1s, 2s, etc.), hazard level (probability of exceedance), GMPE used and location of the chosen site. The de-aggregation is expressed by dividing the entire range of M and R into various bins and the contribution of each combination of M-R is calculated. The M-R combination showing the highest contribution to hazard is identified as parameters for a 'design earthquake'.

The ground motion parameter (PGA, PSA or S_a) for a site from a UHS of a given probability of exceedance and period of interest is known as target ground motion (SA_0). The same ground motion parameters obtained for a specific combination of M and R from a GMPE is known as predicted ground motion (SA). The term 'ε' refers to the number of standard deviations by which the target SA_0 differs from predicted SA.

$$\varepsilon = \frac{\ln SA_0(T) - \ln SA(T)}{\sigma_{lnSA}}$$
(3.6)

Usually, the target and the predicted spectral acceleration are expressed as

$$ln(SA_0) = ln(SA) + E$$
(3.7)

where $E = \varepsilon * \sigma_{lnSa}$ = error term

In the error term, 'ε' has been isolated to make it independent of M and R. Hence, M, R and 'ε' are the three independent variables used in defining design earthquakes.

The following procedure is followed in de-aggregation for a site using CRISIS 2015

- For a chosen period of interest and probability of exceedance, the target intensity measure (SA_0) is obtained from the program.

- The mean (weighted average, $\overline{M}$ and $\overline{R}$) and modal (most likely event, M^* and R^*) values of M and R are calculated.

- The further procedure can be carried out either using $\overline{M} - \overline{R}$ or $M^* - R^*$. Using a specific value of M and R the predicted SA is computed from a chosen GMPE. Additionally, the standard deviation in predicting SA is taken into account.

- The computed values from the earlier steps are substituted in equation 3.1 to calculate ε.

- Finally, the calculated value of ε is used to prepare de-aggregation charts.

3.3.3 Host to Target Adjustment (HTTA)

The input ground motions for site response analysis are usually scaled to match the UHS obtained from PSHA. These input motions need to be consistent with the soil conditions at the base of the soil profile. However, in a few cases, the reference site condition for which the UHS has been derived from PSHA varies significantly from that at the base of the soil profile. Hence, the target spectrum undergoes host to target adjustment (HTTA), wherein the UHS is modified to represent the local site condition. Further, the adjusted UHS is used for selection and scaling of ground motion records as input for site response analysis.

The HTTA is usually performed using $V_{S(30)}$ and κ_0 (site-specific attenuation parameter) estimating large high-frequency motion on hard rock compared to standard rock. In the absence of site-specific values of κ_0, suitable $V_{S(30)}$ - κ_0 correlation can be used. However, recent studies have highlighted that these correlations are not robust (Ktenidou and Abrahamson, 2016) and the measurement of κ may be biased by site amplification resulting in site effects accounted twice (Perron et al, 2017). Further, it was found that this methodology is associated with a high level of uncertainty as explained by Bard et al (2018). The absence of field recordings for the study area and

the demerits associated with the existing HTTA procedures led to the use of a simpler and straightforward approach. It is a common understanding that the amplification phenomena is primarily controlled by the velocity contrast between the rock and soil. Using this approach, recently a GMPE was proposed Laurendeau et al (2013) (abbreviated as LA13), using surface and in-depth recordings of Japan, wherein the site term relied on the V_s alone. This methodology has an advantage as the site response in itself was recorded and not simulated. The empirically derived amplification ratio is given as

$$HTTA\ factor = \frac{Soft\ rock\ (760\ ms^{-1})}{Hard\ rock\ (1500\ ms^{-1})}(T) = \exp\left(C_1(T) * \ln\left(\frac{760}{1500}\right)\right) \qquad (3.8)$$

The coefficient C_1 is estimated from the actual recordings for each spectral period T. It seems questionable about the applicability of amplification factors developed elsewhere for regional conditions. However, most of the seismic hazard studies use nonlinear amplification function developed using California and other active region data (Choi and Stewart, 2005). At least the presently used amplification factor was derived based on actual recordings without any prior assumption about unmeasured parameters such as κ_0. The UHS is multiplied with the HTTA factors to obtain the target spectrum consistent with the site conditions at the base of the soil profile.

3.3.4 Seismic Site Response Analysis

The local site effects are captured by the dynamic simulation of wave propagation through a series of soil layers (with distinct geotechnical characteristics) laid parallel to each other as shown in Figure3.4. This technique is referred to as site/ground response analysis (SRA) and various approaches are available to perform the analysis. The ground response captures impedance, soil nonlinearity and resonance effects of the sediment layers. The site response can be performed in 1D, 2D or 3D, considering linear, equivalent linear or nonlinear soil characteristics using total or effective stress principle. The present study considers the 1- D shear wave propagation to model soil nonlinearity by an equivalent linear (EQL) approach in the frequency domain using SHAKE2000. The effective stress principle accommodating the effect of pore water pressure in the calculation of ground response has been employed. Ground response analysis in one-dimension refers to the response of soil layers to vertically incident SH waves from the underlying rock formation, which was conducted using the program

SHAKE2000 (Ordóñez, 2003). SHAKE2000 assumes a model consisting of horizontally extended, homogenous and isotropic soil layers above the half-space and relatively flat underlying bedrock interface.
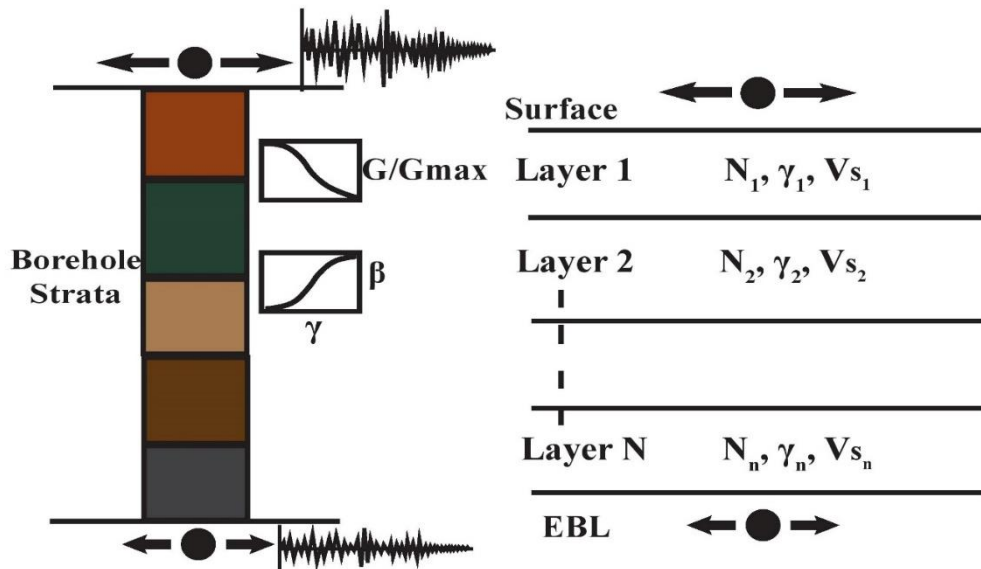
Figure 3.4 Illustration of seismic site response analysis

Each soil layer is characterized by its thickness (D, m), shear wave velocity (V_S, ms^{-1}), unit weight (ρ, kNm^{-3}), damping (η, %), maximum shear stress (τ, kNm^{-2}), and maximum shear strain (γ, %). The model assumes half-space as the rock formation underlying a soil deposit, and the half-space lies at the depth of bedrock. Thus, the transfer function between the half-space and the free surface is convolved with the input motion defined at the bedrock to compute the motion at the free surface.

The site response analysis requires input parameters representing the soil dynamic characteristics in the form of modulus reduction (G/G_{max} vs γ) and damping (η vs γ) curves. The V_S and unit weight (ρ) of each layer constituting the soil column are considered in estimating the shear modulus G_{max}.

$$G_{max} = \rho * V_s^2 \tag{3.9}$$

The equivalent linear approach estimates the modulus reduction (M-R) curve for each soil layer by combining the computed G_{max} and the backbone curves for each distinct subsurface layer. The EQL method uses an iterative procedure to compute strain

compatible secant moduli (G) and damping (D). The iteration converges when the difference in the computed parameters in two successive iterations is less than 5%. However, these parameters are time-invariant and are assigned to each soil layer. The site response analysis determines the natural period of the site, soil amplification, and shape of the response spectrum at the surface. These outcomes are useful in characterizing the ground motion at a given site and evaluating its seismic hazard.

3.3.5   Integration of site response analysis into PSHA

The local site amplification captured using site response analysis is incorporated in PSHA to obtain site-specific hazard estimates. Deterministic and probabilistic approaches are available for integrating the site response analysis with PSHA. In the present study, a probabilistic approach has been adopted by modifying the existing GMPE to accommodate local site effects.

The local site effects on the transmitted ground motion have been captured in the form of a nonlinear function wherein amplification factor (AF(f)) is expressed as a function of input rock motion (S_a^r) for different periods.

$$\ln AF(f) = a + b * \ln(S_a^r(f) + c) + \varepsilon_{\ln AF(f)} * \sigma_{\ln AF(f)} \tag{3.10}$$

The coefficients a, b, and c are obtained from the regression between the amplification factor (AF) and adjusted rock spectral acceleration (S_a^r) in logarithmic space. The term $\sigma_{\ln AF(f)}$ represents the standard deviation in the estimated AF values from nonlinear regression and $\varepsilon_{\ln AF(f)}$ is the standard normal variable. The procedure has been repeated for different spectral periods such as T=0.01s (PGA), 0.2s, 0.8s, 1s, 1.5s, and 3s and for different site categories such as 'sand', 'clay' and 'all soil'.

In order to obtain hazard consistent amplification factor, the amplification ratio $(AF'(f))$ must be computed between the ground motion parameter at the surface and the reference site condition for which hazard was computed.

$$\ln AF'(f) = \ln AF(f) + \bar{Y} \tag{3.11}$$

$\bar{Y}$ represents the median amplification between the reference site condition and the base of the soil profile computed from an ergodic site amplification model (in the present

case, it is LA13 site amplification model). Accordingly, the input motion at the base of the soil profile is modified as

$$\ln S_a^{r'} = \ln S_a^r - \bar{Y} \tag{3.12}$$

The developed nonlinear amplification model was integrated with the existing rock GMPE, hence, transforming it into a site-specific GMPE. A closed form equation was proposed for transforming the GMPE (Bazzuro and Cornel, 2004a).

$$ln\overline{S_a^s(f)} = \ln \overline{S_a^{r'}(f)} + \ln AF'(f) \tag{3.13}$$

The terms $\overline{S_a^{r'}(f)}$ and $\overline{S_a^s(f)}$ represents median reference rock and surface spectral acceleration respectively. One of the advantages of this transformation is that the variability in the resulting surface hazard can be captured. The standard deviation term for the surface hazard considers the variability in the rock hazard as well as site amplification (Goulet et al, 2007).

$$\sigma_{\ln S_a^s(f)} = \sqrt{\left(\frac{b*S_a^r(f)}{C+S_a^r(f)} + 1\right)^2 * \sigma_{\ln S_a^r(f)}^2 + \sigma_{\ln AF(f)}^2} \tag{3.14}$$

The adopted methodology offers an advantage of transforming a generic GMPE by performing site response analysis with lesser ground motions as compared to that required to develop a site-specific GMPE.

3.3.6 Geotechnical site characterization using the topographic slope

Shear wave velocity in the top 30m ($V_{s(30)}$) is the most widely chosen parameter for assessing the dynamic characteristics of the soil. Various in-situ methods are available to determine $V_{s(30)}$ profile but may not always be feasible due to inaccessibility of the site or lack of favorable conditions for testing. In such a scenario, it is desirable to adopt a methodology applicable to any region ruling out the major drawback of in-situ testing methods. A method using topographic slope as a proxy for seismic soil conditions was applied in the study. The freely available elevation data at a uniform sampling for the entire globe is used. The surficial geology contributes to the amplification of ground shaking. In other words, the topographic variations are an indicator of near-surface geomorphology and lithology to the first order, with steep mountains indicating rock, nearly flat basins indicating soil and a transition between the end members as the

intermediate slope. This is based on the fact that more competent material (high velocity) are more likely to maintain steep slopes whereas deep basin sediments are deposited primarily in environments with very low gradients.

In the study, the digital elevation model (DEM) corresponding to a resolution of the 1arc minute with a combination of topography and bathymetry is considered for generating a slope map. The data is obtained from the ETOPO1 global relief model developed by the National Oceanic and Atmospheric Administration (NOAA)(Amante & Eakins, 2009). The data is resampled to 30 arc second before generating the slope values. The slope value at the center of each grid of size approximately 1km x 1km was obtained using ArcGIS v 10.1(ESRI, 2010) which was further used for seismic site characterization. These slope values are correlated to $V_{s\,(30)}$ measurements (Wald and Allen, 2007) and $V_{s\,(30)}$ map is generated for the study area.

The surface level ground motion is visualized as bedrock motion modified by the soil layers and the site coefficient necessary for this estimation was computed from the equations (3.10) and (3.11), adapted from Raghukanth and Iyengar (2007).

$$\ln F_s = a_1 y_{br} + a_2 + ln\delta_s \tag{3.15}$$

$$y_s = y_{br} * F_s \tag{3.16}$$

The site coefficient F_s is estimated for each category (based on $V_{S\,(30)}$) of soil sites in the study area using the regression coefficients a_1 and a_2 with an error δ_s. The regression coefficients are a function of site class as well as the period at which the ground motion parameter is being estimated. This approach provides first-order estimates of the site-specific hazard values.

3.4   Concluding Remarks

The geographical extent of the study area and its associated geology and geomorphology has been detailed in this chapter. The overall methodology adopted in the study has been illustrated using a flowchart. The methodology for performing probabilistic seismic hazard analysis, de-aggregation, site response analysis, and geotechnical site characterization has been explained. The step by step outcome of the procedure has been explained in the subsequent chapters.

CHAPTER 4

PROBABILISTIC SEISMIC HAZARD ANALYSIS

4.1 Introduction

The evaluation of the intensity of ground shaking that can be expected at a specific location involves a considerable amount of uncertainty in location, size, recurrence rate, and attenuation characteristics. Probabilistic seismic hazard analysis (PSHA) aims to quantify these uncertainties and presents the exceedance probability of a certain intensity measure (PGA, PSA, S_a at 5% damping) in a given time frame. The classical Cornell – McGuire approach is used to estimate the hazard level for various return periods by exploring all the possible combinations of magnitude and distances of seismic activity.

Seismic source modeling is the preliminary step of PSHA. The information on local seismicity observed during past few decades helps in understanding the seismic potential and estimating the seismicity parameters. The data on macroseismic observations are limited for an intraplate region especially Peninsular India (PI). Hence, the earthquake data has been collected from various literature and instrumental recordings from global and local sources. The compiled earthquake catalog is further processed and the step by step procedure has been explained in the subsequent sections. The tectonic features such as faults and shear zones and related seismological parameters aid in identifying and mapping seismic sources for the study region.

Ground motion modeling is one of the primary and crucial input parameters in PSHA. GMPEs represents the combination of the source, path, and site characteristics. The mapped seismic sources are combined with the ground motion prediction models to produce a rational estimate of the regional seismic hazard. The seismic hazard of a region is presented in the form of the hazard curve and uniform hazard spectrum (UHS). The aleatory and epistemic uncertainty involved in the formulation of seismic source and ground motion modeling has been explained. Additionally, the sensitivity of the input parameters to different procedures has been addressed. De-aggregation of the computed seismic hazard has been performed to identify the compelling earthquake scenarios of a chosen site of interest. The outcome of de-aggregation aided the selection

of ground motion records whereas the uniform hazard spectra obtained from PSHA is used in scaling the selected ground motion records.

4.2   Regional Tectonics

Southern India consists of three major tectonic domains namely, Dharwar Craton, Eastern Ghat Mobile belt and Southern Granulite terrain. The Dharwar craton is characterized by the Dharwar Schist belt, Kolar Schist belt, and N-S trending Closepet granulite. The collision of the Indian plate with the Eurasian plate lead to subsidence of a portion of Western India, which is submerged in the Arabian Sea. The remaining portion is the present day West Coast. Due to this intercontinental collision PI tilted sloping towards South East causing rapid upliftment on the west coast which is the Western Ghats. Many researchers have asserted Western Continental Margin to be a trailing passive margin and the part of the West Coast stretching along Karnataka to be transitional in nature. The trailing margin has led to the formation of a number of horsts, grabens and faults developed inshore and offshore areas (Sukhtankar et al, 1993).

In order to perform PSHA, a study area within a radius of 350km with Surathkal (13.0108° N, 74.7943° E) as the center has been chosen. The part of the region considered for the study is grouped under seismic zone III and the rest in seismic zone II as per IS 1893 (2016). The earthquake events are mostly shallowly focussed and concentrated along the coastal stretch and few other parts of the study area. The seismic activity observed in the study area is attributed to the neotectonic movements The earthquakes witnessed in the study region are largely due to induced compression resulting from the continuous seafloor spreading.

Mapping of geological features such as faults, lineaments, fractures and shear zones aid in understanding the tectonics and seismicity associated with the region. The geological survey of India has studied, identified and mapped the geological features responsible for tectonic activity in India and its surrounding region. The same has been published in the form of a seismotectonic atlas (SEISAT) (Das et al, 2000). This served as a guide for preparing the fault map for the study region. The faults and lineaments are georeferenced and digitized from SEISAT 32, 33 and 38 on the ArcGIS (ESRI, 2011) mapping tool platform as shown in Figure 4.1.

48

It is very clear from Figure 4.1 that the density of lineaments is quite high and numerous lineaments cross each other. There are two trends in the lineaments, one set of lineaments are running parallel to the coast (NNW-SSE) while the other set is transverse to the West coast. A total of five active shear zones, 111 minor lineaments, 10 major lineaments, 15 gravity faults, and around 40 other faults were mapped. Lineaments of length varying from 20km to 475km are observed.
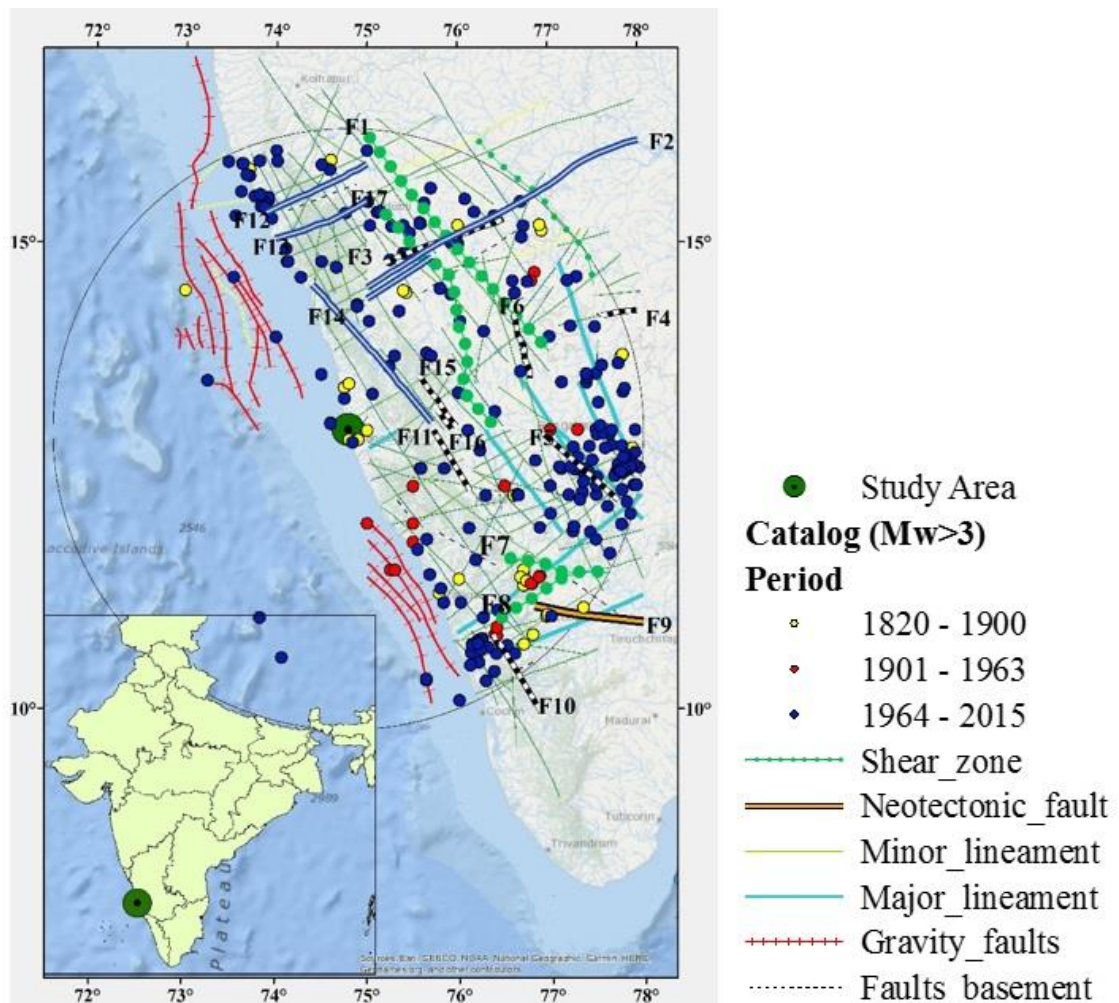
Figure 4.1 Seismotectonic Map depicting the epicentral location of the historic, Pre – Instrumental and Instrumental Earthquakes (Mw > 3) in the study region

Chitradurga Boundary shear (CBS)(F1) of length 345km divides the Dharwar craton into Eastern and Western blocks. A majority of the low to moderate earthquakes and a few major earthquakes can be expected along the shear zones F1 and F17 (length 234km) trending in the NNW-SSE direction. The density and intersection of major lineaments are high over closepet granite and Dharwar group.

Few seismic events reported post-1960 lie very close to Dharma – Tungabhadra fault (156km, F3), Chandragutti Kurnool Lineament (476km, F2) and Bukkapatnam Fault (45km, F4). Clusters of earthquake events in the magnitude range of 2.5 to 5.5 are observed in the vicinity of Chitradurga Boundary Fault (83km, F6) and Arkavathi fault (124km, F5) along with numerous minor lineaments. The region between the Moyar (124km, F7) and Bhavani shear (107km, F8) was observed to be more active with a record of pre-instrumental and instrumental earthquakes.

The N-S trending faults of the Dharwar craton subjected to strike-slip horizontal movements along the Moyar – Bhavani shear zone are speculated to be releasing the stresses accumulated in its interior as a consequence of the Northward movement of the drifting Indian shield (Valdiya, 1989). Studies have revealed the existence of the low-velocity layer in the entire Moyar-Bhavani Shear zone and the region covering these shear zones are interpreted as a collision zone (Reddy and Rao, 2000).

Earthquakes from the instrumental catalog of lower magnitude have been observed near to Sakleshpur – Bettadpura fault (85km, F11). Based on the Epicentral locations close to a fault, it can be inferred that Cauvery fault (133km, F9) and Pattikad Kollengal (101km, F10) fault are active. The coastal region is characterized by offshore faults and lineaments trending parallel to the coastal line in NNW-SSE direction. However, there exist a few lineaments running transverse to the coast such as Chapora, Bennihalla (F13) and Chandragutti Kurnool lineaments in ENE-WSW direction.

Gravimetric and Bathymetric studies on the continental margin have confirmed the extension of onshore ENE – WSW and E-W lineaments over a considerable distance into the offshore regions (Das et al, 2000). Earthquake events of lesser magnitude (Mw 2-3) were observed in the vicinity of Mandari lineament (138km, F12), Bhadra lineament (224km, F14), Chikamaglur fault (80km, F15) and Yagachi fault (29km, F16). A few historic earthquakes have their epicenters close to the west coast and clusters of events with low magnitude is observed to the west of Bhadra lineament.

4.3   Seismicity of the study area

An updated homogenous seismic catalog complete in all aspects (i.e. date and time of occurrence, epicentral location, magnitude, and focal depth) and free from artifacts and

fake events play a major role in characterizing and modeling seismic sources. The study region was considered to be stable and its potential for seismic activity was undermined in the earlier period. As a result, information is available only for significant historic earthquakes in the form of drafted notes, compiled in terms of intensity based on earthquake experiences. The prehistoric events (the 1500s) were collected from the first Indian earthquake catalog compiled by Oldham (1883). In addition, numerous researchers have studied the tectonics of diverse regions and compiled catalogs by collecting data from various reliable sources. The historic earthquake data was collected from the earlier compiled regional catalogs and more details about these sources are listed in Table 4.1.

With the advancement of instrumentation in recording earthquakes, the established seismic network has been capable of recording earthquakes of very low magnitude. The instrumental earthquake data (post-1960s) was collected from various local sources and global sources. The data collected from various sources had listed earthquakes on different Magnitude scales (Ms, m_B, M_L) and Intensity scales (MMI, MSK, EMS − 98), which demanded homogenization before further processing. A single earthquake can have more than one valid magnitude and hence, Ms and m_B had to be ruled out as a choice for a standard scale. M_L and Ms exhibit a saturation level at higher magnitudes and are not effective in representing the actual size of an earthquake. However, a scale defined based on the seismic moment, Mw seemed to overcome these disadvantages and is chosen as a standard scale in homogenizing the catalog. In this regard, the region-specific earthquake magnitude scaling relations proposed by Kolathayar and Sitharam (2012) is employed in the interconversion of magnitude scales and a plot of the relationship between different magnitude scales as well as Intensity has been presented in Figure 4.2 with the aid of events used in the study. The events reported on the intensity scale was dealt with using the outcome of the studies conducted by Muson et al (2010). The study involved a comparison of different intensity scales and derived a correlation to convert different intensity scales to the European Macroseismic scale (Grünthal, 1998). These events were converted to moment magnitude using the relation given in Equation 4.1.

$$M_W = \frac{2}{3}I_O + 1 \qquad (4.1)$$

Table 4.1 Data sources used in building a seismic source model

Category	Reference	Scale	Period range	Epistemic Uncertainty	Area
Regional and National Catalogs	Chandra (1977)	MMI, m_B	1618-1975	-	India
	Srivastav & Ramachandran(1983)	MMI	1839 - 1900	-	India
	Rao & Rao (1984)	MMI, M, M_L, m_B, and M_s	1751-1984		India
	Gangrade et al, (1987)	M_s, M_{ds}	1977-85	Uncertainty in location	India
	Bansal & Gupta(1998)	M_s, m_B, M_L, M_w	1200-1995	-	India
	K G Raj et al, (2001)	Mw	1821-2001	-	Kerala
	Raj K G & Nijagunjappa(2004)	Mw	1828 - 2001	-	Karnataka
	Rajendran et al, (2009)	M_L, MMI	1821-2008		Kerala
	Martin, S. & Szeliga, W. (2010)	EMS-98	1636 - 2009	-	India
	Iyengar et al, (2010)	M_w	1200 - 2008	-	India and surrounding area
	Rastogi B K (2016)	Ms, m_B, M_L, M_w, MMI	1341-2015	-	India
Volumes	T Oldham(1883)	Intensity	1500-1869	-	India
	John Milne (1911)	Intensity	1600 - 1900	-	Many

The resulting database consisted of certain overlapping earthquake information implying multiple entries of the same event. In the preliminary elimination stage, all the duplicate events were removed based on the accuracy and reliability of the source and size of the seismic network. Data reported by multiple sources are prioritized in the following order.

1. International Seismological Centre (ISC).
2. National Earthquake Information Center, United States Geological Survey (NEIC – USGS).
3. Indian Meteorological Department (IMD).
4. National Disaster Management Agency (NDMA)
5. Incorporated Research Institutions for Seismology (IRIS)
6. Geological Survey of India (GSI)
7. Amateur Science Centre (ASC)
8. Events listed by various researchers (Table 4.1).
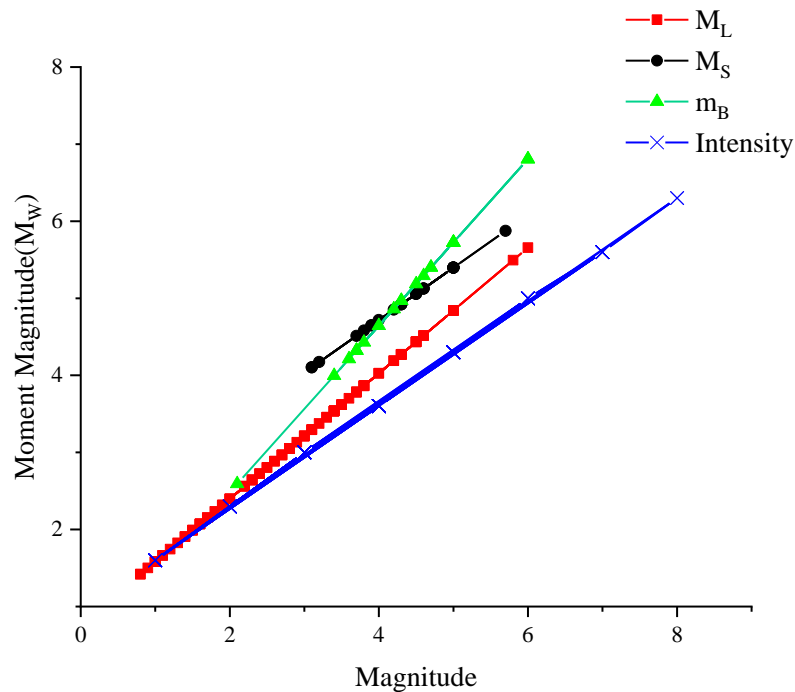
Figure 4.2 Interconversion of events reported on the various magnitude and intensity scales to Moment Magnitude (Mw) scale

In addition, events with their epicenters at a distance farther than 350km from our main location of interest i.e. Surathkal were excluded. The catalog consists of events occurred over a time span of 190 years starting from the early 1820s to late 2015 with a total of 1242 events housing a magnitude range of 0.6 to 6.3 as shown in Figure 4.3(Appendix 1). The majority of events have focal depth within 10 – 15km from the surface demonstrating the inherent property of intraplate earthquakes being shallow focused.
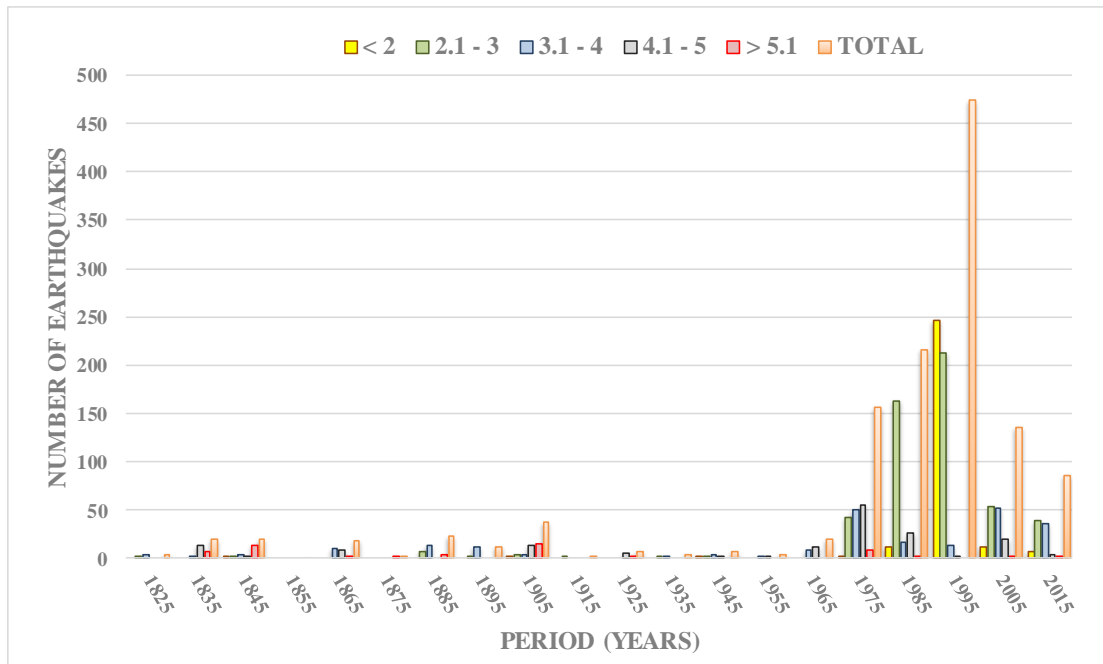
Figure 4.3 Histogram of the compiled earthquake catalog

The spatiotemporal plot of the compiled homogeneous earthquake catalog is presented in Figure 4.4. The period from 1916 to 1933 can be considered as a period of quiescence as none of the sources had recorded seismic activity for this period. In addition, a drastic increase in the number of earthquake events especially in the low magnitude range demonstrates the impact of instrumentation in earthquake monitoring and recording.
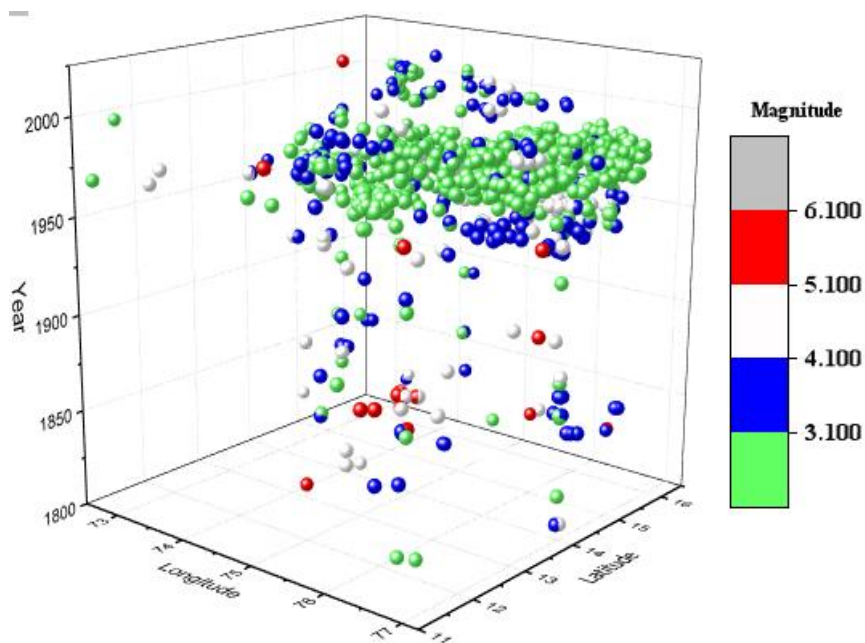
Figure 4.4 Spatio-Temporal Plot of the compiled catalog

54

4.4   Seismic Sources

With the aim of constructing a strong seismic source model, it is essential to collect all the necessary information on neotectonics, local geology, extension, and movement rates and fault plane solutions. Though a number of geological features have been identified in the study region, there is inadequate information available on the style of faulting and slip rates of each of these features. Further, the seismic activity observed in PI cannot be attributed to a particular fault or lineament. In other words, the observed seismic activity is distributed and diffused in nature, as a result, direct fault modeling cannot be adopted for the present study.

In order to bridge the gap between the potential seismotectonic features and the observed seismicity, seismically active zones are identified. Active zones are characterized by numerous earthquake events with few tectonic features such as faults and lineaments in the vicinity. These active zones are geometrically modeled as areal sources with an assumption that the seismicity is uniform within the zone. This is rather a simplification over a continuously observed seismicity but on the contrary, this method checks the overinterpretation of an earthquake catalog covering a short time window compared to the return period of larger earthquakes (Ashish et al, 2016). Additionally, area source zones accommodate the possibility of the existence of unidentified faults in a study region. The segregation of the study area into a number of potential seismogenic sources (area sources) is accomplished with the aid of seismological, geological, tectonic and geodetic information.

Kayal (2008) identified western ghats running parallel to the west coast as a separate seismic zone. Many hot springs and a system of parallel faults under the Deccan traps are believed to exist in this zone. Nath & Thingbaijam (2012) have recommended areal source zones for India, delineated on the basis of seismicity, fault patterns and similarity in fault plane solutions. Kolathayar et al, (2012) identified 104 regional seismic sources based on the pattern of seismic event distribution. The common observation made from all the available literature on seismic source delineation is that the coastal region is considered as a separate seismic zone and in other regions zones are identified based on the fault alignment and spatially distributed seismic events. The seismic zonation adopted in the study attempts to match with the previous hazard studies by considering

55

the focal mechanism observed seismicity and location of faults in the vicinity of the epicenters. The entire study area has been divided into four seismogenic source zones as shown in Figure 4.5.

- Seismic Source Zone 1 (MZ1): A total of 351 events have been reported in this zone and the excessive mining activity being carried out in Bellary and its surrounding area is suspected to be the prime reason for the microseismicity. Earthquake events of magnitude less than 3 are usually harmless to the built environment and majority of the rock blasts are within this magnitude range. Hence, the tectonic events and the possible anthropogenic events with $M_W < 3$ needs to be removed. One of the significant earthquakes witnessed in this zone is the Bellary earthquake (Mw 5.8) of 1843 felt over a radius of 300km. Further, epicenters of few moderate-sized earthquakes have drawn the attention of researchers to categorize this zone to be more active in comparison to its surroundings (Gupta (2006), Bhatia (1999)).

- Seismic Source Zone 2 (MZ2): A total of 295 events have been reported in this zone. All the events are considered to be tectonic and these clusters of events consist of aftershocks and foreshocks that need to be carefully removed from the mainshock. The temporal and spatial variation of seismicity in this zone is found to be sporadic. Mandya, Bangalore, and Kolar have been the epicenter for many earthquakes recorded in this region and Raj and Nijagunappa (2004) recommends upgrading these areas from zone II to III in IS 1893 (2016) based on the remote sensing studies. Studies suggest a reverse/normal fault with dominant strike-slip movement rupturing at close intervals to be the main reason behind low to moderate-sized earthquakes in Bangalore. The maximum reported earthquake event is of magnitude Mw 5.6 and studies have suggested that the Killari earthquake (1993) and Sumatra Earthquake (2004) have triggered a few earthquakes of intensity IV in this zone (Sitharam and Anbazhagan, 2007). The zone encompasses one of the most densely populated areas. Consequently, even a moderate earthquake can cause a great deal of damage.

- Seismic Source Zone 3 (MZ3): A total of 329 events have been recorded in this zone. This zone has witnessed seismic events of a wide range varying from the lower magnitude of Mw 1.1 to a higher magnitude of Mw 6.3. The compiled catalog

consisting of both pre-instrumental and instrumental catalogs suggests that central midland Kerala as more seismically active in comparison to other parts. The focal mechanism solution from the 67 aftershocks of Idukki earthquake (1988) suggests strike-slip movement on an NW-SE plane implying the association with the pre-existing geological structures (Rastogi et al, 1995).

- Seismic Source Zone 4 (MZ4): A few historic earthquakes have their epicenters close to the west coast and clusters of events with low magnitude is observed to the west of Bhadra lineament, summing up to about 251 events in the region. Rao (1992) observed that a large number of micro to moderate earthquakes ranging from M2 to M5 occur close to 13°N. The occurrence of a large number of small magnitude earthquakes can be attributed to the compression the region is experiencing as a result of continuous seafloor spreading. As the West coast is transitional in character and close to the major shear zones, stress cannot accumulate and hence, releases in small amounts resulting in the micro to moderate earthquakes (Subrahmanya, 1996). Based on the macroseismic observations and the linear features in this zone, it can be concluded that the geological features are deep-seated structures active along the Western continental margin of India.

4.5   Estimation of Seismicity parameters

4.5.1   Declustering

An earthquake catalog is composed of independent events (Main shocks) and dependent events (foreshocks and aftershocks). The main shocks also known as parent earthquakes originate due to the build-up of tectonic stresses and are completely unbiased by any previous seismic activity. When the accumulated stresses are released in the form of main shocks, a change in static and dynamic stresses, seismically induced fluid flows and afterslip takes place leading to aftershocks. The separation of background earthquakes which are independent in nature from the dependent events, that are in the form of clusters is known as Declustering. It is necessary to remove these triggered earthquakes as they violate the basic assumption of Poissonian distribution which has been extensively adopted in the study. Aftershocks are identified based on their spatial-temporal proximity to the main shocks and separated by static and dynamic windowing method.
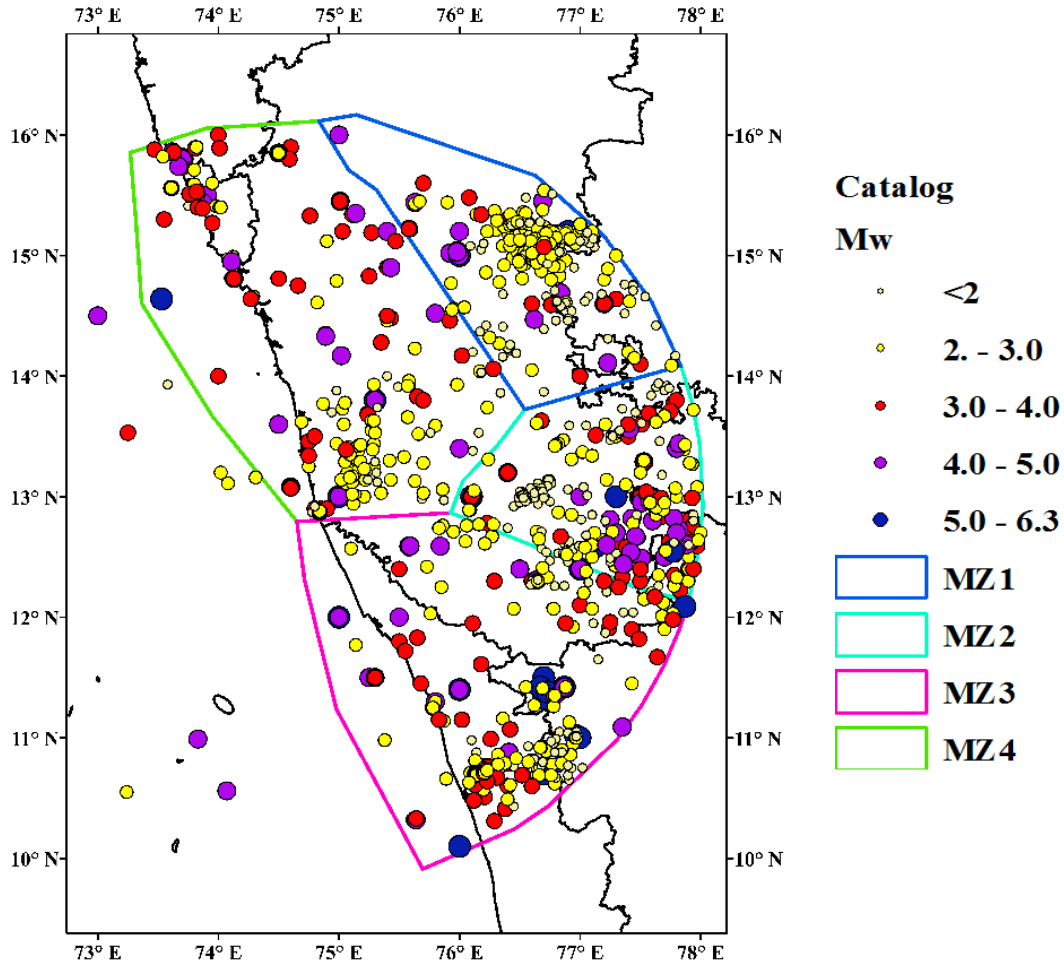
Figure 4.5 Seismic source zones along with the epicenters of the past earthquakes grouped into various divisions

The windowing technique is based on the principle that the main shock is the highest magnitude event and its associated succeeding and preceding events are identified if they occur within a specified time and distance from the main shock.

Gardener and Knopoff (1974) proposed a declustering algorithm assuming a circular spatial window. The duration of the aftershock sequence, as well as its spatial extent, has been derived as a function of the main shock in the sequence. The algorithm is given as

$$D = 10^{0.1238*M+0.983} \text{(km)} \tag{4.2}$$

$$T = \begin{cases} 10^{0.032*M+2.7389} & if\ M \geq 6.5 \\ 10^{0.5409*M-0.547} & else \end{cases} \text{(Days)} \tag{4.3}$$

The algorithm identified that the compiled catalog consisted of 60% (464) dependent events. Figure 4.6 represents the distinction between main shocks and dependent events. During declustering, dense clusters of aftershocks were observed in MZ1. MZ1 and MZ3 have witnessed events of $M_W > 6$, hence, more numbers of aftershocks can be observed in these zones. MZ2 consists of more number of earthquakes of $M_W > 4$ and hence, a swarm of earthquake activity can be observed in this zone. Further, earthquake events of $M_W > 3$ are insignificant and harmless to the built environment. Hence, the final earthquake catalog consisted of 435 main events with $M_W > 3$.
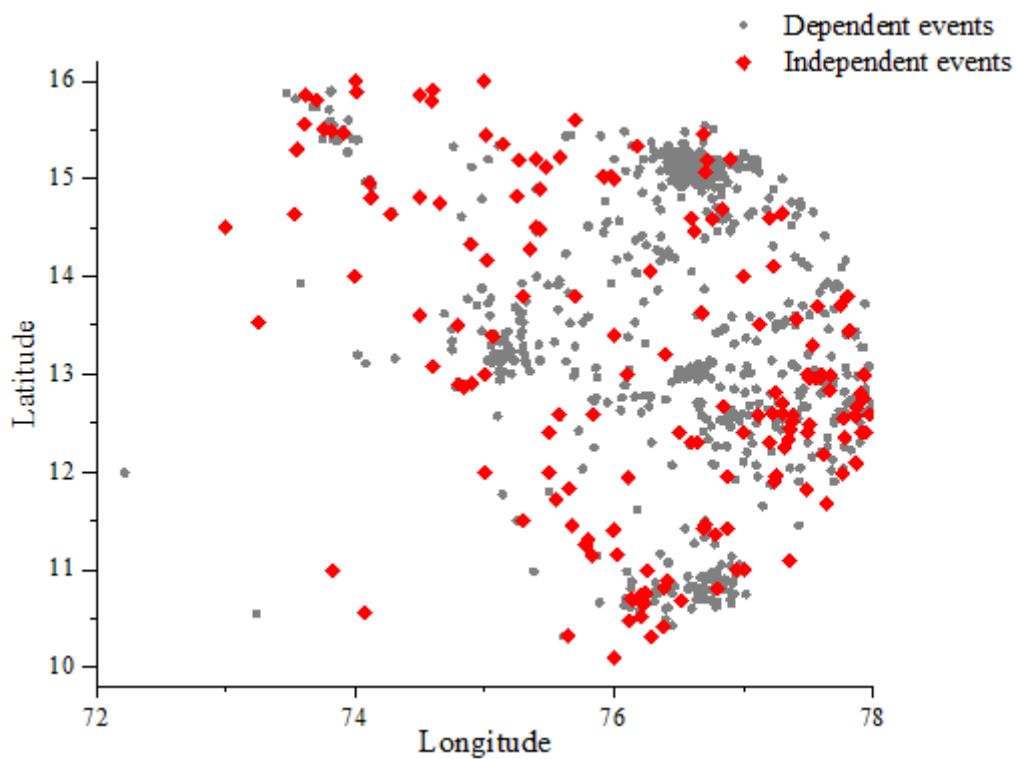
Figure 4.6 Plot showing independent events and dependent events identified from the declustering algorithm

A temporal plot of the declustered catalog consisting of events with $M_W > 3$ has been plotted in Figure 4.7. As evident from Figure 4.7, the entire catalog can be temporally divided into pre-instrumental and instrumental periods. The declustered catalog was found to be incomplete for different magnitude ranges over different periods. The records of higher magnitude events (above Mw 4.5) were found to be more consistent than that of lower magnitude events. As completeness of a catalog plays a major role in obtaining the seismicity parameters, it was essential to determine the period or

duration in which a magnitude of the certain specified range was found to be completely reported.
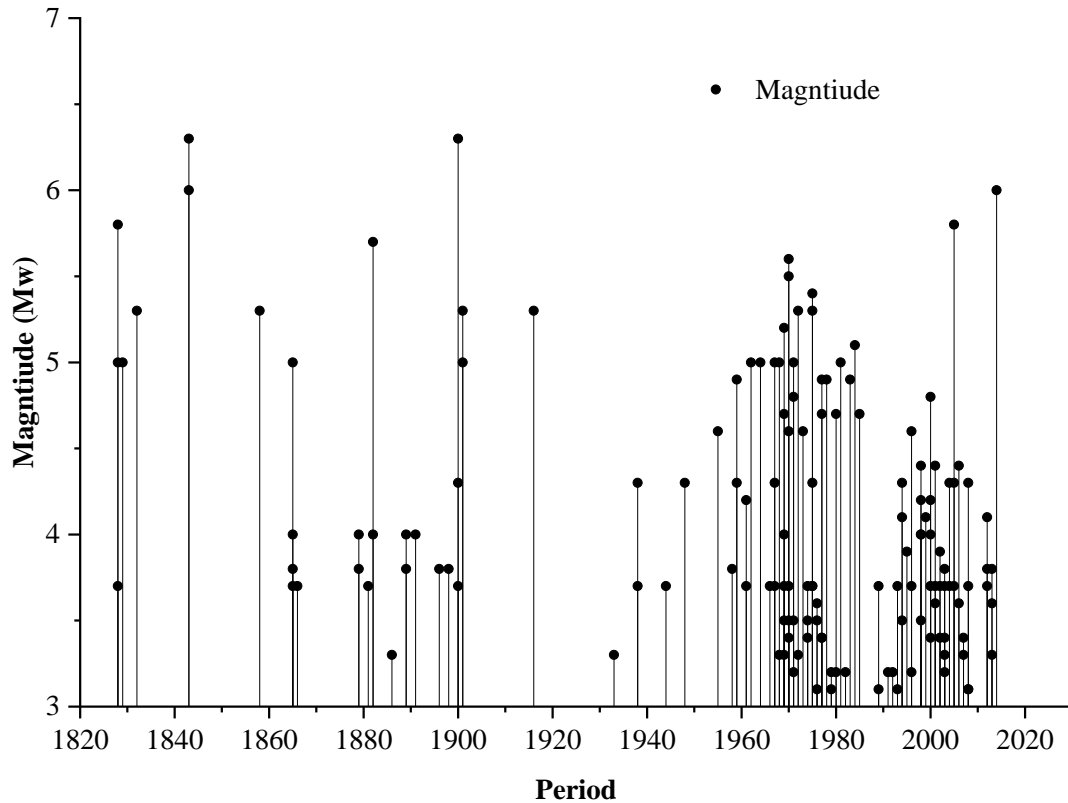
Figure 4.7 Temporal plot of the declustered earthquake catalog

4.5.2 Completeness of the compiled catalog

The completeness magnitude (Mc) is the lowest magnitude in the catalog above which all the earthquake events recorded in a space-time frame are exhaustive. It is crucial to have a factual estimation of Mc, as an estimate on the higher end might lead to scraping off of the usable data due to undersampling while on the lower end might provide erroneous analysis of the seismicity parameters due to incomplete data sets.

Magnitude of Completeness can be computed in two ways, namely,

- Catalog-based method
- Network-based method

The catalog based method is a straightforward approach where the analysis and computation are performed on the compiled catalog data whereas the network-based method is quite complex and time-consuming. The latter method is applicable only for the instrumental data which is available for the last 5 to 6 decades. Hence, the former

method is used in the study. The statistical test on the compiled catalog was performed only for those events of $M_W > 3$ with the maximum observed M_W (M_{obs}) as 6.3.

➢ Stepp's Method:

Determination of magnitude of completeness through an empirical and statistically simple method based on the stability of magnitude recurrence rate was introduced by Stepp (1972). In this method, the entire catalog is grouped into different magnitude classes similar to the previous method with an interval of $\Delta M = 0.5$ and each magnitude class is modeled as a point process. The cumulative number of events in each individual magnitude class is determined for the different time window. The cumulative annual rate of earthquakes is calculated as shown in Table 4.2 starting from magnitude 3 onwards. The threshold magnitude is taken as 3 based on the observations from the previous experiment using visual screening technique where the data below this threshold magnitude was found to be incomplete.

For a particular magnitude range, let x_1, x_2........ x_R be the number of events per unit interval, obtained from the catalog. The unbiased estimate of the mean rate per unit time interval of this sample is

$$x = \frac{1}{N}\sum_{i=1}^{n} x_i \qquad (4.4)$$

Where N = number of intervals.

And its variance is given as

$$\sigma_x^2 = \frac{x}{T} \qquad (4.5)$$

This method is based on the assumption that the occurrence of earthquakes follows a stationary Poisson's process. The standard deviation and rate of earthquake occurrences over the different period and magnitude spaces have been listed in Table 4.2. The completeness test performed on different magnitude ranges has been presented in Figure 4.8. The completeness period of magnitude classes $3.1 - 3.5$, $3.6 - 4.0$, $4.1 - 4.5$, $4.5 - 5.0$ and > 5.0 are found to be 40, 60, 70.80 and 160 years respectively.
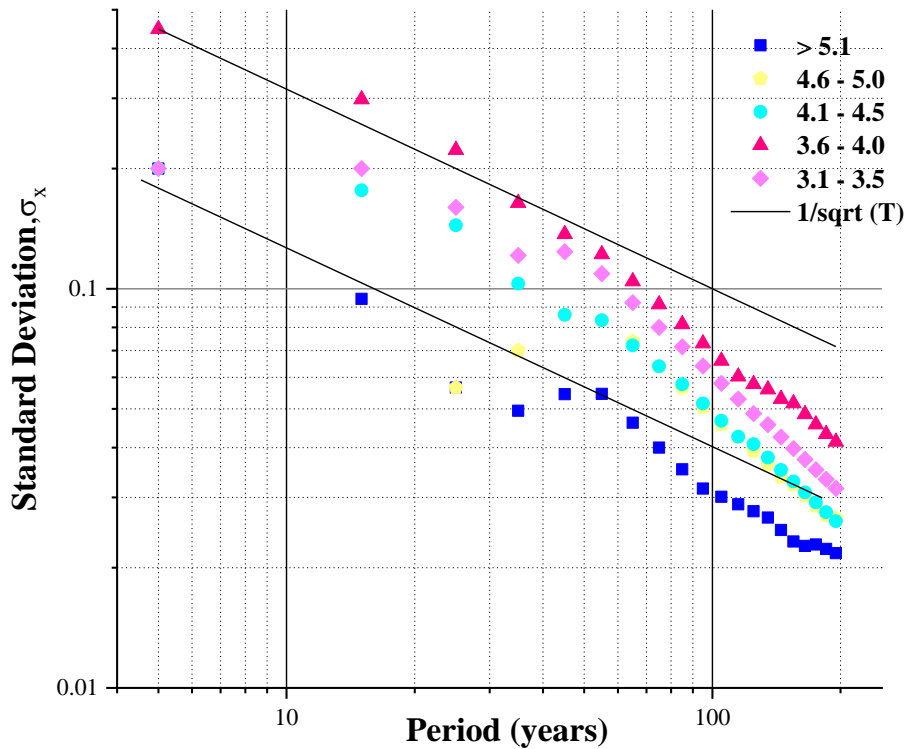
Figure 4.8 Completeness test of the declustered catalog by Stepp's method

Based on the results from the Stepp's method the entire catalog has been divided into the historical catalog and instrumental catalog. The statistical method explained earlier has been superseded by a more robust method for estimating M_C and seismicity parameters. There are various computer programs that are available such as ZMAP, Ha.3 and so on. ZMAP by Wiemer (2001) estimates M_c through various methods such as Maximum curvature technique (MAXC), Entire Magnitude Range (EMR) with an option to bootstrap the samples. The completeness test serves as a key for estimating the region dependent recurrence parameters. The rate of occurrence of earthquakes depends on the completeness of the catalog (Tinti & Mulargia, 1985) and usage of an incomplete catalog leads to an underestimation of the seismicity parameters for that particular magnitude range.

Table 4.2 Distribution of earthquakes in time and magnitude space.

Time period	Time interval (years)	3.1 - 3.5			3.6 - 4.0			4.1 - 4.5			4.6 - 5.0			> 5.1		
		N	N/T	SD	N	N/T	SD	N	N/T	SD	N	N/T	SD	N	N/T	SD
2011 -2015	5	1	0.20	0.20	5	1.00	0.45	1	0.20	0.20	0	0.00	0.00	1	0.20	0.20
2001 -2015	15	9	0.60	0.20	20	1.33	0.30	7	0.47	0.18	0	0.00	0.00	2	0.13	0.09
1991 - 2015	25	16	0.64	0.16	31	1.24	0.22	13	0.52	0.14	2	0.08	0.06	2	0.08	0.06
1981 - 2015	35	18	0.51	0.12	33	0.94	0.16	13	0.37	0.10	6	0.17	0.07	3	0.09	0.05
1971 - 2015	45	31	0.69	0.12	38	0.84	0.14	15	0.33	0.09	15	0.33	0.09	6	0.13	0.05
1961 - 2015	55	36	0.65	0.11	45	0.82	0.12	21	0.38	0.08	21	0.38	0.08	9	0.16	0.05
1951 - 2015	65	36	0.55	0.09	46	0.71	0.10	22	0.34	0.07	23	0.35	0.07	9	0.14	0.05
1941 - 2015	75	36	0.48	0.08	47	0.63	0.09	23	0.31	0.06	23	0.31	0.06	9	0.12	0.04
1931 - 2015	85	37	0.44	0.07	48	0.56	0.08	24	0.28	0.06	23	0.27	0.06	9	0.11	0.04
1921 - 2015	95	37	0.39	0.06	48	0.51	0.07	24	0.25	0.05	23	0.24	0.05	9	0.09	0.03
1911 - 2015	105	37	0.35	0.06	48	0.46	0.07	24	0.23	0.05	23	0.22	0.05	10	0.10	0.03
1901 - 2015	115	37	0.32	0.05	48	0.42	0.06	24	0.21	0.04	24	0.21	0.04	11	0.10	0.03
1891 - 2015	125	37	0.30	0.05	52	0.42	0.06	26	0.21	0.04	24	0.19	0.04	12	0.10	0.03
1881 - 2015	135	38	0.28	0.05	57	0.42	0.06	26	0.19	0.04	24	0.18	0.04	13	0.10	0.03
1871 - 2015	145	38	0.26	0.04	59	0.41	0.05	26	0.18	0.04	24	0.17	0.03	13	0.09	0.02
1861 - 2015	155	38	0.25	0.04	64	0.41	0.05	26	0.17	0.03	25	0.16	0.03	13	0.08	0.02
1851 -2015	165	38	0.23	0.04	64	0.39	0.05	26	0.16	0.03	25	0.15	0.03	14	0.08	0.02
1841 - 2015	175	38	0.22	0.04	64	0.37	0.05	26	0.15	0.03	25	0.14	0.03	16	0.09	0.02
1831 - 2015	185	38	0.21	0.03	64	0.35	0.04	26	0.14	0.03	25	0.14	0.03	17	0.09	0.02
1821 - 2015	195	38	0.19	0.03	65	0.33	0.04	26	0.13	0.03	27	0.14	0.03	18	0.09	0.02

4.5.3   Computation of frequency magnitude recurrence relationship

Seismicity parameters are one of the key elements in quantifying the seismic hazard of a region, out of which frequency magnitude recurrence relationship given by Gutenberg – Richter (G-R) (1944) is one of them.

The G-R recurrence law also known as power law is given as

$$\log \lambda_m = a - bM \tag{4.6}$$

where λ_m refers to the recurrence rate of events with magnitude $\geq M$, 'a' gives a general estimate about the seismicity associated with the study area for a period corresponding to the compiled catalog. A higher 'a' value implies higher seismicity. 'b' represents the relative likelihood of large and small earthquakes. A higher 'b' value signifies a higher number of low magnitude earthquakes and vice- versa. G – R relationship can be interpreted by taking the cumulative number of earthquake events of magnitude exceeding a certain threshold magnitude or in the form of a density law, wherein a number of earthquakes corresponding to a certain magnitude range 'm' is considered. On the other hand, incremental plot accounts for the number of events in a certain magnitude range, that can be zero in case of no available record.

The estimation of 'b' value in G –R recurrence relationship is of utmost importance as it gives a clear picture of the proportion of larger and small earthquakes. One of the easiest methods to obtain this value is by performing linear regression on the compiled database. However, linear regression on the observed earthquake data may deliver biased results due to incompleteness in the catalog and the uncertainty associated with the reported magnitudes (Kijko & Sellevol, 1989). Many researchers suggest that regression should not be performed on cumulative data, as it is dependent on the higher magnitude data contradicting the basic assumption of regression analysis that the data are independent (Naylor et al, 2010).

The most commonly accepted approach for determining the seismicity parameters is the maximum likelihood approach proposed by Aki (1965) which gives the formula to estimate the 'b' value as follows.

$$\beta = \frac{1}{\bar{m} - m_{min}} \tag{4.7}$$

where β = b ln10, $\bar{m}$ = average magnitude and m_{min} is the minimum M_C. This method can accommodate the uncertainty in the recorded magnitude as well as the incomplete data in the catalog which were the major drawbacks to perform regression analysis. In order to adopt maximum likelihood procedure for estimating the seismicity parameters, the entire catalog had to be separated into two different catalogs namely, an extreme catalog which has very few data representing historical seismicity and complete catalog representing instrumental catalog. A Matlab based computer program by name Ha.3 developed by Kijko & Smit (2012) was adopted to estimate the seismicity parameters. A plot of frequency magnitude relationship has been derived for all the identified seismic source zones (MZ1 to MZ4) as shown in Figure 4.9. The seismicity parameters estimated for each of these zones have been tabulated in Table 4.3.

Table 4.3 Seismicity parameters for the seismic source zones and the catalog

Seismic Source Zone	b - value	Recurrence rate	M_c	M_{max}
1	0.511±0.083	0.196±0.06	3.5	6.31±0.25
2	0.613±0.11	0.279±0.06	3.5	5.61±0.25
3	0.69±0.043	0.488±0.1	3.5	6.35±0.25
4	0.765±0.078	0.258±0.05	3.5	6.25±0.27

The seismicity parameters obtained from this study are compared with the studies carried out by other researchers for the same yet wider region and is presented in Table 4.4.

Table 4.4 Comparison of Seismicity Parameters with contemporary studies

Authors	b - value	M_{max}
Bhatia et al, (1999)	0.598	6.5
Jaiswal and Sinha (2006)	0.92 (± 0.052)	6.5
Iyengar et al, (2010)	0.76 (± 0.07)	6.8
Kolathayar and Sitharam (2012)	0.57	6
Ashish et al, (2016)	0.85	6.5
Present study	0.74 (± 0.08)	6.3(± 0.5)

From a statistical perspective, the higher value of 'b' implies that the region is susceptible to a larger percentage of low to moderate-sized earthquakes. However, this can also be attributed to lack of earthquake data and high uncertainty involved in the estimation. It can be observed that the estimated values are in good agreement with that of the other estimations.
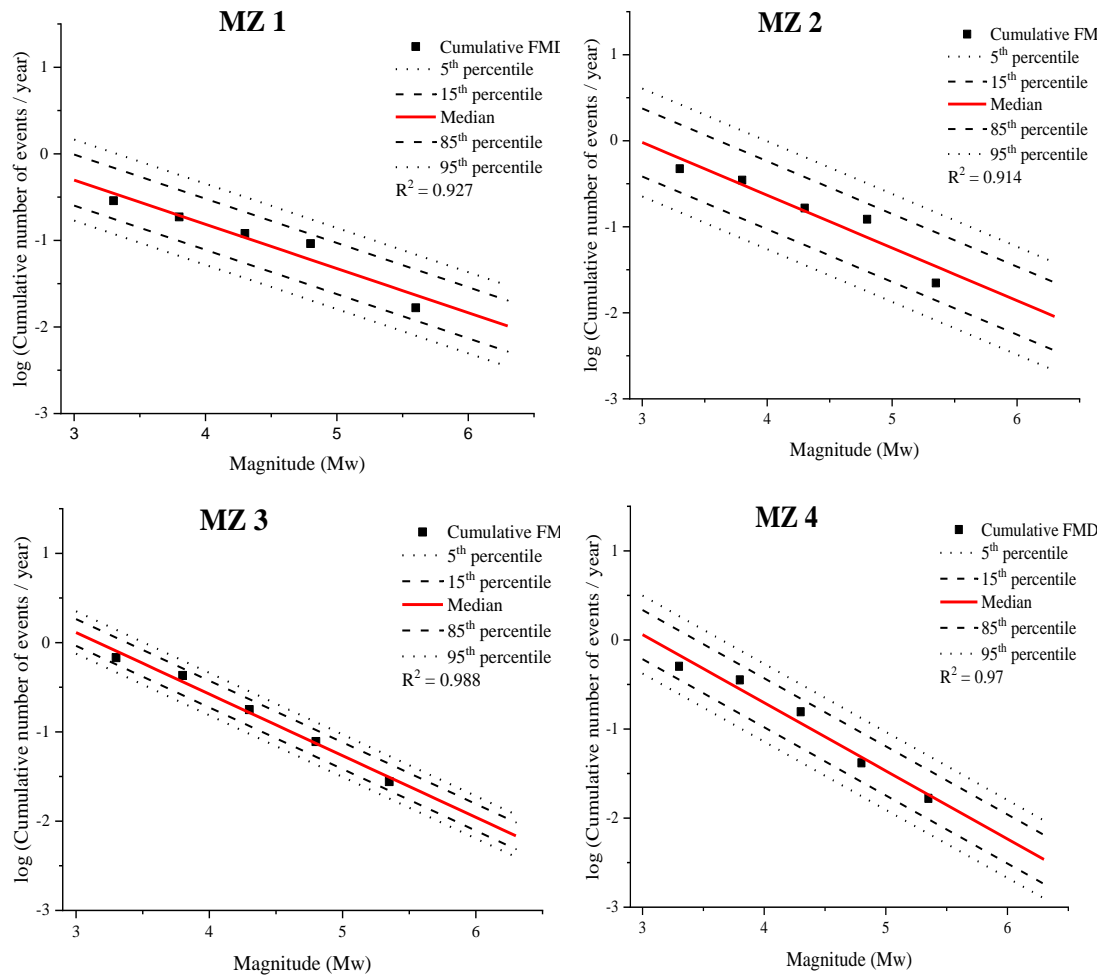
Figure 4.9 Gutenberg-Richter frequency magnitude relationship of all the delineated seismic sources

4.5.4 Uncertainty in developing Seismic Source model

The first essential step in modeling seismicity of a region is to gather all the information and form an exhaustive database related to its associated seismic activity. In order to achieve this, many kinds of literature on regional tectonics, intensity values, studies on individual earthquakes, previous catalogs, and unpublished materials were scrutinized.

The preliminary objective was to compile a regional catalog that includes the most recent events not listed in the previously published material that is free from duplications and fake events. Due to the lack of recording instruments in the earlier period, the historical part of the catalog relies on many regional and national catalogs (Table 4.1). While adopting the data, the sources were chosen in such a way that the catalog is publicly available and its sources are referenced. Priority was given to those catalogs listing events estimated from regional studies and those reported on Mw scale. The major drawback when adopting events from multiple sources is duplication. When multiple recordings of the same event are providing contradictory information, those dataset providing events values in terms of magnitude is chosen. However, the historical events are mostly reported on intensity scales and hence, requires special attention. These events need to be validated through multiple sources (such as previously compiled catalogs, studies on individual earthquakes and the seismicity studies of various regions). In the present study, only those historical events reported in many of the previously compiled catalogs and published reports related to the seismicity of PI have been considered.

There is a great deal of uncertainty involved in the location of the events, its depth, and magnitude. Gangrade et al, (1987) suggest the error in locating an earthquake to vary across India in the range of 0.01° to 0.09°. Srivastav & Ramachandran (1983) exclude the data from the published catalogs and provide a database consisting of events extracted from microfilms of Times of India, Statesman, and Hindu. Priority is given to those catalogs that account for the uncertainty in the reported magnitude. However, in the absence of uncertainty, a default value of 0.5 has been chosen for prehistoric events and 0.25 for historic events and those Mw values obtained from Intensity conversions. Majority of the historic events lack focal depth information and in those cases, a default value of 10km has been chosen. Further, there are certain events in the catalog which have not been verified by multiple sources due to lack of data. Therefore, the compiled catalog consists of Year, Month, Date, and time of occurrence of events along with the information on its location, magnitude or intensity, and focal depth. To account for the uncertainties involved in estimating the b-value, a bootstrap method with 100 bootstraps was implemented. (Chernick, 1999).

In the compiled catalog, it is observed that the completeness of events is homogeneous only for a certain time period. Catalog completeness is a function of the magnitude and substantially varies from region to region (Grünthal, G., & Wahlström, R.,2012). The entire catalog has been divided into two parts namely, Historical Catalog and Instrumental Catalog. The Instrumental Catalog has been derived from various global agencies and hence assumed to be complete. The uncertainty in these events is considered to be ±0.1. In order to accommodate the epistemic uncertainty involved in estimating the recurrence relation, a logic tree was constructed sampling into 5 branches as shown in Figure 4.10. Quantile distribution has been adopted for estimating the G-R recurrence parameters and each branch has been given suitable weights. These seismicity parameters are derived independently for each individual zones and the uncertainty in estimating Mmax has been addressed by considering Mmax(obs), Mmax(obs) + Δ and Mmax(obs) + 2Δ. The weighting factors for Mmax has been chosen based on the history of seismic activity and regional tectonics. The uncertainty (Δ) in estimating the maximum magnitude for the entire study region has been chosen as 0.5 (Iyengar et al, 2010).

The whole of the study area belongs to the same tectonic regime and the source depth is considered to be 10km and hence, the epistemic uncertainty has not been considered for these two parameters. The inadequate information on the tectonic activity in the study area necessitates the choice of area source model and the uncertainty involved in the delineation of these areal seismic sources has not been addressed in the study. The outcome of this approach accounts for various earthquake scenarios and uncertainties in estimating the seismicity patterns, completeness of events, the maximum magnitude. These results serve as an input in predicting the ground motion for various exceedance probabilities in a given time frame.
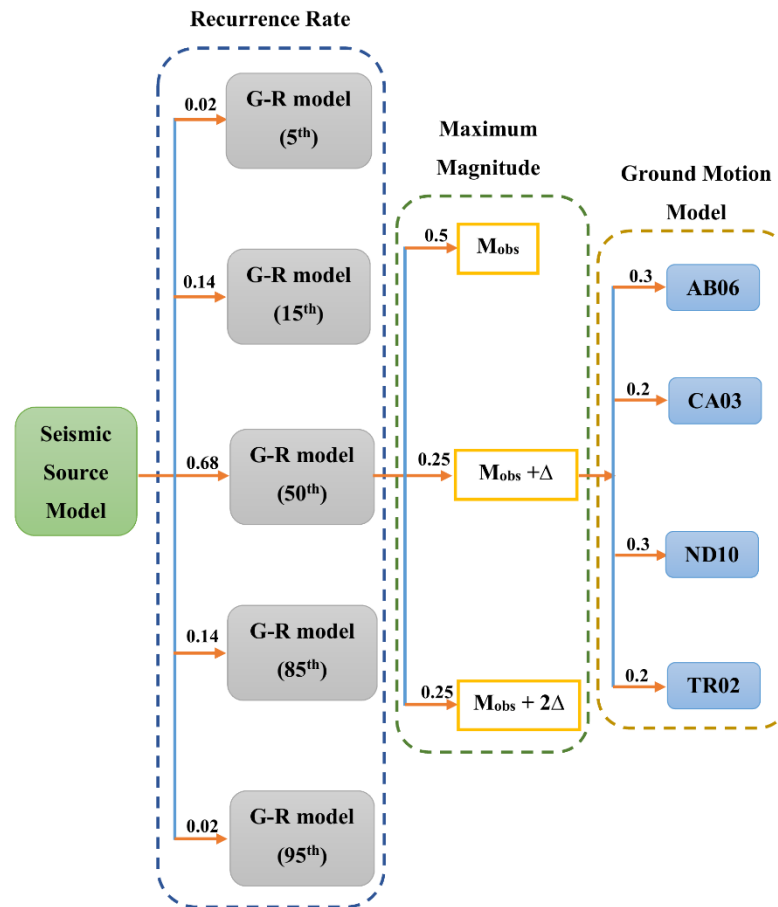
Figure 4.10 Logic tree representing the earthquake recurrence rate model, maximum magnitude, and ground motion models.

4.6 Ground motion modeling

4.6.1 Selection of ground motion prediction equations

The estimation of seismicity parameters provides an overall idea of the potential earthquake magnitudes and its location. The main focus lies in understanding the ground motion that can be expected at the site, which is predicted using Ground Motion Prediction Equations (GMPEs), also known as ground motion prediction models (GMPMs). GMPEs are developed by performing statistical regression on a large database of observed ground motion intensities. GMPEs anticipates the ground motion in terms of intensity measures (PGA, PSA, etc.) as a function of magnitude, distance, faulting mechanism, near-surface site conditions and so on. Due to the lack of strong ground motion data in India, appropriate attenuation laws developed for the regional conditions are scanty. During the investigation of aftershocks of Bhuj earthquake,

Cramer and Kumar (2007) found that the regional tectonics of Peninsular India (PI) is similar to that of Eastern North America (ENA) and the GMPEs developed for ENA are comparable with PI.

The ground motion prediction equations developed for a similar tectonic regime i.e. stable continental region has been considered for preliminary testing. The criteria for selecting GMPEs as suggested by Bommer et al, (2010) was used for the initial screening process. Table 4.5 lists the GMPEs along with their characteristics investigated in the present study. The study region is characterized by low to moderate seismicity and consequently poor in terms of strong motion data. As a result, the data-driven testing methods were not applicable to the present scenario. However, qualitative testing of the applicability of the GMPEs to the regional condition was validated by using macroseismic observations of Bhuj and Jabalpur earthquake given by Singh et al, (2003) as shown in Figure 4.11. The distance (R_{JB}) of the recorded macroseismic data ranges from 91km to 603km and it is to be noted that few of these observations are beyond the applicable distance range of various GMPEs (ND10, RI07, AK14, TR02, HH97). Usually, extrapolation is adapted to compute the ground motion parameter (PGA, PSA) at distance beyond the applicable range. However, these extrapolations may add on to the existing uncertainty in the estimated value and hence, not encouraged. The attenuation equation suggested by Toro (1997) and later modified as Toro (2002) (abbreviated as TR02) was developed for hard rock site condition characterized by an average shear velocity of 1828ms^{-1}. TR02 was found to provide a nearly exact estimation for Bhuj main shock and a reasonable prediction for Jabalpur earthquake.

The functional form of TR02 to predict the spectral acceleration (PGA or S_a) is

$$\ln(Y) = C_1 + C_2 * (M_W - 6) + C_3 * (M_w - 6)^2 - C_4 * \ln(R) - (C_5 - C_4)$$
$$* \max\left(ln\frac{R}{100}, 0\right) - C_6 * R_M + \varepsilon_e + \varepsilon_a$$

(4.8)

where $R = \sqrt{R_{JB} + C_7^2 * [\exp(-1.25 + 0.227 * M)]^2}$

C_1, C_2, C_3, C_4, C_5, C_6, and C_7 are the coefficients, ε_a aleatory uncertainty, ε_e epistemic uncertainty, and R_{JB} is Joyner Boore distance.

Raghukanth & Iyengar (2007) (abbreviated as RI07) and Iyengar et al, (2010) are the equations developed for regional data. The former provides a higher estimate while the latter predicts a rational value, as a result, Iyengar et al, (2010) (abbreviated as ND10) was chosen for the study. Further, RI07 is applicable for a shorter distance range and ND10 is the improvised version of this ground motion model. Hence, RI07 has not been considered to avoid duplication of GMPEs. ND10 was developed for Type A sites and the A type reference site has been defined as layers of a variety of rocks summing the average value of $V_{S\,(30)} > 1500 \text{ms}^{-1}$.

The functional form of ND10 to estimate ground motion parameter is given as

$$ln\left(\frac{S_a}{g}\right) = C_1 + C_2 * M + C_3 * M^2 + C_4 * R + C_5 * \ln(R + C_6 * e^{C_7 * M}) + C_8 * \log(R)$$
$$* f_o + \ln(\varepsilon)$$

(4.9)

where $f_o = \max\left(ln\left(\frac{R}{100}\right), 0\right)$. C_1, C_2, C_3, C_4, C_5, C_6, C_7, and C_8 are the coefficients, R is the hypocentral distance (km), S_a is the spectral acceleration (g) and ε is the residual. The database chosen for deriving the equation suggested by Akkar (2014) mainly comprises of events from a relatively active region and hence, was found to be irrelevant for the present study region in addition to smaller distance range.

Atkinson & Boore (2006) modified as Atkinson & Boore (2011) (abbreviated as AB06) and Campbell (2003) (abbreviated as CA03) was developed for Eastern North America and was observed to provide lower and upper bound estimates respectively for the intended macroseismic data. AB06 developed ground motion relations for hard rock sites in ENA (near surface shear velocity $> 2000 \text{ms}^{-1}$ or NEHRP A) as a function of moment magnitude and closest distance to the fault rupture. The attenuation equation of AB06 is given as

$$\log(PSA) = C_1 + C_2 * M + C_3 * M^2 + (C_4 + C_5 * M) * f_1 + (C_6 + C_7 * M) * f_2$$
$$+ (C_8 + C_9 * M) * f_0 + C_{10} * R_{cd} + S$$

(4.10)

Where $f_0 = \max\left(\log\left(\frac{R_0}{R_{cd}}\right), 0\right)$; $f_1 = \min(\log R_{cd}, \log R_1)$; $f_2 = \max\left(\log\left(\frac{R_{cd}}{R_2}\right), 0\right)$

R_o = 10km, R_1 = 70km and R_2 = 140km. R_{cd} = closest distance to fault rupture, S is the value for soil sites. This GMPE incorporates the seismographic data with a magnitude range of 5 to 7.5 with a distance less than 200km in providing median and standard deviation values for the ground motion parameters (Sa for 5% damped, PGA, PGV). CA03 developed ground motion model by hybrid empirical method incorporating differences in stress drop, source properties, crustal attenuation, regional crustal structure. This empirical attenuation relation is considered to be most appropriate for estimating the ground motion on ENA hard rock with a shear-wave velocity (Vs) of 2800m/s for earthquakes of magnitude Mw≥5.0 and R_{rup}≤ 70km. However, it has been extended to larger distances using stochastic ground motion estimates.

$$\ln(Y) = C_1 + f_1(M_W) + f_2(M_{W,}R_{rup}) + f_3(R_{rup}) \tag{4.11}$$

Where $f_1(M_W) = C_2 * M_W + C_3 * (8.5 - M_W)^2$

$f_2(M_{W,}R_{rup}) = C_4 * \ln(R) + (C_5 + C_6 * M_W) * R_{rup}$;

$R = \sqrt{R_{rup}^2 + (C_7 \exp(C_8 M_w))^2}$

$$f_3(R_{rup}) = \begin{cases} 0 & for\ R_{rup} \leq R_1 \\ C_7(\ln R_{rup} - \ln R_1) & for\ R_1 < R_{rup} \leq R_2 \\ C_7(\ln R_{rup} - \ln R_1) + C_8(\ln R_{rup} - \ln R_2) & for\ R_{rup} > R_2 \end{cases}$$

R_1 = 70km, R_2 = 130km.

Pezeshk (2011) (abbreviated as PK11) predicts a higher PGA and PSA values at shorter distances when compared with the rest of the equations and was opted out of the study. Hwang & Huo (1997) (abbreviated as HH97) provides a reasonable estimate but the applicable distance range is too small and would lead to extrapolation with a higher degree of uncertainty. After preliminary assessment four GMPEs i.e. AB06, TR02, CA03, and ND10 were chosen. The ground motion model developed for the study consists of multiple GMPEs along with its inherent aleatory and epistemic uncertainties developed for both global and regional data.

Table 4.5 Details of the ground motion prediction selected for qualitative testing

GMPE	Region	No. of Records	No. of events	Mw	R type	R range (km)	Component	Period (s)	Style of faulting (stress drop parameter)	Site effect	$V_{S(30)}$ (ms^{-1})	Acronym
Hwang & Huo (1997)	ENA	Simulated data		5-7.5	R_{epi}	1-200	Sa, PGA	0.01 - 3	100-200 bars	$V_{s(30)}$	3500	HH97
Toro (2002)*	CENA	Stochastic Ground motion model		5-8.0	R_{JB}	1-500	Sa, PGA	0.01-2	120bars	dummy variable	1828	TR02
Campbell (2003)*	ENA	Hybrid Empirical method		5 - 8.2	R_{rup}	1-1000	PGA,PSA	0.01 - 4	105 - 215 bars	$V_{s(30)}$	2800	CA03
Raghukanth & Iyengar (2007)	Peninsular India	Simulated data		4 -8.0	R_{hyp}	1-300	Sa, PGA	0.01-4	100-300bars	$V_{s(30)}$	3600	RI07
Iyengar et al, (2010)*	India	Stochastic Finite fault model		4 -8.5	R_{hyp}	1-500	Sa, PGA	0.01 - 4	100-300bars	$V_{s(30)}$	1500	ND10
Atkinson & Boore (2010)*	ENA	Stochastic Finite fault model		3.5 - 8	R_{rup}	1-1000	PSA, PGA, PGV	0.01 - 5	140 bars	$V_{s(30)}$	2000	AB06
Pezeshk (2011)	ENA	Hybrid Empirical method		5 -8.0	R_{rup}	1-1000	PGA,PSA	0.01-10	250bars	$V_{s(30)}$	2000	PK11
Akkar (2014)	Europe & middle east	1041	221	4-7.6	R_{JB}	1-200	PSA, PGA, PGV	0.01-4	N,R,S	Vs30	150-1200	AK14

*GMPEs finally selected for estimating the seismic hazard. CENA - Central and Eastern North America, ENA - Eastern North America.
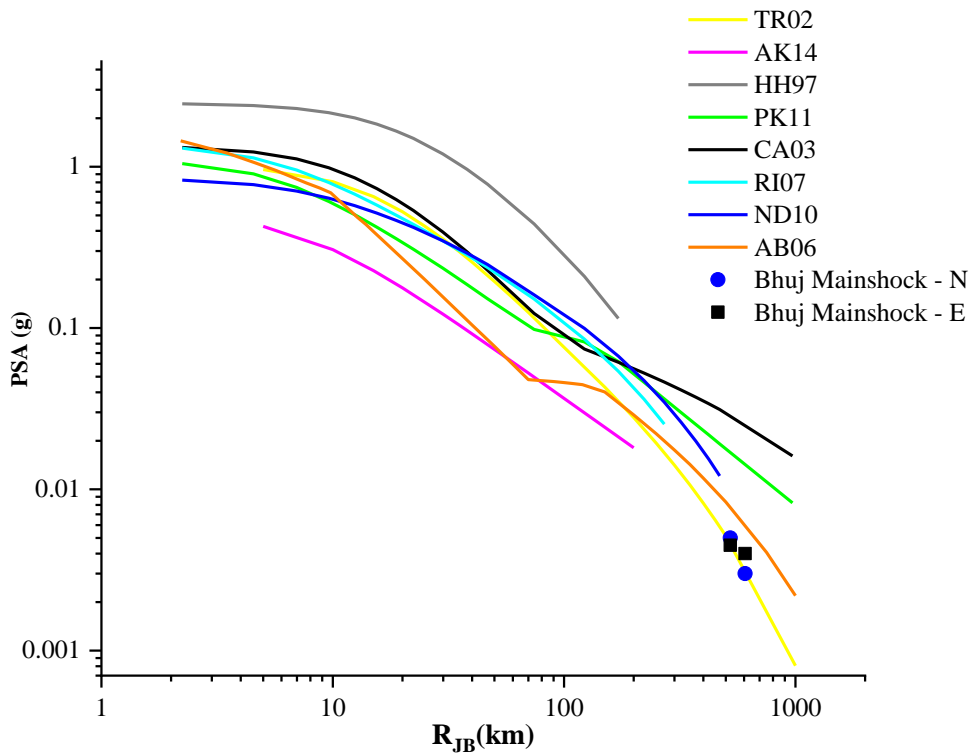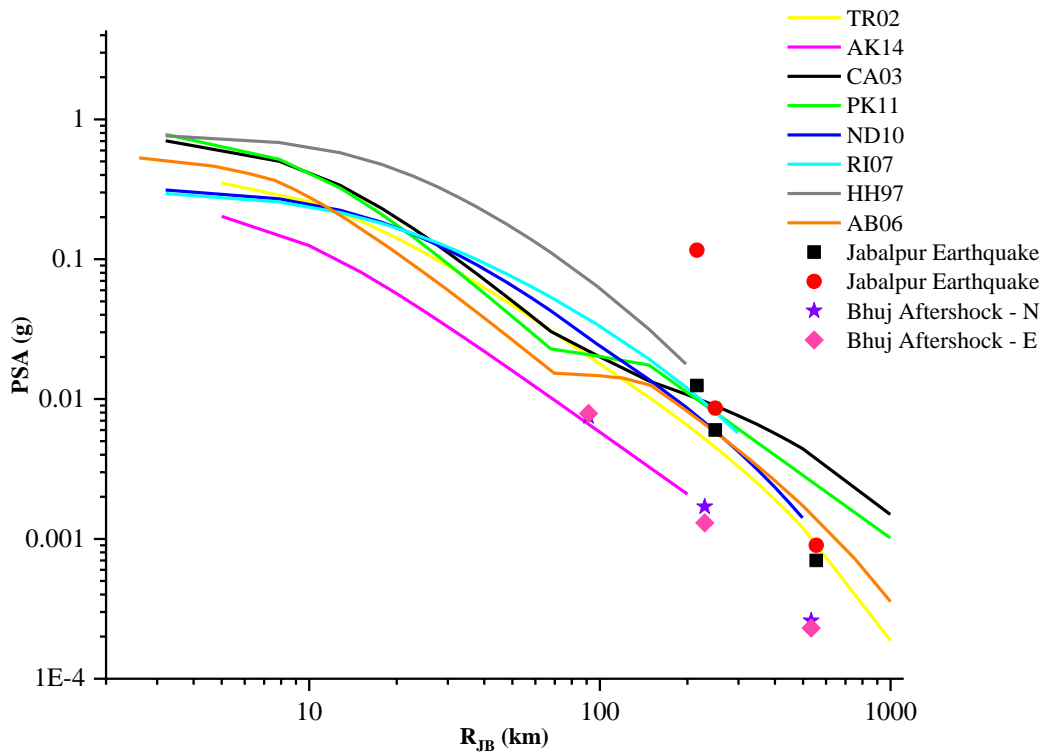
Figure 4.11 Comparison between the GMPEs and the macroseismic recordings during (a) Jabalpur (1997) earthquake and Bhuj aftershock (Mw = 5.7) and (b) Bhuj (2001) (Mw = 7.6)

4.6.2 Qualitative testing of GMPEs

In hazard applications, the non-data driven methods or quality testing methods must be supported by trellis plots and sensitivity analysis (Danciu et al, 2016). Trellis plots are prepared to capture the distribution of ground motion estimates in multidimensional space (M, R, Spectral Period). Trellis plots are presented in three Figures, Figure 4.12, 4.13 and 4.14. Figs 4.12 and 4.14 consist of 12 panels whereas Figure 4.13 consists of 9 panels. Each panel represents a specific earthquake scenario and demonstrates the nonphysical behavior of the attenuation equation. All the GMPEs adopted in this study have developed its own database for the ground motion model incorporating stochastic finite-fault rupture and hybrid empirical methods. Each of these GMPEs has been developed on the different distance scales and they were converted to R_{JB} using the scaling relation developed by EPRI (2004). The attenuation of GMPEs for a various magnitude distance combination has been presented in Figure 4.12. AB06 predicts a lower bound value for all the scenarios whereas ND10 is on the upper bound. For shorter distance (i.e. R_{JB} = 10km) the spectral shape of all the equations remains to be the same but this trend observes a significant period shift in achieving maximum PSA values at far off distances (i.e. R_{JB} = 200km). ND10 demonstrates a well-pronounced peak at larger distances but around the same period range, which is also the case with CA03. AB06 and TR02 witnesses a drastic shift in the period for maximum PSA for higher magnitude and longer distance. This distinctive behavior among GMPEs may be attributed to the difference in their functional forms as well as the data used in developing the equation. TR02 exhibits magnitude saturation at higher magnitudes i.e. Mw = 7. Figure 4.13 represents the magnitude dependent attenuation of the GMPEs considered in the study. TR02 and ND10 represent inelastic attenuation at distances beyond 70-100km and results in steep attenuation. These equations are quite favorable as they can be applied to a wider magnitude-distance range of interest. AB06 exhibits steeper attenuation for PGA at all magnitude ranges but this feature is not so evident at longer spectral periods thereby demonstrating distance saturation. CA03 predicts upper bound values and exhibits distance saturation in all the earthquake scenarios. The magnitude saturation as a function of distance and the spectral period has been presented in Figure4.14. AB06, CA03, and ND10 exhibit magnitude saturation but the same are not evident in TR02.
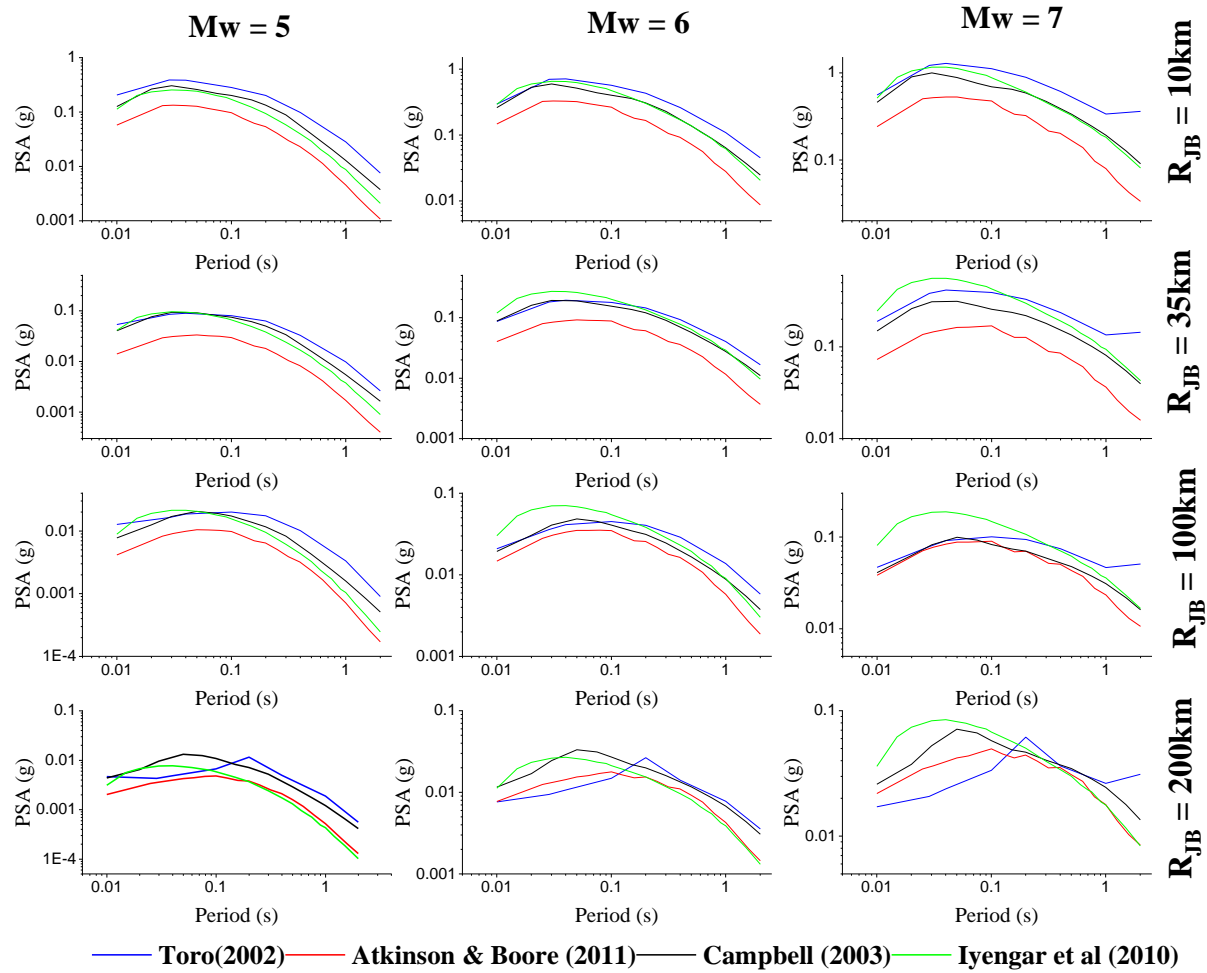
Figure 4.12 Trellis plots for various earthquake scenarios in Magnitude – Source to site distance space for varying spectral period
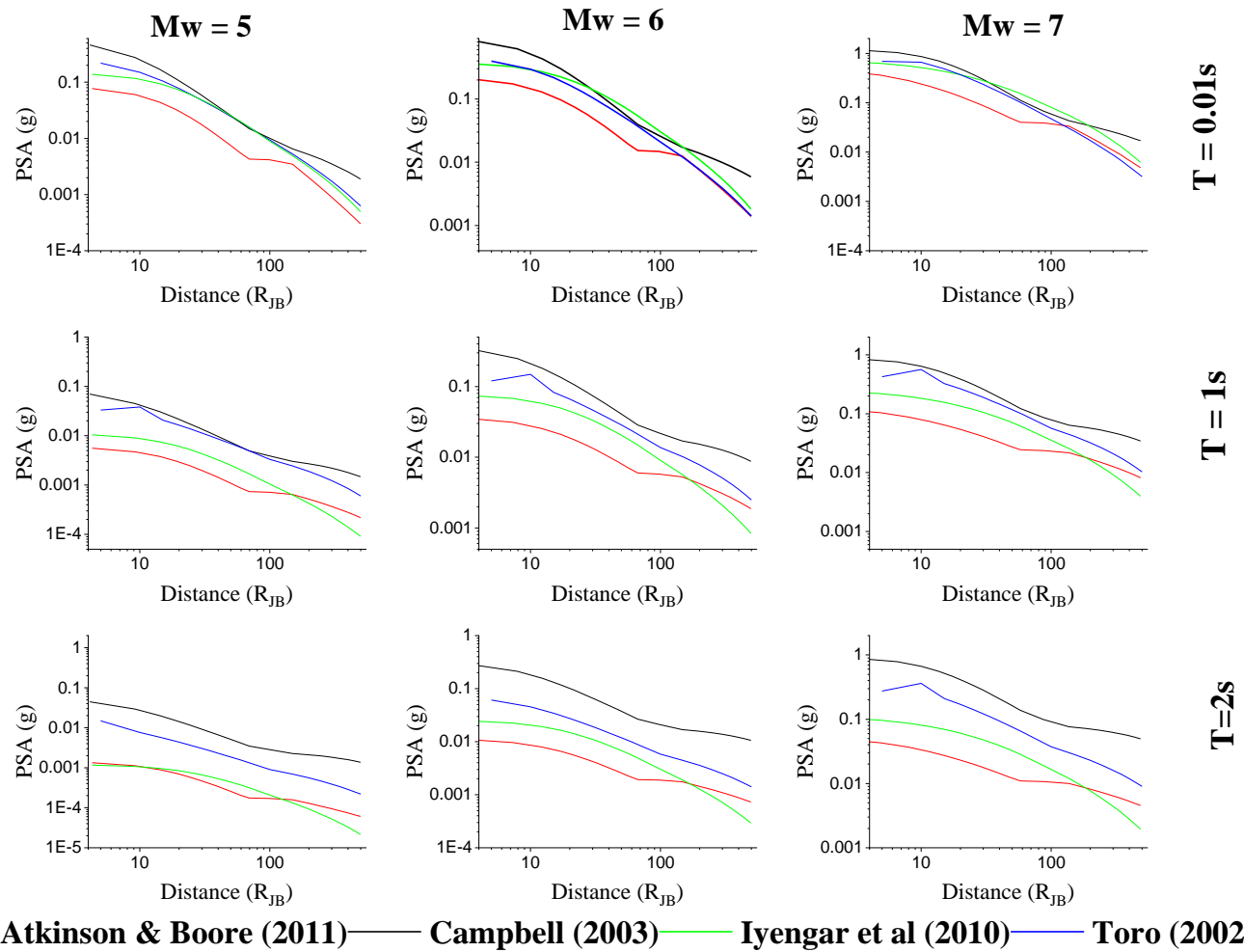
Figure 4.13 Trellis plots for various earthquake scenarios in Magnitude – spectral period space for a varying source to site distance
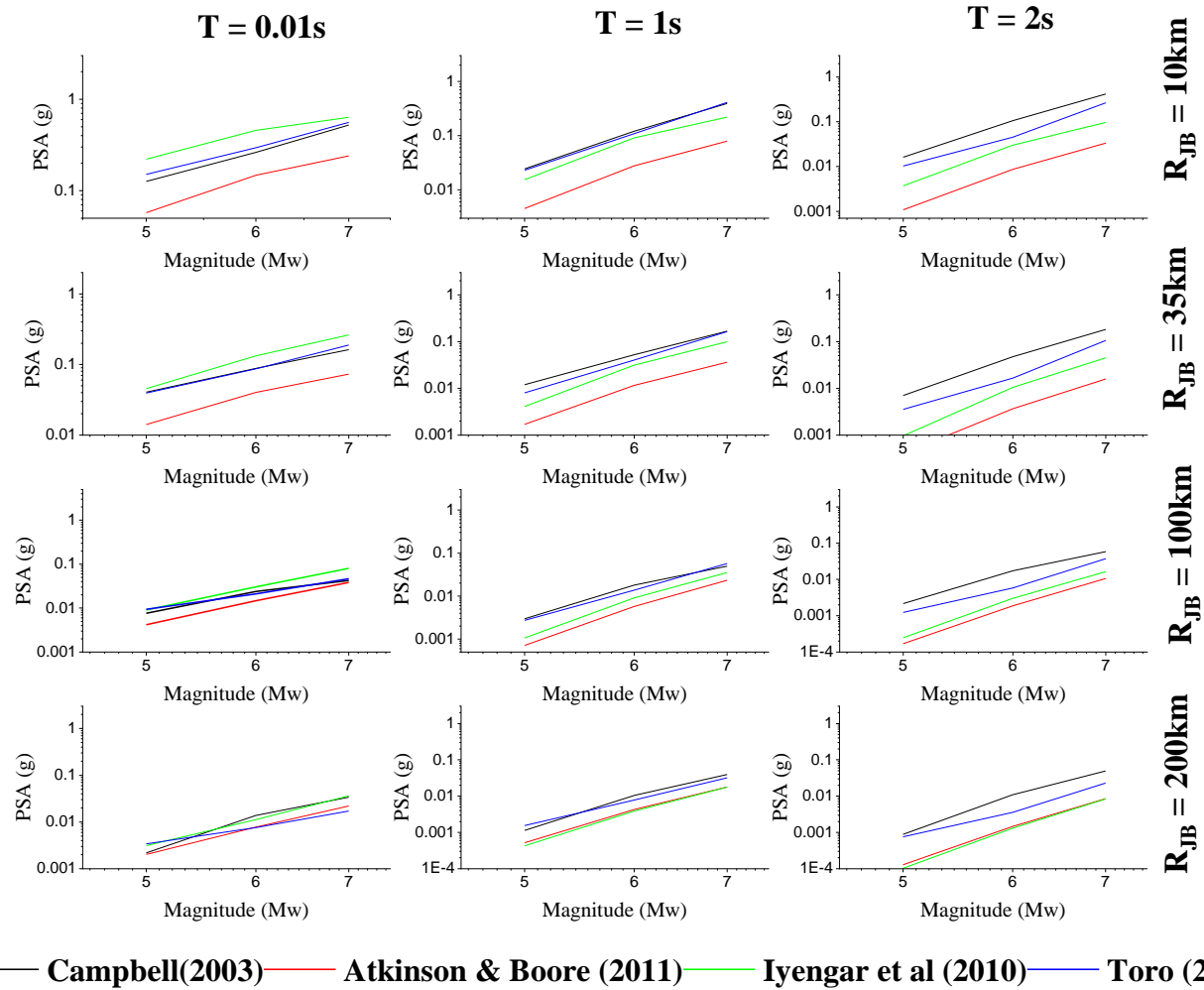
Figure 4.14Trellis plots for various earthquake scenarios in the spectral period – Source to site distance space for varying magnitude range

From all the trellis plots combined together, it can be concluded that AB06 provides a lower bound estimate and CA03 provides an upper bound estimate. In many instances, AB06 and ND10 demonstrate a similar behavior and TR02 toggles between lower and upper bound values along a varied range of magnitude distance combination. The performance of various GMPEs under different earthquake scenario guides in choosing the weighting factors for logic tree combination.

4.6.3 Uncertainties in Ground Motion Prediction model

The uncertainties involved in the formulation and execution of a GMPM can be categorized as aleatory and epistemic uncertainties. Epistemic uncertainty represents the lack of knowledge in understanding and modeling the complex earthquake phenomena. This issue can be overcome with improved data and knowledge such as incorporating multiple ground motion models. These are combined using a logic tree approach with the weighting factors for each model representing the confidence in its prediction as shown in Figure4.10. Aleatory uncertainty represents the natural randomness in earthquake occurrences and cannot be reduced but can provide reasonable estimates with additional data. The impact of aleatory uncertainty in the prediction of ground motion is represented by epsilon 'ε', a fraction of the standard deviation 'σ' of a GMPE. Studies have recognized that the inclusion of σ leads to higher hazard estimates and alternative models influence the overall behavior of the equation. In other words, the aleatory uncertainty controls the shape of the hazard curves while epistemic uncertainty leads to multiple hazard curves equivalent to the logic tree end-branches (Bommer and Abrahamson, 2006). While assigning the weights to each of these branches, it is made sure that each of these equations is mutually exclusive and collectively exhaustive, with the summation of weights of all the branches from a common node being equal to one (Bommer and Scherbaum, 2008). The choice of weighting factors for ground motion models is aided by the trellis plots and sensitivity analysis. The performance of various ground motion models with various weighting factors is analyzed and an appropriate combination is chosen and presented as the final estimate.

The aleatory uncertainty is included in the attenuation equation at the modeling stage and each GMPE treats this uncertainty in a different manner. For instance, TR02 has

the most sophisticated modeling for aleatory and epistemic uncertainty. Despite the fact that the equation uses 20-year-old data TR02 is the most widely accepted ground motion model for stable continental shield region. It represents the lack of data in the form of epistemic uncertainty. The total aleatory uncertainty in the model is considered to be magnitude and distance-dependent whereas epistemic uncertainty is considered to be magnitude dependent alone. The aleatory uncertainty models inter-event variability, stress drop, focal depth, Kappa and Q. Further, the attenuation equation proposed includes variables for aleatory and epistemic uncertainty. CA03 is based on the hybrid empirical method which accommodates aleatory and epistemic uncertainty in the predicted ground motion. The aleatory uncertainty is modeled as lognormal distribution and the values of standard deviation for various magnitude, distance, and spectral period ranges are provided along with the proposed GMPE. Further, the aleatory uncertainty has been included in the proposed equation as a function of magnitude. AB06 includes aleatory uncertainty in the model parameters within the simulation. The epistemic uncertainty considers the stress parameter alone and these uncertainties are modeled as a normal distribution function. ND10 presents a set of values along with the coefficients for the attenuation equation facilitating in plotting mean and mean + sigma values for a region.

In addition to these inherent uncertainties, it is equally important to maintain compatibility among the chosen equations. In other words, different GMPEs produce predictions in terms of different variables (PGA, PSA, SA) using different distance metrics (R_{JB}, R_{hyp}, R_{epi}, R_{rup}) corresponding to different soil conditions. While choosing GMPEs and combining them in a logic tree special attention should be given to these influential parameters. The ground motion models adopted in the study compute the ground motion parameter corresponding to reference sites of distinct shear velocities (Vs(30)) such as $1500 ms^{-1}$ (ND10), $2000 ms^{-1}$ (AB06), $2800 ms^{-1}$ (CA03), $1828 ms^{-1}$ (TR02). However, NEHRP categorizes sites with $V_S > 1500 ms^{-1}$ as site class 'A'. As a result, in the present study, the hazard has been computed at the bedrock level corresponding to NEHRP site class A.

4.6.4 Sensitivity analysis

Selection of GMPEs has been explained in the earlier section. The sensitivity of the weights assigned to each GMPE in logic tree combination in estimating intensity values has been investigated in this section. The epistemic uncertainty involved in the choice of GMPEs is addressed by selecting multiple models and combined using a logic tree. The weights assigned to each of the GMPE requires expert judgment considering their performance in qualitative testing and trellis plots. The results of the trellis plots clearly indicate that CA03 forms the higher end and AB06 form lower end of the hazard estimation. However, ND10 tends to balance and provides a median estimate among the chosen 4 GMPEs. The justification for each of the combinations listed in Table 4.6 is explained in the following section.

Table 4.6 Details of various combinations of weighting factors investigated in the study

GMPE	LT-1	LT-2	LT-3	LT-4	LT-5
AB06	0.3	0.2	0.25	0.2	0.3
CA03	0.2	0.3	0.25	0.2	0.3
ND10	0.3	0.3	0.25	0.2	0.2
TR02	0.2	0.2	0.25	0.4	0.2

4.7 Estimation of Seismic hazard

The probabilistic approach for seismic hazard assessment accommodates all the seismic sources in the study area and predicts the hazard in terms of probability of exceedance for a given intensity level and a predefined time frame. The seismic hazard for the study area has been estimated for NEHRP 'A' site condition ($V_S > 1500ms^{-1}$) by incorporating the seismicity parameters estimated for each of the identified seismogenic source zones along with the attenuation characteristics using the computer program CRISIS 2015. Each source zone is characterized by a minimum and a maximum magnitude and their recurrence parameters. For an area source model, the software assumes a uniform Poissonian distribution of seismicity (i.e. the occurrence of earthquakes in a region is independent of the previous earthquakes for the same region) over the entire source. The software uses a triangulation procedure to discretize the area sources and this discretization is continued until one of the criteria is achieved. The criteria are minimum

triangle size (S) and the ratio of the minimum site to source distance to triangle size (R) and the user has complete flexibility to input these values. As a part of the sensitivity analysis, various combinations of these controlling parameters i.e. S and R were evaluated. However, no significant differences were observed in the hazard values except that the computation time increases with an increase in the values of S and R and a similar observation has been made by Danciu et al, (2010). Initially, each source with 'N' vertices is divided into N-2 triangles and further subdivision continues until the S or R-value specified by the user is achieved. These subdivisions are performed by means of a recursive function. The site to source distance is measured from the computation site to the centroid of the triangle. The seismicity of the area source is assigned to the center of each triangle. CRISIS 2015 uses spatial integration procedure as explained above to sample seismicity source model and predict hazard accounting for all possible locations of the earthquake within the source. The results of the hazard analysis are presented in the form of hazard curves, uniform hazard spectrum, and deaggregation plots. The different combinations of weighting factors for GMPEs from Table 4.6 were investigated and has been plotted in Figure 4.15. The logic tree combination 2 provided higher estimates as CA03 and ND10 as a higher weighting factor as shown in Figure4.15. The combination 3 provides equal weighting factors to all the GMPEs which was in good agreement with that of combination 2. The combination 5 provided an unreasonably lower estimation owing to the lesser weighting factors for ND10 and TR02. On the other hand, a higher weighting factor was provided for TR02 in combination 4. However, this combination suggested that TR02 alone is insufficient in predicting the overall seismic hazard. The choice was to be made between combinations 1 and 3. CA03 gives higher estimation in all the considered scenarios as exhibited in trellis plots. Hence, CA03 had to have the least weighting factor. TR02 is for a higher magnitude range and hence, was given a lesser weighting factor. ND10 is derived based on regional data and performed exceptionally well in qualitative testing. The equation accommodates anelastic attenuation, accounts for exceedance probability of low magnitude events and impact of large earthquakes at far off distances. AB06 provides a significant lower bound estimation in the majority of the scenarios considered but the study region is characterized by low to moderate seismicity. Hence, providing more weighting factor to other attenuation equation would

lead to unrealistic estimates of intensity values. Hence, combination 1 was chosen for the final seismic hazard assessment.
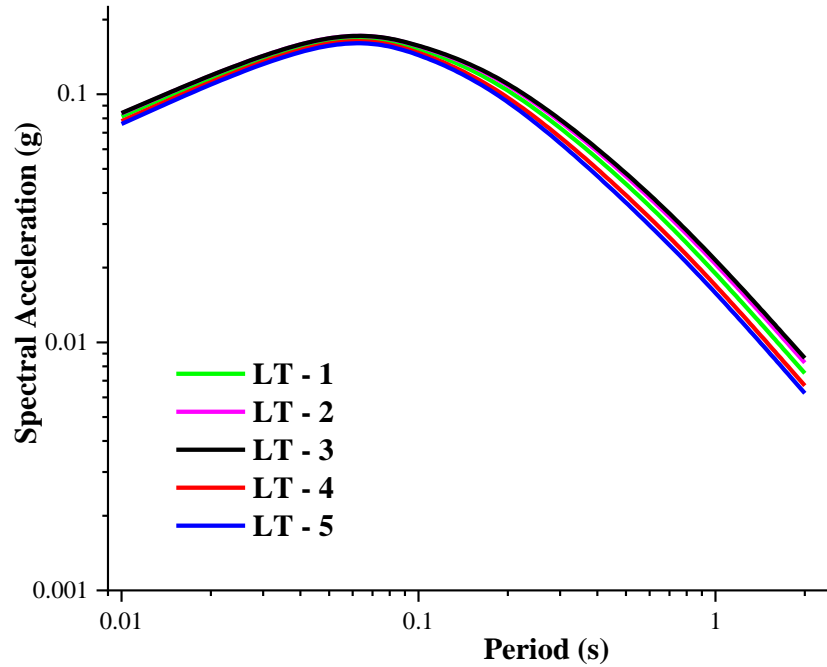
Figure 4.15 Median uniform hazard spectra obtained from various logic tree combinations

The median and percentile uniform hazard spectrum estimated from the chosen logic tree combination 1 has been depicted in Figure 4.16. The contour maps representing the PGA (g) for 10% and 2% probability of exceedance in 50 years has been plotted in Figure 4.17 for the whole of the considered area.
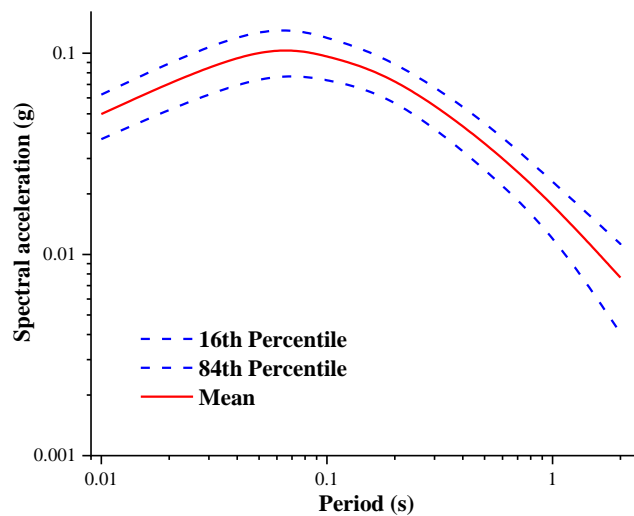
Figure 4.16 Mean and percentile estimation of uniform Hazard spectrum for the chosen logic tree combination (LT-1).
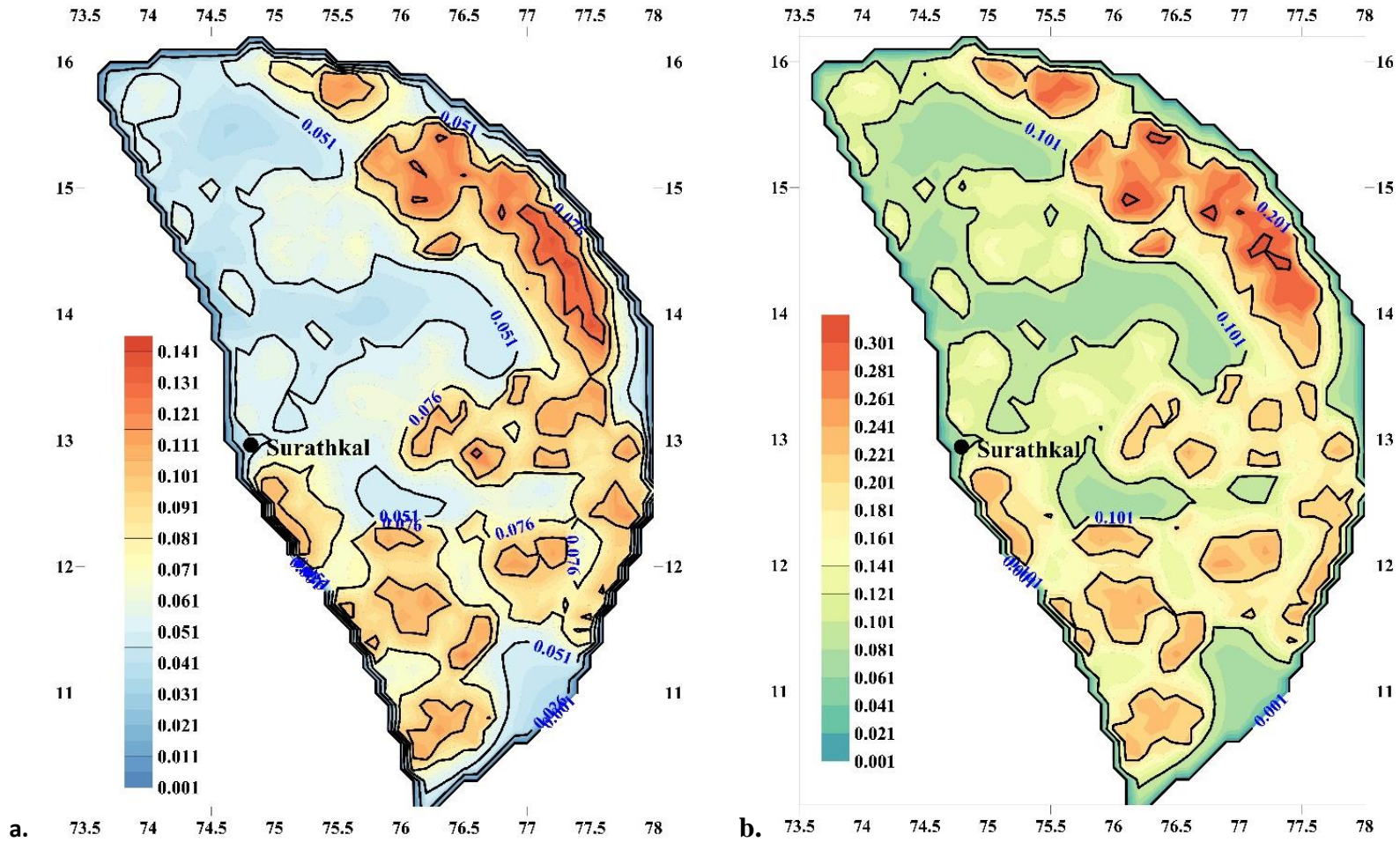
Figure 4.17 Contour maps representing PGA for the study area at (a) 10% and (b) 2% probability of exceedance at the bedrock level condition

The contour maps reveal higher seismic hazard in MZ1 and moderate level seismic hazard is MZ2 and MZ3. The mining activity going on a few locations in MZ1 are suspected to be triggering seismicity in this region and the study recommends further investigation in this area. The hazard curves for the bedrock condition are plotted for Mangalore city (12.81°N, 74.87°E) for various spectral periods as shown in Figure 4.18. It is clear from Figure 4.18 that for a given exceedance probability higher acceleration values can be expected up to 0.05s.
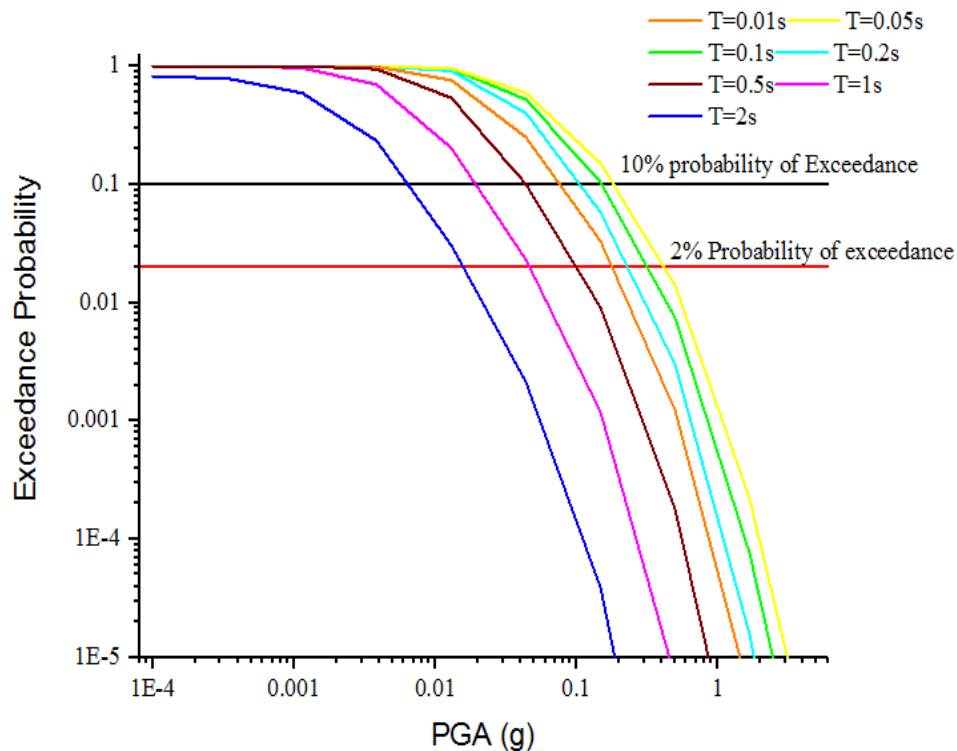
Figure 4.18 Hazard curves for Mangalore city for varying spectral periods in a time frame of 50 years

The UHS for a 10% probability of exceedance in 50 years has been plotted in Figure 4.19 for all the important cities in the study area. Among all the cities, it can be said that Wayanad has higher seismic potential. This major observation is relatable as the city is close to Coimbatore which has been an epicenter for one of the major earthquakes in South India. The plotted UHS can be grouped into three bands based on the estimated acceleration values. Wayanad belongs to the upper band, Kozhikode, Kasargod, and Kannur belong to the mid-band and Surathkal and Udupi belong to the lower band. Given the geographical locations of these places, it can be inferred the seismic potential

is increasing towards South. The inference made is in good agreement with the seismic hazard maps plotted for the region in Figure 4.20. The seismic hazard maps for the study area have been plotted and presented in Figure 4.20 for 10% (Rp = 475 years) and 2% (Rp = 2475 years) probability of exceedance corresponding to bedrock level conditions. The seismic hazard maps suggest gradually increasing trend in seismic hazard towards Kerala. The seismic zonation map of IS 1893 (2016) categorizes the study area under seismic zone III. The findings from the study confirm this geographical division into different seismic zones by the code. However, the zone factor suggested by the code is slightly lower than that obtained from the study. A maximum PGA of 0.16g – 0.24g is observed for a 2% probability of exceedance in 50years, also known as the maximum considered earthquake (MCE). The zone values suggested by the code is 0.16g and 0.24g for zone III and IV respectively. Hence, it can be concluded that the study region fluctuates between seismic zone III and IV of IS 1893 (2016).
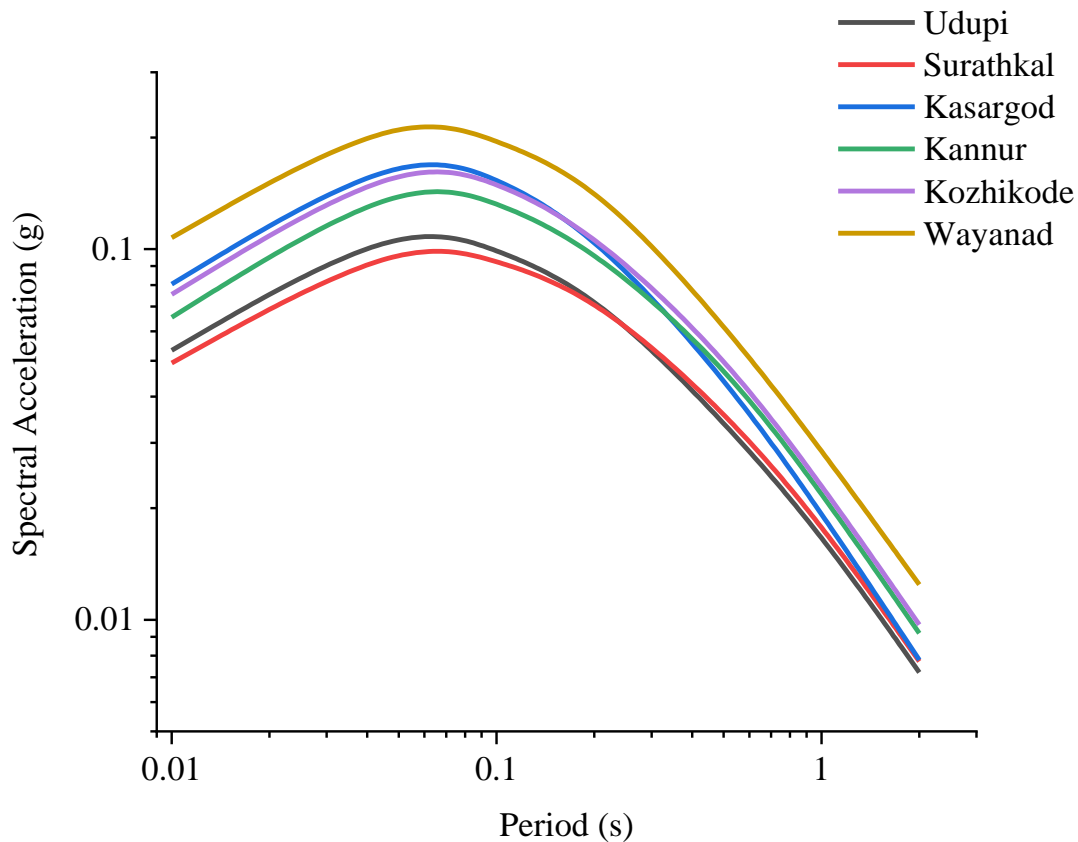
Figure 4.19 Uniform Hazard Spectrum for various important cities at the bedrock level (Vs > 1500ms-1) for a 10% probability of exceedance (R$_p$ - 475 years)
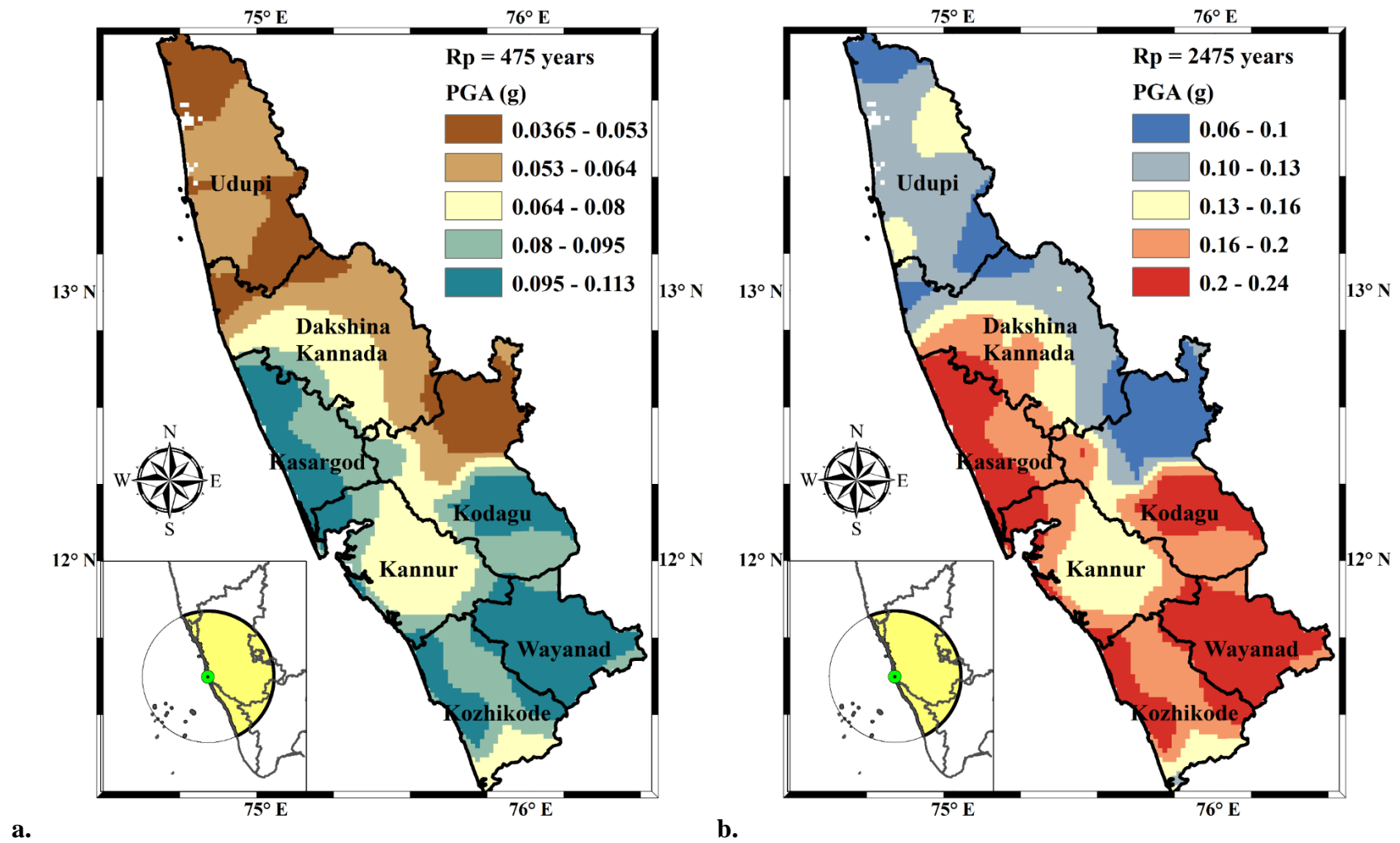
Figure 4.20 Seismic Hazard Maps for the study area corresponding to (a) Rp = 475 years, (b) Rp = 2475 years.

The PGA values estimated at the bedrock level are compared with the predictions made by various researchers for three different regions as listed in Table 4.7.

Table 4.7 Comparison of hazard values predicted for different regions

Intensity levels	Bangalore	Mangalore	Bellary	Authors	Site class
10% probability of exceedance	0.095	0.076	0.112	**Present study**	**$V_s>1500ms^{-1}$**
	0.131	0.044	0.064	**Sitharam et al, (2012)**	**Bedrock**
	0.024	0.023	0.038	**Iyengar et al, (2010)**	**NEHRP 'A'**
	0.05	0.08	0.05	**BIS (2016)**	**Rock/ stiff soil**
	0.11	0.08	0.12	**Nath and Thingbhaijam (2012)**	**B-C boundary**
	0.10	-	-	**Jaiswal and Sinha (2007)**	**Hard rock**
	0.06	0.1	0.08	**Sitharam and Kolathayar (2013)**	**$V_s>1500ms^{-1}$**
	0.057	0.06	0.10	**Ashish et al, (2016)**	**$V_s>1100ms^{-1}$**

Jaiswal and Sinha (2007) performed seismic hazard for PI using a zoneless approach and this study uses GMPEs which have been superseded by a more recent and sophisticated ground motion models. Further, the study was almost a decade ago thereby creating space for improved knowledge and additional data in recent years. However, the hazard predicted for Bangalore seems to be in good agreement with that of the present estimation and the city wise predicted PGA values are not available for improved discussion in the matter. Iyengar et al, (2010) predict relatively lesser values for all the considered region corresponding to NEHRP site class A. The study adopts areal source zones and makes use of regionally developed GMPEs for different parts of the country. This was the first attempt to develop a common attenuation equation with spatially varying coefficients for each identified individual tectonic regime. However, the major limitation of this study is the use of single GMPE making epistemic uncertainty dominant in the hazard prediction. Sitharam et al, (2012) performed both deterministic and probabilistic seismic hazard analysis for Karnataka state alone by

adopting linear and areal source models for PSHA. The study underestimates the seismic potential of both Mangalore and Bellary and slightly overestimates for Bangalore. The attenuation equation used in the study has been superseded by a more recent publication and is believed to be the reason for the difference in the predicted values with that of the present study. Nath & Thingbhaijam (2012) have adopted the smoothened gridded seismicity model as well as the uniform seismicity areal source model. A major coincidence with this study is the use of a similar trend in areal source delineation and same GMPEs but with varying weighting factors for each GMPE. Ashish et al, (2016), and Nath and Thingbhaijam (2012) demonstrated the seismic potential of Bellary to be higher than the other two locations supporting the results obtained in this study. Ashish et al, (2016) used multiple source models such as areal source, gridded seismicity model and fault source model to estimate the seismic hazard for entire PI. The computed hazard values match well with that of the present study except for a slight underestimation for Bangalore region. The difference in the predicted hazard values from the present study and that of Sitharam & Kolathayar (2013) is quite significant and the reason behind this difference is due to the use of single GMPEs by the latter. Overall, the present study is believed to have produced a rational estimate of the seismic hazard values by incorporating the available datasets on earthquake events and regionally applicable ground motion models.

4.8   De-aggregation of seismic hazard

PSHA integrates all the possible earthquake scenarios (magnitude – distance) and predicts the hazard level but difficult to identify the relative contribution of the seismic sources for a chosen site of interest. In order to obtain the specific scenario earthquake (a combination of magnitude, and distance) contributing to the specified hazard level, de-aggregation of the seismic hazard is mandatory. The de-aggregation of the computed seismic hazard provides better insights into the significance of various influential parameters contributing to hazard (Bazzurro & Cornell, 1999). The investigation of the most influential earthquake scenario consists of three essential parameters such as magnitude (M), distance (R), and epsilon (ε). These three parameters have a significant influence on the exceedance probability. De-aggregation was performed using CRISIS 2015 and the program provides flexibility to the user to input the intensity level or the

probability level (i.e. 2% or 10% probability exceedance), time frame (say 50 years), magnitude, distance, and epsilon. Epsilon (ε) represents the measure of the contribution to hazard above or below the mean predicted value. The contribution of the smallest earthquakes is significant when $\varepsilon>1$ and for larger earthquakes $\varepsilon<1$ (Halchuk et al, 2007). For a chosen range of M, R, ε the de-aggregation plots represents the probability of exceedance as a percentage of total exceedance probability (for all magnitude, distance, and epsilon equal to $-\infty$) (Aguilar-Meléndez et al, 2017).

In a stable continental region such as the present study area, the contribution comes from a wide range of magnitudes and distances. In order to capture the importance of small earthquakes at a close distance to large earthquakes at far off distance, mean M and R-value were chosen from de-aggregation plots. The ε value was calculated as the number of standard deviations by which the target ground motion deviated from the median value predicted from a GMPE for a given M and R (Bazzurro and Cornell, 1999). The de-aggregation plots for each GMPE have been presented in Figure 4.21 to 4.24.
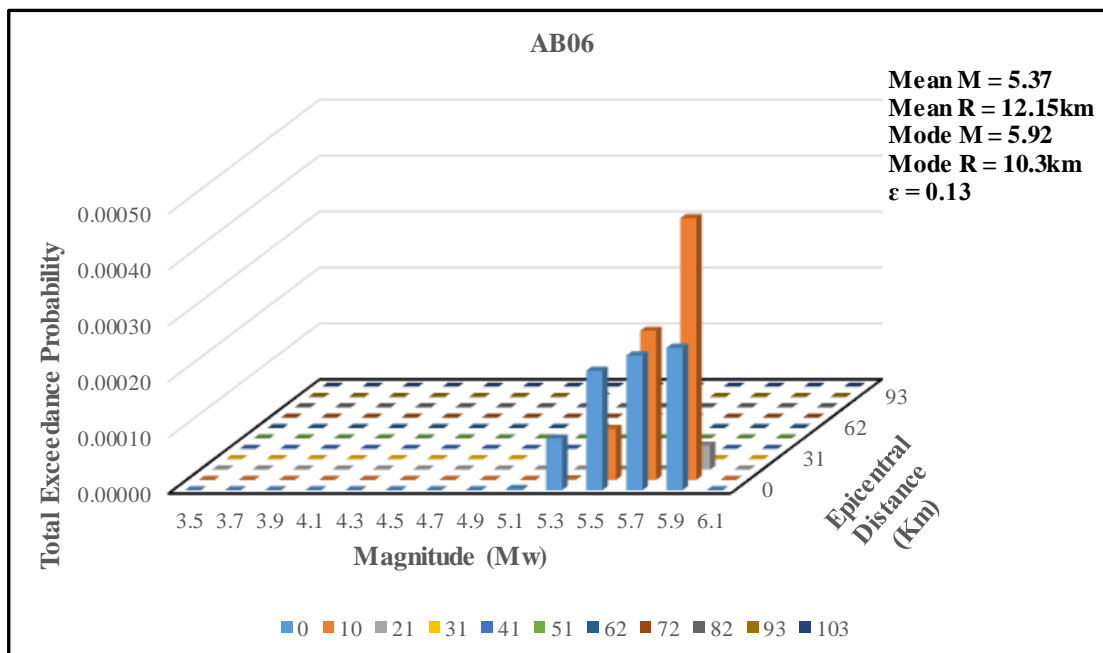
Figure 4.21 De-aggregation plot for AB06 with intensity 0.121g for 2% probability of exceedance.

AB06 provided relatively lower estimates throughout the study and highlights the importance of moderate-sized earthquakes (Mw 5-6) at smaller distances ($R_{epi}< 25km$).

Additionally, the impact of an Mw 6 earthquake up to 50km distance has been well demonstrated. CA03 provides an upper bound estimate and recommends that an Mw 6 earthquake has a significant impact only till 30km. In addition, it underestimates the significance of low magnitude earthquakes in de-aggregation. The possible reason for this estimation is the higher magnitude range (Mw 5-8.2) incorporated in the modeling phase of the GMPE.
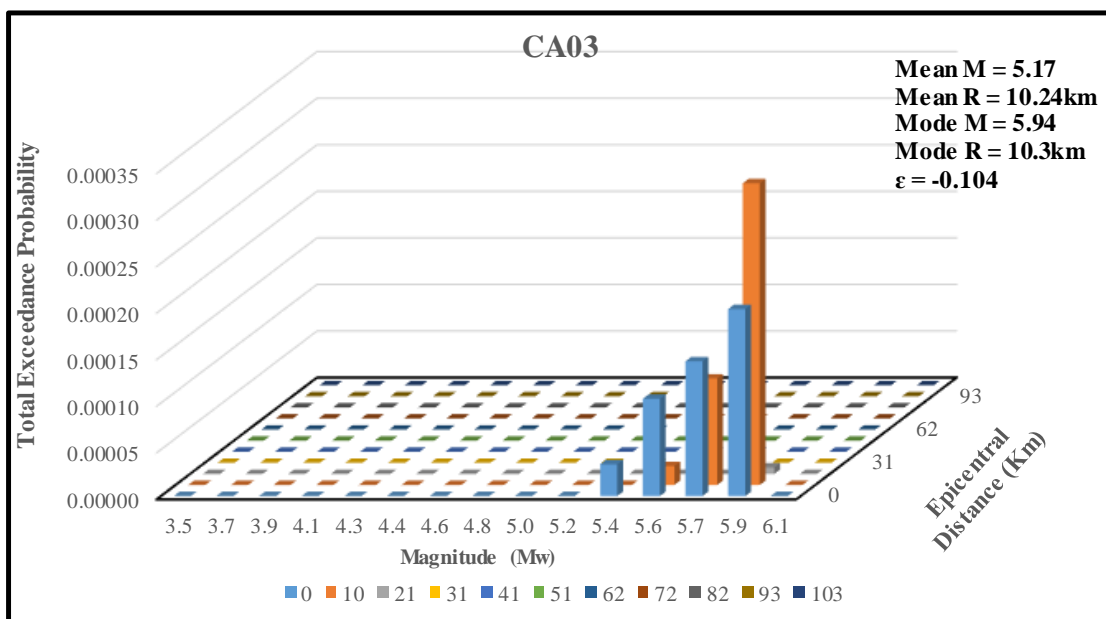
Figure 4.22 De-aggregation plot for CA03 with intensity 0.229g for 2% probability of exceedance

ND10 provides a reasonable de-aggregation accommodating the significance of earthquakes (Mw > 5) at distances with 20km and for events with Mw 6 up to 50km. This GMPE is derived from the regional data and is expected to best represent the local attenuation characteristics. Further, it shows increased exceedance probability for increasing magnitude and near source distances. TR02 highlights the significance of lower magnitude events at a near-source distance (<10km) and higher magnitude events (Mw>6) at distances greater than 30km. In conclusion, all the GMPEs highlight the importance of near-source effect irrespective of the size of an earthquake event but larger magnitude events can cause a significant impact at far off distances say 50km. In general, de-aggregation is carried out to determine controlling earthquakes consistent with the uniform hazard spectrum to generate time histories that are representative of

the target hazard level. These time histories can be used for various engineering purpose and in this study these results are used in selecting ground motions for site response analysis.
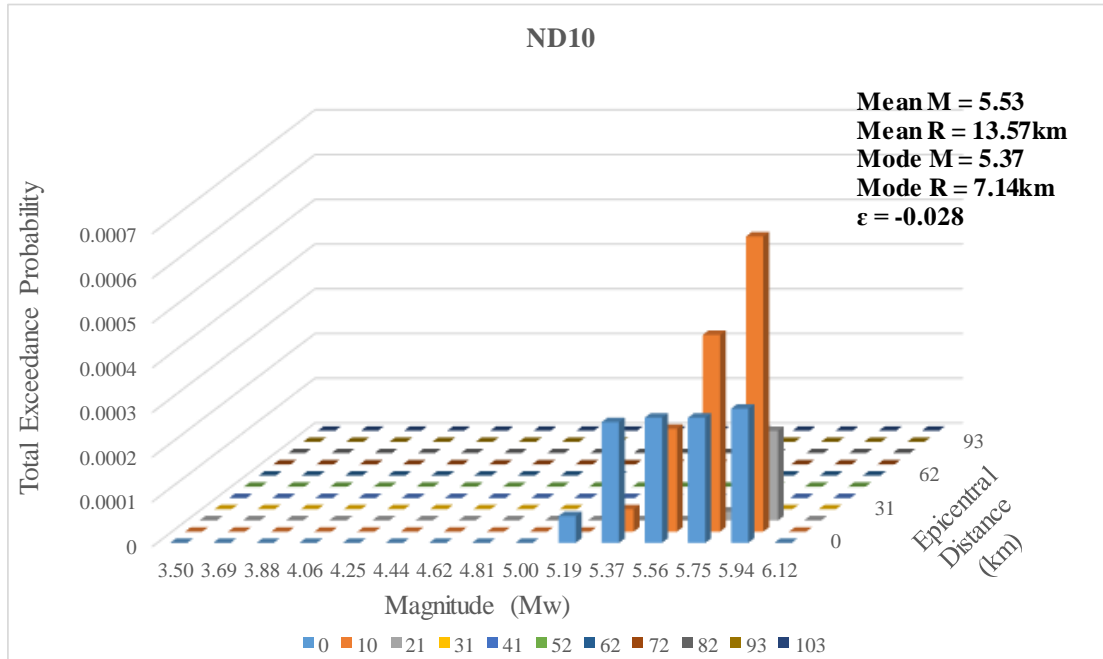
Figure 4.23 De-aggregation plot for ND10 with intensity 0.17g for 2% probability of exceedance
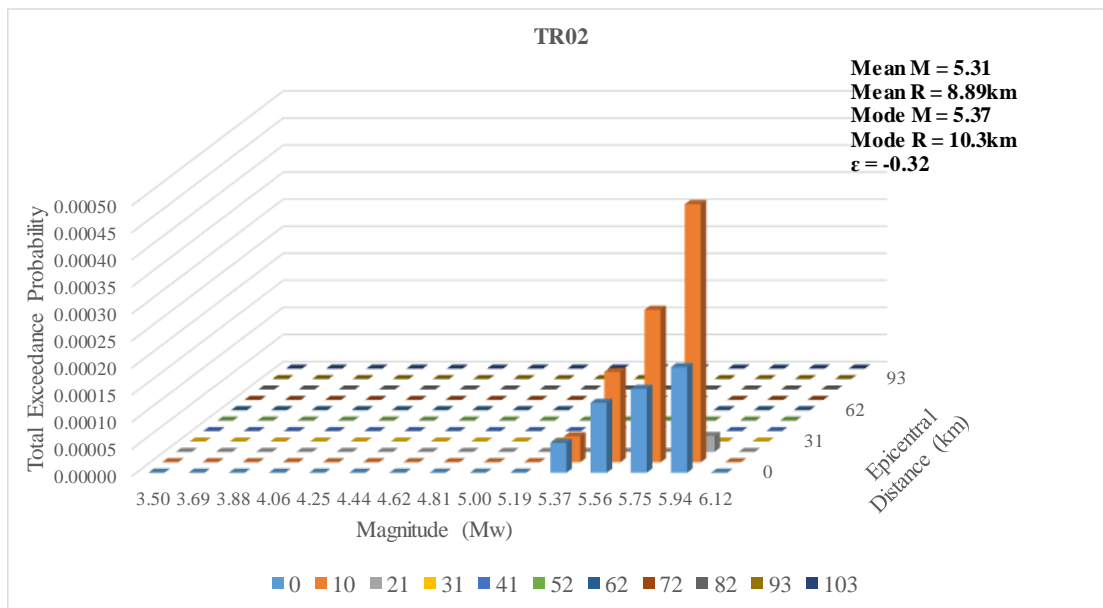
Figure 4.24 De-aggregation plot for TR02 with intensity 0.177g for 2% probability of exceedance

4.9   Concluding Remarks

The seismic hazard was estimated using Cornel – McGuire approach for the whole of South West India. Seismic sources were modeled as areal sources owing to diffused seismicity of the region. The seismicity parameters have been estimated using a maximum likelihood approach. The following observations are found to be noteworthy.

1. The records of the seismic data have witnessed significant improvement in the last 5 decades owing to better instrumentation in the recording of earthquake events.

2. Reactivation of dormant faults is noticed in Shimoga during the 1975 earthquake. Though, there were no records of earlier seismic activity in this region.

3. The catalog is divided into sub-catalogs with different magnitude of completeness (M_C) and catalog period.

4. The estimated seismicity parameters suggest a larger proportion of lower magnitude events in the study region.

5. The epistemic and aleatory uncertainty involved in the seismic source and ground motion modeling has been explained explicitly.

6. The study area is categorized under seismic zone III by IS 1893 (2016). The study reveals that the estimated PGA values are higher than 0.16g (Zone factor).

7. The hazard values estimated for the study region are in good agreement with the studies conducted in recent years.

CHAPTER 5

SEISMIC SITE CHARACTERIZATION

5.1   Introduction

A seismic hazard analysis is said to be complete only when the local site effects are considered in the estimation. The seismic waves traveling from the source located at depth to the surface undergo significant modification depending on the dynamic characteristics of the subsurface material. A hazard estimate failing to capture the local site effects suffer from inaccuracy and hence, the inclusion of local site response in PSHA is fundamental.

The seismic site characterization involves assessing the dynamic properties of the medium constituting the subsurface. In most of the cases, the shear wave velocity in the top 30m ($V_{S(30)}$) from the surface is used as an indirect measure for understanding the dynamic characteristics. Higher the value of $V_{S(30)}$, stronger is the material (soil) and lesser amplification and vice versa. Various in-situ methods such as seismic refraction survey, seismic reflection survey, surface wave methods, crosshole method, downhole method, and suspension logging are available to estimate V_S. The measured V_S is used in modeling the soil material to estimate amplification by site response analysis. However, these in-situ methods require skilled labor apart from being expensive and time-consuming. Hence, these methods are not feasible under all circumstances. On the other hand, Standard Penetration test (SPT) is widely practiced and there have been studies correlating the SPT resistance 'N' value to $V_{S(30)}$.

In the present study, the SPT borehole data is collected for the Southern part of the study area and shear velocity profile is generated for each bore log. Site response analysis using the equivalent linear approach is performed on SHAKE 2000. The nonlinear behavior of the soil material is considered by using the intensity measure of the input rock motion (S_a^r) as the independent variable for deriving the amplification function AF(f). These amplification functions are derived for different soil types i.e. 'Sand', 'Clay' and 'All soil' at different periods of interest i.e 0.01s, 0.2s, 0.8s, 1s, 1,5s, and 3s. The amplified ground motion time histories are further used in generating elastic

design response spectra for three different site categories (I, II and III) consistent with the site classification of IS 1893 (2016) (Hard rock, medium stiff soil and soft soil).

The local soil data was not available for the entire study area and hence, an alternate method has been employed to map the seismic site characteristics. The digital elevation model (DEM) is available for the entire globe at a uniform sampling. The topographic slope is calculated from the DEM using ArcGIS v10.1. Wald & Allen (2007) suggested topographic variations as an indicator of near-surface geomorphology and lithology to the first order. Hence, the topographic slope is used to produce $V_{S(30)}$ map for the whole of the study area. Further, using regionally developed amplification equation, the surface level seismic hazard maps are generated.

5.2   Geotechnical characterization

The soil data were collected for the Southern Part of the study area stretching between 10.08°N to 12.72°N (latitude) and 74.86°E to 76.85°E (longitude) as shown in Figure 5.1. The soil data were mainly from the Northern Kerala region comprising of 7 districts i.e Kasargod, Kannur, Kozhikode (Calicut), Wayanad, Malappuram, Palakkad, and Ernakulam.

The topography, climate, and local geology have influenced the local soil formation. Laterite is the most prominent soil type in the study region formed due to weathering of rocks and serves as an excellent building material. This type of soil is observed in heavy rainfall region with humid tropical conditions and rich in iron and aluminum oxides. The surface soils appear in reddish brown to yellowish red in color with a texture varying from gravelly loam to gravelly clay loam. Apart from laterites, the study region is geotechnically characterized by coastal alluvium developed from recent marine deposits and fluvial sediment along the coastal stretch. This soil type is predominantly 'sand' with smaller quantities of silt and clay. In general, the soil deposits observed in Palakkad and Thrissur are deep and well drained with fairly high gravel content and loamy to 'clay' texture. Hence, the collected borehole samples consisted of 'sand' deposits close to the coastal tract and 'clay' deposits as well as a mixture of laterites, sand, and clay in the rest of the study region. and 'clay' deposits as well as a mixture of laterites, sand, and clay in the rest of the study region.
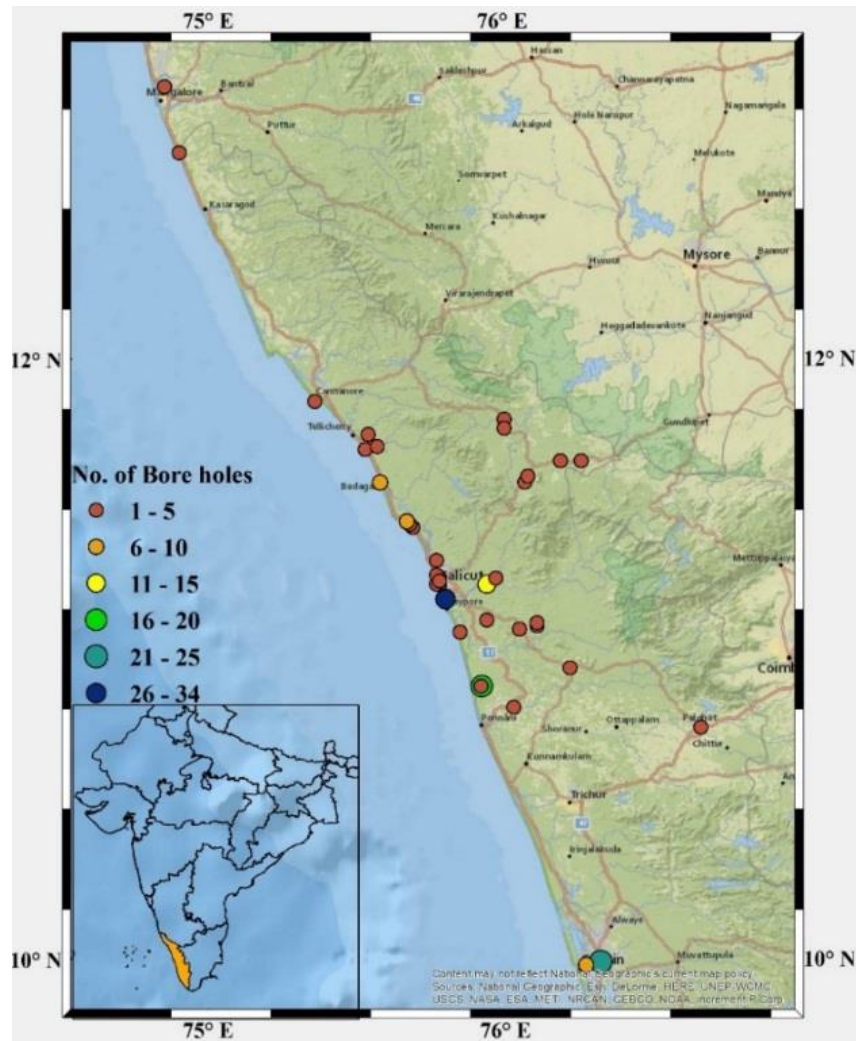
Figure 5.1 Physical map indicating the location and number of boreholes used for the study

The study region has exposures of gneissic rocks close to the beaches and a few other places. The typical geological strata for the Calicut region in the order of their appearance from the ground surface is 'sand', 'clay' sand, clay, laterite, lateritic clay, weathered rock, hard basement rock (gneiss), fractured rock and hard rock (Nazimuddin, 1993) as shown in Figure 5.2. The depth to bedrock varied from 20m to 35m depending on the topography (Joji, 2009). Most of the boreholes were terminated upon reaching the hard rock strata. In places such as Ernakulam and Palakkad, the weathered geological units were observed between 2 to 16m. In such cases, the validation for the depth to bedrock was derived by referring to the electrical resistivity surveys carried out in the region (Balakrishnan, 2009). However, in Malapurram the

depth to compact bedrock is in the range of 50 to 200m (Venkiteswaran and Rao, 1980). In Kannur, the depth to weathered rock ranges between 3 and 20m.
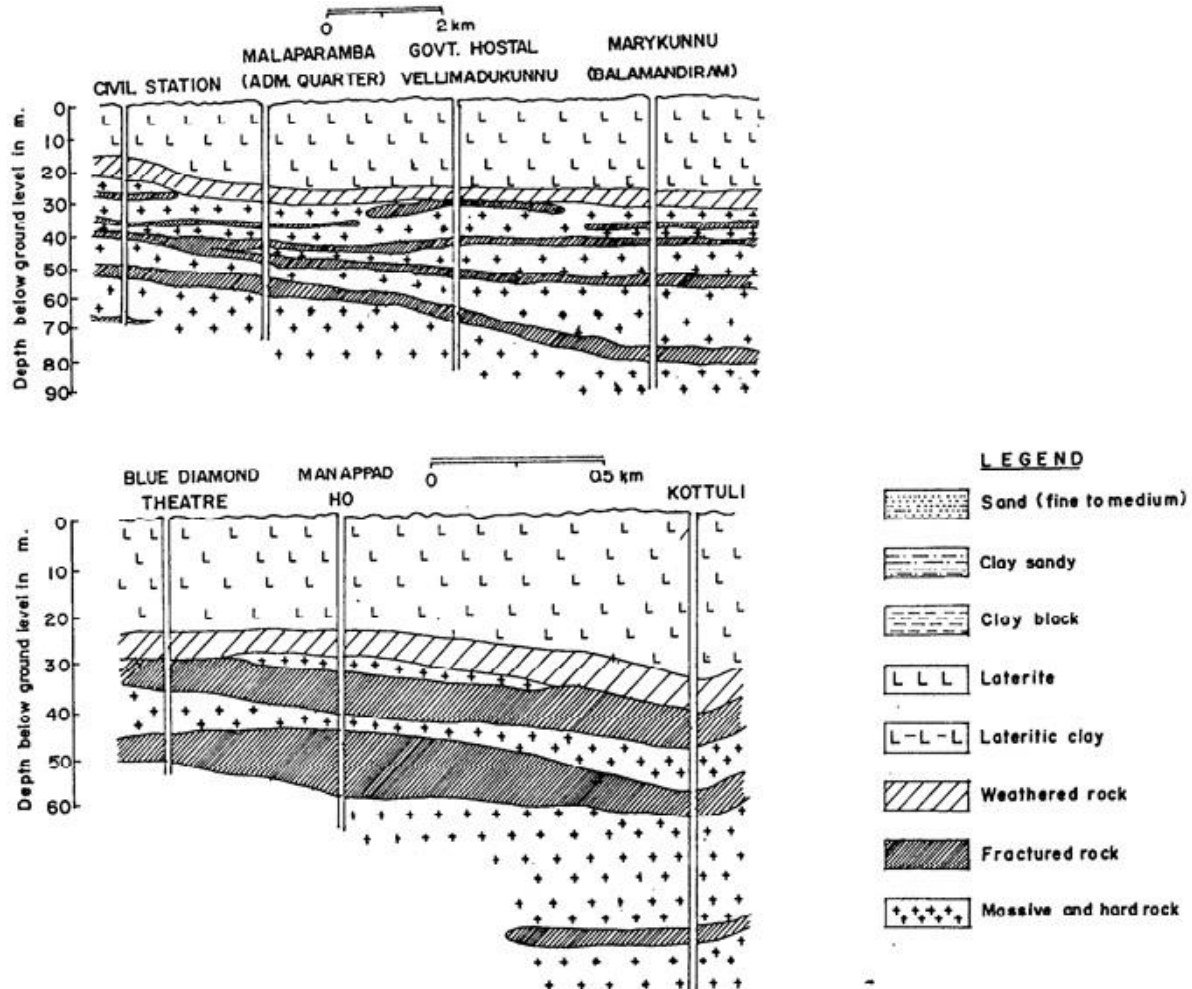
Figure 5.2 Soil stratigraphy illustrating the geological formation in the target area (Nizamuddin, 1993)

The depth of the soil profiles used in the study has been presented in Figure 5.3. The depth of the soil column varies from 6m to 35m. Few boreholes terminated at a depth of 48m. Based on vast literature survey (CGWB (2002), Gopinath, G. (2003), Vinayachandran and Joji (2007), Sreenath G (2009), and Saritha S and Vikas C (2009), Brijesh (2017)) and the collected borehole data, it can be concluded that the overall depth to Engineering Bedrock ($V_{S(30)} > 760ms^{-1}$) is within 50m from the surface and the same has been applied for soil profiling in the study.
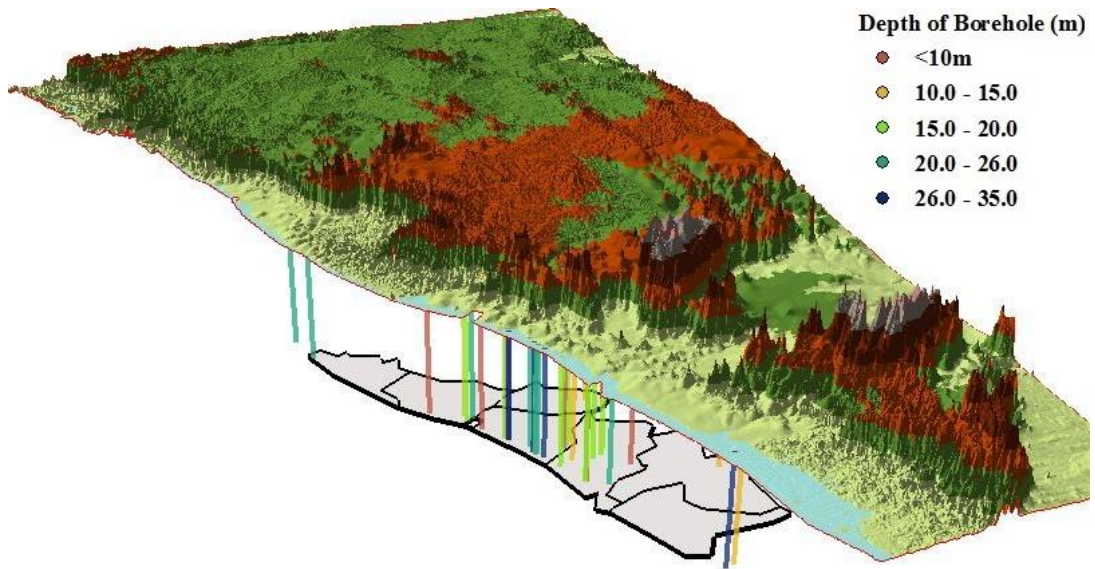
Figure 5.3 Topographical map in the vicinity of borehole locations with the borehole depths dropped as a shadow

5.3   Site classification based on N_{SPT} and $V_{S(30)}$

The soil characteristics form an integral part in modeling the soil profile for seismic site amplification studies. In this regard, the subsurface geology and geotechnics were studied using borehole data determined as per the guidelines of BIS 2131 (1981). The geotechnical data consisting of bore logs with standard penetration test 'N' value, unit weight, index properties, grain size distribution, and shear strength parameters were collected from the Dept. of Civil Engineering, National Institute of Technology Calicut. Additionally, reports of electrical resistivity studies and groundwater information booklets by Central Ground Water Board, Govt. of India were referred to understand the subsurface geological and geotechnical formations. The borehole information was collected from approximately 40 locations in the study area with a minimum of two boreholes and a maximum of 30 boreholes at each location. However, on processing the collected data, few borehole samples were discarded due to missing data on N-value, unit weight or grain size distribution. The collected borehole data can be categorized into different site classes based on the weighted average of 'N' value for soil layers existing from the surface to a depth (d) of 30m.

$$N_{SPT} = \frac{\sum_{i=1}^{n} d_i}{\sum_{i=1}^{n} \frac{d_i}{N_i}} \tag{5.1}$$

99

where $\sum_{i=1}^{n} d_i$ = 30m (or 100ft), i = number of layers, N_i = corrected SPT 'N' value in layer 'i'. IS 1893 (2016) has classified site classes into three groups based on the SPT 'N' value as shown in Table 5.1. The collected borehole information was classified based on the N_{SPT} and elastic design spectrum was generated for these soil types. The bore logs were cataloged and categorized based on N_{SPT} as shown in Figure 5.4 As evident from Figure 5.4, a major part of the collected samples belong to soil category I (N > 30) and III (N < 15).
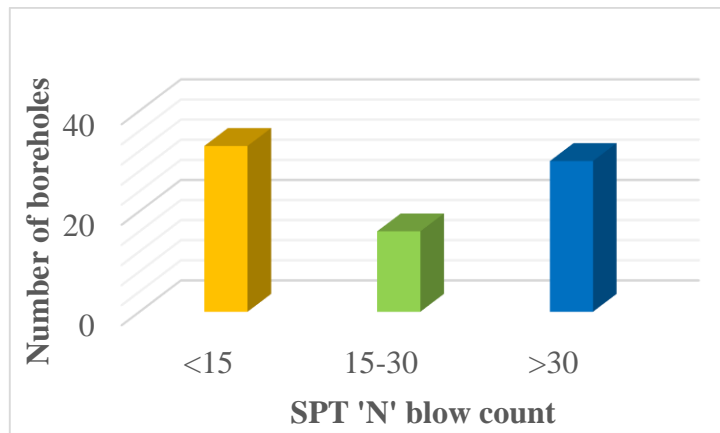
Figure 5.4 Histogram of the soil bore logs collected for the study

The study attempts to highlight the significance of soil type as one of the influential factors in determining the local site amplification. In this regard, the compiled borehole data was classified into three soil types i.e Sand, Clay and All soil based on the predominant soil content and grain size distribution. Overall 30 samples for 'all soil', 15 samples for 'clay' and 6 samples for 'sand' were considered for further analysis. A typical stratigraphy witnessed in a sample borehole of each soil type is shown in Figure 5.5. Most of the deposits reach weathered rock at a very shallow depth (<30m).

Table 5.1 Classification of soils based on NSPT for determining elastic design spectrum (IS 1893, 2016)

Soil Type	Description		N_{SPT} (weighted average)
I Rock/ Hard Soils	**a.**	Well graded gravel (GW) or well-graded sand (SW), both with less than 5% passing 75µm sieve (fines).	**>30**
	b.	Well graded gravel-sand mixtures with or without fines (GW-SW)	
	c.	Poorly graded sand (SP) or clayey sand (SC)	
	d.	Stiff to hard clays	
II Medium/ Stiff soils	**a.**	Poorly graded sands or poorly graded sands with gravel (SP) with little or no fines	**15 to 30**
	b.	Stiff to medium stiff fine-grained soils, like silts of low compressibility (ML) or clays of low compressibility	
III Soft Soils	**a.**	Silts of intermediate compressibility (Ml)	**<15**
	b.	Silts of high compressibility (MH)	
	c.	Clays of intermediate compressibility (CI)	
	d.	Clays of high compressibility (CH)	
	e.	Silts and clays of intermediate to high compressibility (MI-MH or CI-CH)	
	f.	Silt with clay of intermediate compressibility (MI-CI)	
	g.	Silt with clay of high compressibility (MH-CH)	
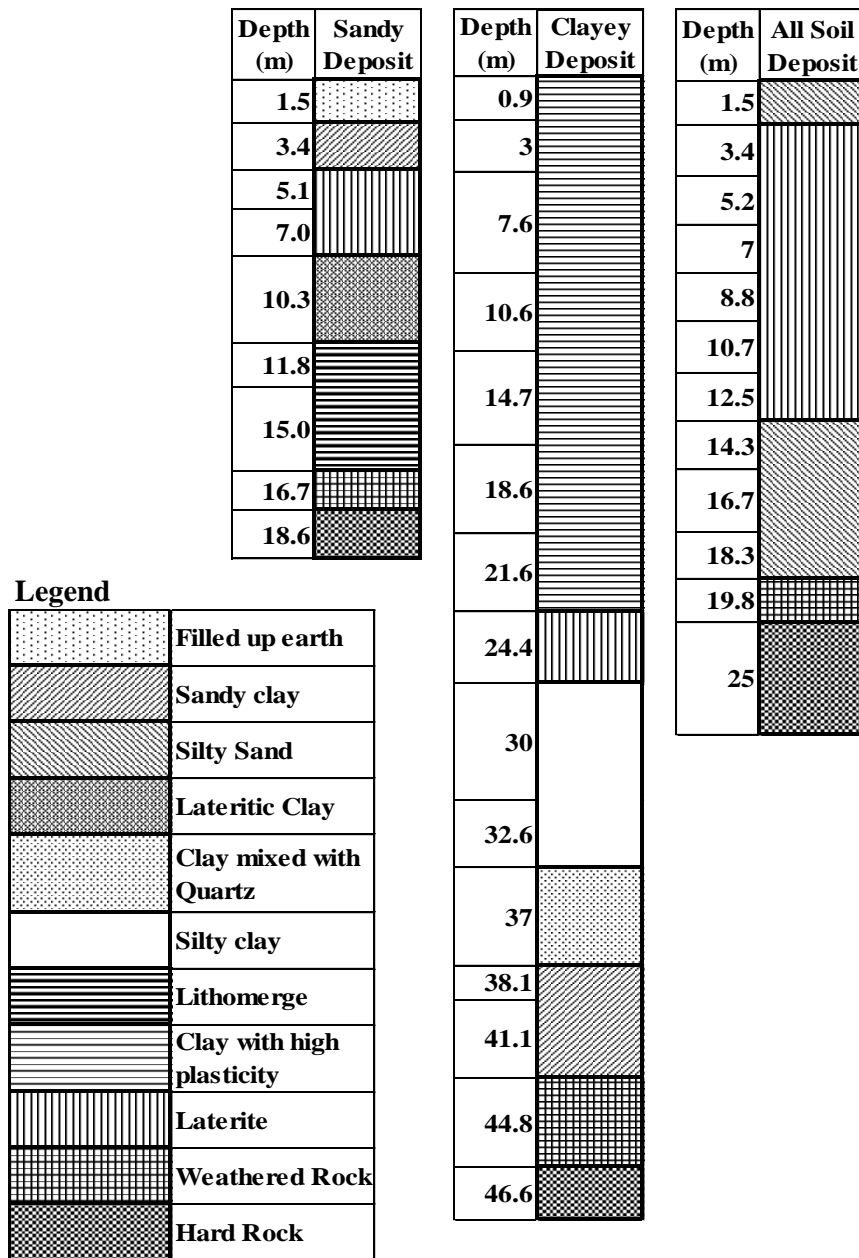
Figure 5.5 Stratigraphy of all the three representative soil types used in the study

The shear velocity (Vs) profile for all the boreholes was estimated using $V_S - N$ correlation. In order to reduce the uncertainty involved in the estimation of Vs, multiple correlations were investigated as shown in Figure 5.6. The details about each of these correlations have been tabulated in Table 5.2. Importance to regionally developed correlations and based on uncorrected SPT 'N' values was given during the selection process in order to maintain homogeneity.

Table 5.2 Vs – N Correlations investigated in the study

Authors	Correlation	Soil Type	Region
Maheshwari et al. (2010)* - **UM1**	$V_s = 89.31*N^{0.358}$ $V_s = 100.53*N^{0.265}$ $V_s = 95.64*N^{0.301}$	Clay Sand All Soil	Chennai
Hanumanthrao & Ramana (2008) – **HR**	$V_s = 79*N^{0.434}$ $V_s = 82.6*N^{0.43}$ $V_s = 86*N^{0.42}$	Sand All Soil Silty Sand/ sand Silt	Delhi
Unal Dikmen (2009) – **UD**	$V_s = 58*N^{0.39}$ $V_s = 73*N^{0.33}$ $V_s = 60*N^{0.36}$ $V_s = 44*N^{0.48}$	All Soil Sand Silt Clay	Turkey
Chatterjee & Choudhury (2013)* - **CC1**	$V_s = 78.21*N^{0.38}$ $V_s = 77.11*N^{0.39}$ $V_s = 54.82*N^{0.53}$ $V_s = 58.02*N^{0.46}$	All Soil Clay Silty Sand Silt	Kolkata
Kirar, Maheshwari et al. (2016) – **KMM**	$V_s = 100.31*N^{0.348}$ $V_s = 94.4*N^{0.379}$ $V_s = 99.5*N^{0.345}$	Sand Clay All Soil	Roorkee
Maheshwari et al. (2010)* - **UM2**	$V_s = 90.75*N^{0.304}$ $V_s = 96.29*N^{0.266}$ $V_s = 83.27*N^{0.365}$	All Soil Sand Clay	Chennai
Hasaneebi & Ulusay (2007)* - **NR**	$V_s = 90*N^{0.309}$ $V_s = 90.8*N^{0.319}$ $V_s = 97.9*N^{0.269}$	All Soil Sand Clay	Turkey
Anbazhagan et al.(2012) – **AZ**	$V_s = 68.96*N^{0.51}$ $V_s = 60.17*N^{0.56}$ $V_s = 106.63*N^{0.39}$	All Soil Sand Clay	Lucknow
Sil & Haloi (2017)* - **SH**	$V_s = 75.478*N^{0.3799}$ $V_s = 79.217*N^{0.3699}$ $V_s = 99.708*N^{0.3358}$	All Soil Sand Clay	Any region
Mhaske & Choudhury (2011)* - **MC**	$V_s = 72*N^{0.4}$	All Soil	Mumbai
Thokchom et al. (2017) * - **TK**	$V_s = 2.641*N +189.6$ $V_s = 3.925*N + 143.1$ $V_s = 3.395*N+156.8$ $V_s = 3.311*N+160.5$	Sand Silt Clay All Soils	Dholera, Western India.
Chatterjee & Choudhury (2013)* - **CC2**	$V_s = 78.63*N^{0.37}$ $V_s = 78.03*N^{0.38}$ $V_s = 58.62*N^{0.45}$ $V_s = 56.44*N^{0.51}$	All Soil Clay Silt Silty Sand	Kolkata

* correlations finalized for estimating the V_S profile. Nomenclature ending with numbers 1 and 2 represents correlation derived based on uncorrected and corrected SPT 'N' values respectively.
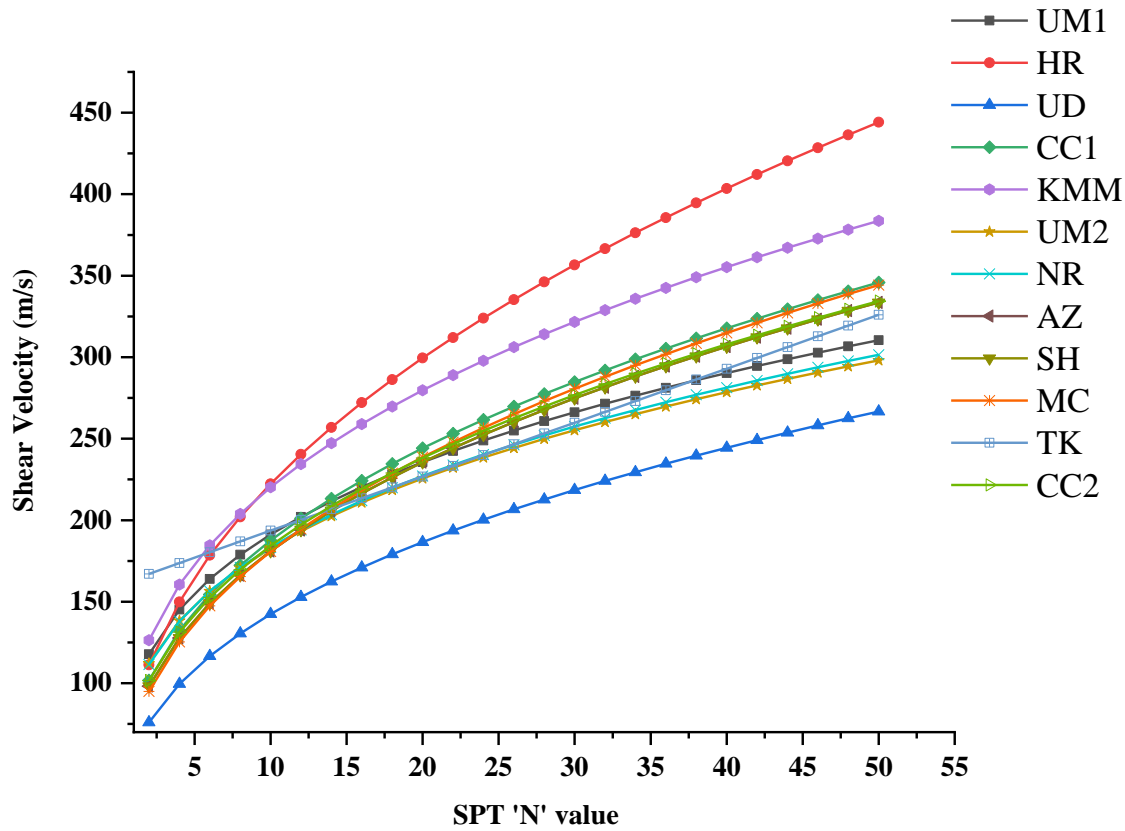
Figure 5.6 Comparison of the Vs – N correlations investigated in the study

As evident from Figure 5.6, few correlations resulted in extreme estimations such as HR, KMM, and UD. These correlations were eliminated and a total of six correlations were used for the final estimation of the shear velocity profile. The estimated shear velocity profile from all the six correlations along with the median and standard deviation is shown in Figure 5.7.

Most of the amplification studies use $V_{S(30)}$ as a predictor variable. Hence, the preliminary step was to prove that the use of $V_{S(30)}$ alone to identify the amplification that can be expected from a site is inadequate. As a result, the generated shear velocity profiles for the collected bore logs have been categorized based on the NEHRP recommendations as listed in Table 5.3. The $V_{S(30)}$ was calculated using the formula

$$V_{S(30)} = \frac{\sum_{i=1}^{n} d_i}{\sum_{i=1}^{n} \frac{d_i}{V_{Si}}} \tag{5.2}$$

where V_{Si} is the shear wave velocity of layer 'i'
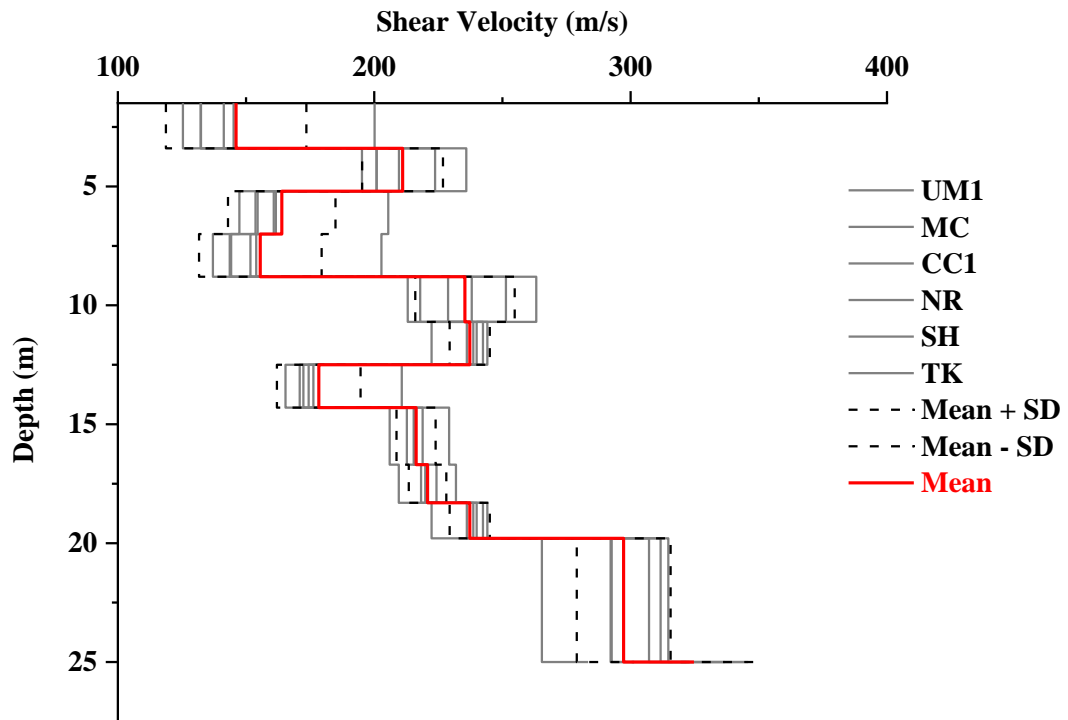
Figure 5.7 Shear velocity profile of a typical clay deposit

Table 5.3 Site classification based on $V_{S(30)}$ in NEHRP provisions (BSSC, 2003)

NEHRP Category	Description	Average Shear Wave Velocity ($V_{S(30)}$)
A	Hard rock	> 1500 ms^{-1}
B	Firm to hard rock Dense soil	760 - 1500 ms^{-1}
C	soft rock	360 – 760 ms^{-1}
D	Stiff soil	180 – 360 ms^{-1}
E	Soft Soil	< 180 ms^{-1}
F	Special study soils (liquefiable soils, sensitive clays, organic soils, soft clays > 36 m)	

The boreholes classified based on $V_{S(30)}$ have been plotted in Figure5.8. Majority of the soil deposits have $V_{S(30)}$ in the range of 350 – 400ms^{-1} and that is the boundary between NEHRP 'C' and 'D' site categories. Except for a few boreholes belonging to the 'C' category, the rest lies in 'D' site class. The geological strata observed in Figure 5.2 is in agreement with the stratification of the collected bore log (Figure 5.5). Also, few boreholes terminate at a shallow depth as evident from Figure 5.3 which was justified

in Figure 5.2. Additionally, the estimated V_S profiles suggest stiff soil deposits with few soft soil deposits. Based on these observations, it can be concluded that the collected number of samples have been able to represent the local site conditions adequately.
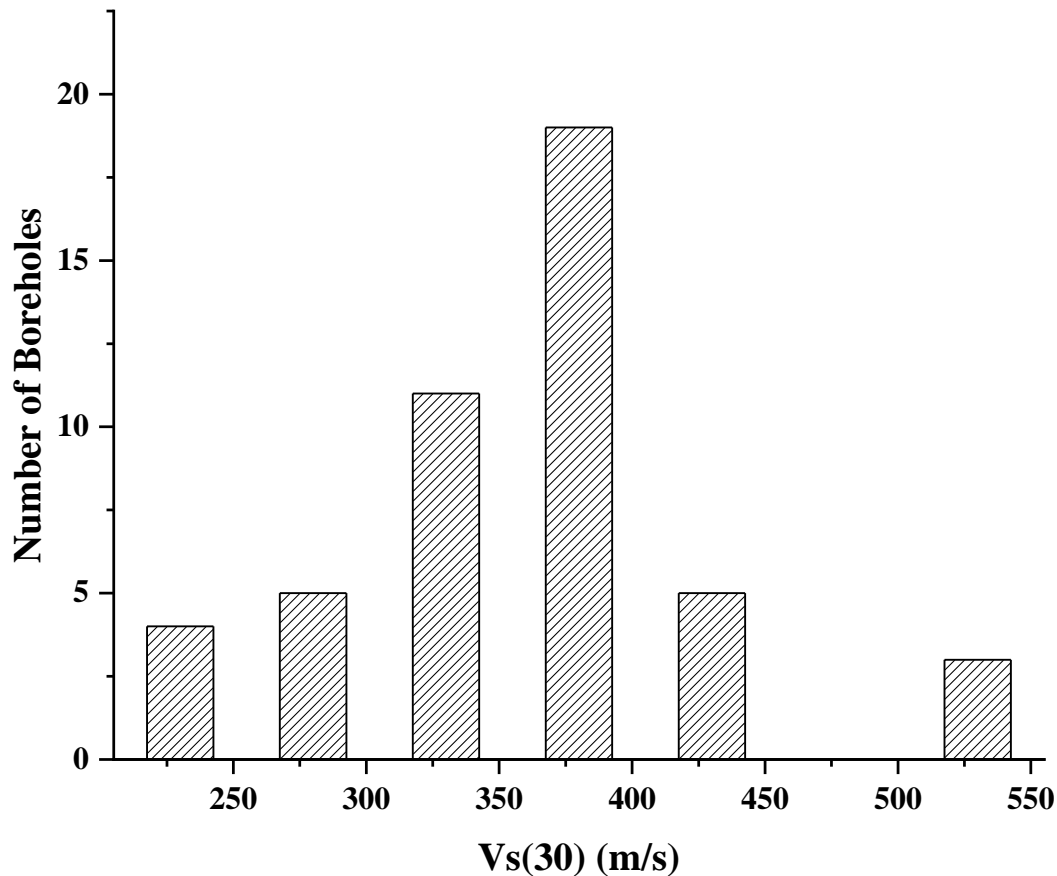
Figure 5.8 Histogram of the number of soil profiles simulated in the study

5.4 Soil modeling

The dynamic characteristics of the soil material need to be estimated and modeled to estimate the local site response. The modulus reduction (M-R) curves i.e shear modulus reduction (G/G_{max}) versus cyclic shear strain (γ_c) and damping (D) curves (i.e. damping versus γ_c) are essential in modeling the dynamic behavior of soils. Various in-situ and laboratory tests such as Cyclic tri-axial shear or resonant column shear apparatus can be used to estimate the dynamic properties. However, in the absence of experimental programs, M-R curves and Damping curves can be obtained from the literature. Based on experimental investigation, many classical M-R and damping curves have been proposed in the past. In the present study, the standard empirical relations of G/G_{max}

(Figure 5.9) and D (Figure 5.10) as a function of cyclic shear strain (γ_c) for sand and clay have been used to model the dynamic soil response. These curves are referred to as backbone curves and represent the nonlinear hysteretic behavior of various soil types. The damping in the soils can be accounted to the cyclic shear causing slippage between soil grains and leading to complex interactions between solid and fluid phases. This produces a lag in time between the application of stress and the development of the resulting strains. The damping ratio calculated by considering the area under the stress-strain loops are found to be nearly independent of loading frequency within the frequency range of interest. Hence, it is commonly referred to as hysteretic (Stewart and Afshari, 2015). The investigated boreholes consisted of weathered rocks and the same has been modeled as Rockfill. Based on the observation from Figures 5.9 and 5.10, the curves for rock demonstrate a linear trend when compared to the other material. The nonlinear trend of the curves for Sand and Clay depicts the nonlinear behavior of the material. The rockfill was also observed to be almost linear when compared to Sand and Clay.
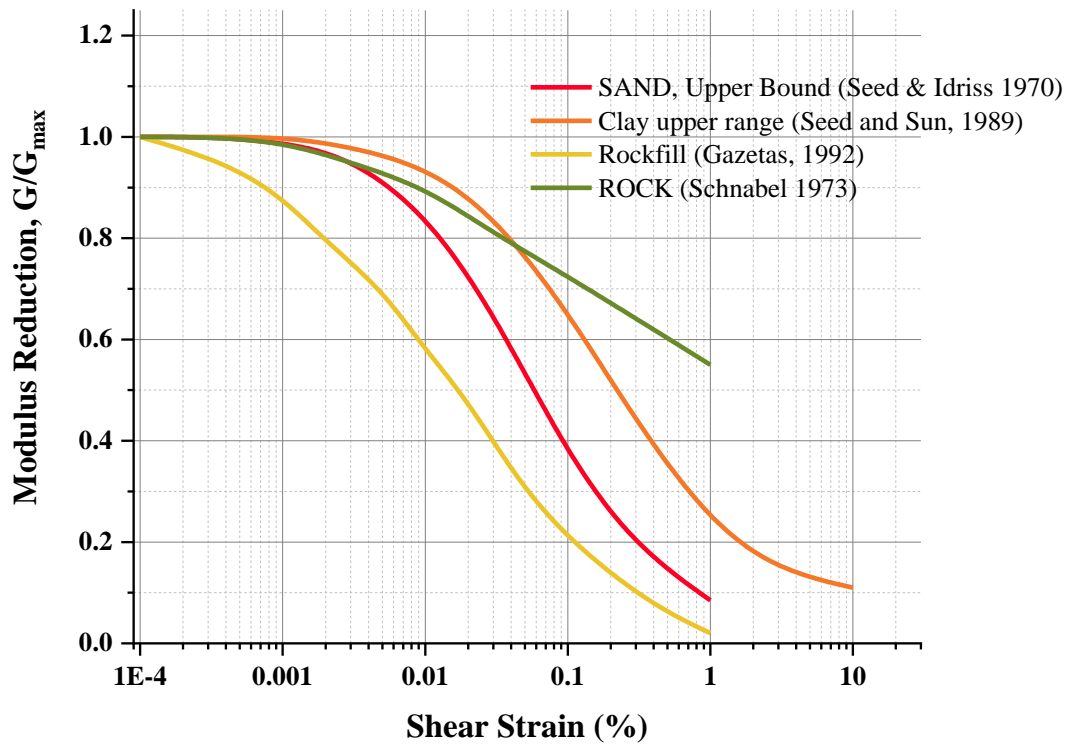
Figure 5.9 Shear modulus reduction curves as a function of cyclic strain for different soil types
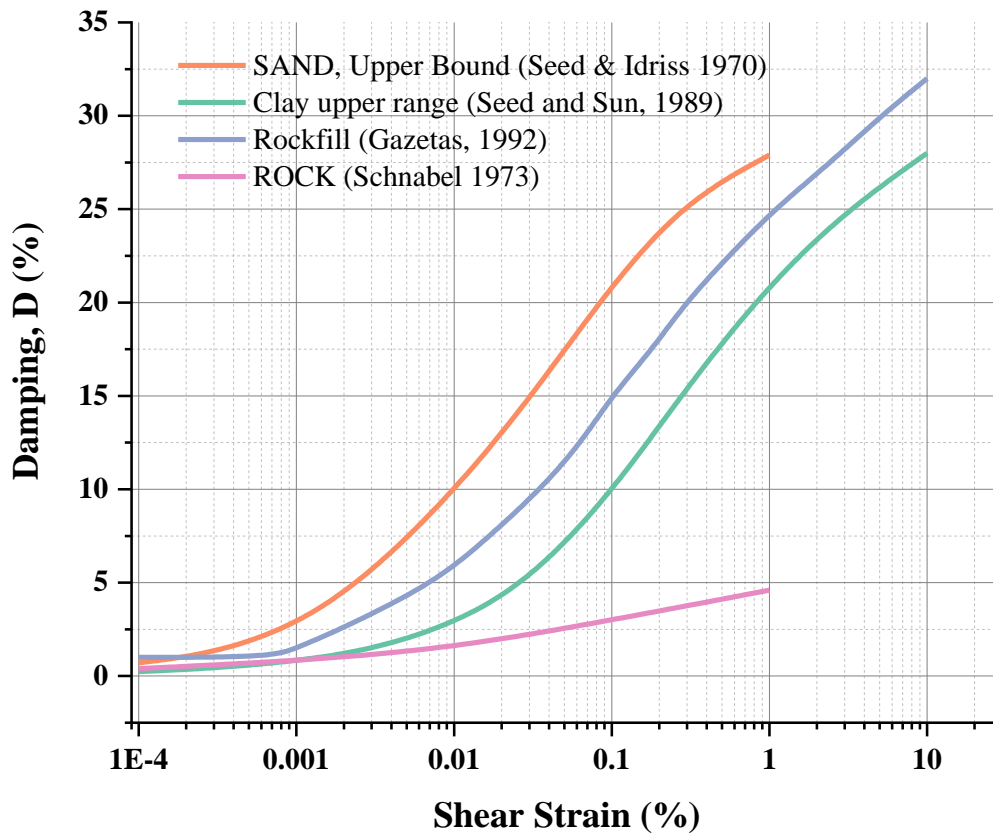
Figure 5.10 Damping ratio curves as a function of shear strain for different soil types

The M-R and damping curves chosen for each soil strata in a soil column are tabulated in Table 5.4, 5.5 and 5.6. The tables represent the soil modeling details for the soil strata depicted in Figure 5.5.

Table 5.4 Input parameters for soil modeling of a site categorized as 'sand'

Depth, m	Thickness, m	SPT 'N' value	Unit weight kN/m³	Description	Modulus reduction curve and damping curve
1.5	1.5	1	18.64	filled up earth	SAND, Upper bound (Seed & Idriss, 1970)
3.4	1.9	6	19.62	'sand' clay	
5.1	1.7	25	21.58	laterite	
7	1.9	33	22.56		
10.3	3.3	50	21.58	lateritic clay	CLAY, Upper range (Seed & Sun, 1989)
11.8	1.5	43	19.62	lithomerge	SAND, Upper bound (Seed & Idriss, 1970)
15	3.2	43	20.60		
16.7	1.7	42	19.62	Weathered rock	Rock Fill (Gazetas, 1992)

Table 5.5 Input parameters for soil modeling of a site categorized as 'All soil'

Depth, m	Thickness, m	SPT 'N' value	Unit weight kN/m³	Description	Modulus reduction curve and damping curve
1.5	1.5	4	19.62	Silty Sand	Soil Plasticity Index = 0 (Vucetic & Dobry, 1991)
3.4	1.9	13	20.70	Soft Laterite	
5.2	1.8	6	23.54	Medium Hard Laterite	
7	1.8	5	22.56	Soft Laterite	
8.8	1.8	18	17.17		
10.7	1.9	20	18.54		
12.5	1.8	8	17.56		
14.3	1.8	15	13.44	Silty Sand	
16.7	2.4	16	20.21		
18.3	1.6	20	17.56		
19.8	1.5	39	16.09	Weathered Rock	Rock Fill (Gazetas, 1992)

Table 5.6 Input parameters for soil modeling of a site categorized as 'clay'

Depth, m	Thickness, m	SPT 'N' value	Unit weight kN/m^3	Plasticity Index	Description	Modulus reduction curve and damping curve
0.9	1.5	7	20.60	23	'clay' Sand (Yellow)	CLAY (PI = 20 - 40, Sun et al, 1988)
3	2.1	18	19.62	27	Stiff clay Yellow	
7.6	4.6	2	16.87	40	Clay (Yellow)	
10.6	3	5	15.01	37	Clay with Organic matter	
14.7	4.1	5	15.50	-	Clay (grey)	CLAY, Upper range (Seed & Sun, 1989)
18.6	3.9	6	15.70	50	Clay	CLAY (PI = 40 - 80, Sun et al, 1988)
21.6	3	9	16.68	-		CLAY, Upper range (Seed & Sun, 1989)
24.4	2.8	50	19.52	20	Lateritic Soil	CLAY (PI = 20 - 40, Sun et al, 1988)
30	5.6	24	15.79	49	Silty clay	CLAY(PI = 40 - 80, Sun et al, 1988)
32.6	2.6	20	15.30	53		
37	4.4	17	14.72	-	Clay mixed with Quartz	CLAY, Upper range (Seed & Sun, 1989)
38.1	1.1	50	14.72	-	'sand' Clay	
41.1	3	19	14.72			
44.8	3.7	48	19.62	-	Weathered Rock	Rock Fill (Gazetas, 1992)

5.5   Selection and scaling of ground motion records

The generation of input motions for site response analysis consists of three main phases. The first phase involves defining the target spectrum representative of the regional

seismic hazard. The second phase deals with the selection of ground motion records compatible with the target spectrum. The third phase involves the modification of the chosen records with respect to the target spectrum. The practice of selecting ground motion varies widely and no definitive guidelines or strict procedures exist. However, the codal provision provides a general guideline to consider a minimum of five recorded or simulated rock outcrop horizontal ground motion records from events with magnitude and distance range consistent with those controlling Maximum Considered Earthquake (MCE) ground motion (ASCE, 2017). In the present study, the Uniform Hazard Spectrum (UHS) derived from PSHA was modified to obtain the target spectrum. The UHS is adjusted to obtain a target spectrum consistent with the local site condition by applying HTTA factor as shown in Figure 5.11.

The median UHS represents the time varied ground motion parameter (Sa at 5% damping). The developed UHS is a combination of different magnitude and distances contributing to the seismic hazard and is specific to a given Probability of Exceedance (POE). The objective of the study is to quantify the seismic site amplification by computing local site response. The input ground motions are selected considering seismic de-aggregation results and scaled with respect to the developed UHS. However, the UHS resulting from a single hazard level may not be sufficient for developing amplification equation. Hence, multiple hazard levels were considered. The design ground motions specified in the Indian seismic code correspond to 10% POE in 50 years i.e. Design Basis Earthquake (DBE). With DBE as the standard design condition, two more hazard levels i.e., 10*DBE and 0.25*DBE were defined based on the recommendations from Stewart and Afshari (2015). The DBE (abbreviated as HM) represents the median hazard level whereas 10* DBE (abbreviated as HL) and 0.25*DBE (abbreviated as HH) represents lower and higher hazard levels of the considered range. HL correspond to 65% POE and HH correspond to 2.5% POE in 50 years.

Once the range of the target spectrum was set, the next crucial step was to identify the range of magnitude and distance combination controlling the hazard at a site. De-aggregation performed for all the three hazard levels suggested events with magnitude (Mw) in the range of 4-6.5 occurring within a distance of 60km to be controlling the

111

hazard. The ground motion records were chosen from a similar tectonic regime as that of the study region (i.e. stable continental region) consistent with the de-aggregation findings. Ground motions recorded on a rock site with $V_{S(30)}$ corresponding to NEHRP 'B' ($>760ms^{-1}$) had to be considered to be consistent with the site condition of the derived target spectra.

With the aforementioned criteria, the ground motions were selected from the PEER NGA East website and European ground motion database (Luzi et al, 2016) In order to minimize the uncertainty in ground motion selection, multiple recordings were considered. Studies on the sensitivity of site response analysis to the number of input ground motions reveal at least 10, and preferably 20 ground motions to be considered when incorporating site effects into PSHA (Rathje et al, 2010). Based on the recommendations (Stewart and Afshari, 2015) and preliminary analysis, 11 ground motions for each hazard level summing up to 33 ground motions were considered for each soil column. The details of the ground motion records used in the study are given in Table 5.7. A few records have been repeated with different scaling factors to match the target spectrum. However, care was taken not to use more than four ground motions from the same event for a given hazard level.

Variety of scaling techniques exists in making the recorded ground motions compatible with the target spectrum. A recent study (Ansal et al, 2018) briefed the impact of different scaling techniques on the overall outcome of site response analysis. In the present study, the recorded acceleration time histories are modified through spectral matching (Al-Atik and Abrahamson, 2010) to match the target spectrum at each period using SEISMOMATCH (Seismosoft, 2016). The scaling factor was limited to 4 and the number of iterations to 20 as higher values may alter the ground motion to an extent where the record may lose its original nonstationary characteristics.
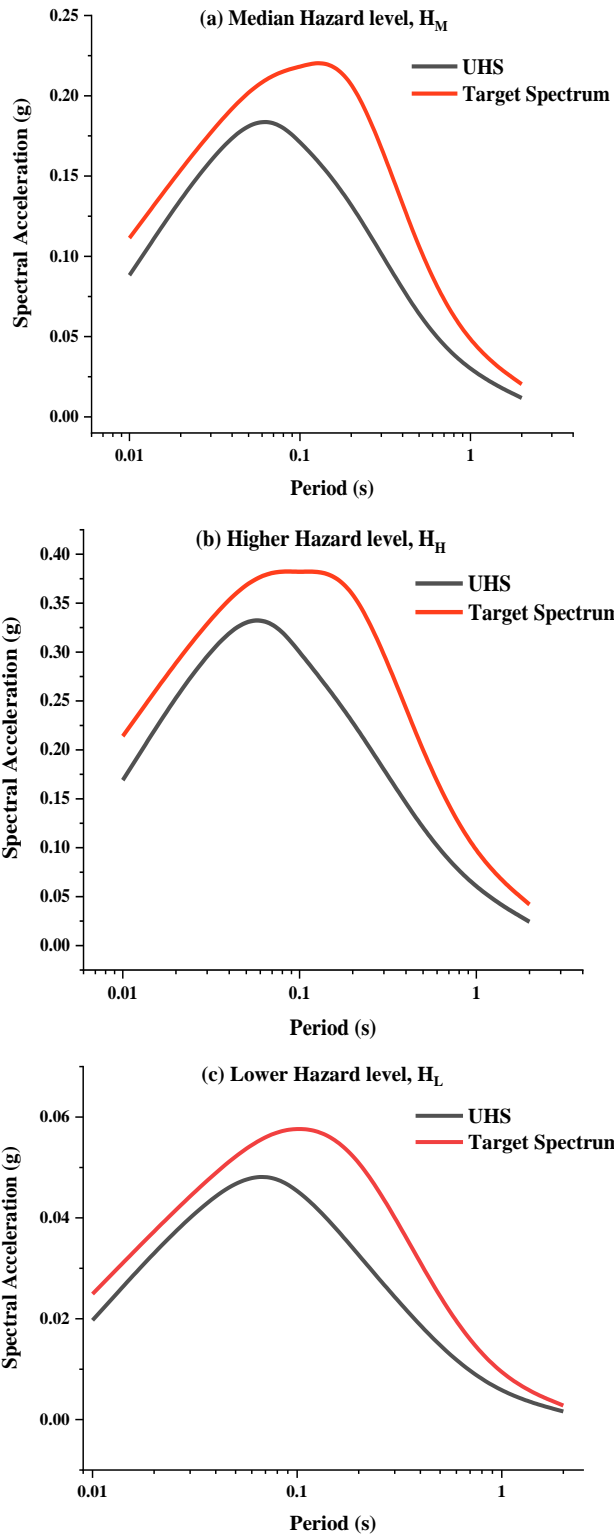
Figure 5.11 Plots depicting the UHS obtained from the earlier PSHA study and the modified UHS termed as 'Target Spectrum'

Table 5.7 Details of ground motions used in the study

Earthquake name	Acronym	Date	Mw	R_{rup} (km)	$V_{S(30)}$/ Site class	PGA (g)	Scaled PGA	Hazard level
RiviereDuLoup	RSN1688	06-03-2005	4.65	19.05	2000	0.045	0.100	Median hazard level, H_M
RiviereDuLoup	RSN1771	06-03-2005	4.65	41.75	1026	0.070	0.124	
Greenbrier	RSN6934	28-02-2011	4.68	6.27	1403	0.030	0.135	
Greenbrier	RSN7052	28-02-2011	4.68	54.07	1288	0.001	0.126	
ValDesBois	RSN4027	23-06-2010	5.1	52.94	1700	0.018	0.102	
Sicily	IT.NOT	13-12-1990	5.6	48.30	A	0.090	0.111	
Central Italy	3A.MZ14	26-10-2016	5.9	36.60	A	0.515	0.108	
Central Italy	3A.MZ19	26-10-2016	5.9	30.40	A	0.096	0.118	
Central Italy	3A.MZ21	26-10-2016	5.9	30.70	A	0.183	0.104	
Central Italy	3A.MZ19_30	30-10-2016	6.5	22.60	A	0.363	0.114	
Central Italy	3A.MZ29	30-10-2016	6.5	26.90	A	0.689	0.131	
RiviereDuLoup	RSN1688	06-03-2005	4.65	19.05	2000	0.045	0.172	Higher hazard level, H_H
RiviereDuLoup	RSN1771	06-03-2005	4.65	41.75	1026	0.070	0.237	
ValDesBois	RSN4027	23-06-2010	5.1	52.94	1700	0.018	0.174	
Greenbrier	RSN6934	28-02-2011	4.68	6.27	1403	0.030	0.231	
Greenbrier	RSN7052	28-02-2011	4.68	54.07	1288	0.001	0.227	
LaMalbaie	RSN1199	13-06-2003	3.53	10.06	2000	0.056	0.205	
LaMalbaie	RSN1192	13-06-2003	3.53	52.75	2000	0.000	0.218	
Central Italy	3A.MZ11	26-10-2016	6.5	24.8	A	0.044	0.170	
Central Italy	IT.ACC	26-10-2016	6.5	18.6	A	0.090	0.172	
Sicily	IT.NOT	13-12-1990	5.6	48.3	A	0.090	0.214	
Sicily	IT.SRT	13-12-1990	5.6	36.9	A	0.107	0.180	
L'Aquila	IT.ANT	06-04-2009	6.1	26.2	A	0.0198	0.0226	Lower hazard level, H_L
L'Aquila	IT.LSS	06-04-2009	6.1	41.5	A	0.0096	0.0191	
L'Aquila	IT.SUL	06-04-2009	6.1	53.7	A	0.0336	0.0229	
Sicily	IT.NOT	13-12-1990	5.6	48.3	A	0.0886	0.0253	
Sicily	IT.SRT	13-12-1990	5.6	36.9	A	0.1053	0.0263	
Bovec	RF.SVAL	12-04-1998	5.7	23.5	A	0.0249	0.0196	
Bovec	RF.MOG	12-04-1998	5.7	40.5	A	0.0151	0.0246	
RiviereDuLoup	RSN1681	06-03-2005	4.65	39.01	2000	0.0212	0.0232	
ValDesBois	RSN4027	23-06-2010	5.1	52.94	1700	0.0482	0.0276	
Central Italy	3A.MZ11	26-10-2016	5.9	31	A	0.0432	0.0192	
Central Italy	3A.MZ14	26-10-2016	5.9	36.6	A	0.0505	0.0271	

The comparison of the target spectrum along with the scaled records and mean matched spectrum is shown in Figures 5.12, 5.13 and 5.14. Since median UHS was chosen for the study, a slightly flexible range of scaled ground motions have been considered to represent varied input acceleration values.
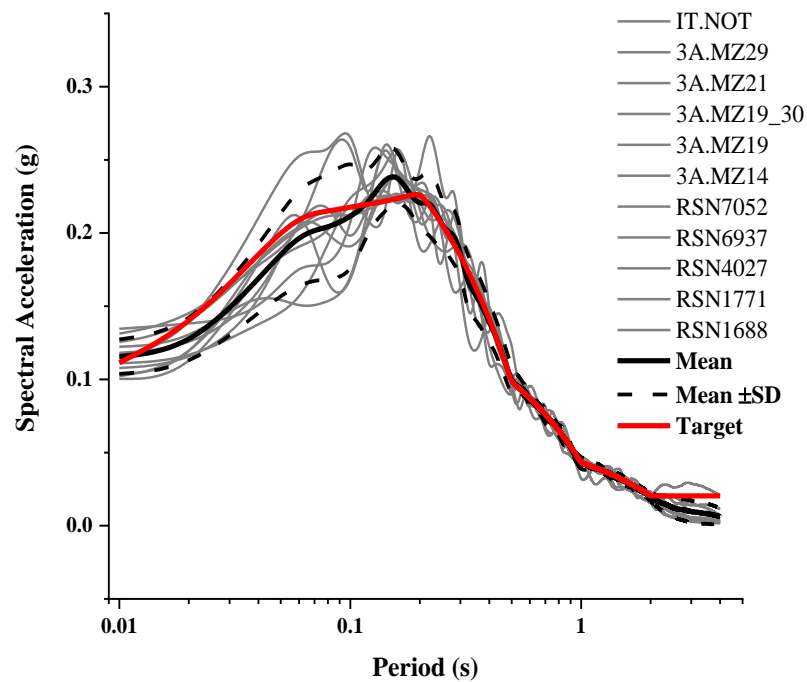
Figure 5.12 Plot of 5% damped rock acceleration spectrum of ground motions scaled to H_M
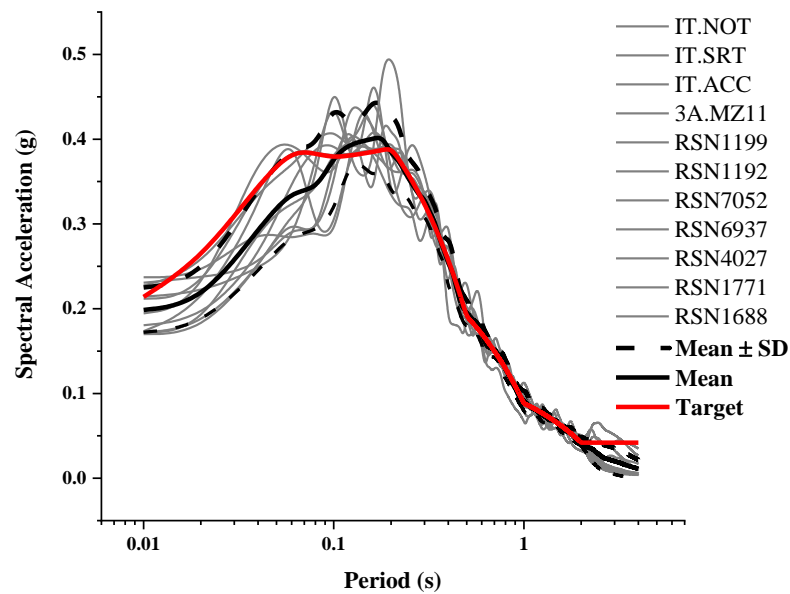
Figure 5.13 Plot of 5% damped rock acceleration spectrum of ground motions scaled to H_H
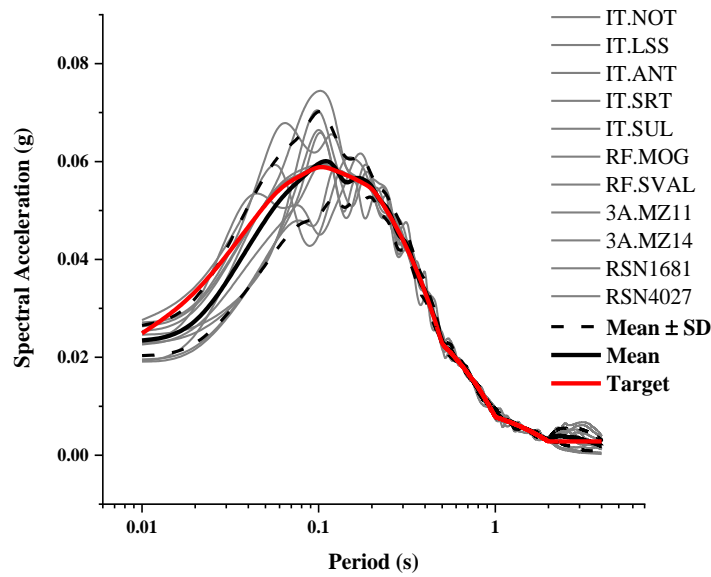
Figure 5.14 Plot of 5% damped rock acceleration spectrum of ground motions scaled to H_L

5.6 Site response analysis

The compiled borehole information along with the selected and scaled input motions served as input to equivalent linear analysis. The dynamic characteristics of the local soil are explained through different output parameters such as amplification and surface response spectrum. Due to space constraint, the results of all the simulated soil columns are not presented. Instead, three representative soil profiles having shear $Vs_{(30)}$ in the range of 331-332ms^{-1} but different soil type were chosen. Figures 5.15, 5.16 and 5.17 represents the amplification spectrum derived for all the 33 selected ground motions for the three soil types. It is interesting to note that two wide peaks are observed at 0.12s – 0.16s and 0.28s – 0.36s in all the three cases. The 'sand' site amplifies the ground motion at the bedrock by a factor of 4.64 near its predominant site period 0.33s. However, in spite of having the same $Vs_{(30)}$, a higher spectral amplification of 5.52 was observed at 0.36s for all soil site. A 'clay' site with $Vs_{(30)}$ of 331ms^{-1} produces the surface motion amplified 7.05 times the input motion at 0.28s. The significant difference in site amplification among the three considered profiles highlights the drawback of generic site amplification factors based on $Vs_{(30)}$ to capture the soil dynamic characteristics. In all the cases, higher variability was observed close to the first two soil resonant frequencies (i.e. first two peaks) and PGA. Relatively higher variability was observed in 'clay' deposits representing the large differences in the

116

intensity of input motions. The amplification characteristics of all the simulated soil profiles are presented in three different categories based on the predominant soil type.
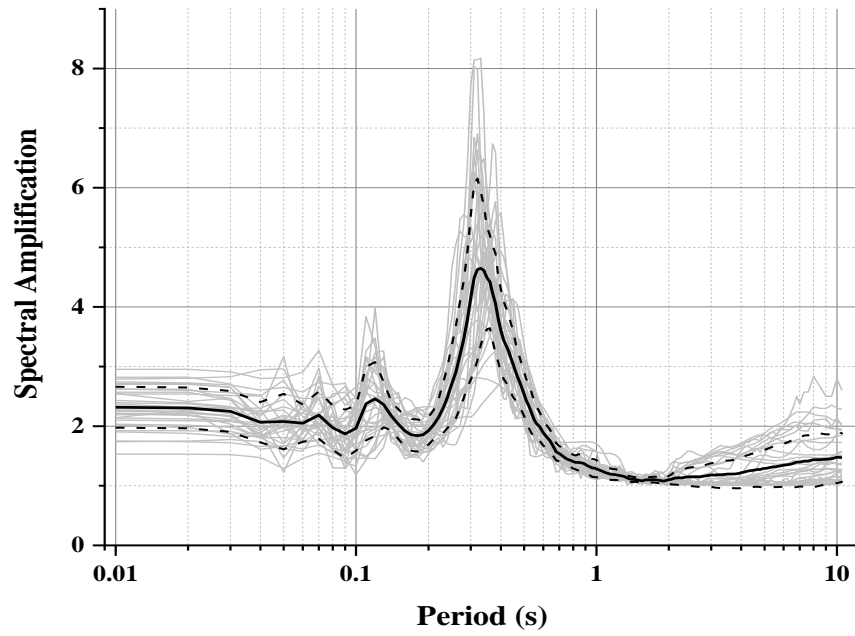
Figure 5.15 Amplification spectrum for 'Sand' type of soil
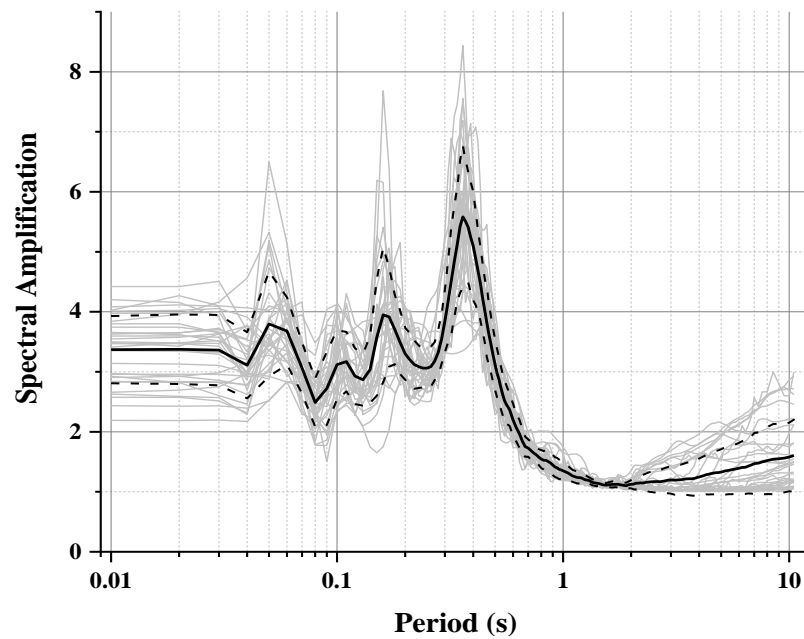
Figure 5.16 Amplification spectrum for 'All soil' type
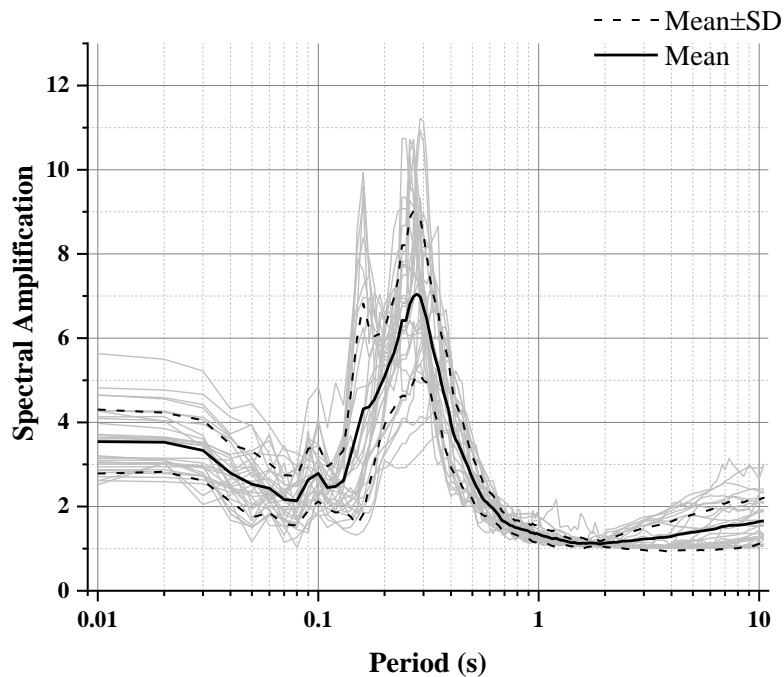
Figure 5.17 Amplification spectrum for 'Clay' type of soil

Figure 5.18 represents the median amplification function along with the standard deviation and 95% confidence interval as a function of rock spectral acceleration assessed at different spectral periods. The amplification function varying with the period (AF(f)) for different input motion acceleration values (PGA and S_a (f)) was compiled for all the numerically modeled soil deposits belonging to 'all soil' site category. Each soil profile generated 33 data points from the input ground motions for each period window. The plots for T=0.8s, 1s, and 1.5s clearly distinguish the difference in the input ground motion scaled corresponding to three different hazard levels. At T = 0.01s (PGA) and 0.2s, the amplification observed is higher compared to other periods. Additionally, the nonlinear behavior of the soil is well represented in these two periods. The natural site period of the analyzed soil columns lies in the range of 0.3-0.5s. However, at T = 0.8s, 1s and 1.5s the trend of the fitted curve changes from a negative slope to positive slope and is characterized by lower amplification factors. It can be inferred that a negative correlation exists at periods below the fundamental site period. The nonlinear regression coefficients obtained for T=3s is not statistically significant as evident from the bottom right panel of Figure 5.18. Though the values of AF(f) are considerably less, sustained amplifications are observed at longer periods implying that the site characteristics are critical for longer period ground motions.

118
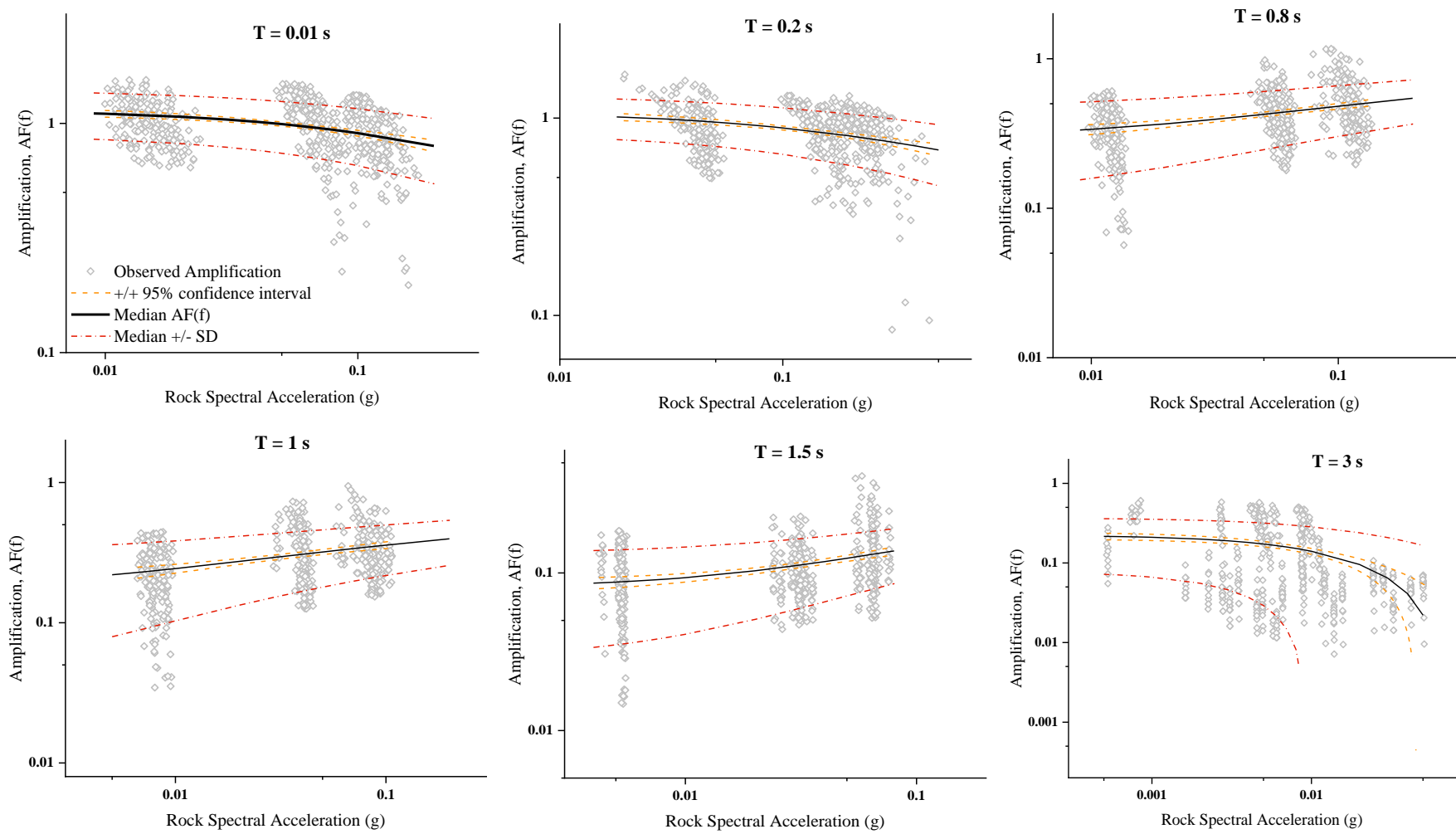
Figure 5.18 Amplification factors regressed against rock spectral acceleration for 'all soil' sites.
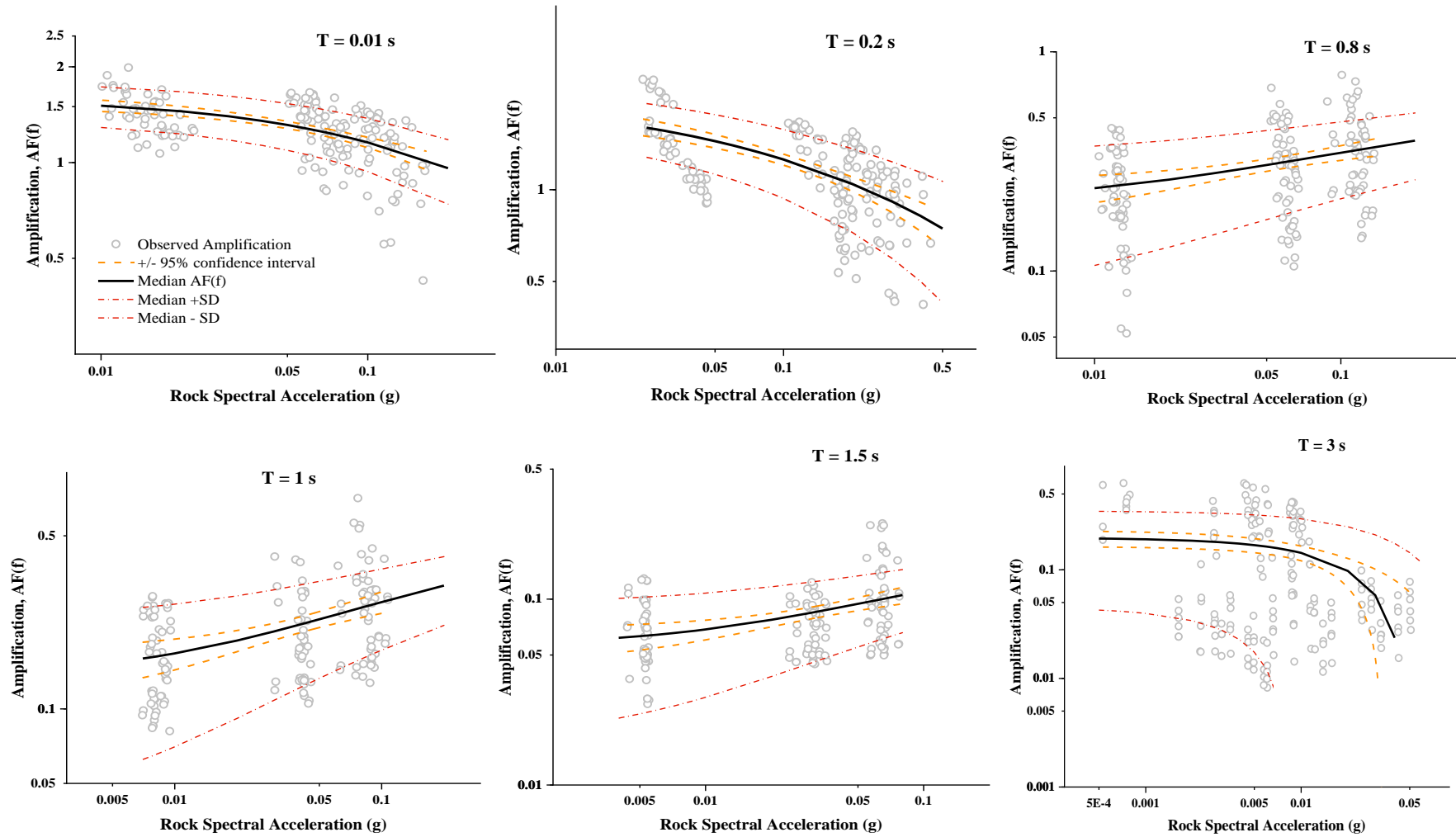
Figure 5.19 Amplification factors regressed against rock spectral acceleration for 'sand' sites
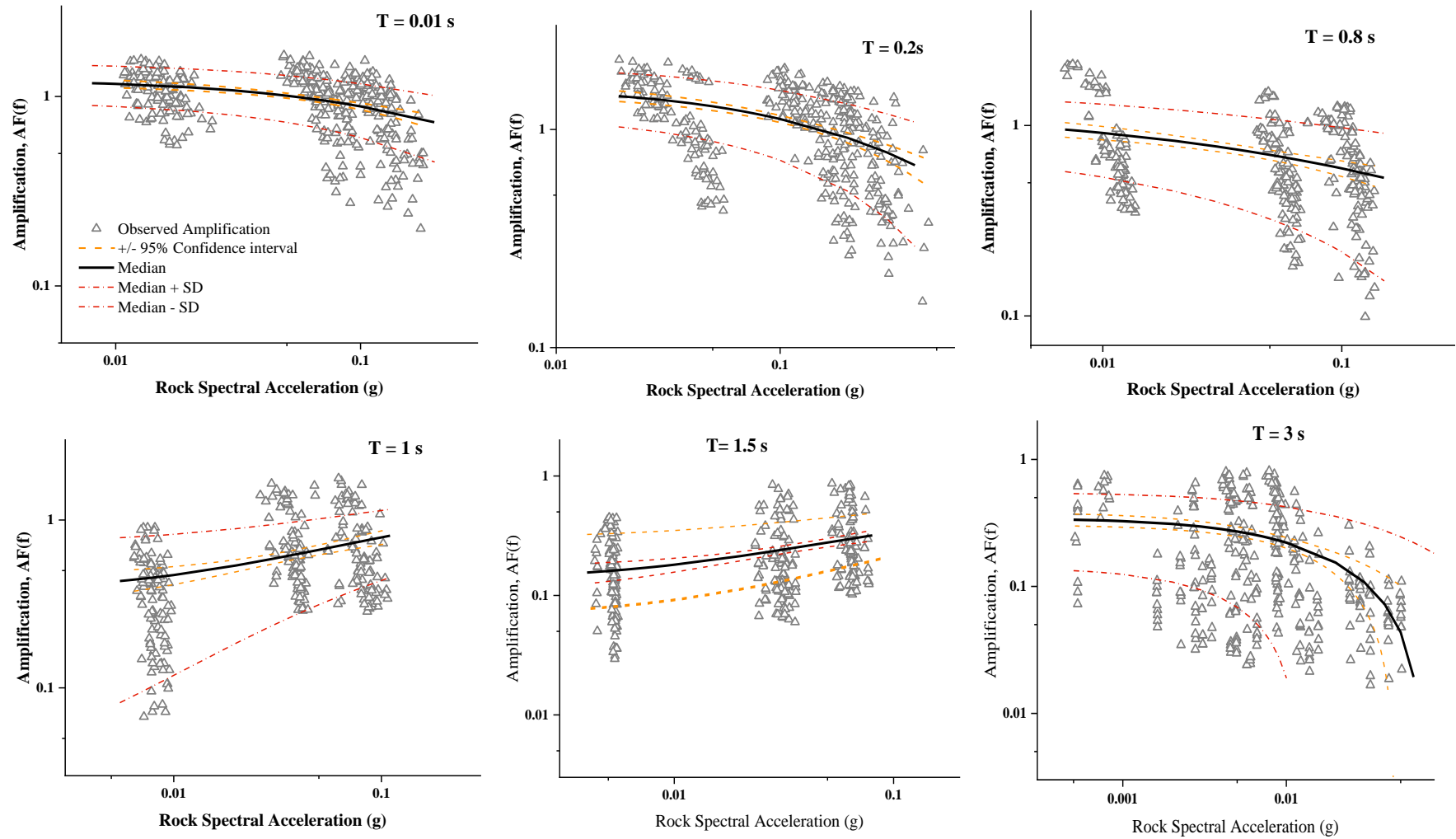
Figure 5.20 Amplification factors regressed against rock spectral acceleration for 'clay' sites

Figure 5.19 represents the amplification functions derived for 'sand' site for different spectral periods. The observed amplification data points are sparse and widely distributed in comparison with the previous plot due to a lesser number of simulated soil profiles. However, they were sufficient to draw a nonlinear amplification function for different spectral periods.

The natural period of the soil profiles lies in the range of 0.31s – 0.38s. The amplification for the depicted soil type i.e. sand tends to be highly nonlinear especially at periods below the average site period. Significant variability is visible for higher spectral acceleration values at T=0.02s, demonstrating larger variation at T=0.8s, 1s, and 1.5s. This is mainly due to the large differences in intensity of the selected input ground motions as evident from Figures 5.12, 5.13, and 5.14. Similar to the previous Figure5.18, an upward shift was observed at intermediate and longer period range (T = 0.8s – 1.5s). The inability of the equivalent linear methodology to converge to a solution for high-intensity records is the reason behind this upward shift (Papaspiliou et al, 2012). Additionally, the equivalent linear method estimates higher amplification at the smaller period range and overestimates resonant responses when the soil becomes nonlinear (Kim et al, 2016). Further, the amplification reduces drastically for periods after the resonant vibration period of the sites.

Another interesting observation made during the study is the shift in the natural period depending on the strain induced by various ground motions. In order to explain this phenomenon, a typical 'sand' site with a predominant period of vibration of 0.33s was considered (Figure 5.15). Ground motions with lower PGA values especially scaled to H_L indicated a lower period of vibration in the range of 0.317s – 0.319s. On the other hand, ground motions scaled to H_H indicated a higher period of vibration in the range of 0.348s – 0.358s. Though the shift from the predominant period of vibration is small for the considered ground motions, a higher shift can be witnessed in the case of ground motions with higher acceleration values.

Figure5.20 depicts the nonlinear regression in logarithmic space between amplification factor and input rock spectral acceleration for 'clay'. The amplification observed at T=0.01s and 0.2s is less when compared with 'sand' deposit. However, the 'clay' sites have demonstrated sustained amplification at longer periods (T= 1s and 1.5s). While

the majority of the soil deposits have their natural period around 0.4s, there are a few deposits with a period as high as 0.7 – 0.9s displaying a diverse range. However, the shift in the natural period depending on the induced strain was noticed similar to the 'sand' site. Due to this phenomena, resonance is attained by soil profiles at the elongated site period (T = 0.8, 1s and 1.5s) driving the regression towards a positive correlation. As a result, the upward shift in the fitted median amplification curve was observed at these periods. The 'clay' deposits exhibit stronger linearity compared to 'sand' deposits by producing higher amplification at T=0.8s. The 'clay' site demonstrated consistently higher AF(f) compared to the other soil categories implying amplification of longer period ground motions. Overall, 'clay' sites demonstrate slower stiffness degradation and hence, less nonlinear when compared to 'sand' sites.

The nonlinear regression of amplification factors against rock spectral acceleration provide a mean value as well as the variability between the observed value and the fitted mean value. This variability commonly referred to as the standard deviation for the three site categories investigated in the study has been shown in Figure 5.21.
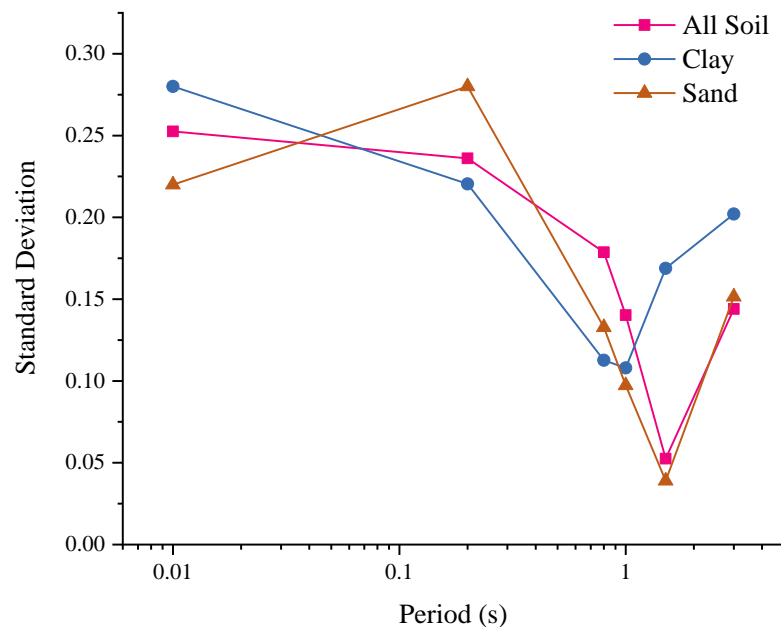
Figure 5.21 Plot of the standard deviation of the derived amplification function

The standard deviation of the 'all soil' site seems to be in the mid-range compared to the other two over the entire period range. A large number of soil profiles considered under this category tends to have reduced the overall variability. However, the highest

value of 0.28 was observed in 'clay' (T = 0.01s) and 'sand' (T = 0.2s) type sites at a different yet lower spectral period. The general trend of the curves suggests that the standard deviation is high for periods below the site periods and drops drastically for greater periods. It is important to note that the standard deviation does not exceed 0.3, in agreement with the findings of Bazzurro and Cornel (2004). As higher variability was observed in 'sand' deposit at T=0.2s, the residual plot for the same has been presented in Figure 5.22.
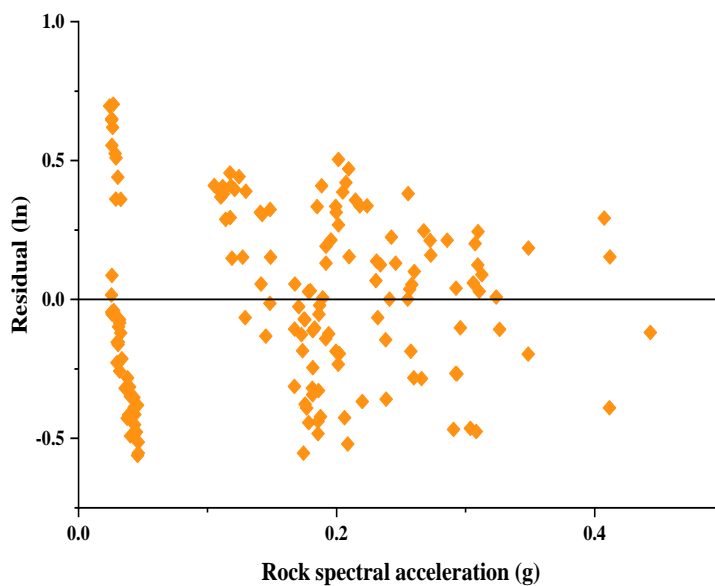
Figure 5.22 Residual plot of fitted AF(f) with respect to Sa (0.2s) for 'sand' type

The ground motion records scaled to H_L tend to have acceleration value ($S_a(0.2s)$) in the range of 0.3g, due to which huge overlapping of the ordinates can be seen. However, the amplification varies slightly, moving the X ordinate about the same Y ordinate leading to higher residuals in the fit. This can be balanced by choosing ground motions with varied acceleration values as evident in input values $S_a(0.2s) > 0.2g$. Another interesting observation is that the nonlinear curve fits well at higher acceleration values demonstrating strong nonlinearity in 'sand' soils.

The $V_{S(30)}$ is widely accepted as an index for soil amplification. However, the present study suggests that the soil characteristics affect the amplification to a greater extent. In order to validate this, three profiles of same $V_{s(30)}$ but of different soil type are considered for plotting mean amplification in Figure 5.23. As evident from the Figure5.23, the sand exhibits higher amplification at lower input values but decreases

gradually with the increase in PGA demonstrating its nonlinear behavior. For the 'clay' site, amplification reduces as the intensity increases and de-amplification can be noticed for PGA values as small as 0.005g. However, there is still a very clear amplification at longer periods as shown in Figure 5.20. An important observation made during the analysis of 'clay' deposits is that as the soil plasticity index increases, the behavior of the soils became less nonlinear. The overall amplification is lesser in 'All soil' type when compared to the other two soil types. However, the amplification does not substantially reduce for higher PGA values implying less nonlinearity in the soil sediment.
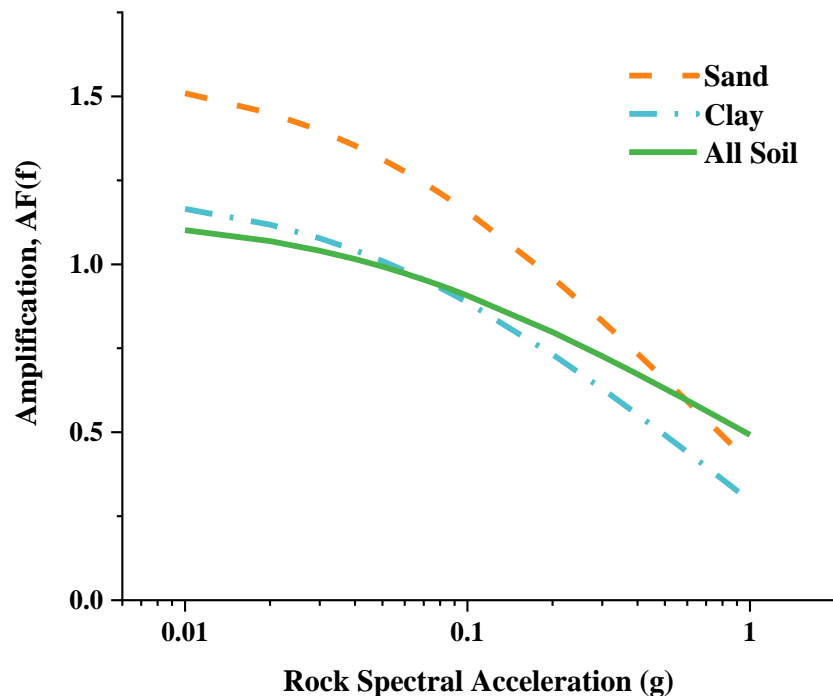
Figure 5.23 Mean site amplification of all three soil types at T=0.01s

The fluctuation in the recorded acceleration values at the interface of each constituent layer in a soil profile has been shown in Figure 5.24. The PGA at the bottom of the soil profile is almost the same for the three distinct soil types. As the propagation progresses through various soil layers toward the surface the transmitted ground motion undergoes modification consistent with the dynamic characteristics and the same is evident from Figure5.24. The three soil types with the same shear velocity are still dependent on the other soil characteristics in modifying the behavior of the ground motion. Maximum amplification can be observed in the 'clay' deposit for a smaller depth. A similar trend has been followed by the all soil type but amplification becomes significant in the top

10m. In the case of 'sand' deposit, a gradual amplification was observed with the top 6m being crucial in altering the PGA value. The PGA values at the surface are 0.21g, 0.15g, and 0.20g for clay, sand and all soil respectively. The careful examination of each ground motion record along the depth revealed that records with PGA < 0.1g tend to produce higher amplification when compared to records with PGA>0.2g. It is mainly due to the fact that as the intensity of the applied motion increases the nonlinear behavior of the soil becomes predominant and dampens the observed surface PGA. The strong nonlinearity of the 'sand' sites as observed in Figure14 tends to reduce the intensity of the ground motion at the surface.
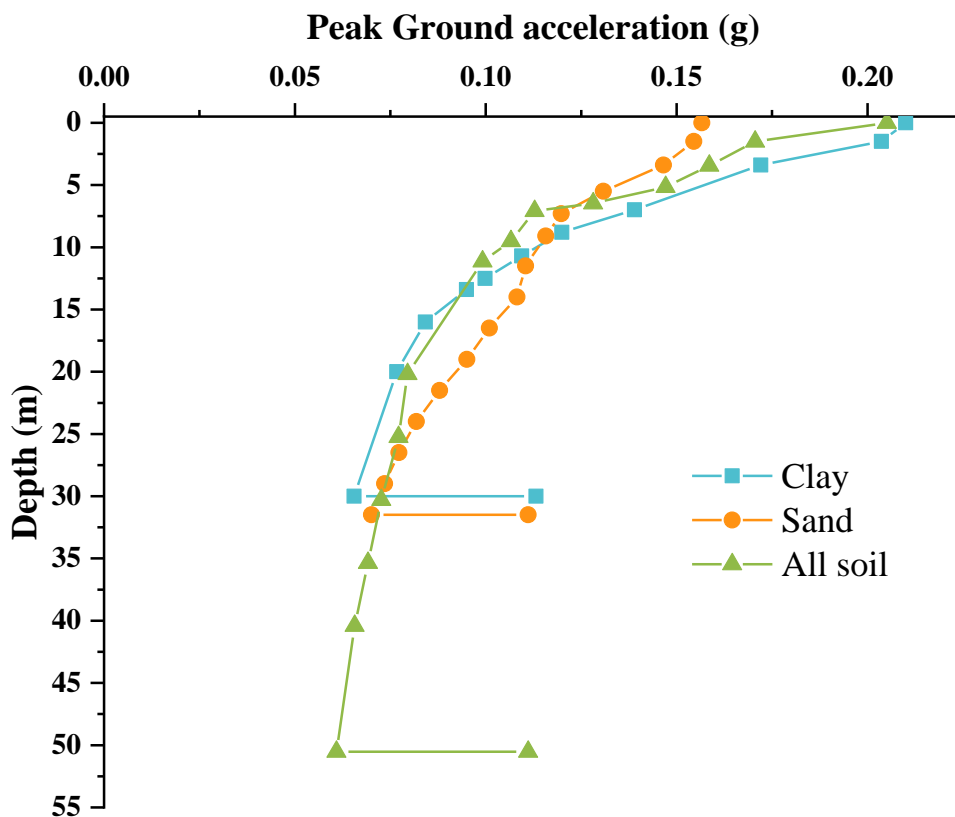
Figure 5.24 Plot of variation of PGA along with the depth of the soil profile for different sites

The site-specific seismic hazard analysis was performed by transforming the GMPE to include developed site amplification equation for various spectral periods. The hazard curves have been compared for two different spectral periods for varying site condition in Figure5.25. At T = 0.01s, the surface level hazard curve can be seen distinctly varying from that of rock at lower spectral acceleration values. However, as PGA increases

beyond 0.3g, the trend tends to be diminishing and closely merging towards the rock hazard curve. This behavior is mainly due to the fact that the amplification equation was derived as a function of input motion at the bedrock level, which in turn induces the strong nonlinear effect. At T = 1s, the intensity values are lower and as a result, the nonlinear effect is minimal. Hence, the difference in the estimated intensity values between the two site conditions for T=1s is greater than the same at T=0.01s.
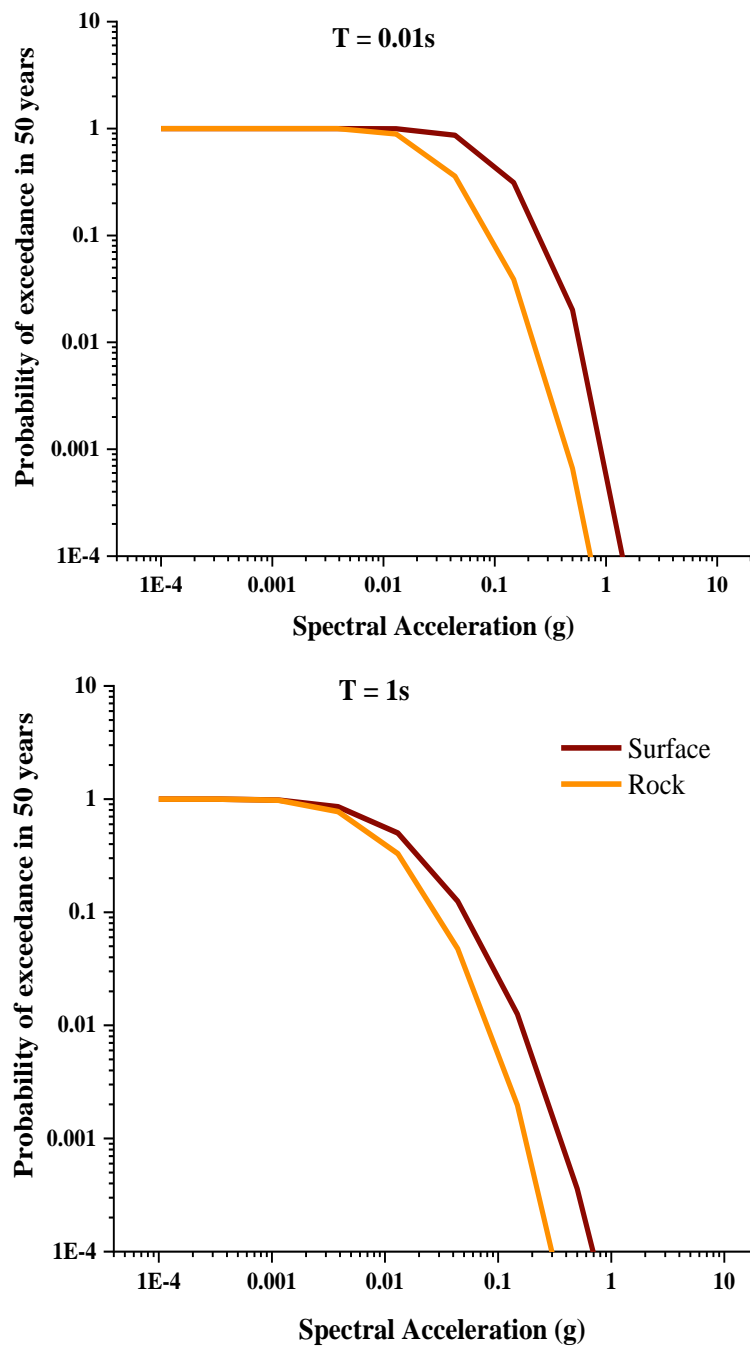
Figure 5.25 Hazard curves for the rock and 'all soil' condition

The computed surface UHS was compared with the elastic spectrum recommended by various codes as well as the target spectrum as shown in Figure5.26. The soft soil condition was taken for computing the spectra from the Indian code. The code underestimates the amplification potential of regional soils and hence cannot be used for site-specific applications. A similar comparison was made with EC-8 by choosing the ground type as 'C' and importance class as II for generating the site-specific spectra. The codal provision underestimates the spectral values at smaller periods (T<0.5s) and overestimates at higher values. A similar observation was made when compared with the ASCE elastic spectrum for soil class D. However, the ASCE spectrum provides a better estimation and captures the site amplification reasonably well among the three codal provisions.

The lower estimation of the spectra resulting from the study for a certain period range may be due to overdamping by EQL analysis. As expected the 'sand' site provides higher spectral acceleration followed by clay and all soil. However, a shift in the predominant frequency was observed only for the 'clay' type. The shift can be attributed to the fact that the 'clay' soil produces significant amplification even at longer periods (T = 0.5s − 1s) and a few of the soil profiles under 'clay' site category have natural period in the range of 0.8-1s causing resonance at the prolonged period. It is a common understanding that modeling taller soil column can modify the predominant period of spectral amplification. However, Bazzurro and Cornel (2004) state that the amplification at the surface does not vary significantly for frequencies beyond the fundamental period of vibration (f_{sc}) of the soil column. It was observed that f_{sc} shifts towards lower resonant frequency as the intensity of the input motion increases and this explains the lower predominant frequency observed in Figure 5.26. Hence, the generated surface spectrum is suitable for site-specific applications.

The seismic hazard map depicting the PGA values at the surface has been presented in Figure5.27. Majority of the study area are susceptible to moderate to high seismic hazard and the current codal provision underestimates the seismic as well as the amplification potential of the study area. As per IS 1893 (2016), the study area belongs to zone III and susceptible to moderate ground shaking of PGA 0.16g. The PGA values for design basis earthquake intensity level (10% probability of exceedance in 50 years)

128

varies between $0.11 - 0.35$g. Hence, the findings highlight the necessity for site-specific studies in the Southern region of India whose seismic potential has been underestimated over the years.
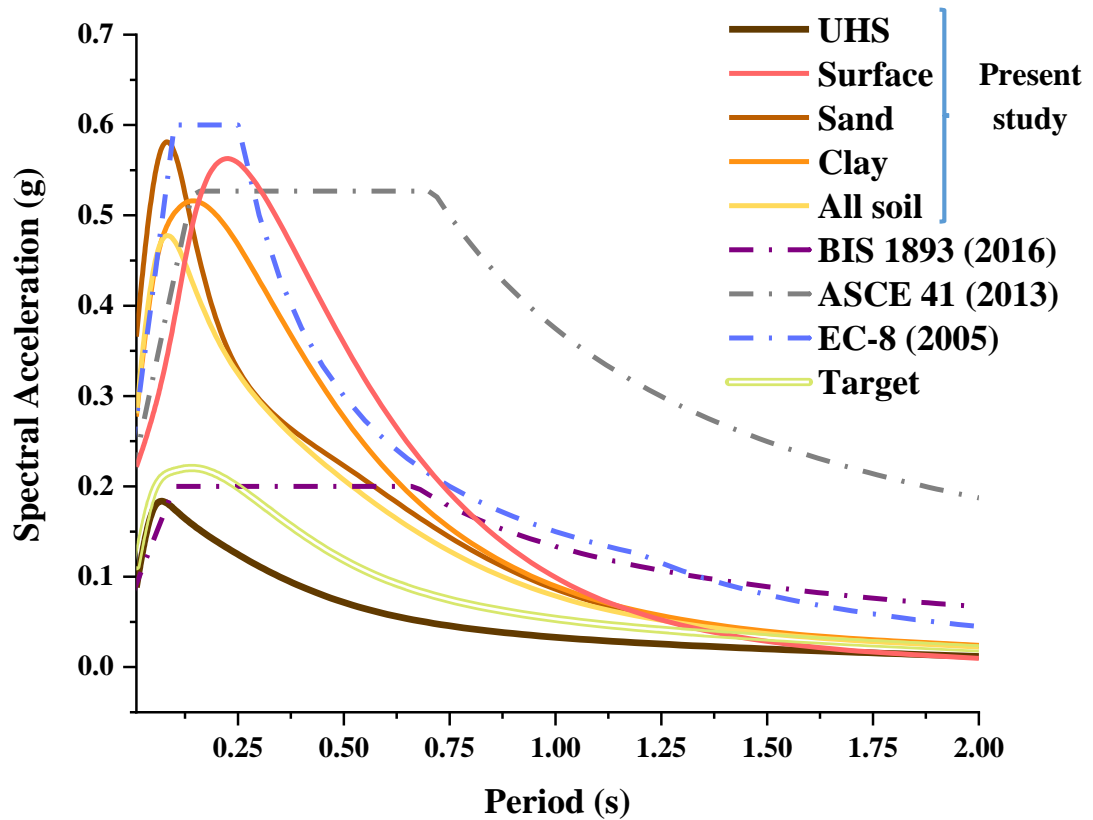
Figure 5.26 Comparison of site-specific spectra obtained from the study with that of the codal provisions and the target spectrum
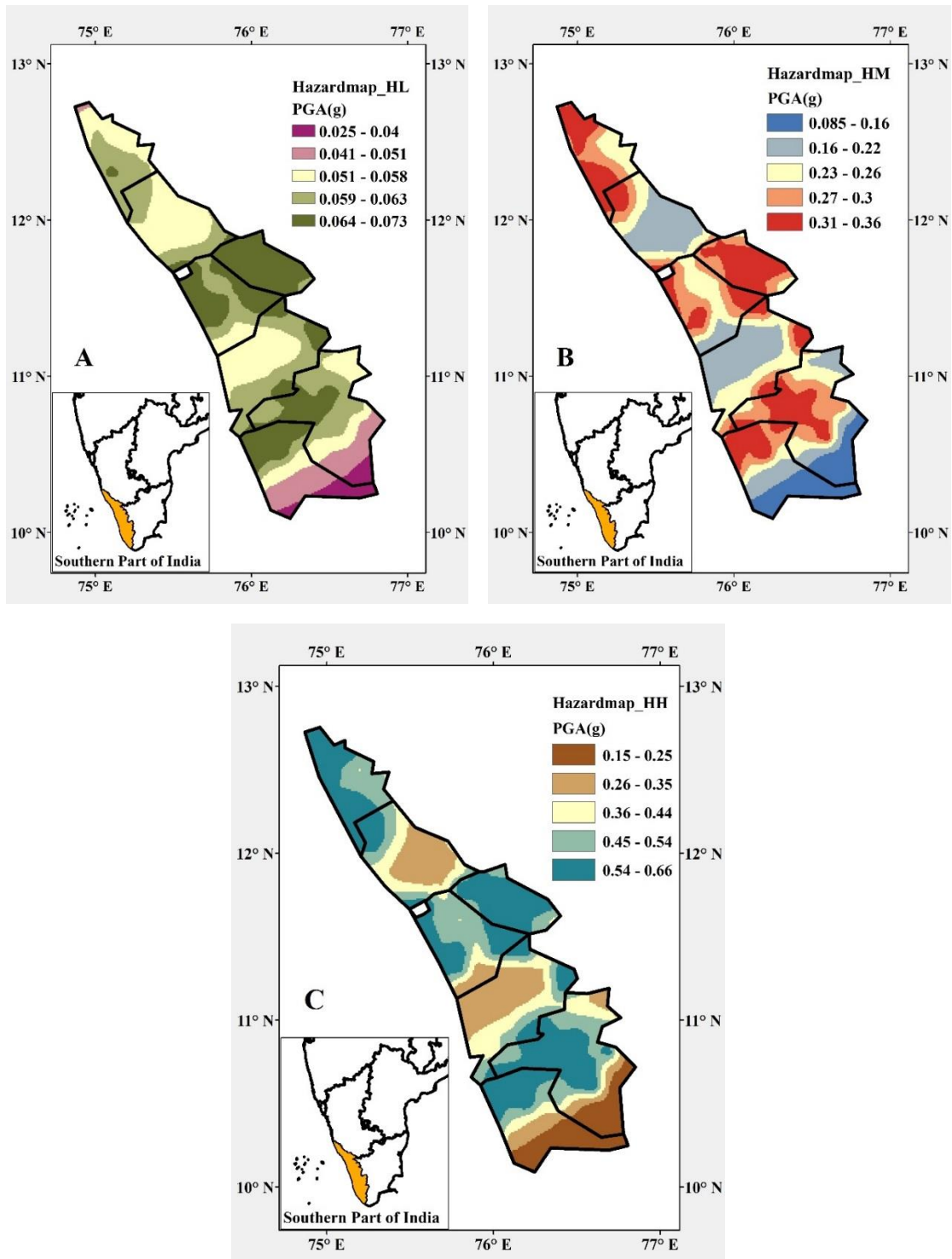
Figure 5.27 Seismic hazard maps for the study region for A. 65% probability of exceedance, B. 10% probability of exceedance and C. 2.5% probability of exceedance in 50 years

5.7 Elastic Design Response Spectra

The surface-level ground motion time histories simulated from site response analysis was used to generate elastic design response spectrum for the study region. The soil columns were categorized based on SPT 'N' value to match the site classification of IS 1893 (2016). The ground motion time histories for each soil category were normalized corresponding to the maximum value of the acceleration a_{max}. The response spectrum was generated corresponding to each normalized time history. The mean and mean + 1 standard deviation of the response spectrum was calculated for each soil type. These curves are further idealized corresponding to maximum acceleration, displacement and velocity in their respective sensitive regions as shown in Figure 5.28.
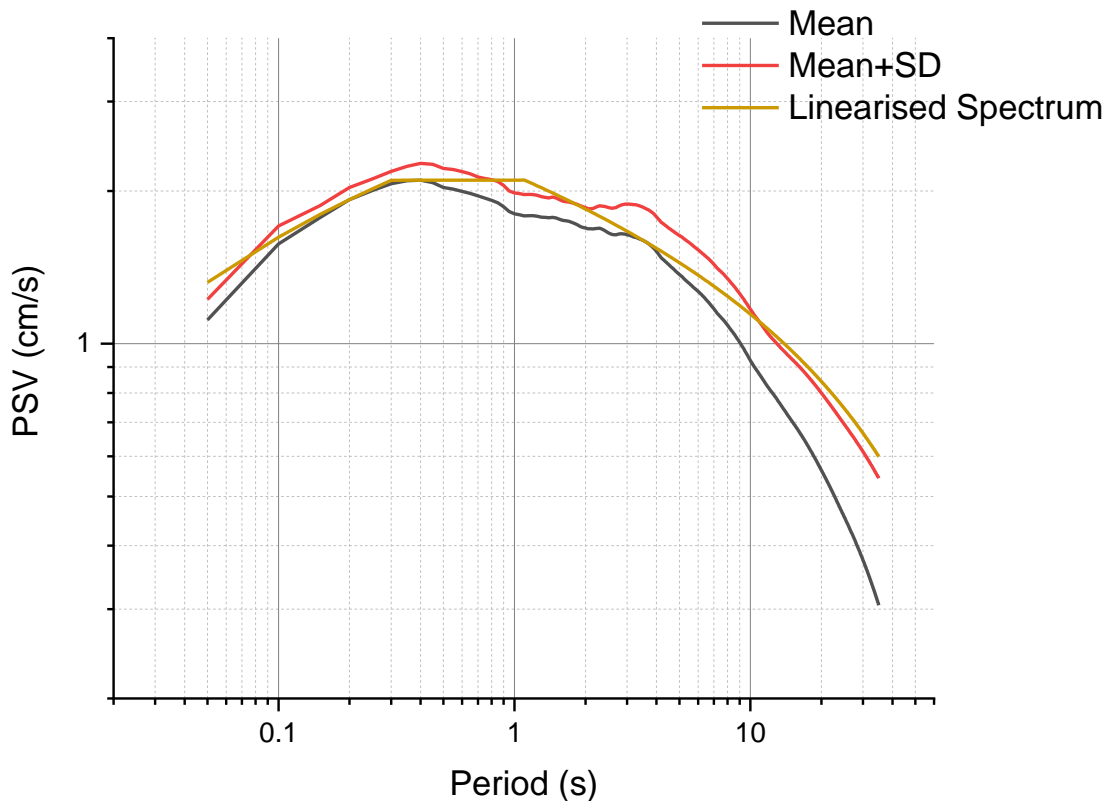
Figure 5.28 Construction of design response spectrum and idealized spectrum

A total of 528 ground motions were used for the Type I category of soils i.e Rock/ Hard soils. In the logarithmic space, power distribution was adopted to derive equations for the design spectrum. The elastic design spectrum for all the types of soils can be generated from the developed equations 5.3 to 5.5. Equation 5.3 gives the expression for generating the power spectrum as shown in Figure 5.29.

$S_a/g = 2.85$ $T \leq 0.25s$

$S_a/g = 0.73/T^2$ $0.25s < T \leq 1.1s$ (5.3)

$S_a/g = 0.79/T^2$ $1.1s < T \leq 4s$

$S_a/g = 0.05$ $T > 4s$
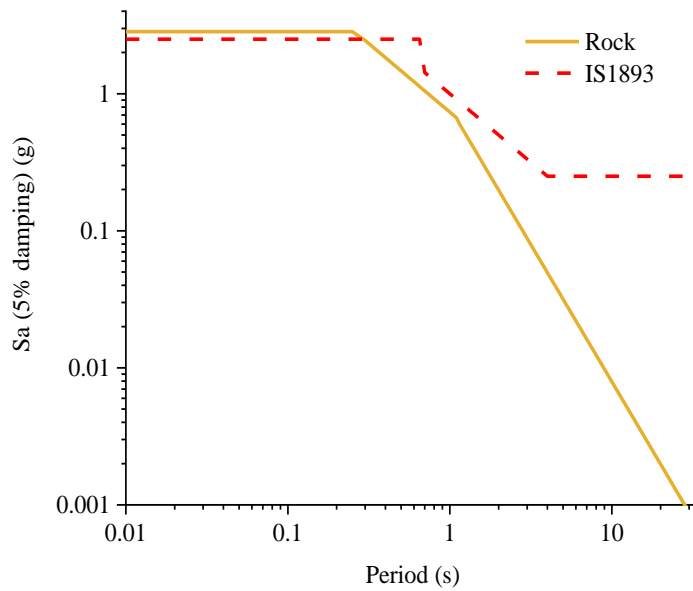
Figure 5.29 Elastic design Spectrum for Type I soils

Similarly, 759 ground motions were simulated and used for deriving the design spectrum for Type II soils. The equation to generate the spectrum shown in Figure 5.30 is given as

$S_a/g = 3$ $T \leq 0.32s$

$S_a/g = 0.95/T$ $0.3s < T \leq 0.85s$ (5.4)

$S_a/g = 0.82/T^2$ $0.85s < T \leq 4s$

$S_a/g = 0.05$ $T > 4s$

The design spectrum for soft soil category/type III soils was generated using 165 ground motions (Figure 5.30). All the derived spectrum are with respect to a damping ratio of 5%.

$S_a/g = 3.7$ $T \leq 0.3s$

$S_a/g = 1.07/T^2$ $0.3s < T \leq 0.85s$ (5.5)

$S_a/g = 0.923/T^2$ $0.85s < T \leq 4s$

$S_a/g = 0.05$ $T > 4s$
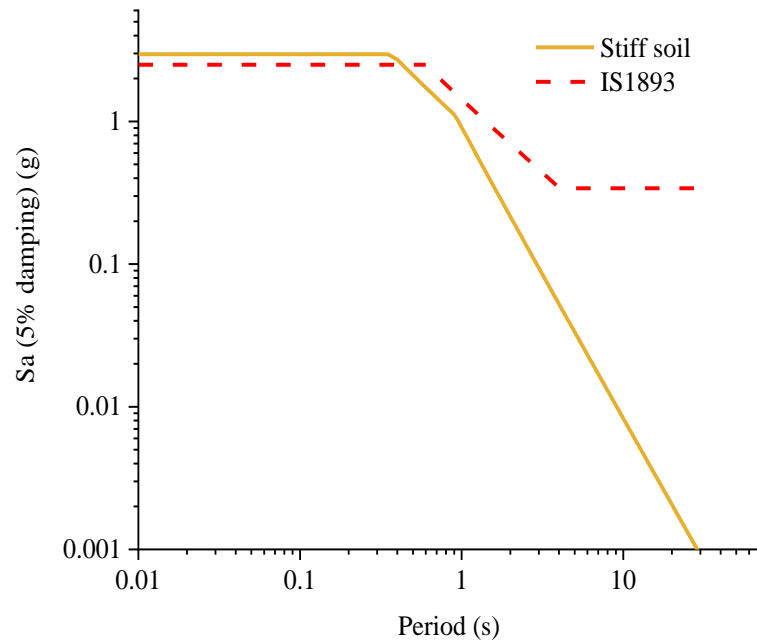
Figure 5.30 Elastic design Spectrum for Type II soils
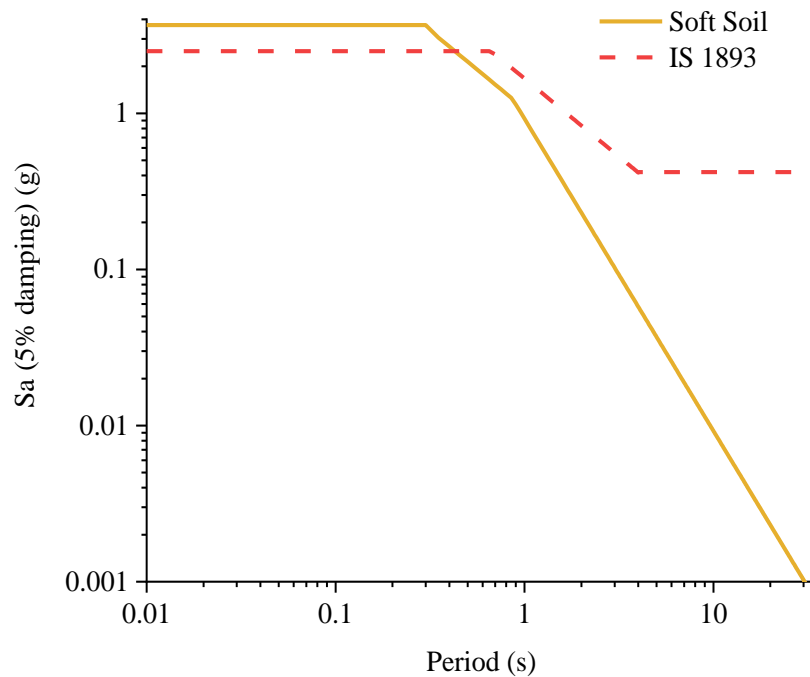
Figure 5.31 Elastic design Spectrum for Type III soils

In Figures 5.29, 5.30 and 5.31, the generated design spectrum has been compared with that of IS 1893 (2016). The generated spectrum matches well with that of the code but except in Type III category. Additionally, the code overestimates the spectral values at longer periods.
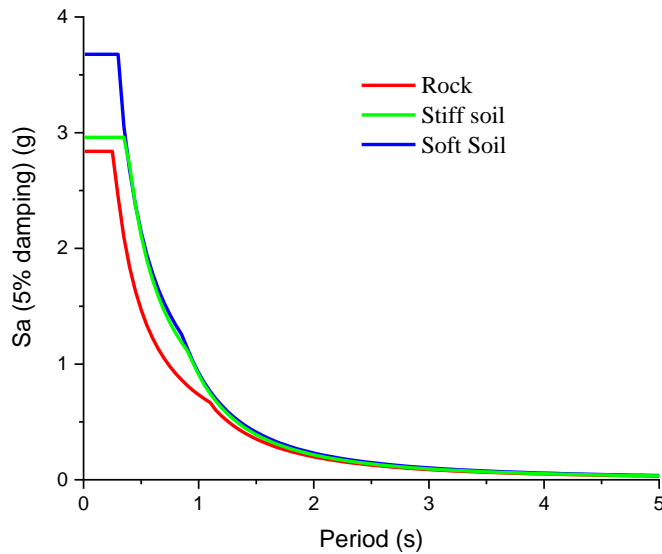
Figure 5.32 Comparison of all the three generated design response spectrum

Comparison of the derived design spectrum for all the three categories in Figure 5.32 suggests that the width of the plateau is wider for soft soil when compared to the other two. Also, each curve begins at a different PSA value and does not coincide as in the case of IS 1893 (2016) spectrum.

5.8 Site characterization using Topographic slope

The topographic slope was calculated on ArcGIS v10.1 and correlated to $V_{S(30)}$ using the correlation proposed by Wald and Allen (2007). The $V_{S(30)}$ map for the study area has been shown in Figure 5.33. The majority of our study area is classified under NEHRP site category D and the Western Ghats and other hill stations such as Nilgiris, B R hills are grouped under site class B and C. The identification of site classes based on the shear velocity is helpful in computing site amplification factor for each individual site category. The resulting surface level ground motion is visualized as bedrock motion modified by the soil layers. The amplification factor for each site category was calculated and multiplied with the bedrock motion. The amplification factor observed for each site class is listed in Table 5.8. It is evident from Table 5.8 that the sites corresponding to lower shear velocity are subjected to higher amplification when compared with that of the sites with higher shear velocity. Site class B and C suffers maximum amplification whereas few regions with higher PGA values at the bedrock level have witnessed lesser amplification.

Table 5.8 Spectral Amplification observed for various site classes classified based on shear velocity

Shear Velocity (V_s)- m/s	Amplification Factor
180 - 359	1.33 to 1.85
360 - 649	1.62 to 1.82
650 - 749	1.67 to 1.82
750 - 799	1.63 to 1.80
800 - 959	1.63 to 1.64

In seismic hazard estimation, PGA has been chosen as the standard ground motion parameter for understanding the seismic potential in different regions.
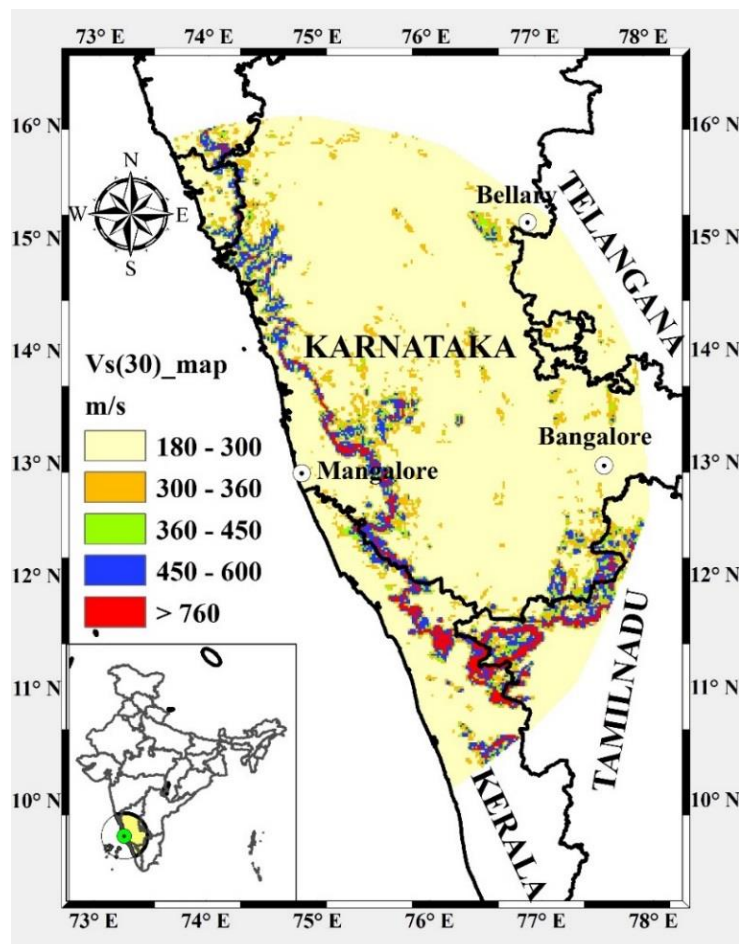
Figure 5.33 Vs (30) map generated from the slope values for the study area

The hazard maps corresponding to 10% and 2% probability of exceedance for the study area has been plotted in Figure 5.34, illustrating the variation of PGA at the surface

level. The highest value in the order of 0.23g - 0.30g was observed in the Bellary and Raichur districts at the surface level for 10% probability of exceedance. The predominant shear velocity estimated in this region is $180 - 240ms^{-1}$ with few areas having a higher velocity in the range of $300 - 360ms^{-1}$. This region is under constant mining activity and numerous earthquakes of moderate intensity and few major ones have been witnessed in the past. This region comes under seismogenic source zone 1 (SZ1) and the majority of the earthquakes are believed to be occurring due to the excessive mining activity and tectonics of Chitradurga Boundary shear along with its associated faults. For Bengaluru region, the projected PGA value a the surface level is around $0.12g – 0.176g$ for an estimated shear velocity in the range of $180 - 300ms^{-1}$ implying that the region is more susceptible to seismic hazard than mentioned in the code. The site amplification studies carried out by Vipin et al (2009) demonstrates amplification factor in the range $1 – 2$ for a major portion of Bengaluru with some parts experiencing higher amplification and these results are found to be in good agreement with the current research findings.

The central part of Karnataka comprising of Shimoga, Chikmagalur, Chitradurga, Mysore, and Mandya districts are susceptible to low to moderate ground shaking. The mountains existing in Shimoga and Chikmagalur are mainly part of Western Ghats and not much amplification of ground motion has been observed in these districts. The Southern Coastal region covering Dakshina Kannada, a major portion of Kerala, Kodagu, and Nilgiri districts are subjected to frequent moderate ground shaking. A part of our study area encompassing Kerala is predicted to have higher seismic activity and the seismic hazard due to Bhavani and Moyar shear in association with Kaveri, Tirupur and Bhavani fault. The seismic hazard was computed for the neighboring state Goa and it was found that South Goa is more Vulnerable when compared to North Goa. Though Goa, Uttara Kannada, Dakshina Kannada, and Kerala lie on the same coastal stretch, the seismic hazard has shown an increasing trend as one move towards South.

Additionally, the design spectrum generated from different methods used in the study has been compared with the codal provisions of different countries in Figure 5.35. The solid lines represent the findings from the study and the dashed lines represent the codal provisions. Significant amplification of the UHS estimated at a reference site condition

136

can be observed. can be observed An interesting observation made from Figure 5.35 is that the site-specific study matches satisfactorily with the EC-8 and ASCE 41. This is due to the fact that both these codes consider input ground motion as one of the important factors in determining amplification at any given site. The spectrum generated from site response accommodates nonlinear behavior of soils and so does ASCE 41. Hence, the two curves match very well until T = 0.3s. Also, the elastic spectrum generated using topographic slope method predicts satisfactory acceleration values and can be used as first-order estimates in the absence of site-specific data. IS 1893 and ASCE 41 overestimates the spectral values at longer periods.

5.9   Concluding remarks

The present study attempts to investigate the influence of local site amplification and incorporate the same for hazard computation in a probabilistic manner. In this regard, a number of borehole data were collected, processed and compiled in a systematic manner. The dynamic characteristics of the constituent layers in each bore log were modeled using suitable modulus reduction and damping curves. These modeled soil profiles were subjected to recorded ground motions selected and scaled to a target spectrum. The nonlinear behavior of the soil to various input motions was captured using an equivalent linear approach. The computed amplification factors for various input motion intensity level (Spectral acceleration at 5% damping, Sa) was correlated using a nonlinear regression equation for various spectral periods. The amplification equations were developed for each soil type such as 'Clay', 'Sand' and 'all soil'. The site-specific PSHA was performed by transforming a generic GMPE into a site-specific one and integrating with the already developed seismic source model for the study area. The ground motion time histories generated at the surface level from site response analysis was used to derive the elastic design spectrum for different soil categories. In the absence of soil data for the whole of the study region, topography has been used as a proxy for $V_{S(30)}$ and amplification for different ranges of $V_{S(30)}$ was estimated. The estimates made in the study using Topography are for preliminary consideration alone and site-specific studies have to be undertaken for construction of important building sand infrastructures.
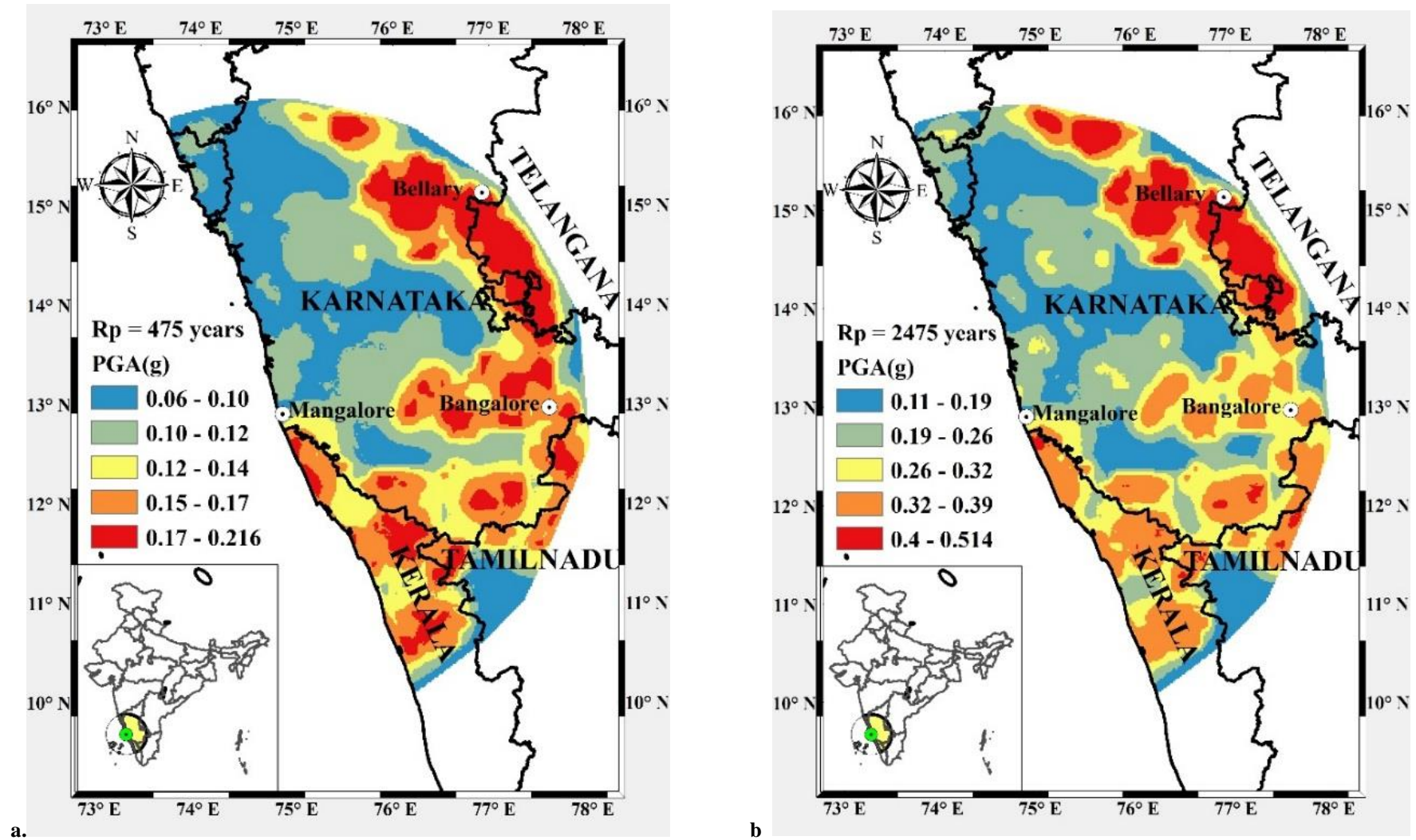
Figure 5.34 Hazard maps representing PGA value at 10% (a) and 2% (b) probability of exceedance at the surface level

138
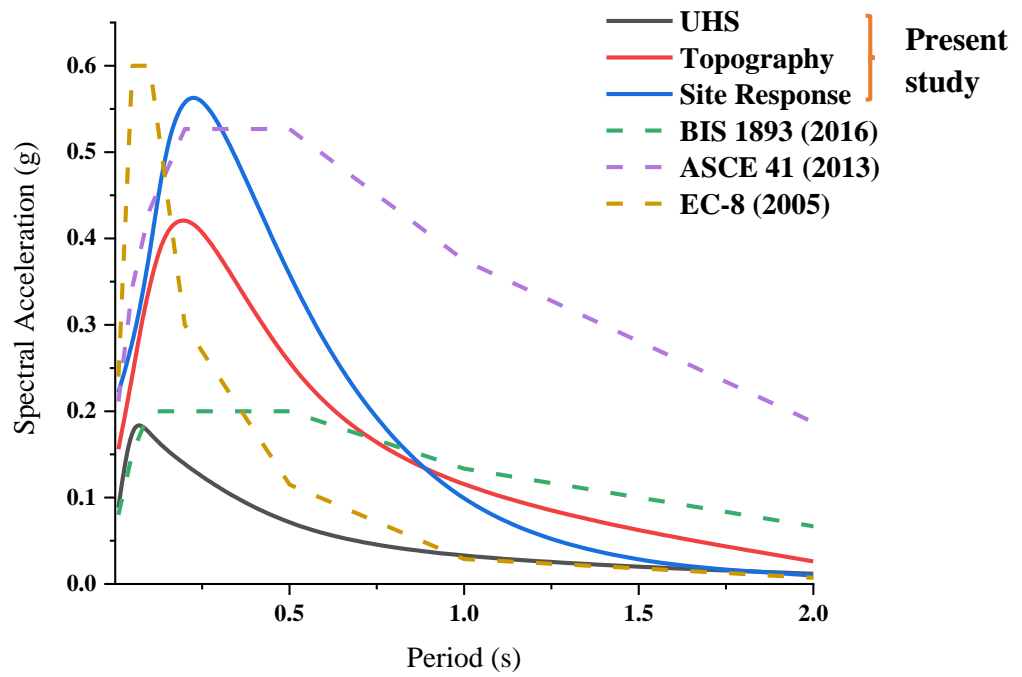
Figure 5.35 Comparison of the design spectra obtained from the study with that of the codal provisions

CHAPTER 6

CONCLUSIONS

6.1   Summary

The first step towards seismic hazard assessment is the evaluation of past earthquakes in the region. In the present study, the earthquake data was collected for the study region from various global and local sources. The recording of earthquakes was not instrumentally advanced till 1960. Hence, the earthquake events from the pre-instrumental period were mainly from the previously compiled catalogs and regional seismicity studies. An earthquake catalog spanning over 190 years with a few prehistoric events from the early 16th century has been compiled. The compiled catalog can be temporally classified into Historic and Instrumental catalogs. Diffused seismicity is one of the attributes of stable continental regions such as the study area. Hence, area seismic sources zones were adopted for modeling the seismic sources. The area source zones were identified and delineated based on the tectonic features, predominant focal mechanism, and observed seismicity. The seismicity parameters were estimated for each of these source zones using the maximum likelihood method.

The GMPEs developed for regions of the similar tectonic regime were tested qualitatively and four suitable candidate GMPEs were selected for hazard estimation. The epistemic uncertainties involved in formulating seismic source and ground motion models (GMPEs) is addressed by the logic tree approach. Sensitivity analysis has been performed for GMPEs with different weighting factors in a logic tree combination. The probabilistic seismic hazard analysis (PSHA) has been carried out using the methodology proposed by Cornell (1968) for a reference site condition ($V_S > 1500 ms^{-1}$) using CRISIS 2015.

The geotechnical characterization was accomplished using two different techniques. In the first approach, the information on local soil deposits was collected for North Kerala in the form of SPT bore logs. The local shear wave velocity (V_S) profile was developed for each of the soil columns. Hazard consistent ground motions were selected and scaled to perform site response analysis on the modeled soil columns. The local site effect has been captured by performing 1D equivalent linear analysis using SHAKE

2000. The amplification models as a function of input ground motion for 'sand', 'clay' and 'other soil' have been developed for different periods. These amplification models are incorporated into PSHA by transforming the GMPEs as explained by Bazzurro and Cornell (2004). The resulting uniform hazard spectrum (UHS) for all the three soil types was compared with the elastic spectrum of various codes. The synthetic ground motions generated from site response analysis are further used to propose an elastic design spectrum for different soil types. The soil categories are similar to the classification of IS 1893 (2016). The site-specific elastic design spectrum for a damping ratio of 5% has been developed for different soil types and compared with that of the codal provisions.

The topography of the study area poses difficulty in obtaining site-specific geotechnical information at a micro level. The topographic slope was calculated to obtain the $V_{S(30)}$ map for the study area. Once the $V_{S(30)}$ had been estimated for the entire region, it was easier to calculate the local amplification using suitable generic amplification functions. The findings and conclusions drawn from each phase of the study have been presented in the following sections.

6.2   Probabilistic Seismic Hazard Analysis

Based on the results presented in the study, the following conclusions have been drawn.

1. While attempting to understand the seismicity of the study area, it was observed that few dormant faults have undergone reactivation in the recent times and one such example is Shimoga earthquake (12th May 1975) as there were no records of past seismic activity in this region in the entire catalog duration.

2. The coastal region has witnessed very few major earthquakes ($M_W > 5$) and some of the shocks have originated away from the shore. The Bengaluru city is more frequently subjected to low magnitude earthquakes (M_W 2 - 3) compared to any other region.

3. The seismic hazard estimated for each of the mapped seismogenic source zones demonstrated that the seismic source zone 1 (SZ 1) is more vulnerable than the rest. The ongoing mining activity in Bellary and Raichur district is suspected to be the main reason for the increased seismic activity.

4. The estimated seismicity parameters (b < 1) reveal a larger proportion of small magnitude earthquakes in the study region.

5. The qualitative testing and sensitivity analysis of candidate GMPEs revealed that although the models have been developed for a similar tectonic regime, they may overestimate the values of ground motion parameter. Hence, the selection of GMPEs and assigning weighting factors in a logic tree requires the utmost attention.

6. The study area belongs to seismic zone III (IS 1893, 2016) with a zone factor of 0.16g. However, the seismic hazard maps suggest that the PGA value varies between 0.16g – 0.24g. Hence, the seismic potential of the study region is between seismic zone III and IV.

7. The comparison of the estimated hazard values with other studies reveal that the catalog period, choice of GMPEs and evaluation of aleatory and epistemic uncertainty in the input parameters are the crucial factors influencing hazard estimation.

8. The de-aggregation of the predicted seismic hazard revealed that earthquakes of range (M_w) 4–6 occurring within a distance of 35kms to be the most influential for any given site of interest. The outcome implied that nearby sources make a significant contribution to the seismic hazard of a specific site and also higher magnitude events have a larger spatial extent.

9. The seismic hazard tends to be increasing towards the South. Further, the seismic zoning map recommended by the IS 1893(2016) is Intensity-based and not an effective standard for comparing the seismic hazard estimated using a probabilistic approach.

6.3   Site Response Analysis

The present study attempts to investigate the influence of local site amplification and incorporate the same for hazard computation in a probabilistic manner. In this regard, a number of borehole data were collected, processed and compiled in a systematic manner. The dynamic characteristics of the constituent layers in each bore log were modeled using suitable modulus reduction and damping curves. These modeled soil profiles were subjected to recorded ground motions selected and scaled to a target spectrum. The uniform hazard spectrum (UHS) for a reference site condition

($V_s > 1500ms^{-1}$) was already developed from PSHA for the study region. The UHS was modified to generate a target spectrum compatible with the local site condition. The target spectrum was developed for three hazard levels and the selected ground motion records were spectrally matched with the respective target spectrum. The nonlinear behavior of the soil to various input motions was captured using an equivalent linear approach. The computed amplification factors for various input motion intensity level (Spectral acceleration at 5% damping, S_a) was correlated using a nonlinear regression equation for various spectral periods. The amplification equations were developed for each soil type such as 'Clay', 'Sand' and 'all soil'. The site-specific PSHA was performed by transforming a generic GMPE into a site-specific one and integrating with the already developed seismic source model for the study area. Additionally, the local site effects were studied by plotting incremental changes in the PGA value of the ground motion transmitted through each soil layer. The computed surface uniform hazard spectrum was compared with the elastic spectrum recommended by various seismic codes. The findings of the study are summarised below.

1. The soil profiles modeled in the study belongs to NEHRP 'C' ($360-760ms^{-1}$) and 'D' ($180 - 360ms^{-1}$) site categories and the study region belongs to seismic zone III (moderate level shaking).

2. The average spectral amplification observed is 3 for 'All soil' sites, 5 for 'clay' sites and 3.5 for 'sand' sites of the study region.

3. 'Sand' sites exhibit nonlinear behavior by undergoing large amplification for smaller intensity measure but reduce substantially as the spectral acceleration values (S_a^r) values exceed 0.1g. Among the three considered soil types, the 'sand' site is by far the highly nonlinear material and 'all soil' is less nonlinear.

4. 'Clay' sites exhibit amplification even at longer periods (T=0.8s, 1s, and 1.5s) but become less nonlinear with the increase in plasticity index. Hence, the 'clay' site plays a major role in the event of long-period seismic waves.

5. Three soil profiles of V_{S30} in the similar range demonstrated distinct amplification characteristics. The 'sand' site amplifies 33% (max. value) more than all soil and 29% more than the 'clay' site for lower S_a^r values. However, as the S_a^r (> 0.5g) increases all soil amplifies 9% more than 'sand' soil. This observation implies that

the local site amplification cannot be determined by $V_{s\,(30)}$ alone as the soil characteristics also influence the amplification.

6. The amplification characteristics observed in various spectral period frames suggests that PGA offers an unbiased and better prediction of amplification function. The same parameters studied at different spectral period suffer from resonance (site-specific effect) and demerits of the EQL method (computational capacity).

7. The comparison of the computed response spectra suggests that the seismic codes underestimate the spectral acceleration values for $T < 0.25s$ and overestimates for $T > 1s$. The elastic response spectrum from NEHRP matches the estimated site-specific spectrum at the short period range.

8. The seismic hazard map suggests higher values of intensity measure (PGA) in the mid – Kerala region and the same extending towards South.

The present investigation aims to highlight the influence of soil type in local site effects and correlate amplification to the soil type instead of the conventional $V_{S(30)}$. The study addresses the dilemma in adjusting a host response spectrum to target region and has implemented a procedure to reduce the uncertainty in various input parameters. The overall amplification has been captured and integrated with the rock PSHA in the most robust way possible. The study provides a seismic hazard map at the surface level for the different probability of exceedance. These maps coupled with the site-specific spectrum can be used to plan, design and construct infrastructures of socio-economic importance.

6.4   Site characterization using topography

1. The shear wave velocity ($V_{S(30)}$) map developed from topographic amplification revealed competent material near the hilly terrain and loose soil deposits in the plains and near coastal line. Majority of the study area belongs in the $V_{S(30)}$ range of $180 – 360$ ms^{-1} corresponding to Site class 'D' of NEHRP site classification.

2. A maximum of 60% to 80% of amplification has been observed in the study area. Hence, the topographic slope can be used as a proxy for a first order site characterization of any given area.

The present investigation is an attempt to understand the seismic potential of an intraplate region. The study area has not received much attention over the years and the present study attempts to create awareness among the engineers and researchers about the impending seismic and geotechnical disaster. The outcome of the study will be of immense use in the future for planning and designing seismic resilient infrastructures.

6.5 Recommendation for future work

1. The investigation suspects mining-induced seismicity in Bellary and Raichur districts though there is no mention of this in the prior literature. Hence, the study recommends site-specific investigations in this region.

2. The seismicity parameters were estimated assuming Poissonian distribution of earthquakes. However, an investigation can be carried out considering non-Poissonian nature of earthquakes too.

3. The diffused seismicity observed in the region can be modeled using the Gridded seismic source model or zone free method.

4. The present study incorporated a probabilistic approach in estimating the seismic hazard. Deterministic as well as Neo deterministic approaches can be adopted for seismic hazard analysis.

5. The present study mainly focused on seismic hazard and local site amplification. The study can be further continued to assess secondary effects such as liquefaction potential and its hazard assessment.

6. The study can be further extended by estimating the seismic risk and developing risk maps for the study area.

7. The outcome of the study can be further improved by accurate in-situ measurements of $V_{S(30)}$ and computing nonlinear site response in the time domain. The research findings are region-specific but the methodology adopted in the study can be repeated with reliable data for other regions as well.

REFERENCES

Abrahamson, N. A., Silva, W. J., and Kamai, R. (2014). "Summary of the ASK14 Ground Motion Relation for Active Crustal Regions." *Earthquake Spectra*, 30, 1025–1055.

Aguilar-Meléndez, A., Schroeder, M. G. O., De la Puente, J., González-Rocha, S. N., Rodriguez-Lozoya, H. E., Córdova-Ceballos, A., and Campos-Rios, A. (2017). "Development and Validation of Software CRISIS to Perform Probabilistic Seismic Hazard Assessment with Emphasis on the Recent CRISIS2015*." Computación y Sistemas*, 21(1), 67-90.

Aki, K. (1965). "Maximum Likelihood Estimate of b in the Formula logN = a - bM and Its Confidence Limits." *Bulletin of the Earthquake Research Institute*, 43, 237-239.

Akkar, S., Sandıkkaya, M. A., and Bommer, J. J. (2014). "Empirical Ground-Motion Models for Point-And Extended- Source Crustal Earthquake Scenarios in Europe and the Middle East." *Bulletin of Earthquake Engineering*, 12(1), 359-387.

Al-Atik, L., and Abrahamson, N. A. (2010). "An Improved Method for Nonstationary Spectral Matching." *Earthquake Spectra*, 26(6), 601-617. doi: https://doi.org/10.1193/1.3459159

Allen, T. I., and Wald, D. J. (2009). "On the Use of High-Resolution Topographic Data as A Proxy for Seismic Site Conditions (VS30)." *Bulletin of the Seismological Society of America*, 99(2A), 935–943. doi: http://doi.org/10.1785/0120080255

Amante, C. and Eakins, B.W. (2009). "ETOPO1 1 Arc-Minute Global Relief Model: Procedures, Data Sources and Analysis." NOAA Technical Memorandum NESDIS NGDC-24. National Geophysical Data Center, NOAA. doi:10.7289/V5C8276M [last accessed on 28th Feb 2018].

Amateur Seismic Centre, http://www.asc-india.org/, Pune, India (last accessed on 31st March 2017).

American Society of Civil Engineers. (2017). "Minimum Design Loads and Associated Criteria for Buildings and Other Structures, ASCE/SEI 7-16." Reston, VA. https://doi.org/10.1061/9780784414248

Anbazhagan, P., Kumar, A., and Sitharam, T. G. (2013). "Seismic Site Classification and Correlation Between Standard Penetration Test N Value and Shear Wave Velocity for Lucknow City in Indo-Gangetic Basin." *Pure and Applied Geophysics*, 170 (3), 299-318. doi: https://doi.org/10.1007/s00024-012-0525-1

Anbazhagan, P., Sreenivas, M., Ketan, B., Moustafa, S. S. R., and Al-Arifi, N. S. N. (2016). "Selection of Ground Motion Prediction Equations for Seismic Hazard Analysis of Peninsular India." *Journal of Earthquake Engineering*, 20(5), 699–737. doi: http://doi.org/10.1080/13632469.2015.1104747

Anderson, J. G. (1986). "Seismic Strain Rates in the Central and Eastern United States." *Bulletin of the Seismological Society of America,* 76, 272–290.

Andreotti, G., Famà, A., and Lai, C. G. (2018). "Hazard-Dependent Soil Factors for Site-Specific Elastic Acceleration Response Spectra of Italian and European Seismic Building Codes." *Bulletin of Earthquake Engineering*, 16(12), 5769–5800. doi: http://doi.org/10.1007/s10518-018-0422-9

Ansal, A., Tönük, G., and Kurtuluş, A. (2018). "Implications of Site-Specific Response Analysis." In: Pitilakis K. (Eds) Recent Advances In Earthquake Engineering In Europe. ECEE 2018. Geotechnical, Geological and Earthquake Engineering, vol 46. Springer, Cham, 51-68. doi: https://doi.org/10.1007/978-3-319-75741-4_2

Aristizábal, C., Bard, P. Y., Beauval, C., Lorito, S., and Selva, J. (2016). "Guidelines and Case Studies of Site Monitoring to Reduce the Uncertainties Affecting Site-Specific Earthquake Hazard Assessment." Deliverable D3. 4—STREST—harmonized approach to stress tests for critical infrastructures against natural hazards. STREST deliverable, 3.

American Society of Civil Engineers. (2013). "Seismic Evaluation and Retrofit of Existing Buildings." Reston, VA. doi: https://doi.org/10.1061/9780784412855

Ashish, Lindholm, C., Parvez, I. A., and Kühn, D. (2016). "Probabilistic Earthquake Hazard Assessment for Peninsular India." *Journal of Seismology*, 20(2), 629-653.

Atkinson, G. M., and Boore, D. M. (2006). "Earthquake Ground-Motion Prediction Equations for Eastern North America." *Bulletin of the Seismological Society of America*, 96(6), 2181-2205.

Atkinson, G. M., and Boore, D. M. (2011). "Modifications to Existing Ground-Motion Prediction Equations in Light of New Data." *Bulletin of the Seismological Society of America*, 101(3), 1121-1135.

Balakrishnan, P. (2009). "Hydrogeological and Hydrochemical Studies of the Periyar River Basin, Central Kerala", Doctoral dissertation, Cochin University of Science and Technology, Kerala, India.

Balasubrahmanyan, M. N. (2006). "Geology and Tectonics of India an Overview" (No. 9). MN Balasubrahmanyan.

Bansal, B. K., and Gupta, S. (1998). "A Glance Through the Seismicity of Peninsular India." *Journal of the Geological Society of India*, 52(1), 67-80.

Barani, S., and Spallarossa, D. (2017). "Soil Amplification in Probabilistic Ground Motion Hazard Analysis." *Bulletin of Earthquake Engineering*, 15(6), 2525-2545. http://doi.org/10.1007/s10518-016-9971-y

Barani, S., De Ferrari, R., and Ferretti, G. (2013). "Influence of Soil Modeling Uncertainties on Site Response." *Earthquake Spectra*, 29(3), 705–732. doi: http://doi.org/10.1193/1.4000159

Bard, P. Y., Bora, S. S., Hollender, F., Laurendeau, A., and Traversa, P. (2018). "Are The Standard Vs 30-Kappa Host-To-Target Adjustments the Best Way to Get Consistent Hard-Rock Ground Motion Prediction? In Best Practices in Physics-based Fault Rupture Models for Seismic Hazard Assessment of Nuclear Installations: issues and challenges towards full Seismic Risk Analysis." May 2018, Cadarache France. https://hal.archives-ouvertes.fr/hal-01826648

Baruah, S., Baruah, S., Kalita, A., Biswas, R., Gogoi, N., Gautam, J. L., Sanoujam, M., and Kayal, J. R. (2012). "Moment Magnitude – Local Magnitude Relationship for the Earthquakes of the Shillong-Mikir Plateau, Northeastern India Region: A New Perspective." *Geomatics, Natural Hazards and Risk*, 3(4), 365-375. doi: 10.1080/19475705.2011.596577

Baturay, M. B., and Stewart, J. P. (2003). "Uncertainty and Bias in Ground-Motion Estimates from Ground Response Analyses." *Bulletin of the Seismological Society of America*, 93 (5): 2025-2042. doi: http://doi.org/10.1785/0120020216

Bazzurro, P., and Cornell, C. A. (1999). "Disaggregation of Seismic Hazard." *Bulletin of the Seismological Society of America*, 89(2), 501-520.

Bazzurro, P., and Cornell, C. A. (2004). "Ground-Motion Amplification in Nonlinear Soil Sites with Uncertain Properties." *Bulletin of the Seismological Society of America*, 94(6), 2090-2109. doi: http://doi.org/10.1785/0120030215

Bazzurro, P., and Cornell, C. A. (2004). "Nonlinear Soil-Site Effects in Probabilistic Seismic Hazard Analysis." *Bulletin of the Seismological Society of America*, 94(6), 2110-2123.

BC Hydro, 2008, Seismic Source Characterization for the Probabilistic Seismic Hazard Analysis for the BC Hydro Service Area: draft report, BC Hydro and Power Authority.

Bhatia, S. C., Kumar, M. R., and Gupta, H. K. (1999). "A Probabilistic Seismic Hazard Map of India and Adjoining Regions." *Annals of Geophysics*, 42(6), 1153-1164.

Bommer, J. J., and Scherbaum, F. (2008). "The Use and Misuse of Logic Trees in Probabilistic Seismic Hazard Analyses." *Earthquake Spectra*, 24(4), 997–1009.

Bommer, J. J., Douglas, J., Scherbaum, F., Cotton, F., Bungum, H., and Fah, D. (2010). "On the Selection of Ground-Motion Prediction Equations for Seismic Hazard Analysis." *Seismological Research Letters*, 81(5), 783-793. doi: http://doi.org/10.1785/gssrl.81.5.783

Bommer, J. J., Scherbaum, F., Bungum, H., Cotton, F., Sabetta, F., and Abrahamson, N. A. (2005). "On the Use of Logic Trees for Ground-Motion Prediction Equations in The Seismic-Hazard Analysis." *Bulletin of the Seismological Society of America*, 95(2), 377-389. doi: http://doi.org/10.1785/0120040073

Boore, D. M., Stewart, J. P., Seyhan, E., and Atkinson, G. A. (2014). "NGA-West2 Equations for Predicting PGA, PGV, And 5% Damped PSA for Shallow Crustal Earthquakes." *Earthquake Spectra*, 30, 1057–1085.

Bott, M. H. P., and Dean, D. S. (1972). "Stress Systems at Young Continental Margins." *Nature*, 235(54), 23-25.

Brijesh, V. K., Diljith, V. P. and Ayisha, V. A. (2017). "Geophysical Resistivity Surveys and Well Lithologs of Filter Point Wells for Aquifer Delineation Around Tavanur, Malappuram District, Kerala." In National Conference on recent trends in Geoscience, Material Science and Civil Engineering, Mysore, India, 23rd – 24th March 2017.

BS EN1998-1 (2005) "Eurocode 8: Design of structures for earthquake resistance-part 1: general rules, seismic actions and rules for buildings." *European Committee for Standardization*, Brussels.

BSSC (2003). NEHRP recommended provisions for seismic regulation for new buildings and other structures (FEMA 450), Part 1: Provisions, Building Safety seismic council for the federal Emergency Management Agency, Washington D. C; 2003

Bureau of Indian Standard (BIS). (2016). IS 1893 - Indian Standard Criteria for Earthquake Resistant Design of Structures, Part 1 - General Provisions and Buildings. Bureau of Indian Standards, New Delhi, India.

Bureau of Indian Standard (BIS). (2016). IS 2131 - Method for Standard Penetration Test for Soils, Bureau of Indian Standards, New Delhi, India.

Burke, K., Dewey, L.F., Edelstein, A., Kidd, W.S.F., Nelson, K.D., Sengor, A.M.C. and Stroup, J. (1978). Rift and sutures of the world (NASA-CR-175201) compiled for Goddard Space Flight Center, Greenbelt, Maryland. Albany Global Tectonics

Burks, L. S., and Baker, J. W. (2012). "Occurrence of Negative Epsilon in Seismic Hazard Analysis Deaggregation, and Its Impact On Target Spectra Computation." *Earthquake Engineering & Structural Dynamics*, 41(8), 1241-1256.

Calais, E., Camelbeeck, T., Stein, S., Liu, M., and Craig, T. J. (2016). "A New Paradigm for Large Earthquakes in Stable Continental Plate Interiors." *Geophysical Research Letters*, 43(20), 10,621-10,637.

Campbell, K. W. (2003). "Prediction of Strong Ground Motion Using the Hybrid Empirical Method and Its Use in the Development of Ground-Motion (Attenuation) Relations in Eastern North America." *Bulletin of the Seismological Society of America*, 93(3), 1012-1033.

Campbell, K. W., and Bozorgnia, Y. (2014). "NGA-West2 Ground Motion Model for the Average Horizontal Components of PGA, PGV, and 5% Damped Linear Acceleration Response Spectra." *Earthquake Spectra*, 30, 1087–1115.

Central Ground Water Board, (2002). "Mapping of Hard Rock Aquifer System and Aquifer Management Plan, Palakkad District, Kerala", Draft report.

CEUS Ground Motion Project Final Report, EPRI, Palo Alto, CA, Dominion Energy, Glen Allen, VA, Entergy Nuclear, Jackson, MS, and Exelon Generation Company, Kennett Square,PA: 2004. 1009684.

Chandra, U. (1977). "Earthquakes of Peninsular India - A Seismotectonic Study." *Bulletin of the Seismological Society of America*, 67(5), 1387-1413.

Chandrasekharam, D. (1985). "Structure and Evolution of the Western Continental Margin of India Deduced from Gravity, Seismic, Geomagnetic and Geochronological Studies." *Physics of the Earth and Planetary interiors*, 41(2-3), 186-198.

Chatterjee, K., and Choudhury, D. (2013). "Variations in Shear Wave Velocity and Soil Site Class in Kolkata City Using Regression and Sensitivity Analysis." *Natural Hazards*, 69(3), 2057-2082. doi: https://doi.org/10.1007/s11069-013-0795-7

Chernick, M. R. (1999). "Bootstrap Methods: A Practitioner's Guide." New York: Wiley Series in Probability and Statistics.

Chiou, B. S. J. and Youngs, R. R. (2006). "PEER-NGA Empirical Ground Motion Model for the Average Horizontal Component of Peak Acceleration and Pseudo-Spectral Acceleration for Spectral Periods of 0.01 To 10 Seconds." Interim Report for USGS Review, 219.

Choi, Y., and Stewart, J. P. (2005). "Nonlinear Site Amplification as Function of 30 M Shear Wave Velocity." *Earthquake Spectra*. 21(1), 1-30. doi: http://doi.org/10.1193/1.1856535

Chopra, S., Kumar, D., Rastogi, B. K., Choudhury, P., and Yadav, R. B. S. (2013). "Estimation of Seismic Hazard in Gujarat Region, India." *Natural hazards*, 65(2), 1157-1178.

Christine, G. A., and Jonathan, P. (2007). "Probabilistic versus Deterministic Implementation of Nonlinear Site Factors in Seismic Hazard." UCLA: Civil and Environmental Engineering. Retrieved from https://escholarship.org/uc/item/4nm9q7ps

Cornell, C. A. (1968). "Engineering Seismic Risk Analysis." *Bulletin of the Seismological Society of America*, 58, 1583-1606.

Cotton, F., Scherbaum, F., Bommer, J. J., and Bungum, H. (2006). "Criteria for Selecting and Adjusting Ground-Motion Models for Specific Target Regions: Application to Central Europe and Rock Sites." *Journal of Seismology*, 10(2), 137–156. doi: http://doi.org/10.1007/s10950-005-9006-7

Cramer, C. H., and Kumar, A. (2003). "2001 Bhuj, India, Earthquake Engineering Seismoscope Recordings and Eastern North America Ground-Motion Attenuation Relations." *Bulletin of the Seismological Society of America*, 93(3), 1390-1394.

Danciu, L., Kale, Ö., and Akkar, S. (2016). "The 2014 Earthquake Model of the Middle East: Ground Motion Model and Uncertainties." *Bulletin of Earthquake Engineering*, 16(8), 3497–3533. doi: https://doi.org/10.1007/s10518-016-9989-1

Danciu, L., Monelli, D., Pagani, M. and Wiemer, S. (2010). "GEM1 Hazard: Review of PSHA Software." GEM Technical Report 2010-2, GEM Foundation, Pavia, Italy.

Das Gupta, S., Narula, P. L., Acharyya, S. K., and Banerjee, J. (2000). "Seismotectonic Atlas of India and Its Environs." *Geological Survey of India*.

Das, R., Sharma, M. L., and Wason, H. R. (2016). "Probabilistic Seismic Hazard Assessment for Northeast India Region." *Pure and Applied Geophysics*, 173(8), 2653-2670.

Delavaud, E., Cotton, F., Akkar, S., Scherbaum, F., Danciu, L., Beauval, C., … Theodoulidis, N. (2012). "Toward A Ground-Motion Logic Tree for Probabilistic Seismic Hazard Assessment in Europe." *Journal of Seismology*, 16(3), 451–473. doi: http://doi.org/10.1007/s10950-012-9281-z

Desai, S. S., and Choudhury, D. (2014). "Spatial Variation of Probabilistic Seismic Hazard for Mumbai and Surrounding Region." *Natural Hazards*, 71(3), 1873-1898.

Dessai, A. G. (2011). "The Geology of Goa Group: Revisited." *Journal of the Geological Society of India*, 78, 233. doi: https://doi.org/10.1007/s12594-011-0083-7

Dikmen, Ü. (2009). "Statistical Correlations of Shear Wave Velocity and Penetration Resistance for Soils." *Journal of Geophysics and Engineering*, 6(1), 61-72. doi: https://doi.org/10.1088/1742-2132/6/1/007

ESRI 2011. ArcGIS Desktop: Release 10. Redlands, CA: Environmental Systems Research Institute.

Gangrade, B. K., Prasad, A. G. V., and Sharma, R. D. (1987). "Earthquakes from Peninsular India: Data from The Gauribidanur Seismic Array (No. BARC--1347)." Bhabha Atomic Research Centre, India.

Gardner, J. K., and Knopoff, L. (1974). "Is the Sequence of Earthquakes in Southern California, With Aftershocks Removed, Poissonian?" *Bulletin of the Seismological Society of America*, 64(5), 1363-1367.

Gazetas, G. and Dakoulas, P. (1992). "Seismic Analysis and Design of Rockfill Dams: State-of-the-Art." *Soil Dynamics and Earthquake Engineering*, 11(1), 27-61. doi: https://doi.org/10.1016/0267-7261(92)90024-8

Gopinath, G. (2003). "An Integrated Hydrogeological Study of the Muvattupuzha River Basin, Kerala, India.", Doctoral dissertation, Cochin University of Science and Technology, Kerala, India.

Goulet, C. A., Stewart, J. P., Bazzurro, P., and Field, E. H. (2007). "Integration of Site-Specific Ground Response Analysis Results into Probabilistic Seismic Hazard Analyses." In Proceedings, *4th International Conference on Earthquake Geotechnical Engineering*.

Grünthal, G. (Ed.) (1998) European Macroseismic Scale 1998 (EMS-98) European Seismological Commission, sub commission on Engineering Seismology, Working Group Macroseismic Scales. Conseil de l'Europe, Cahiers du Centre Européen de Géodynamique et de Séismologie, Vol. 15, Luxembourg.

Grünthal, G., and Wahlström, R. (2012). "The European-Mediterranean Earthquake Catalogue (EMEC) for the Last Millennium." *Journal of Seismology*, 16(3), 535–570. doi: http://doi.org/10.1007/s10950-012-9302-y

GSI. (2005). Geology and Mineral Resources of the States of India, Part IX – Kerala. Miscellaneous Publication No. 30, Geological Survey of India, New Delhi.

GSI. (2006). Geology and Mineral Resources of the States of India, Part VII – Karnataka and Goa. Miscellaneous Publication No. 30, Geological Survey of India, New Delhi.

Guha, S.K., Gosavi, P.D., Nand, K., Padale, J.G. and Marwadi, S.C. (1974). "Koyna Earthquakes (October 1963 to December 1973)." Report of the Central Water and Power Research Station, Poona, India.

Gupta, I. D. (2006). "Delineation of Probable Seismic Sources in India and Neighbourhood by A Comprehensive Analysis of Seismotectonic Characteristics of the Region." *Soil Dynamics and Earthquake Engineering*, 26(8), 766-790.

Gutenberg, B., and Richter, C. F. (1944). "Frequency of Earthquakes in California." *Bulletin of the Seismological Society of America*, 34(4), 185-188.

Halchuk, S., Adams, J., and Anglin, F. (2007). "Revised Deaggregation of Seismic Hazard for Selected Canadian Cities." In Proceedings, *9th Canadian Conference on Earthquake Engineering*, 420-432.

Hanumantharao, C., and Ramana, G. V. (2008). "Dynamic Soil Properties for Microzonation of Delhi, India." *Journal of earth system science*, 117 (2), 719-730. doi: https://doi.org/10.1007/s12040-008-0066-2

Hasancebi, N., and Ulusay, R. (2007). "Empirical Correlations Between Shear Wave Velocity and Penetration Resistance for Ground Shaking Assessments." *Bulletin of Engineering Geology and the Environment*, 66(2), 203-213. doi: https://doi.org/10.1007/s10064-006-0063-0

Hong, H. P., and Goda, K. (2006). "A Comparison of Seismic-Hazard and Risk Deaggregation." *Bulletin of the Seismological Society of America*, 96(6), 2021-2039.

Hwang, H., and Huo, J. R. (1997). "Attenuation Relations of Ground Motion for Rock and Soil Sites in Eastern United States." *Soil Dynamics and Earthquake Engineering*, 16(6), 363-372.

Incorporated Research Institutions for Seismology, Earthquake browser, http://www.iris.edu/hq/ (last accessed on 26th October 2016).

Indian Meteorological Department, New Delhi, India. (Through Personal communication)

International Seismological Centre, Online Bulletin, http://www.isc.ac.uk, Internatl. Seismol. Cent., Thatcham, United Kingdom, 2014 (last accessed on 31st October 2016).

Iyengar, R. N., and Ghosh, S. (2004). "Microzonation of Earthquake Hazard in Greater Delhi Area." *Current Science*, 87(9), 1193-1202.

Iyengar, R. N., Chadha, R. K., Balaji Rao, K., and Raghukanth, S. T. G. (2010). "Development of Probabilistic Seismic Hazard Map of India." *The National Disater Management Authority*, 86.

Jade, S. (2004). "Estimates of Plate Velocity and Crustal Deformation in the Indian Subcontinent Using GPS Geodesy." *Current Science*, 86(10), 1443-1448.

Jaiswal, K., and Sinha, R. (2006). "Probabilistic Modeling of Earthquake Hazard in Stable Continental Shield of the Indian Peninsula." *ISET Journal of Earthquake Technology*, 43(3), 49-64.

Jaiswal, K., and Sinha, R. (2007). "Probabilistic Seismic Hazard Estimation for Peninsular India." *Bulletin of the Seismological Society of America*, 97(1B), 318-330.

Johnston, A. C. (1996). "Seismic Moment Assessment of Earthquakes in Stable Continental Regions---III. New Madrid 1811-1812, Charleston 1886 And Lisbon 1755." *Geophysical Journal International*, 126(2), 314–344. doi: http://doi.org/10.1111/j.1365-246X.1996.tb05294.x

Joji, V. S. (2009). "Ground Water Information Booklet of Kozhikode District, Kerala State." Central Ground Water Board, Ministry of Water Resources, Government of India.

Raj, K. G., Paul, M. A., Hegde, V.S. and Nijagunappa, R. (2001). "Lineaments and Seismicity of Kerala—A Remote Sensing Based Analysis." *Journal of the Indian Society of Remote Sensing*, 29(4), 203-211.

Kaila, K. L., Gaur, V. K., and Narain, H. (1972). "Quantitative Seismicity Maps of India." *Bulletin of the Seismological Society of America*, 62(5), 1119-1132.

Kayal, J. R. (2008). "Microearthquake Seismology and Seismotectonics of South Asia." Springer Science & Business Media.

Khattri, K. N. (1994). "A Hypothesis for the Origin of Peninsular Seismicity." *Current Science*, 67, 590–597.

Khattri, K. N., Rogers, A. M., Perkins, D. M., and Algermissen, S. T. (1984). "A Seismic Hazard Map of India and Adjacent Areas." *Tectonophysics*, 108(1-2), 93111-108134.

Kijko, A., and Sellevoll, M. A. (1989). "Estimation of Earthquake Hazard Parameters from Incomplete Data Files. Part I. Utilization of Extreme and Complete Catalogs with Different Threshold Magnitudes." *Bulletin of the Seismological Society of America*, 79(3), 645-654.

Kijko, A., and Smit, A. (2012). "Extension of The Aki-Utsu B-Value Estimator for Incomplete Catalogs." *Bulletin of the Seismological Society of America*, 102(3), 1283-1287.

Kim, B., Hashash, Y. M. A., Stewart, J. P., Rathje, E. M., Harmon, J. A., Musgrove, M. I., … and Silva, W. J. (2016). "Relative Differences Between Nonlinear and Equivalent-Linear 1-D Site Response Analyses." *Earthquake Spectra*, 32(3), 1845-1865. doi: http://doi.org/10.1193/051215EQS068M

Kirar, B., Maheshwari, B. K., and Muley, P. (2016). "Correlation Between Shear Wave Velocity (Vs) and SPT Resistance (N) for Roorkee Region." *International Journal of Geosynthetics and Ground Engineering*, 2, 9. doi: https://doi.org/10.1007/s40891-016-0047-5

Kolathayar, S., and Sitharam, T. G. (2012). "Characterization of Regional Seismic Source Zones in and Around India." *Seismological Research Letters*, 83(1), 77-85.

Kolathayar, S., Sitharam, T. G. and Vipin, K. S. (2012). "Spatial Variation of Seismicity Parameters Across India and Adjoining Areas." *Natural Hazards*, 60(3), 1365-1379. doi: https://doi.org/10.1007/s11069-011-9898-1

Kramer, S. L. (1996). "Geotechnical Earthquake Engineering." Prentice–Hall International Series in Civil Engineering and Engineering Mechanics. Prentice-Hall, New Jersey.

Ktenidou, O. J., and Abrahamson, N. A. (2016). "Empirical Estimation of High-Frequency Ground Motion on Hard Rock." *Seismological Research Letters*, 87(6), 1465-1478. doi: https://doi.org/10.1785/0220160075

Laurendeau, A., Cotton, F., Ktenidou, O. J., Bonilla, L. F., and Hollender, F. (2013). "Rock and Stiff-Soil Site Amplification: Dependency on VS30 and Kappa (κ0)." *Bulletin of the Seismological Society of America*, 103(6), 3131-3148. doi: https://doi.org/10.1785/0120130020

Lemoine, A., Douglas, J., and Cotton, F. (2012). "Testing the Applicability of Correlations Between Topographic Slope and VS30 for Europe." *Bulletin of the Seismological Society of America*, 102(6), 2585–2599. doi: http://doi.org/10.1785/0120110240

Luzi, L., Puglia, R., Russo, E., D'Amico, M., Felicetta, C., Pacor, F., et al. (2016). "The Engineering Strong-Motion Database: A Platform to Access Pan-European Accelerometric Data." *Seismological Research Letters*, 87(4), 987-997. doi: https://doi.org/10.1785/0220150278

Maheswari, R. U., Boominathan, A., and Dodagoudar, G. R. (2010). "Use of Surface Waves in Statistical Correlations of Shear Wave Velocity and Penetration Resistance of Chennai Soils." *Geotechnical and Geological Engineering*, 28(2), 119-137. doi: https://doi.org/10.1007/s10706-009-9285-9

Maiti, S. K., Nath, S. K., Adhikari, M. D., Srivastava, N., Sengupta, P., and Gupta, A. K. (2017). "Probabilistic Seismic Hazard Model of West Bengal, India." *Journal of Earthquake Engineering*, 21(7), 1113-1157.

Mandal, P. (1999). "Intraplate Stress Distribution Induced by Topography and Crustal Density Heterogeneities Beneath the South Indian Shield, India." *Tectonophysics*, *302*(1-2), 159-172.

Martin, S., and Szeliga, W. (2010). "A Catalog of Felt Intensity Data for 570 Earthquakes in India from 1636 to 2009." *Bulletin of the Seismological Society of America*, 100(2), 562-569.

Matsuoka, M., Wakamatsu, K., Fujimoto, K. and Midorikawa, S. (2005.) "Nationwide Site Amplification Zoning Using GIS Based Japan Engineering Geomorphologic Classification Map." Proceedings 9th International Conference on Structural Safety and Reliability, pp. 239–246.

Mhaske, S. Y., and Choudhury, D. (2011). "Geospatial Contour Mapping of Shear Wave Velocity for Mumbai City." *Natural Hazards*, 59(1), 317-327. doi: https://doi.org/10.1007/s11069-011-9758-z

Milne, J. (1911). "A Catalogue of Destructive Earthquakes: AD 7 to AD 1899." The Association.

Molnar, P., and Tapponnier, P. (1975). "Cenozoic Tectonics of Asia: Effects of A Continental Collision." *Science*, 189, 419–426.

Molnar, P., and Tapponnier, P. (1979). "The Collision Between India and Eurasia (1979)." In: Earthquakes and Volcanoes, Procs., from Scientific American. San Francisco: WH Freeman and Company, 62–73.

Musson, R. M., Grünthal, G., and Stucchi, M. (2010). "The Comparison of Macroseismic Intensity Scales." *Journal of Seismology*, 14(2), 413-428.

Nath, S. K., and Thingbaijam, K. K. S. (2011). "Peak Ground Motion Predictions in India: An Appraisal for Rock Sites." *Journal of Seismology*, 15(2), 295–315. doi: http://doi.org/10.1007/s10950-010-9224-5

Nath, S. K., and Thingbaijam, K. K. S. (2012). "Probabilistic Seismic Hazard Assessment of India." *Seismological Research Letters*, 83(1), 135-149.

National Earthquake Information Center 2003 USA PDE reportings http://neic.usgs.gov/neis/epic/ (last accessed on 28th November 2016)

Naylor, M., Orfanogiannaki, K., and Harte, D. (2010). "Exploratory Data Analysis: Magnitude, Space, and Time." *Community Online Resource for Statistical Seismicity Analysis*, doi: 10.5078/corssa-92330203. Available at http://www.corssa.org.

Nazimuddin, M. (1993). "Coastal Hydrology of Kozhikode, Kerala", Doctoral dissertation, Cochin University of Science and Technology, Kerala, India. http://hdl.handle.net/10603/3629

Oldham, T. A. (1883). "Catalogue of Indian Earthquakes from the Earliest Time to the End of AD 1869." Memoirs of the Geological Survey of India 19 Part 3 (1883).

Ordonez, Gustavo A. (2012). "SHAKE2000 – A Computer Program for the 1-D Analysis of Geotechnical Earthquake Engineering Problems." GeoMotions, LLC; Lacey, Washington, USA.

Papaspiliou, M., and Kontoe, S. (2013). "Sensitivity of Site Response Analysis on the Number of Ground Motion Records and Implications for PSHA." *Bulletin of Earthquake Engineering*, 11(5), 1287–1304. doi: http://doi.org/10.1007/s10518-013-9459-y

Papaspiliou, M., Kontoe, S., and Bommer, J. J. (2012). "An Exploration of Incorporating Site Response into PSHA-Part II: Sensitivity of Hazard Estimates to Site Response Approaches." *Soil Dynamics and Earthquake Engineering*, 42, 316-330. doi: https://doi.org/10.1016/j.soildyn.2012.05.001

Perron V., Hollender F., Bard P., Gélis C., Guyonnet-Benaize C., Hernandez B., and Ktenidou O. (2017). "Robustness of Kappa (κ) Measurement in Low-to-Moderate Seismicity Areas: Insight from a Site-Specific Study in Provence, France*." Bulletin of the Seismological Society of America*, 107(5), 2272–2292. doi: https://doi.org/10.1785/0120160374

Pezeshk, S., Zandieh, A., and Tavakoli, B. (2011). "Hybrid Empirical Ground-Motion Prediction Equations for Eastern North America Using NGA Models and Updated Seismological Parameters." *Bulletin of the Seismological Society of America*, 101(4), 1859–1870. doi: http://doi.org/10.1785/0120100144

Prasad, S. K., Vijayendra, K. V., and Nayak, S. (2019). "Issues on Seismic Site Characterization." In Frontiers in Geotechnical Engineering, 217-248. Springer, Singapore.

Radhakrishna, B. P. (1993). "Neogene Uplift and Geomorphic Rejuvenation of the Indian Peninsula." *Current Science,* 64(11 & 12), 787–793.

Raghu Kanth, S., and Iyengar, R. N. (2007). "Estimation of Seismic Spectral Acceleration in Peninsular India." *Journal of Earth System Science*, 116(3), 199-214.

Raj, K. G., and Nijagunappa, R. (2004). "Major Lineaments of Karnataka State and their Relation to Seismicity: A Remote Sensing Based Analysis." *Journal-Geological Society of India*, 63(4), 430-439.

Rajendran, C. P., John, B., Sreekumari, K. and Rajendran, K. (2009). "Reassessing The Earthquake Hazard in Kerala Based on the Historical and Current Seismicity". *Journal of the Geological Society of India*, 73(6), 785-802.

Rao, B. R. (1992). "Seismicity and Geodynamics of the Low-To High-Grade Transition Zone of Peninsular India." *Tectonophysics*, 201(1-2), 175-185.

Rao, B. R., and Rao, P. S. (1984). "Historical Seismicity of Peninsular India." *Bulletin of the Seismological Society of America*, 74(6), 2519-2533.

Rastogi, B. K. (1992). "Seismotectonics Inferred from Earthquakes and Earthquake Sequences in India During The 1980s." *Current Science*, *62*, 101-108.

Rastogi, B. K. (2016). "Seismicity of Indian Stable Continental Region." *Journal of Earthquake Engineering*, 3, 57-93.

Rastogi, B. K., Chadha, R. K., and Sarma, C. S. P. (1995). "Investigations of June 7, 1988 Earthquake of Magnitude 4.5 Near Idukki Dam in Southern India." *Pure and Applied Geophysics*, 145(1), 109-122.

Rathje, E. M., Kottke, A. R., and Trent, W. L. (2010). "Influence of Input Motion and Site Property Variabilities on Seismic Site Response Analysis." *Journal of Geotechnical and Geoenvironmental Engineering*, 136(4). doi: http://doi.org/10.1061/(ASCE)GT.1943-5606.0000255

Reddy, P. R. (2003). "Need for High-Resolution Deep Seismic Reflection Studies in Strategic Locales of South India." *Current Science,* 84 (8), 973-974.

Reddy, P. R., and Rao, V. V. (2000). "Structure and Tectonics of the Indian Peninsular Shield–Evidences from Seismic Velocities." *Current Science*, 78(7), 899-906.

Reiter, L. (1991). "Earthquake Hazard Analysis: Issues and Insights." Columbia University Press, NewYork.

Rota, M., Lai, C. G., and Strobbia, C. L. (2011). "Stochastic 1D Site Response Analysis at A Site in Central Italy." *Soil Dynamics and Earthquake Engineering*, 31(4), 626–639. http://doi.org/10.1016/j.soildyn.2010.11.009

Rout, M. M., and Das, J. (2018). "Probabilistic Seismic Hazard for Himalayan Region Using Kernel Estimation Method (Zone-Free Method)." *Natural Hazards,* 93(2), 967-985.

Sandikkaya, M. A., Akkar, S., and Bard, P. Y. (2018). "A Probabilistic Procedure to Describe Site Amplification Factors for Seismic Design Codes." *Soil Dynamics and Earthquake Engineering*, (In press). doi: http://doi.org/10.1016/j.soildyn.2018.01.050

Saritha, S. and Vikas, C. (2009). "Ground Water Information Booklet of Kannur District, Kerala State." Central Ground Water Board, Ministry of Water Resources, Government of India.

Scordilis, E. M. (2006). "Empirical Global Relations Converting M S and M B to Moment Magnitude." *Journal of seismology*, 10(2), 225-236.

Seeber, L., Armbruster, J.G. and Jacob, K.H. (1999). "Probabilistic Assessment of Earthquake Hazard for the State of Maharashtra, India." The Government of Maharashtra Earthquake Rehabilitation Cell, Mumbai, 60p.

Seed, H. B. and Sun, J. H. (1989). "Implication of Site Effects in the Mexico City Earthquake of September 19, 1985 for Earthquake-Resistance-Design Criteria in the San Francisco Bay Area of California." Report No. UCB/EERC-89/03, University of California, Berkeley, California.

Seed, H. B., and Idriss, I. M. (1970). "Soil Moduli and Damping Factors for Dynamic Response Analysis." Report no. EERC 70-10. University of California, Berkeley, California.

*Se*ismosoft (2016) "Seismomatch 2016 – A Computer Program for Spectrum Matching of Earthquake Records," available from http://www.seismosoft.com

Shukla, J., and Choudhury, D. (2012). "Seismic Hazard and Site-Specific Ground Motion for Typical Ports of Gujarat." *Natural Hazards*, 60(2), 541–565. doi: http://doi.org/10.1007/s11069-011-0042-z

Sil, A., and Haloi, J. (2017). "Empirical Correlations with Standard Penetration Test (SPT)-N for Estimating Shear Wave Velocity Applicable to Any Region." *International Journal of Geosynthetics and Ground Engineering*, 3: 22. doi: https://doi.org/10.1007/s40891-017-0099-1

Singh, S. K., Bansal, B. K., Bhattacharya, S. N., Pacheco, J. F., Dattatrayam, R. S., Ordaz, M., and Hough, S. E. (2003). "Estimation of Ground Motion for Bhuj (26

January 2001; Mw 7.6) And for Future Earthquakes in India." *Bulletin of the Seismological Society of America*, 93(1), 353-370.

Sitharam, T. G., and Anbazhagan, P. (2007). "Seismic Hazard Analysis for the Bangalore Region." *Natural Hazards*, 40(2), 261-278.

Sitharam, T. G., and Kolathayar, S. (2013). "Seismic Hazard Analysis of India Using Areal Sources." *Journal of Asian Earth Sciences*, 62, 647-653.

Sitharam, T. G., James, N., Vipin, K. S., and Raj, K. G. (2012). "A Study on Seismicity and Seismic Hazard for Karnataka State." *Journal of Earth System Science*, 121(2), 475-490.

Sreenath, G. (2009). "Ground Water Information Booklet of Kozhikode District, Kerala State." Central Ground Water Board, Ministry of Water Resources, Government of India.

Sriram, K., and Prasad, K. N. (1979). "Observations on the Geomorphology of Goa." *Journal of the Geological Society of India*, 20(12), 608-614.

Srivastava, H. N., and Ramachandran, K. (1985). "New Catalogue of Earthquakes for Peninsular India During 1839-1900." *Mausam*, 36(3), 351-358.

Stepp, J. C. (1973). "Analysis of Completeness of the Earthquake Sample in the Puget Sound Area." NOAA Tech. Report ERL 267-ESL30, Boulder, Colorado.

Stewart, J. P., and Afshari, K. (2015). "Guidelines for Performing Hazard-Consistent One-Dimensional Ground Response Analysis for Ground Motion Prediction. GEER Reconnaissance of Central Italy Earthquake Sequence View Project Seismic Soil Liquefaction View Project." Retrieved from https://www.researchgate.net/publication/308052147

Stewart, J. P., Douglas, J., Javanbarg, M., Bozorgnia, Y., Abrahamson, N. A., Boore, D. M., ... and Stafford, P. J. (2015). "Selection of Ground Motion Prediction Equations for The Global Earthquake Model." *Earthquake Spectra*, 31(1), 19-45.

Stucchi, M., Rovida, A., Gomez Capera, A. A., Alexandre, P., Camelbeeck, T., Demircioglu, M. B., ... and Giardini, D. (2013). "The SHARE European Earthquake Catalogue (SHEEC) 1000-1899." *Journal of Seismology,* 17(2), 523–544. doi: http://doi.org/10.1007/s10950-012-9335-2

Subrahmanya, K. R. (1996). "Active Intraplate Deformation in South India." *Tectonophysics*, 262(1-4), 231-241.

Sukhtankar R.K. 2004. "Indian Perspective of Coastal Quaternary Research: An Overview." IX IGCS Prof. Jhingram Memorial Lecture, IGC Roorkee: 1-22.

Sukhtankar, R. K., Pandian, R. S., and Guha, S. K. (1993). "Seismotectonic Studies of the Coastal Areas of India, Pakistan, Bangladesh, and Burma." *Natural Hazards*, *7*(3), 201-210.

Sun, J. I., Golesorkhi, R., and Seed, H. B. (1988). "Dynamic Moduli and Damping Ratios of Cohesive Soils." Report No. UCB/EERC-88/15, University of California, Berkeley, California.

Sykes, L. R. (1970). "Seismicity of The Indian Ocean and A Possible Nascent Island Arc Between Ceylon and Australia." *Journal of Geophysical Research*, 75(26), 5041-5055.

Thokchom, S., Rastogi, B. K., Dogra, N. N., Pancholi, V., Sairam, B., Bhattacharya, F., and Patel, V. (2017). "Empirical Correlation of SPT Blow Counts Versus Shear Wave Velocity for Different Types of Soils in Dholera, Western India." *Natural Hazards*, 86(3), 1291-1306. doi: https://doi.org/10.1007/s11069-017-2744-3

Tinti, S., and Mulargia, F. (1985). "Effects of Magnitude Uncertainties on Estimating the Parameters in The Gutenberg-Richter Frequency-Magnitude Law." *Bulletin of the Seismological Society of America*, *75*(6), 1681-1697.

Toro, G. R. (2002). "Modification of The Toro Et Al. (1997) Attenuation Equations for Large Magnitudes and Short Distances." Risk Engineering Technical Report.

Urhammer, R. (1986), "Characteristics of Northern and Central California Seismicity." *Earthquake Notes*, 57(1), 21.9

US Nuclear Regulatory Commission, 2007. "A Performance-Based Approach to Define the Site Specific Earthquake Ground Motion." Regulatory Guide 1.208, Washington D.C.

Valdiya, K. S. (1989). "Neotectonic Implication of Collision of Indian and Asian Plates." *Indian Journal of Geology*, 61, 1-13.

Valdiya, K. S. (2001). "Tectonic Resurgence of the Mysore Plateau and Surrounding Regions in Cratonic Southern India." *Current Science*, 81(8), 1068–1089.

Valdiya, K. S. (2013). "Recent Tectonic Movements in the Kaveri Catchment, Southern India." *Journal of the Indian Institute of Science*, 77(3), 267-273.

Venkiteswaran, C. S., and Rao, B. V. L. N. (1980). "Report On the Geophysical Investigations for Structural Studies in The Hard Rock Areas of Mallapuram District, Kerala State." (Field. Pure and Applied Chemistry (Vol. 52).

Verma, M., and Bansal, B. K. (2013). "Seismic Hazard Assessment and Mitigation In India: An Overview." *International Journal of Earth Sciences*, 102(5), 1203-1218.

Vinayachandran, N., and Joji, V. S. (2007). "Ground Water Information Booklet of Wayanad District, Kerala State." Central Ground Water Board.

Vucetic, M. and Dobry, R. (1991). "Effect of Soil Plasticity on Cyclic Response." *Journal of Geotechnical Engineering*, 117(1), 89-107. doi: https://doi.org/10.1061/(ASCE)0733-9410(1991)117:1(89)

Wald, D. J., and Allen, T. I. (2007). "Topographic Slope as A Proxy for Seismic Site Conditions and Amplification." *Bulletin of the Seismological Society of America*, 97(5), 1379–1395. doi: http://doi.org/10.1785/0120060267

Walling, M. Y., and Mohanty, W. K. (2009). "An Overview on the Seismic Zonation and Microzonation Studies in India." *Earth-Science Reviews*, 96(1-2), 67-91.

Wiemer, S. (2001). "A Software Package to Analyze Seismicity: ZMAP." *Seismological Research Letters*, 72(3), 373–382. doi: http://doi.org/10.1785/gssrl.72.3.373

Wills, C. J., Petersen, M. D., Bryant, W. A., Reichle, M. S., Saucedo, G. J., Tan, S. S., Taylor, G. C. and Trei- man, J. A. (2000). "A Site-Conditions Map for California Based on Geology and Shear Wave Velocity." *Bulletin of the Seismological Society of America*, 90(6B), S187–S208.

APPENDIX – 1

COMPOSITE REGIONAL EARTHQUAKE CATALOG

Catalog Period – 1507AD to 2015 AD; Number of earthquake events – 1242

The distances for all the events are calculated from Surathkal with coordinates – 13.0108° N, 74.7943° E

Sl. No	Longitude	Latitude	Year	Month	Date	MW	Depth	Distance (km)
1	77.56	12.96	1507	7	1	3.7	0	300
2	77.59	12.97	1507	8	1	3.0	0	303
3	76.87	11.42	1823	2	9	2.3	0	287
4	76.70	11.33	1823	2	9	3.0	0	279
5	73.00	14.50	1828	8	22	4.8	0	255
6	75.00	13.00	1828	8	22	5.3	0	22
7	75.00	13.00	1828	8	22	5.7	0	22
8	73.00	14.50	1828	8	22	4.9	0	255
9	75.00	13.00	1828	8	22	4.9	0	22
10	73.62	15.86	1828	8	22	3.7	0	341
11	75.00	13.00	1828	8	22	5.7	0	22
12	73.00	14.50	1828	8	22	5.0	0	255
13	75.00	13.00	1828	8	22	4.3	0	22
14	75.00	13.00	1828	8	22	5.8	0	22
15	75.00	13.00	1828	8	22	4.4	0	22
16	77.60	13.00	1829	3	12	4.3	0	304
17	77.60	13.00	1829	3	13	4.7	0	304
18	77.58	12.96	1829	3	12	3.7	0	302
19	75.00	12.00	1829	3	12	5.7	0	115
20	77.60	13.00	1829	3	12	5.0	0	304
21	77.60	13.00	1829	3	13	4.3	0	304
22	77.60	13.00	1829	3	13	4.4	0	304
23	73.70	15.80	1832	10	4	5.0	0	332
24	73.70	15.80	1832	10	4	5.3	0	332
25	73.70	15.80	1832	10	4	4.9	0	332
26	76.90	15.20	1843	3	31	5.7	0	333
27	76.90	15.20	1843	3	31	6.0	0	333
28	76.00	15.20	1843	3	12	4.7	0	276
29	76.90	15.20	1843	3	12	3.9	0	333
30	76.90	15.20	1843	3	31	5.3	0	333
31	76.90	15.20	1843	3	31	5.4	0	333

32	76.90	15.20	1843	3	31	3.7	0	333
33	76.00	15.00	1843	4	1	5.7	0	257
34	76.90	15.20	1843	4	1	5.7	0	333
35	76.90	15.20	1843	4	1	6.2	0	333
36	76.00	15.00	1843	4	1	5.6	0	257
37	77.59	12.96	1843	4	1	1.7	0	303
38	75.80	14.51	1843	4	1	3.0	0	199
39	76.92	15.14	1843	4	1	3.7	0	330
40	76.90	15.20	1843	4	1	6.3	0	333
41	76.00	15.00	1843	4	1	6.0	0	257
42	76.90	15.20	1843	4	1	5.7	0	333
43	76.90	15.20	1843	4	1	6.1	0	333
44	76.90	15.20	1843	4	1	5.4	0	333
45	76.00	11.40	1858	8	13	3.7	0	222
46	76.00	11.40	1858	8	23	3.7	0	222
47	76.00	11.40	1858	8	23	4.3	0	222
48	76.00	11.40	1858	8	13	4.7	0	222
49	76.00	11.40	1858	8	13	4.3	0	222
50	76.00	11.40	1858	8	23	5.3	0	222
51	76.00	11.40	1858	8	23	4.0	0	222
52	76.00	11.40	1858	8	23	4.7	0	222
53	76.00	11.40	1858	8	23	4.3	0	222
54	76.00	11.40	1858	8	23	5.0	0	222
55	76.62	12.30	1865	6	4	3.7	0	213
56	76.95	11.00	1865	6	24	3.7	0	324
57	76.60	12.30	1865	6	4	4.0	0	211
58	76.60	12.30	1865	6	4	3.8	0	211
59	76.00	11.40	1865	8	13	4.3	0	222
60	76.00	11.40	1865	8	23	5.0	0	222
61	76.60	12.30	1865	8	23	3.8	0	211
62	76.80	10.80	1865	8	23	3.8	0	329
63	75.43	14.48	1866	2	12	3.7	0	177
64	77.85	12.75	1879	6	17	3.7	0	333
65	77.78	13.78	1879	4	28	3.7	0	334
66	77.82	12.73	1879	6	17	3.7	0	330
67	77.90	12.80	1879	6	17	3.8	0	338
68	77.80	13.80	1879	4	28	4.0	0	337
69	77.80	13.80	1879	4	28	3.8	0	337
70	77.59	12.97	1881	12	31	2.3	0	303
71	74.84	12.87	1881	12	31	2.3	0	17
72	76.79	11.35	1881	12	31	3.0	0	285
73	75.78	11.25	1881	12	31	3.7	0	223

74	76.69	11.42	1881	12	31	3.7	0	272
75	76.70	11.46	1882	2	28	5.7	0	270
76	77.58	12.96	1882	4	0	3.0	0	302
77	76.70	11.50	1882	2	28	5.6	0	267
78	75.78	11.26	1882	2	28	3.0	0	222
79	76.69	11.41	1882	2	28	3.7	0	272
80	77.58	12.96	1882	4	1	3.7	0	302
81	77.50	13.00	1882	4	1	3.8	0	293
82	77.59	12.97	1882	4	1	3.7	0	303
83	77.58	12.96	1882	4	1	3.0	0	302
84	77.60	13.00	1882	4	1	4.0	0	304
85	76.70	11.50	1882	4	1	5.6	0	267
86	75.40	14.46	1886	2	12	3.0	0	174
87	75.40	14.50	1886	2	12	3.3	0	178
88	74.85	12.90	1889	3	31	3.7	0	14
89	74.85	12.90	1889	3	31	3.7	0	14
90	74.90	12.90	1889	3	31	4.0	0	17
91	74.80	12.90	1889	3	31	3.8	0	12
92	74.84	12.87	1889	8	12	3.7	0	17
93	74.80	12.90	1889	8	12	3.8	0	12
94	77.58	12.96	1891	2	17	3.7	0	302
95	77.59	12.98	1891	2	17	3.7	0	303
96	77.60	12.96	1891	2	17	3.7	0	304
97	77.60	13.00	1891	2	17	4.0	0	304
98	74.75	13.46	1896	1	3	3.7	0	50
99	74.80	13.50	1896	1	3	3.8	0	54
100	77.58	12.97	1897	6	12	2.3	0	302
101	74.50	15.85	1898	10	15	3.0	0	317
102	74.60	15.90	1898	10	15	3.0	0	322
103	74.60	15.90	1898	10	15	3.8	0	322
104	76.80	10.80	1900	1	7	6.3	0	329
105	76.80	10.80	1900	2	7	5.7	70	329
106	76.80	10.80	1900	2	7	6.2	0	329
107	76.70	10.70	1900	2	8	5.7	70	330
108	76.70	10.70	1900	2	8	6.2	0	330
109	76.70	10.70	1900	2	8	5.6	0	330
110	74.75	13.34	1900	2	8	2.3	0	37
111	75.78	11.25	1900	2	8	3.7	0	223
112	77.59	12.97	1900	2	8	4.3	0	303
113	76.88	11.43	1900	2	8	4.3	0	287
114	76.64	12.31	1900	2	8	4.3	0	215
115	77.35	11.09	1900	2	8	4.3	0	351

116	76.97	11.01	1900	2	8	5.0	0	325
117	76.79	11.35	1900	2	8	5.0	0	285
118	76.69	11.40	1900	2	8	5.0	0	273
119	76.70	11.33	1900	2	8	5.7	0	279
120	76.87	11.42	1900	2	8	5.7	0	287
121	76.67	11.42	1900	2	8	5.7	0	270
122	76.73	11.38	1900	2	8	5.7	0	278
123	76.96	11.02	1900	2	8	5.7	0	323
124	76.80	10.80	1900	2	8	4.3	0	329
125	76.70	10.70	1900	2	8	6.0	0	330
126	76.80	10.80	1900	2	8	5.7	0	329
127	76.80	10.80	1900	2	8	5.7	0	329
128	75.00	12.00	1901	4	27	5.0	0	115
129	75.00	12.00	1901	4	27	5.3	0	115
130	75.00	12.00	1901	4	27	4.6	0	115
131	75.00	12.00	1901	4	27	4.9	0	115
132	75.00	12.00	1901	4	27	4.7	0	115
133	75.50	12.00	1901	4	27	5.0	0	136
134	74.78	12.87	1905	4	5	1.7	0	16
135	76.36	10.77	1907	8	25	3.0	0	302
136	77.00	13.00	1916	1	7	4.8	0	239
137	77.50	13.00	1916	1	7	5.0	0	293
138	77.50	13.00	1916	1	7	5.3	0	293
139	77.00	13.00	1916	1	7	4.9	0	239
140	77.30	13.00	1916	1	7	5.3	0	272
141	77.50	13.00	1916	1	7	4.9	0	293
142	77.50	13.00	1916	1	7	4.7	0	293
143	75.50	12.40	1933	1	7	3.3	0	102
144	74.84	12.87	1934	1	15	2.3	0	17
145	75.00	15.45	1934	1	15	3.0	0	272
146	74.50	15.85	1938	3	14	4.3	0	317
147	76.79	11.35	1938	9	10	3.0	0	285
148	76.39	10.81	1938	9	10	3.7	0	300
149	76.41	10.79	1938	9	10	3.7	0	303
150	77.57	12.97	1944	2	29	1.7	0	301
151	76.78	11.35	1944	2	29	3.7	0	284
152	76.84	14.69	1948	2	6	4.3	0	289
153	76.80	14.60	1948	2	6	3.8	0	279
154	76.64	12.30	1955	7	11	3.7	0	215
155	76.50	12.40	1955	7	11	4.6	0	197
156	77.58	12.97	1958	10	30	3.7	0	302
157	77.50	13.00	1958	10	30	3.8	0	293

158	75.30	11.50	1959	7	27	3.7	0	177
159	75.30	11.50	1959	7	27	4.0	0	177
160	76.41	10.88	1959	9	21	4.3	0	295
161	75.30	11.50	1959	7	21	4.9	0	177
162	75.25	11.50	1959	7	27	4.9	0	175
163	75.30	11.50	1959	7	27	4.1	0	177
164	75.30	11.50	1959	7	27	3.8	0	177
165	75.50	11.80	1959	7	27	4.0	0	155
166	75.80	11.30	1961	9	1	4.0	0	220
167	74.12	14.81	1961	9	2	3.7	0	213
168	75.80	11.30	1961	9	1	4.1	0	220
169	75.80	11.30	1961	9	1	4.2	0	220
170	76.87	11.42	1962	2	7	5.0	0	287
171	75.80	11.30	1964	10	1	4.7	0	220
172	75.80	11.30	1964	10	1	4.3	0	220
173	75.80	11.30	1964	10	1	5.0	0	220
174	75.80	11.30	1964	10	1	4.4	0	220
175	77.75	13.71	1966	1	1	3.7	0	329
176	74.50	15.85	1967	12	10	2.3	0	317
177	76.91	15.14	1967	12	10	2.3	0	329
178	73.81	15.48	1967	12	10	2.3	0	294
179	77.70	13.67	1967	12	10	2.3	0	323
180	75.63	14.23	1967	12	10	2.3	0	163
181	74.98	14.79	1967	12	10	2.3	0	199
182	75.98	13.93	1967	12	10	2.3	0	164
183	76.37	15.27	1967	12	10	2.3	0	303
184	75.13	15.35	1967	12	10	2.3	0	263
185	76.14	15.34	1967	12	10	2.3	0	297
186	74.84	12.87	1967	12	10	2.3	0	17
187	75.63	13.13	1967	12	10	2.3	0	92
188	77.58	12.95	1967	12	10	3.0	0	302
189	74.69	13.62	1967	12	10	3.0	0	69
190	75.92	14.45	1967	12	10	3.0	0	201
191	75.58	13.92	1967	12	10	3.0	0	132
192	74.75	13.25	1967	12	10	3.0	0	27
193	75.73	12.42	1967	12	10	3.0	0	121
194	73.70	15.73	1967	12	10	3.7	0	324
195	75.03	15.20	1967	12	10	3.7	0	245
196	75.65	13.83	1967	12	10	3.7	0	130
197	77.51	13.60	1967	12	10	3.7	0	301
198	74.76	15.33	1967	12	10	3.7	0	258
199	73.25	13.53	1967	12	10	3.7	0	177

200	73.47	15.88	1967	12	10	3.7	0	349
201	76.02	14.17	1967	12	10	3.7	0	185
202	73.81	15.89	1967	12	10	3.7	0	337
203	75.35	14.28	1967	12	10	3.7	0	153
204	74.89	14.35	1967	12	10	3.7	0	149
205	75.24	13.69	1967	12	10	3.7	0	90
206	75.01	15.45	1967	12	10	4.3	0	272
207	77.53	13.29	1967	12	10	4.3	0	298
208	75.63	15.44	1967	12	10	4.3	0	285
209	73.91	15.47	1967	12	10	4.3	0	289
210	73.91	15.50	1967	12	10	4.3	0	293
211	73.87	15.44	1967	12	10	4.3	0	288
212	75.80	14.52	1967	12	10	4.3	0	200
213	74.13	14.81	1967	12	10	4.3	0	212
214	73.67	15.74	1967	12	10	4.3	0	327
215	75.02	14.17	1967	12	10	4.3	0	131
216	73.62	15.86	1967	12	10	4.3	0	341
217	75.92	15.02	1967	12	10	5.0	0	254
218	74.29	14.66	1967	12	10	3.0	0	191
219	74.50	15.85	1967	12	10	3.0	0	317
220	74.13	14.82	1967	12	10	3.0	0	213
221	73.82	15.50	1967	12	10	3.0	0	296
222	74.50	15.85	1967	12	11	3.0	0	317
223	74.13	14.81	1967	12	11	3.0	0	212
224	74.50	15.85	1967	12	24	3.0	0	317
225	74.13	14.81	1967	12	24	3.0	0	212
226	73.82	15.90	1967	12	24	3.0	0	338
227	73.63	15.86	1967	12	24	3.7	0	341
228	73.82	15.49	1967	12	25	3.0	0	295
229	77.78	12.35	1968	5	10	3.3	0	332
230	77.91	12.40	1968	8	2	5.0	0	345
231	77.83	12.22	1968	8	26	3.7	0	341
232	77.23	14.11	1969	2	5	4.7	0	290
233	77.74	12.62	1969	5	6	3.6	0	322
234	77.87	12.09	1969	6	4	5.2	0	349
235	77.35	12.33	1969	8	15	3.3	0	288
236	77.72	12.54	1969	9	21	4.7	0	322
237	77.74	12.55	1969	9	29	4.6	0	324
238	77.30	14.64	1969	11	26	3.7	0	326
239	77.51	13.61	1969	4	13	1.7	0	301
240	77.59	12.97	1969	4	13	2.3	0	303
241	76.78	11.26	1969	4	13	2.3	0	291

242	73.81	15.49	1969	4	13	2.3	0	295
243	74.50	15.85	1969	4	13	3.0	0	317
244	75.14	15.35	1969	4	13	3.0	0	263
245	76.65	12.31	1969	4	13	3.0	0	216
246	77.50	14.10	1969	4	13	3.5	0	317
247	76.60	14.60	1969	4	13	3.5	0	263
248	77.50	12.30	1969	4	13	3.2	0	304
249	77.50	13.00	1969	4	13	4.0	0	293
250	77.12	12.58	1970	1	19	5.6	0	257
251	76.10	13.00	1970	2	12	5.5	0	142
252	77.93	12.75	1970	2	12	3.4	0	341
253	77.20	14.60	1970	2	20	4.6	0	314
254	76.93	13.31	1970	2	12	3.0	0	234
255	76.27	12.67	1970	2	12	3.0	0	165
256	76.05	12.63	1970	2	12	3.0	0	143
257	76.23	12.78	1970	2	12	3.7	0	158
258	76.29	12.30	1970	2	12	3.7	0	181
259	76.65	12.30	1970	2	12	3.7	0	216
260	76.10	13.00	1970	2	12	5.0	0	142
261	77.20	14.60	1970	2	20	3.9	3	314
262	76.10	13.00	1970	2	12	4.8	0	142
263	77.00	12.40	1970	3	27	4.4	0	249
264	77.10	12.60	1970	3	27	3.8	0	254
265	76.10	13.00	1970	2	12	3.8	0	142
266	75.70	13.80	1970	2	12	3.5	0	131
267	77.00	12.40	1971	1	17	4.6	0	249
268	77.00	12.40	1971	1	17	4.9	0	249
269	77.00	12.40	1971	3	6	4.6	0	249
270	77.00	12.40	1971	3	6	4.9	0	249
271	77.00	12.40	1971	3	27	4.7	0	249
272	77.00	12.40	1971	3	27	4.9	0	249
273	77.51	12.49	1971	5	23	4.8	0	300
274	77.65	12.95	1971	5	30	4.6	0	310
275	77.43	11.90	1971	9	5	3.5	0	312
276	77.24	11.91	1971	12	16	3.2	0	293
277	77.00	12.40	1971	1	17	5.0	13	249
278	77.00	12.40	1971	3	6	5.0	16	249
279	77.00	12.40	1971	3	27	5.0	14	249
280	77.00	12.40	1971	1	17	4.4	0	249
281	77.00	12.40	1971	3	6	4.4	0	249
282	77.00	12.40	1971	3	27	4.4	0	249
283	77.00	12.40	1971	1	17	4.4	0	249

284	77.00	12.40	1971	3	6	4.4	0	249
285	77.00	12.40	1971	3	27	4.4	0	249
286	77.00	12.40	1971	1	17	4.3	0	249
287	77.00	12.40	1971	3	6	4.3	0	249
288	77.00	12.40	1971	3	27	4.4	0	249
289	77.00	12.40	1971	3	27	4.1	0	249
290	77.50	13.00	1971	3	27	3.5	0	293
291	76.10	13.00	1971	3	27	3.5	0	142
292	77.00	12.10	1971	3	27	3.3	0	260
293	77.38	12.51	1972	2	15	3.3	0	286
294	77.00	12.40	1972	4	24	3.7	0	249
295	77.00	12.40	1972	5	16	4.9	0	249
296	77.00	12.40	1972	5	16	5.1	0	249
297	77.00	12.40	1972	5	17	4.8	0	249
298	77.00	12.40	1972	5	17	5.1	0	249
299	77.00	11.00	1972	7	29	5.3	0	328
300	77.00	12.40	1972	4	24	4.8	7	249
301	77.00	12.40	1972	4	24	3.9	0	249
302	77.00	12.40	1972	5	16	4.7	0	249
303	77.00	12.40	1972	5	16	4.6	0	249
304	77.00	12.40	1972	5	17	4.6	0	249
305	77.25	12.81	1973	10	20	4.6	0	267
306	77.97	12.59	1974	1	15	3.4	0	348
307	77.32	12.25	1974	12	19	3.5	0	287
308	77.87	12.66	1974	12	20	3.7	0	336
309	77.27	12.57	1975	1	7	3.1	0	273
310	75.30	13.80	1975	5	12	5.4	0	103
311	76.00	15.00	1975	5	12	4.8	0	257
312	76.00	15.00	1975	5	12	5.3	0	257
313	77.67	12.83	1975	12	28	3.7	0	312
314	76.24	13.31	1975	5	12	3.0	0	160
315	77.59	12.97	1975	5	12	3.0	0	303
316	75.00	15.45	1975	5	12	3.0	0	272
317	76.17	14.04	1975	5	12	3.0	0	188
318	75.14	15.35	1975	5	12	3.0	0	263
319	75.92	14.46	1975	5	12	3.7	0	202
320	76.68	13.63	1975	5	12	3.7	0	215
321	74.84	12.87	1975	5	12	3.7	0	17
322	75.40	14.90	1975	5	12	3.7	0	220
323	75.24	13.68	1975	5	12	3.7	0	89
324	74.75	13.34	1975	5	12	3.7	0	37
325	74.89	14.33	1975	5	12	4.3	0	147

326	76.69	15.45	1975	5	12	4.3	0	340
327	75.30	13.80	1975	5	12	4.7	15	103
328	76.00	15.00	1975	5	12	5.0	0	257
329	76.00	15.00	1975	5	12	4.9	0	257
330	75.30	13.80	1975	5	12	5.0	0	103
331	77.64	11.67	1976	3	3	3.1	0	343
332	77.93	13.27	1976	3	4	3.0	0	341
333	77.91	13.28	1976	6	18	3.0	0	339
334	77.25	11.96	1976	12	11	3.6	0	291
335	77.86	12.57	1976	12	24	3.5	0	336
336	77.49	11.82	1977	2	4	3.4	0	321
337	73.83	15.55	1977	5	25	3.0	0	301
338	77.86	13.39	1977	7	12	3.0	0	335
339	77.51	12.95	1977	9	24	4.7	0	294
340	77.13	13.51	1977	10	24	3.4	0	259
341	76.30	15.21	1977	12	1	2.4	0	293
342	73.24	10.55	1977	12	9	2.9	0	322
343	75.98	15.04	1977	12	11	4.6	0	259
344	76.83	14.83	1977	12	17	2.2	0	299
345	75.98	15.03	1977	12	1	4.9	11	258
346	76.37	15.28	1978	1	2	2.4	0	304
347	76.72	15.08	1978	1	8	2.0	0	310
348	76.82	15.15	1978	2	5	2.6	0	323
349	77.20	14.80	1978	3	1	2.2	0	327
350	75.38	10.98	1978	3	10	3.0	0	235
351	77.23	14.89	1978	3	10	2.2	0	336
352	76.54	14.98	1978	5	10	2.6	0	289
353	76.70	15.13	1978	6	2	2.2	0	313
354	77.30	15.00	1978	6	6	2.8	0	349
355	77.10	12.50	1978	6	26	2.3	0	257
356	75.95	14.56	1978	7	13	2.2	0	213
357	77.80	13.40	1978	8	8	4.6	0	328
358	77.49	12.66	1978	11	9	2.5	0	295
359	76.09	12.89	1978	12	17	2.2	0	141
360	77.82	13.44	1978	8	8	4.9	12	331
361	77.90	12.30	1979	6	4	2.6	0	346
362	77.90	12.40	1979	6	9	3.0	0	344
363	77.94	12.40	1979	6	9	3.2	0	348
364	77.30	12.60	1979	9	21	3.1	0	276
365	76.64	15.04	1980	2	10	2.2	0	301
366	77.30	12.70	1980	5	3	4.7	0	274
367	77.40	14.20	1980	5	4	2.4	0	311

368	75.54	13.33	1980	8	16	2.4	0	88
369	76.62	14.47	1980	9	3	3.2	0	255
370	76.06	12.76	1980	11	24	2.2	0	140
371	76.70	15.17	1980	12	13	2.2	0	316
372	74.50	13.60	1980	12	20	3.0	0	73
373	76.97	15.20	1980	12	21	2.2	0	338
374	77.50	12.40	1980	12	25	3.2	0	301
375	77.90	12.50	1980	12	25	2.3	0	342
376	74.50	13.60	1980	12	20	4.7	12	73
377	76.62	14.47	1980	9	3	4.7	5	255
378	76.40	15.30	1980	11	18	3.9	0	308
379	76.80	10.64	1981	1	25	2.2	0	342
380	76.59	15.02	1981	2	9	2.2	0	296
381	76.55	15.10	1981	2	11	2.2	0	300
382	75.03	13.73	1981	2	13	2.2	0	84
383	76.53	15.36	1981	2	21	2.2	0	321
384	74.07	10.56	1981	2	24	5.0	0	284
385	76.79	10.62	1981	2	26	2.2	0	343
386	76.71	15.23	1981	3	17	2.2	0	322
387	76.36	15.08	1981	7	16	2.2	0	285
388	77.80	13.00	1981	8	17	2.8	0	326
389	76.76	15.05	1981	9	28	2.2	0	310
390	76.45	15.15	1981	10	9	2.2	0	297
391	76.65	15.10	1981	10	22	2.2	0	307
392	76.78	15.15	1981	10	26	2.2	0	320
393	76.82	15.10	1981	11	2	2.6	0	319
394	76.94	10.95	1981	11	23	2.2	0	327
395	76.65	15.17	1981	11	28	2.2	0	313
396	76.63	15.12	1981	12	8	2.2	0	307
397	75.58	12.56	1982	1	14	2.6	0	99
398	75.58	12.56	1982	3	13	2.6	0	99
399	76.77	15.08	1982	4	20	2.2	0	314
400	76.75	15.16	1982	4	30	2.2	0	319
401	76.45	15.15	1982	5	6	2.2	0	297
402	75.12	13.33	1982	5	10	2.2	0	50
403	76.83	15.17	1982	7	11	2.4	0	325
404	76.97	12.52	1982	7	15	2.2	0	242
405	76.04	14.57	1982	8	8	2.4	0	219
406	76.72	15.19	1982	8	12	3.2	0	319
407	76.89	15.20	1982	9	9	2.2	0	332
408	76.74	15.13	1982	9	13	2.2	0	315
409	76.84	15.15	1982	9	14	2.2	0	324

410	76.41	15.17	1982	10	1	2.2	0	297
411	76.69	15.20	1982	10	6	2.9	0	318
412	76.60	15.03	1982	10	31	2.2	0	297
413	75.10	12.57	1982	11	11	2.8	0	59
414	76.64	12.71	1982	11	25	2.2	0	203
415	76.69	14.92	1982	11	27	2.2	0	295
416	76.64	15.10	1982	12	1	2.2	0	306
417	76.73	12.33	1982	12	11	2.2	0	223
418	76.88	14.96	1982	12	16	2.9	0	312
419	77.01	15.23	1982	12	18	2.2	0	343
420	75.94	14.55	1982	12	24	2.2	0	211
421	76.70	15.08	1982	12	25	2.2	0	308
422	76.58	15.17	1982	12	31	2.2	0	308
423	76.74	15.13	1983	1	4	2.6	0	315
424	76.56	15.08	1983	1	8	2.2	0	299
425	76.54	14.93	1983	1	10	2.2	0	285
426	76.58	15.06	1983	1	13	2.2	0	298
427	76.72	15.11	1983	1	16	2.2	0	312
428	76.60	14.05	1983	1	22	2.3	0	227
429	76.44	14.98	1983	1	23	2.2	0	282
430	76.71	15.10	1983	1	24	2.6	0	311
431	76.71	15.10	1983	1	25	2.2	0	311
432	76.29	15.37	1983	1	28	2.2	0	308
433	76.71	15.04	1983	1	31	2.2	0	306
434	76.71	15.07	1983	2	5	2.2	0	308
435	76.78	15.11	1983	2	13	2.2	0	317
436	76.78	15.09	1983	2	15	2.2	0	315
437	73.58	13.93	1983	2	24	2.0	0	166
438	76.64	15.18	1983	2	24	2.4	0	313
439	76.37	15.24	1983	2	26	2.2	0	300
440	76.51	15.02	1983	3	12	2.4	0	290
441	76.57	15.27	1983	3	13	2.2	0	316
442	76.64	15.01	1983	3	14	2.2	0	298
443	76.62	15.08	1983	3	15	2.2	0	303
444	76.60	15.03	1983	3	17	2.2	0	297
445	76.59	15.05	1983	3	21	2.2	0	298
446	76.61	15.02	1983	3	25	2.2	0	297
447	76.61	14.99	1983	3	27	2.2	0	295
448	75.21	13.00	1983	3	29	2.2	0	45
449	75.83	12.59	1983	4	6	2.4	0	122
450	76.64	15.15	1983	4	6	2.2	0	310
451	76.62	15.08	1983	4	8	2.2	0	303

452	76.61	15.11	1983	4	9	2.2	0	305
453	76.62	15.02	1983	4	11	2.2	0	298
454	76.72	15.18	1983	4	19	2.2	0	318
455	77.19	12.64	1983	4	21	3.0	0	263
456	76.61	15.08	1983	4	22	2.2	0	302
457	77.10	12.60	1983	4	22	3.0	0	254
458	76.78	15.20	1983	4	23	2.2	0	324
459	76.69	15.09	1983	4	24	2.6	0	309
460	77.10	15.20	1983	4	27	2.2	0	348
461	76.74	15.09	1983	4	30	2.2	0	312
462	76.76	15.13	1983	5	6	2.2	0	317
463	77.22	13.14	1983	5	11	2.2	0	263
464	76.53	15.00	1983	5	18	2.2	0	290
465	76.77	15.15	1983	5	30	2.2	0	319
466	77.12	12.70	1983	5	30	2.3	0	255
467	76.12	13.05	1983	6	14	2.8	0	144
468	76.61	15.13	1983	7	10	2.4	0	306
469	78.00	12.70	1983	7	28	2.3	0	349
470	75.14	11.77	1983	8	31	2.2	0	143
471	76.68	15.11	1983	9	7	2.2	0	310
472	76.63	15.10	1983	9	30	2.2	0	305
473	76.68	15.11	1983	10	2	2.6	0	310
474	73.83	10.99	1983	10	7	4.9	0	248
475	74.31	13.16	1983	10	7	2.2	0	55
476	76.00	13.40	1983	10	21	3.7	0	138
477	76.68	14.87	1983	12	8	2.2	0	290
478	76.00	13.40	1983	10	2	4.9	6	138
479	76.66	15.12	1984	2	13	2.5	0	309
480	76.69	15.06	1984	2	25	2.1	0	306
481	76.68	15.05	1984	3	14	2.4	0	305
482	76.64	15.08	1984	3	19	2.2	0	304
483	77.70	12.50	1984	3	20	5.0	0	320
484	77.80	12.70	1984	3	20	4.8	0	328
485	75.06	13.16	1984	4	17	2.2	0	33
486	74.98	13.88	1984	4	26	2.0	0	99
487	75.12	13.16	1984	4	30	2.0	0	39
488	76.73	15.03	1984	4	30	2.1	0	307
489	76.71	15.04	1984	5	12	2.4	0	306
490	75.22	13.14	1984	5	17	2.0	0	48
491	76.71	15.14	1984	5	31	2.4	0	314
492	77.29	12.43	1984	6	17	2.1	0	278
493	76.66	15.12	1984	6	21	2.2	0	309

494	76.71	15.02	1984	6	26	2.2	0	304
495	76.73	15.03	1984	7	15	2.4	0	307
496	76.52	15.02	1984	8	7	2.2	0	291
497	76.67	15.10	1984	8	10	2.2	0	308
498	76.68	15.10	1984	8	27	2.2	0	309
499	76.68	15.10	1984	8	28	2.8	0	309
500	76.31	15.29	1984	9	10	2.2	0	301
501	76.67	15.17	1984	9	21	2.6	0	314
502	76.68	15.10	1984	10	16	2.2	0	309
503	76.74	15.06	1984	10	21	2.6	0	310
504	75.80	13.59	1984	10	25	2.2	0	126
505	77.60	12.20	1984	11	15	2.2	0	318
506	76.64	14.98	1984	11	21	2.2	0	296
507	76.74	15.04	1984	11	31	2.2	0	308
508	76.52	15.28	1984	12	8	2.2	0	313
509	77.43	12.82	1984	3	20	4.6	10	287
510	76.64	12.31	1984	3	20	3.0	0	215
511	77.53	13.29	1984	3	20	3.7	0	298
512	77.92	12.62	1984	3	20	3.7	0	342
513	77.59	12.97	1984	3	20	4.3	0	303
514	77.60	12.80	1984	3	20	4.3	0	305
515	77.78	12.53	1984	3	20	4.3	0	328
516	77.82	12.73	1984	3	20	4.3	0	330
517	77.75	12.56	1984	3	20	4.3	0	324
518	77.88	12.60	1984	3	20	4.3	0	338
519	77.78	12.82	1984	3	20	4.3	0	324
520	77.80	12.58	1984	3	20	5.0	0	329
521	77.77	12.55	1984	3	20	5.1	0	327
522	77.43	12.82	1984	3	20	4.4	0	287
523	77.43	12.82	1984	3	20	4.5	0	287
524	77.80	12.70	1984	3	20	4.6	0	328
525	75.80	11.30	1984	3	20	3.0	0	220
526	76.69	15.09	1985	1	10	2.0	0	309
527	77.10	12.60	1985	1	12	2.1	0	254
528	77.50	13.20	1985	1	24	2.1	0	294
529	76.83	14.91	1985	3	13	2.6	0	305
530	76.44	15.27	1985	3	15	2.0	0	307
531	76.66	15.08	1985	4	11	2.0	0	306
532	77.30	13.50	1985	5	5	2.8	0	277
533	77.40	13.50	1985	5	7	3.1	0	287
534	76.70	15.15	1985	5	15	2.4	0	314
535	76.74	15.10	1985	7	9	2.0	0	313

536	76.68	15.04	1985	9	3	2.0	0	304
537	76.60	14.97	1985	9	18	2.2	0	292
538	76.64	14.98	1985	9	21	2.2	0	296
539	76.77	15.06	1985	9	25	2.2	0	312
540	76.78	15.06	1985	10	17	2.0	0	313
541	77.40	12.60	1985	10	17	2.3	0	286
542	76.71	15.08	1985	10	29	2.4	0	309
543	76.70	15.54	1985	11	1	2.2	0	348
544	76.69	15.07	1985	11	4	2.2	0	307
545	77.41	13.56	1985	5	7	4.7	8	290
546	77.40	13.60	1985	5	7	3.3	0	290
547	76.70	15.24	1986	1	11	2.4	0	322
548	76.63	15.12	1986	1	17	2.4	0	307
549	75.29	13.24	1986	1	22	2.2	0	59
550	76.52	15.18	1986	1	24	2.2	0	305
551	75.10	13.21	1986	1	29	2.1	0	40
552	76.69	15.17	1986	1	30	2.3	0	315
553	76.59	15.06	1986	2	4	2.7	0	299
554	76.72	15.06	1986	2	5	2.4	0	308
555	76.52	14.81	1986	2	9	2.3	0	273
556	76.73	15.15	1986	2	19	2.8	0	316
557	76.57	15.05	1986	3	18	2.1	0	297
558	76.79	15.03	1986	3	18	2.3	0	311
559	75.16	13.22	1986	3	19	2.1	0	46
560	76.64	15.04	1986	3	20	2.4	0	301
561	76.74	14.99	1986	3	21	2.0	0	304
562	75.85	12.73	1986	3	22	2.0	0	119
563	76.61	15.06	1986	3	28	2.3	0	300
564	76.76	15.07	1986	4	2	2.2	0	312
565	76.73	15.08	1986	4	4	2.3	0	311
566	76.80	15.20	1986	4	7	2.5	0	326
567	75.16	13.18	1986	4	15	2.6	0	44
568	76.66	15.14	1986	4	20	2.5	0	311
569	76.63	15.23	1986	4	27	2.0	0	316
570	76.48	15.20	1986	4	28	2.0	0	304
571	76.45	15.11	1986	4	29	2.7	0	294
572	76.67	15.21	1986	5	3	2.6	0	317
573	75.08	13.41	1986	5	5	2.9	0	54
574	76.23	15.20	1986	9	24	2.1	0	288
575	76.77	15.12	1986	9	24	2.0	0	317
576	76.96	15.10	1986	9	29	2.2	0	329
577	76.71	15.15	1986	10	1	2.6	0	315

578	76.63	15.01	1986	10	2	2.0	0	298
579	76.75	15.07	1986	10	7	2.0	0	311
580	76.48	15.03	1986	10	8	2.5	0	289
581	77.10	12.07	1986	10	8	2.7	0	271
582	76.57	15.17	1986	10	9	2.2	0	307
583	76.60	12.30	1986	10	9	2.0	0	211
584	76.72	15.10	1986	10	10	2.2	0	312
585	76.54	15.03	1986	10	13	2.6	0	293
586	76.63	15.13	1986	10	15	2.4	0	308
587	76.61	15.01	1986	10	16	2.4	0	296
588	76.54	14.98	1986	10	17	2.5	0	289
589	75.69	12.98	1986	10	19	2.0	0	97
590	76.55	15.21	1986	10	20	2.3	0	309
591	76.88	14.61	1986	10	20	2.4	0	287
592	76.68	15.16	1986	10	22	2.0	0	314
593	76.70	15.07	1986	10	28	2.5	0	308
594	76.69	15.19	1986	10	30	2.0	0	317
595	75.29	13.44	1986	10	31	2.7	0	72
596	75.13	13.12	1986	11	10	2.0	0	38
597	76.50	14.97	1986	11	12	2.3	0	285
598	74.98	13.44	1986	11	14	2.3	0	52
599	76.64	10.69	1986	11	18	2.2	0	327
600	76.71	15.14	1986	11	18	2.8	0	314
601	76.42	15.34	1986	11	20	2.1	0	313
602	76.73	15.17	1986	11	22	2.6	0	318
603	76.65	15.09	1986	11	25	2.0	0	306
604	74.08	13.11	1986	11	27	2.4	0	78
605	74.02	13.20	1986	11	29	2.6	0	86
606	76.68	15.10	1986	12	3	2.1	0	309
607	76.66	15.08	1986	12	4	2.8	0	306
608	75.05	13.78	1986	12	5	2.3	0	90
609	76.56	15.14	1986	12	5	2.7	0	304
610	76.67	15.13	1986	12	8	2.6	0	311
611	75.06	13.11	1986	12	9	2.8	0	31
612	76.82	15.19	1986	12	9	2.2	0	326
613	76.88	15.18	1986	12	12	2.3	0	330
614	76.78	14.91	1986	12	13	2.4	0	301
615	76.58	15.18	1986	12	15	2.0	0	309
616	75.16	13.38	1986	12	21	2.3	0	57
617	76.75	15.07	1986	12	26	2.5	0	311
618	76.54	15.03	1986	12	27	2.2	0	293
619	75.04	13.60	1986	12	29	2.3	0	71

620	76.75	15.20	1986	12	29	2.6	0	322
621	76.78	15.19	1986	12	30	2.1	0	323
622	75.16	13.22	1987	1	2	2.3	0	46
623	76.70	15.14	1987	1	6	2.6	0	313
624	76.66	15.14	1987	1	7	2.6	0	311
625	76.18	15.05	1987	1	13	2.0	0	272
626	76.55	15.35	1987	1	13	2.1	0	322
627	75.07	13.20	1987	1	21	2.3	0	37
628	77.69	12.12	1987	1	22	2.6	0	330
629	76.58	15.26	1987	1	25	2.1	0	316
630	76.68	15.10	1987	1	27	2.8	0	309
631	76.57	15.07	1987	1	29	2.0	0	298
632	76.88	10.88	1987	2	2	2.0	0	328
633	75.10	13.16	1987	2	6	2.1	0	37
634	76.69	15.12	1987	2	14	2.0	0	311
635	75.12	12.94	1987	2	18	2.6	0	36
636	76.81	15.13	1987	2	19	2.0	0	321
637	76.80	15.15	1987	2	24	2.7	0	321
638	76.86	13.47	1987	2	25	2.2	0	229
639	76.71	15.13	1987	2	26	2.5	0	313
640	75.11	13.12	1987	3	5	2.9	0	36
641	76.37	14.92	1987	3	5	2.1	0	272
642	76.51	15.27	1987	3	6	2.1	0	312
643	75.90	15.44	1987	3	16	2.1	0	295
644	75.15	13.02	1987	4	1	2.0	0	39
645	76.76	14.80	1987	4	3	2.2	0	291
646	76.63	15.14	1987	4	13	2.1	0	309
647	75.16	13.42	1987	4	15	2.4	0	60
648	76.42	15.25	1987	4	17	2.1	0	304
649	75.05	13.29	1987	4	30	2.4	0	42
650	75.11	13.02	1987	5	7	2.9	0	34
651	76.65	10.75	1987	5	9	2.2	0	323
652	76.74	15.13	1987	5	12	2.0	0	315
653	77.22	12.21	1987	5	13	2.0	0	278
654	75.42	13.30	1987	5	19	2.7	0	75
655	75.22	13.14	1987	5	23	2.4	0	48
656	75.18	13.29	1987	5	28	2.5	0	52
657	75.11	13.17	1987	5	30	2.4	0	39
658	75.09	13.35	1987	6	4	2.6	0	49
659	76.65	15.22	1987	6	15	2.2	0	317
660	76.63	15.14	1987	7	30	2.8	0	309
661	75.02	13.14	1987	8	31	2.4	0	28

662	76.71	15.18	1987	9	3	2.6	0	318
663	75.09	13.16	1987	9	6	2.3	0	36
664	76.76	12.08	1987	9	6	2.0	0	237
665	76.08	12.89	1987	9	13	2.7	0	140
666	76.68	14.96	1987	10	20	2.2	0	297
667	76.64	14.94	1987	10	28	2.2	0	293
668	76.73	15.12	1987	11	3	2.2	0	314
669	76.57	15.01	1987	11	4	2.7	0	293
670	76.69	15.38	1987	11	4	2.6	0	333
671	76.71	15.04	1987	11	9	2.2	0	306
672	77.76	14.09	1987	11	19	2.3	0	342
673	76.51	14.92	1987	12	7	2.1	0	282
674	75.27	13.55	1987	12	10	2.3	0	79
675	76.77	10.78	1987	12	10	2.1	0	328
676	76.58	15.04	1987	12	21	2.6	0	297
677	76.70	15.07	1988	1	6	2.0	0	308
678	76.61	15.02	1988	1	8	2.3	0	297
679	76.77	10.88	1988	1	8	2.2	0	320
680	76.82	13.44	1988	1	13	2.1	0	224
681	76.61	15.02	1988	1	15	2.2	0	297
682	76.20	15.10	1988	1	18	2.0	0	277
683	76.46	15.27	1988	1	25	2.3	0	309
684	76.53	15.00	1988	1	25	2.0	0	290
685	76.64	13.61	1988	1	25	2.2	0	211
686	76.59	15.12	1988	1	27	2.1	0	304
687	76.66	15.05	1988	1	28	2.5	0	303
688	76.50	14.96	1988	1	29	2.1	0	284
689	76.44	15.26	1988	2	1	2.2	0	307
690	75.21	13.23	1988	2	4	2.2	0	51
691	75.29	13.93	1988	2	4	2.7	0	115
692	76.70	15.17	1988	2	4	2.4	0	316
693	76.50	14.96	1988	2	5	2.4	0	284
694	76.47	15.25	1988	2	8	2.0	0	308
695	76.63	15.03	1988	2	17	2.5	0	299
696	76.74	10.79	1988	2	17	2.0	0	325
697	75.28	13.39	1988	2	19	2.1	0	67
698	75.87	11.14	1988	2	19	2.4	0	239
699	75.31	13.20	1988	2	20	2.0	0	60
700	76.43	15.25	1988	2	26	2.0	0	305
701	76.49	14.95	1988	3	4	2.2	0	283
702	75.18	13.43	1988	3	5	2.4	0	63
703	76.48	15.28	1988	3	5	2.2	0	311

704	76.22	14.86	1988	3	21	2.4	0	257
705	76.77	10.78	1988	3	21	2.5	0	328
706	76.80	15.02	1988	3	23	2.3	0	311
707	76.72	15.18	1988	3	29	2.2	0	318
708	75.43	13.14	1988	4	7	2.2	0	70
709	75.49	13.91	1988	4	19	2.0	0	125
710	76.75	15.10	1988	4	19	2.1	0	314
711	76.70	14.97	1988	4	21	2.5	0	300
712	76.76	15.00	1988	4	23	2.2	0	306
713	76.80	13.43	1988	5	2	2.2	0	222
714	77.00	15.26	1988	5	2	2.3	0	345
715	76.70	15.11	1988	5	5	2.4	0	311
716	75.27	13.63	1988	5	16	2.4	0	86
717	76.85	15.03	1988	5	18	2.0	0	316
718	75.35	13.03	1988	5	21	2.9	0	60
719	75.30	13.29	1988	5	28	2.0	0	63
720	75.61	10.32	1988	6	14	2.1	0	312
721	76.77	15.51	1988	7	1	2.0	0	350
722	75.86	12.76	1988	7	26	3.0	0	119
723	76.73	14.93	1988	8	11	2.0	0	299
724	76.50	15.12	1988	10	10	2.1	0	298
725	76.42	15.08	1988	10	27	2.9	0	289
726	76.60	15.02	1988	11	22	2.2	0	296
727	76.42	15.13	1988	11	23	2.4	0	294
728	75.57	13.66	1988	11	30	2.3	0	111
729	76.50	15.13	1988	12	4	2.4	0	299
730	76.83	15.03	1988	12	31	2.0	0	314
731	77.58	12.97	1988	8	20	1.7	0	302
732	77.06	13.01	1989	1	12	2.0	0	246
733	76.68	12.57	1989	1	13	1.1	0	210
734	76.72	12.54	1989	2	8	1.9	0	215
735	76.70	10.90	1989	2	10	1.5	0	313
736	76.93	12.85	1989	2	10	2.1	0	232
737	77.06	15.19	1989	2	11	1.8	0	344
738	76.91	12.55	1989	2	12	1.3	0	235
739	77.70	11.90	1989	2	16	2.8	0	339
740	76.92	12.58	1989	2	25	1.1	0	236
741	76.68	12.71	1989	3	9	1.2	0	207
742	77.68	13.18	1989	3	18	1.4	0	313
743	77.25	12.46	1989	3	19	1.5	0	273
744	77.21	13.60	1989	3	22	2.2	0	270
745	77.57	13.69	1989	3	26	3.7	0	310

746	76.58	12.98	1989	3	27	1.4	0	194
747	76.87	12.61	1989	4	10	1.3	0	230
748	77.63	12.17	1989	5	9	2.0	0	322
749	77.66	13.46	1989	5	29	1.8	0	314
750	77.66	13.46	1989	6	2	1.6	0	314
751	76.91	10.65	1989	8	5	1.8	0	349
752	76.70	14.39	1989	8	20	1.3	0	257
753	76.70	15.07	1989	8	23	3.1	0	308
754	76.28	12.77	1989	8	24	3.0	0	163
755	76.11	13.38	1989	9	5	1.6	0	148
756	76.90	12.62	1989	9	12	1.3	0	232
757	76.93	14.54	1989	10	15	1.1	0	287
758	76.16	13.53	1989	10	16	2.0	0	159
759	76.65	10.76	1989	10	18	1.8	0	322
760	74.87	13.77	1989	10	29	2.4	0	85
761	76.75	10.68	1989	11	30	1.8	0	335
762	76.82	12.53	1989	12	1	1.1	0	226
763	77.01	12.81	1989	12	5	1.8	0	241
764	77.44	14.76	1989	12	26	1.4	0	346
765	76.38	10.41	1989	3	15	3.7	0	337
766	76.36	14.68	1990	1	9	1.7	0	251
767	76.70	13.87	1990	2	12	2.0	0	227
768	76.75	12.47	1990	2	20	1.1	0	221
769	76.86	12.52	1990	2	22	1.4	0	231
770	74.94	13.70	1990	2	26	1.8	0	78
771	76.79	12.26	1990	2	26	1.1	0	232
772	76.88	12.55	1990	2	27	1.7	0	232
773	76.78	12.07	1990	3	6	2.8	0	240
774	76.91	12.63	1990	3	13	1.4	0	233
775	77.12	15.07	1990	3	13	1.9	0	340
776	77.94	13.72	1990	3	18	2.7	0	349
777	76.69	10.69	1990	3	27	1.7	0	331
778	76.45	10.76	1990	3	31	1.8	0	309
779	76.67	10.80	1990	4	16	1.8	0	320
780	75.93	14.77	1990	5	4	2.1	0	231
781	76.90	14.48	1990	8	17	1.9	0	280
782	77.37	14.76	1990	9	2	1.5	0	339
783	77.44	14.75	1990	9	20	1.7	0	345
784	76.17	14.37	1990	11	21	1.3	0	212
785	77.08	15.10	1991	1	14	1.9	0	339
786	76.86	12.53	1991	1	22	0.9	0	230
787	77.44	14.71	1991	1	29	1.2	0	342

788	77.15	11.65	1991	2	5	1.7	0	297
789	76.79	14.71	1991	3	11	1.8	0	287
790	76.10	10.98	1991	3	17	1.6	0	267
791	76.91	13.59	1991	3	25	1.8	0	238
792	76.28	14.06	1991	3	28	3.2	0	198
793	76.21	12.61	1991	5	4	2.2	0	160
794	77.63	13.62	1991	5	5	2.7	0	314
795	76.90	10.69	1991	5	10	1.7	0	345
796	76.59	12.27	1991	5	15	1.6	0	212
797	77.54	14.66	1991	6	30	1.7	0	349
798	77.25	12.49	1991	7	18	1.6	0	273
799	76.72	14.66	1991	8	4	1.9	0	277
800	77.77	12.03	1991	8	23	2.1	0	341
801	76.90	12.46	1991	9	1	1.2	0	237
802	76.72	10.69	1991	9	5	1.8	0	333
803	76.59	10.83	1991	9	21	1.5	0	312
804	76.65	12.94	1991	9	21	1.1	0	201
805	76.97	11.05	1991	10	3	1.7	0	322
806	76.93	10.75	1991	10	10	1.7	0	342
807	76.69	10.80	1991	10	15	1.5	0	321
808	76.64	10.81	1991	10	17	1.6	0	317
809	76.14	10.88	1991	10	19	1.6	0	279
810	77.98	12.64	1991	11	1	2.2	0	348
811	77.90	12.60	1991	11	22	2.0	0	340
812	76.79	13.42	1991	11	23	2.3	0	221
813	77.63	12.85	1991	11	30	2.3	0	308
814	77.41	14.62	1991	12	3	2.1	0	334
815	77.65	12.35	1991	12	4	2.7	0	318
816	77.65	12.26	1991	12	5	1.7	0	321
817	77.07	12.29	1991	12	9	1.3	0	260
818	77.18	14.68	1991	12	9	1.5	0	317
819	76.71	13.00	1991	12	19	1.2	0	208
820	72.22	11.99	1991	12	28	1.5	0	302
821	76.80	10.67	1991	12	31	1.5	0	340
822	77.71	12.55	1992	1	1	2.2	0	320
823	76.77	10.88	1992	1	6	2.3	0	320
824	77.25	13.51	1992	1	7	1.6	0	272
825	77.32	13.54	1992	1	9	1.5	0	280
826	77.02	13.37	1992	1	18	2.2	0	244
827	77.46	13.70	1992	1	19	1.8	0	298
828	76.91	11.13	1992	1	21	2.5	0	311
829	77.30	13.51	1992	2	4	1.6	0	277

830	76.74	13.14	1992	2	5	1.0	0	211
831	76.83	11.05	1992	2	6	1.9	0	311
832	76.74	13.13	1992	2	18	2.4	0	211
833	76.80	10.99	1992	2	21	1.9	0	313
834	76.94	12.56	1992	2	21	1.3	0	238
835	77.03	13.08	1992	2	23	1.0	0	242
836	77.63	14.42	1992	2	27	1.1	0	344
837	76.95	14.90	1992	3	2	1.9	0	313
838	77.11	15.14	1992	3	4	1.4	0	344
839	76.99	12.59	1992	3	7	1.3	0	243
840	77.25	13.50	1992	3	7	1.1	0	271
841	76.67	15.28	1992	3	15	1.7	0	323
842	76.68	10.93	1992	3	19	2.2	0	309
843	77.32	13.53	1992	3	19	1.1	0	279
844	76.73	10.94	1992	4	3	2.0	0	312
845	76.90	11.04	1992	4	21	2.0	0	317
846	76.43	14.21	1992	4	23	1.8	0	221
847	77.37	14.52	1992	4	29	1.9	0	325
848	76.23	13.74	1992	4	30	2.1	0	175
849	76.36	14.16	1992	5	5	2.0	0	212
850	76.58	15.27	1992	6	1	1.5	0	316
851	76.72	10.89	1992	7	2	2.8	0	316
852	77.23	14.31	1992	7	23	1.2	0	300
853	77.25	13.47	1992	8	3	0.9	0	271
854	77.10	12.85	1992	8	9	1.1	0	251
855	77.59	13.84	1992	8	9	0.7	0	316
856	77.21	11.87	1992	8	12	1.9	0	291
857	77.63	13.91	1992	8	12	1.8	0	323
858	77.27	13.50	1992	8	14	0.6	0	273
859	77.65	13.94	1992	8	14	1.4	0	326
860	77.72	13.92	1992	8	16	1.5	0	332
861	77.70	13.88	1992	8	18	1.7	0	329
862	77.33	13.55	1992	8	22	0.9	0	281
863	76.69	10.91	1992	8	25	2.0	0	312
864	76.68	13.05	1992	8	27	1.3	0	204
865	77.74	13.90	1992	8	27	1.8	0	334
866	77.87	13.43	1992	8	27	2.8	0	336
867	76.80	10.92	1992	9	5	2.0	0	319
868	75.27	15.19	1992	9	12	3.2	0	248
869	76.40	12.74	1992	9	20	1.5	0	177
870	76.34	13.86	1992	9	30	1.7	0	192
871	75.14	11.77	1992	10	20	2.3	0	143

872	77.94	12.85	1992	10	28	1.1	0	341
873	77.88	12.98	1992	11	4	1.1	0	334
874	75.40	14.00	1992	11	23	1.9	0	128
875	77.94	12.80	1992	11	27	1.4	0	342
876	76.85	10.79	1992	11	28	2.4	0	333
877	76.09	15.08	1992	11	29	2.0	0	269
878	76.92	10.86	1992	12	5	2.5	0	333
879	77.07	14.66	1992	12	5	1.6	0	307
880	76.80	14.46	1992	12	16	1.6	0	270
881	76.90	14.46	1992	12	24	1.4	0	279
882	77.05	13.59	1993	1	28	1.7	0	252
883	75.86	13.06	1993	1	30	2.7	0	116
884	76.76	10.69	1993	1	31	2.9	0	335
885	74.90	15.12	1993	2	16	2.7	0	235
886	77.45	14.15	1993	4	6	3.0	0	314
887	75.83	12.74	1993	4	7	2.8	0	116
888	75.30	13.53	1993	4	20	3.0	0	80
889	76.50	15.27	1993	5	2	2.0	0	311
890	76.76	14.59	1993	5	18	3.1	0	275
891	75.29	13.63	1993	6	3	2.8	0	87
892	77.05	12.68	1993	6	15	1.4	0	247
893	76.87	12.26	1993	6	16	1.7	0	240
894	75.70	13.28	1993	6	23	2.5	0	103
895	76.11	14.20	1993	7	18	1.9	0	194
896	77.03	15.12	1993	7	19	1.7	0	336
897	77.59	12.94	1993	7	24	2.9	0	303
898	75.76	13.53	1993	7	26	1.9	0	119
899	76.90	13.06	1993	7	28	1.3	0	228
900	77.42	12.60	1993	8	16	1.1	0	288
901	76.88	14.61	1993	9	26	1.8	0	287
902	75.58	13.96	1993	10	5	2.2	0	135
903	77.97	13.08	1993	10	12	2.9	0	344
904	77.41	13.07	1993	11	9	2.0	0	283
905	77.20	12.30	1993	11	14	3.7	0	273
906	77.78	12.26	1993	11	23	2.6	0	335
907	77.04	14.62	1993	11	25	1.6	0	301
908	76.80	14.61	1993	11	29	1.5	0	280
909	76.85	10.90	1993	12	14	2.1	0	324
910	74.84	12.87	1993	9	30	2.3	0	17
911	76.92	15.14	1993	9	30	3.0	0	330
912	76.79	11.35	1993	9	30	3.0	0	285
913	75.57	13.92	1993	9	30	3.0	0	131

914	77.38	12.58	1993	9	30	3.7	0	285
915	75.01	15.45	1993	9	30	3.7	0	272
916	75.11	15.34	1993	9	30	3.7	0	261
917	73.55	15.30	1993	9	30	3.7	0	288
918	73.82	15.49	1993	12	8	3.0	0	295
919	76.57	10.93	1994	2	22	1.9	0	302
920	77.02	10.75	1994	3	2	2.0	0	349
921	76.85	10.88	1994	3	12	1.9	0	326
922	76.47	14.19	1994	4	2	1.6	0	224
923	77.44	12.04	1994	4	7	1.9	0	307
924	77.36	12.04	1994	4	15	1.8	0	299
925	77.53	12.15	1994	5	26	2.4	0	312
926	76.90	10.77	1994	6	23	2.0	0	339
927	77.44	12.78	1994	6	23	2.1	0	288
928	76.62	10.83	1994	6	24	1.9	0	314
929	76.09	10.71	1994	6	28	2.7	0	292
930	77.11	11.95	1994	7	17	1.5	0	278
931	76.69	10.79	1994	7	28	1.9	0	322
932	76.16	12.77	1994	9	8	2.3	0	151
933	76.45	12.07	1994	9	20	2.6	0	208
934	76.36	11.16	1994	9	28	2.3	0	267
935	76.55	15.48	1994	9	29	2.0	0	333
936	76.18	14.03	1994	9	30	2.0	0	188
937	76.79	10.88	1994	9	30	1.9	0	321
938	77.68	12.01	1994	10	1	2.2	0	333
939	75.32	13.74	1994	10	10	1.9	0	99
940	75.95	12.71	1994	10	10	2.6	0	130
941	75.06	13.39	1994	10	21	3.5	0	51
942	75.32	13.12	1994	10	21	1.8	0	58
943	76.62	10.82	1994	11	1	2.0	0	314
944	75.66	13.52	1994	11	3	2.1	0	109
945	76.67	10.92	1994	11	7	2.1	0	309
946	75.24	13.14	1994	11	14	2.0	0	50
947	76.66	12.65	1994	11	17	2.5	0	206
948	76.25	10.75	1994	12	2	4.1	16	297
949	73.82	15.49	1994	2	1	3.0	0	295
950	76.21	10.75	1994	2	1	4.3	0	295
951	76.82	12.87	1995	2	12	2.3	0	220
952	76.36	14.41	1995	2	18	1.7	0	230
953	75.87	12.97	1995	3	1	1.4	0	117
954	76.35	14.26	1995	3	4	1.9	0	218
955	74.00	14.00	1995	3	12	3.9	0	139

956	77.78	12.62	1995	3	12	1.2	0	327
957	76.85	12.69	1995	3	22	2.0	0	226
958	76.22	14.42	1995	4	4	1.7	0	220
959	76.33	14.78	1995	4	21	2.3	0	257
960	76.68	10.77	1995	6	6	1.9	0	323
961	76.84	14.58	1995	7	3	1.7	0	281
962	76.67	13.08	1995	8	12	1.1	0	203
963	76.69	10.80	1995	8	12	1.9	0	321
964	76.68	13.09	1995	8	13	1.2	0	205
965	76.76	13.12	1995	8	14	1.1	0	213
966	76.66	13.04	1995	8	16	1.2	0	202
967	76.76	13.11	1995	8	21	1.3	0	213
968	76.59	13.00	1995	8	24	1.3	0	195
969	76.74	13.14	1995	8	26	1.3	0	211
970	76.65	13.11	1995	8	27	1.3	0	201
971	77.35	13.73	1995	9	7	0.9	0	288
972	76.68	13.02	1995	9	10	1.6	0	204
973	76.63	13.07	1995	9	11	1.2	0	199
974	76.65	13.05	1995	9	13	1.2	0	201
975	76.40	14.23	1995	9	16	1.9	0	220
976	76.42	14.26	1995	9	17	1.8	0	224
977	77.47	12.85	1995	9	17	1.4	0	291
978	76.73	13.09	1995	9	19	1.3	0	210
979	76.76	10.97	1995	9	21	1.9	0	312
980	76.45	12.92	1995	9	22	1.3	0	180
981	76.68	13.07	1995	9	23	1.0	0	204
982	76.66	13.04	1995	9	28	1.2	0	202
983	76.69	13.04	1995	10	1	1.2	0	205
984	77.54	13.02	1995	10	1	2.4	0	298
985	76.75	12.96	1995	10	7	1.5	0	212
986	76.70	12.99	1995	10	8	1.4	0	207
987	76.81	14.62	1995	10	14	1.6	0	282
988	76.50	12.95	1995	10	16	0.9	0	185
989	76.52	13.04	1995	10	18	1.4	0	187
990	76.33	14.27	1995	10	19	2.2	0	217
991	76.25	14.32	1995	10	21	2.3	0	214
992	76.54	12.98	1995	10	30	0.9	0	189
993	76.58	13.01	1995	10	31	0.9	0	194
994	76.51	13.02	1995	11	1	1.7	0	186
995	76.62	12.99	1995	11	3	1.1	0	198
996	76.59	13.07	1995	11	6	1.2	0	195
997	76.62	13.03	1995	11	7	1.2	0	198

998	76.53	13.01	1995	11	8	1.3	0	188
999	76.53	13.00	1995	11	9	1.2	0	188
1000	76.53	12.98	1995	11	10	1.5	0	188
1001	76.53	12.98	1995	11	11	1.2	0	188
1002	76.53	12.98	1995	11	13	1.2	0	188
1003	76.51	13.01	1995	11	14	1.0	0	186
1004	76.50	13.04	1995	11	15	1.3	0	185
1005	77.30	12.53	1995	11	15	1.2	0	277
1006	76.49	12.99	1995	11	16	1.3	0	184
1007	77.00	15.12	1995	11	17	1.9	0	334
1008	76.53	12.99	1995	11	18	1.1	0	188
1009	76.56	12.97	1995	11	21	1.2	0	191
1010	76.55	12.96	1995	11	22	1.3	0	190
1011	77.80	12.33	1995	11	24	2.2	0	335
1012	76.54	12.98	1995	11	26	1.9	0	189
1013	76.53	12.98	1995	11	27	1.6	0	188
1014	76.53	12.98	1995	11	28	1.2	0	188
1015	76.55	12.96	1995	11	30	1.3	0	190
1016	77.69	12.89	1995	12	4	2.4	0	314
1017	76.53	13.02	1995	12	9	1.4	0	188
1018	76.51	13.01	1995	12	12	1.3	0	186
1019	77.21	12.80	1995	12	15	1.8	0	263
1020	76.52	13.01	1995	12	17	1.4	0	187
1021	76.53	12.99	1995	12	22	1.5	0	188
1022	74.00	16.00	1996	4	26	3.7	0	343
1023	77.00	14.00	1996	11	10	3.2	0	263
1024	75.40	15.20	1996	1	9	4.6	2	252
1025	75.40	15.20	1996	1	9	4.4	0	252
1026	75.40	15.20	1996	1	9	4.5	0	252
1027	76.40	13.20	1998	2	4	4.0	10	175
1028	76.40	13.20	1998	2	4	4.2	21	175
1029	75.43	14.90	1998	7	19	4.4	22	221
1030	74.50	14.81	1998	11	25	3.5	2	202
1031	76.84	12.67	1998	2	4	4.0	21	225
1032	75.70	15.60	1998	7	19	3.9	0	304
1033	76.40	13.20	1998	2	4	4.0	0	175
1034	75.70	15.60	1998	7	19	4.0	0	304
1035	75.64	10.33	1999	9	11	3.9	15	312
1036	75.64	10.32	1999	9	11	4.1	3	313
1037	75.64	10.33	1999	9	11	3.8	3	312
1038	75.00	16.00	2000	3	12	4.8	0	333
1039	75.25	14.83	2000	8	14	2.8	37	208

1040	74.60	13.07	2000	1	1	4.0	9	22
1041	77.79	14.17	2000	3	9	1.5	6	349
1042	73.75	15.41	2000	3	15	1.5	0	289
1043	74.59	15.80	2000	4	24	3.8	11	311
1044	75.25	14.83	2000	8	14	3.4	6	208
1045	74.50	15.85	2000	9	5	3.0	0	317
1046	76.96	11.00	2000	12	12	3.0	0	325
1047	76.79	11.35	2000	12	12	3.0	0	285
1048	77.43	11.45	2000	12	12	3.0	0	335
1049	76.88	11.42	2000	12	12	3.0	0	288
1050	76.62	11.27	2000	12	12	3.0	0	277
1051	76.69	11.41	2000	12	12	3.0	0	272
1052	75.68	11.45	2000	12	12	3.7	0	199
1053	76.21	10.51	2000	12	12	3.7	0	318
1054	74.60	13.08	2000	1	1	4.2	9	22
1055	74.59	15.80	2000	4	24	4.0	11	311
1056	74.60	13.08	2000	1	1	3.7	9	22
1057	74.60	13.07	2000	1	1	3.7	0	22
1058	74.59	15.80	2000	4	24	3.4	0	311
1059	77.36	12.44	2001	1	29	4.3	15	286
1060	76.12	10.48	2001	8	25	3.1	15	316
1061	73.54	15.82	2001	8	26	2.2	33	340
1062	77.36	12.44	2001	1	29	4.4	2	286
1063	76.12	10.48	2001	8	25	3.6	0	316
1064	73.54	15.82	2001	8	26	3.0	14	340
1065	76.97	11.00	2001	1	7	3.0	0	326
1066	75.78	11.25	2001	1	7	3.0	0	223
1067	74.12	14.99	2001	1	26	2.3	0	232
1068	77.60	12.95	2001	1	26	3.0	0	304
1069	74.84	12.87	2001	1	29	2.3	0	17
1070	77.27	12.71	2001	1	29	2.3	0	271
1071	77.10	13.34	2001	1	29	2.3	0	252
1072	77.03	12.20	2001	1	29	2.3	0	259
1073	76.94	11.92	2001	1	29	3.0	0	263
1074	77.79	13.07	2001	1	29	3.0	0	325
1075	77.04	12.58	2001	1	29	3.0	0	248
1076	77.05	12.38	2001	1	29	3.0	0	255
1077	76.89	12.52	2001	1	29	3.0	0	234
1078	76.65	12.30	2001	1	29	3.0	0	216
1079	77.38	13.10	2001	1	29	3.0	0	280
1080	76.69	12.41	2001	1	29	3.0	0	216
1081	77.93	12.99	2001	1	29	3.7	0	340

1082	77.58	12.96	2001	1	29	4.3	0	302
1083	77.46	12.67	2001	1	29	4.3	0	292
1084	77.42	12.54	2001	1	29	4.3	0	290
1085	77.53	13.30	2001	9	25	2.3	0	298
1086	74.84	12.88	2001	9	25	2.3	0	16
1087	77.58	12.97	2001	9	25	3.0	0	302
1088	77.22	12.60	2001	1	29	4.4	2	267
1089	77.22	12.60	2001	1	29	4.3	0	267
1090	76.12	10.48	2001	8	25	3.1	0	316
1091	77.36	12.44	2001	1	29	4.2	0	286
1092	77.36	12.44	2001	1	29	4.3	0	286
1093	76.25	10.76	2001	8	25	3.4	0	296
1094	76.08	15.48	2002	7	10	3.6	10	307
1095	76.08	15.48	2002	7	10	3.9	14	307
1096	75.63	15.43	2002	7	10	2.3	0	284
1097	75.67	15.45	2002	7	10	2.3	0	287
1098	75.01	15.45	2002	7	10	2.3	0	272
1099	75.47	15.12	2002	7	10	3.7	0	245
1100	75.58	15.23	2002	7	10	3.7	0	261
1101	76.18	15.34	2002	7	10	3.9	14	299
1102	76.18	15.34	2002	7	10	3.5	0	299
1103	76.24	10.76	2002	8	1	3.4	11	296
1104	74.27	14.64	2003	7	12	3.5	30	190
1105	75.59	15.22	2003	11	4	3.5	5	260
1106	74.27	14.64	2003	7	12	3.8	13	190
1107	75.58	15.22	2003	11	4	3.8	18	260
1108	74.66	14.75	2003	7	12	3.8	13	194
1109	75.59	15.22	2003	11	4	3.4	18	260
1110	75.58	15.22	2003	11	4	3.3	0	260
1111	75.65	11.83	2003	1	12	3.3	17	161
1112	76.88	11.95	2003	11	4	3.4	18	255
1113	75.55	11.72	2003	11	8	3.7	15	165
1114	76.11	11.95	2003	11	8	3.2	16	185
1115	76.20	10.57	2003	12	8	2.2	19	312
1116	74.13	14.81	2004	1	7	1.7	0	212
1117	73.95	15.27	2004	1	7	1.7	0	267
1118	73.81	15.59	2004	1	7	1.7	0	306
1119	73.82	15.49	2004	1	7	1.7	0	295
1120	73.83	15.40	2004	1	7	1.7	0	285
1121	74.08	14.97	2004	1	7	3.0	0	231
1122	74.13	14.92	2004	1	7	3.0	0	224
1123	74.11	14.95	2004	1	7	4.3	0	228

1124	74.80	12.92	2004	12	26	1.7	0	10
1125	76.65	12.31	2004	12	26	1.7	0	216
1126	77.59	13.00	2004	12	26	3.0	0	303
1127	77.61	13.00	2004	12	26	3.0	0	305
1128	77.63	12.91	2004	12	26	3.0	0	308
1129	77.55	13.03	2004	12	26	3.0	0	299
1130	77.67	12.99	2004	12	26	3.7	0	312
1131	77.55	13.04	2004	12	26	3.7	0	299
1132	76.13	10.81	2004	4	17	2.6	19	285
1133	76.66	10.69	2004	4	18	2.5	0	328
1134	76.30	10.76	2004	7	22	2.5	8	299
1135	76.55	11.42	2004	12	28	2.9	6	260
1136	76.00	10.10	2005	7	25	5.8	10	349
1137	76.42	10.61	2005	2	13	2.3	10	320
1138	77.58	12.96	2005	3	14	1.7	0	302
1139	73.95	15.60	2005	3	14	3.0	0	302
1140	75.01	15.45	2005	3	14	3.0	0	272
1141	73.98	15.41	2005	3	14	3.0	0	281
1142	73.94	15.27	2005	3	14	3.0	0	267
1143	73.80	15.59	2005	3	14	3.0	0	306
1144	73.80	15.71	2005	3	14	3.0	0	319
1145	74.01	15.40	2005	3	14	3.0	0	279
1146	74.82	14.61	2005	3	14	3.0	0	178
1147	74.50	15.85	2005	3	14	3.7	0	317
1148	75.01	15.45	2005	3	14	3.7	0	272
1149	75.14	15.35	2005	3	14	3.7	0	263
1150	74.13	14.81	2005	3	14	3.7	0	212
1151	73.82	15.49	2005	3	14	3.7	0	295
1152	73.83	15.40	2005	3	14	3.7	0	285
1153	75.84	12.59	2005	6	19	4.3	0	123
1154	77.58	12.96	2005	7	24	2.3	0	302
1155	76.18	11.61	2005	8	26	3.2	11	217
1156	77.58	12.97	2005	10	8	1.7	0	302
1157	76.13	10.61	2006	12	20	3.5	10	304
1158	76.40	10.60	2006	12	20	3.2	11	320
1159	76.31	10.67	2006	12	21	3.0	10	308
1160	76.22	10.66	2006	12	27	3.8	5	304
1161	76.60	10.60	2006	12	27	3.6	10	333
1162	76.57	10.80	2006	2	27	2.2	19	313
1163	76.32	10.86	2006	3	1	2.9	17	291
1164	76.34	10.76	2006	3	25	2.6	14	302
1165	74.50	15.85	2006	4	17	1.7	0	317

1166	73.81	15.49	2006	4	17	1.7	0	295
1167	73.94	15.27	2006	4	17	2.3	0	267
1168	73.80	15.59	2006	4	17	2.3	0	306
1169	73.81	15.49	2006	4	17	2.3	0	295
1170	73.83	15.40	2006	4	17	2.3	0	285
1171	73.81	15.49	2006	5	21	1.7	0	295
1172	76.23	10.74	2006	5	21	2.2	7	297
1173	76.38	10.79	2006	6	3	2.6	21	301
1174	76.23	10.74	2006	6	17	2.0	19	297
1175	76.45	10.43	2006	7	4	2.0	23	339
1176	76.42	10.61	2006	7	20	2.3	22	320
1177	75.85	12.25	2006	7	27	2.4	6	143
1178	76.97	11.01	2006	10	7	1.7	0	325
1179	76.22	10.62	2006	11	29	2.0	20	308
1180	76.13	10.61	2006	12	20	3.8	13	304
1181	76.31	10.67	2006	12	21	3.5	19	308
1182	76.22	10.66	2006	12	27	4.0	1	304
1183	76.31	10.67	2006	12	21	3.5	19	308
1184	76.22	10.66	2006	12	27	4.0	1	304
1185	76.14	10.70	2006	12	20	4.4	0	296
1186	76.14	10.70	2006	12	27	3.9	0	296
1187	76.22	10.66	2006	12	27	3.7	1	304
1188	76.13	10.61	2006	12	20	3.4	13	304
1189	76.20	10.75	2006	12	11	2.8	2	294
1190	76.14	10.70	2006	12	20	3.4	13	296
1191	76.14	10.70	2006	12	20	2.5	15	296
1192	76.14	10.70	2006	12	21	3.1	19	296
1193	76.32	10.78	2006	12	22	2.6	2	299
1194	76.13	10.69	2006	12	22	2.7	10	296
1195	76.14	10.69	2006	12	23	2.8	3	297
1196	76.29	10.31	2007	10	2	2.8	10	342
1197	76.14	10.69	2007	2	1	3.3	19	297
1198	76.47	10.83	2007	4	30	2.1	16	304
1199	76.47	10.83	2007	5	4	2.2	15	304
1200	76.40	10.49	2007	6	8	2.7	4	330
1201	76.23	10.64	2007	8	14	3.3	18	307
1202	76.29	10.31	2007	10	2	3.4	23	342
1203	76.21	10.73	2007	10	2	3.1	23	297
1204	76.14	10.69	2007	10	3	2.2	2	297
1205	76.20	10.71	2007	10	3	3.1	4	298
1206	76.20	10.72	2007	10	3	2.5	4	297
1207	76.08	10.63	2007	10	5	2.8	3	300

1208	76.21	10.72	2007	10	6	2.9	1	298
1209	76.21	10.71	2007	10	10	2.7	11	299
1210	76.21	10.71	2007	10	12	2.5	20	299
1211	76.23	10.73	2007	11	2	2.3	22	298
1212	76.40	10.49	2007	12	16	2.5	3	330
1213	73.61	15.56	2008	1	4	2.3	10	311
1214	73.61	15.56	2008	1	4	3.1	19	311
1215	74.50	15.85	2008	9	17	3.0	0	317
1216	77.58	12.95	2008	9	17	3.0	0	302
1217	74.02	15.40	2008	9	17	3.0	0	278
1218	73.76	15.51	2008	9	17	3.7	0	299
1219	73.95	15.27	2008	9	17	3.7	0	267
1220	73.82	15.53	2008	9	17	3.7	0	299
1221	73.83	15.40	2008	9	17	3.7	0	285
1222	73.87	15.39	2008	9	17	3.7	0	283
1223	75.14	15.35	2008	9	17	4.3	0	263
1224	73.61	15.56	2008	1	4	3.1	19	311
1225	73.61	15.56	2008	1	4	2.3	19	311
1226	75.89	10.66	2008	2	11	3.0	13	287
1227	75.76	12.03	2008	2	12	2.8	0	151
1228	76.52	10.69	2008	12	1	3.1	20	319
1229	77.70	12.95	2009	8	11	2.3	0	315
1230	77.62	12.17	2012	5	27	3.7	18	321
1231	76.02	11.15	2012	6	20	3.7	8	246
1232	75.58	12.59	2012	10	14	4.1	8	97
1233	77.77	11.98	2012	11	28	3.8	22	343
1234	76.02	11.15	2012	6	20	3.7	8	246
1235	75.59	12.59	2012	10	14	4.1	8	98
1236	77.77	11.98	2012	11	28	3.8	22	343
1237	74.01	15.89	2013	1	8	3.3	10	331
1238	75.83	11.15	2013	2	26	3.6	17	236
1239	76.26	10.99	2013	12	8	3.8	4	276
1240	76.42	11.07	2013	12	9	3.8	10	279
1241	73.53	14.64	2014	8	24	6.0	23	227
1242	75.70	13.03	2015	2	25	2.7	0	98

PUBLICATIONS

Journals

1. **C. Shreyasvi**, Katta Venkataramana, Chopra, S (2019). "Local site-effect incorporation in probabilistic seismic hazard analysis – A case study from southern peninsular India, an intraplate region", *Soil dynamics and earthquake engineering*, 123(2019) 381-398. DOI: 10.1016/j.soildyn.2019.04.035

2. **C. Shreyasvi**, K. Venkataramana, Chopra, S., and Rout, M., M. (2019). "Probabilistic Seismic Hazard Analysis for Mangalore city and its adjoining regions, A part of Indian Peninsular: An Intraplate region". *Pure and Applied Geophysics*, 176(6), 2263-2297 DOI: 10.1007/s00024-019-02110-w.

Book Chapters

1. **C. Shreyasvi**, and Venkataramana, K. (2019). "Quantification of Seismic Hazard for Mangalore Region". Geotechnics for Natural and Engineered Sustainable Technologies, Springer. (In press)

2. **C. Shreyasvi**, Katta Venkataramana (2019), "Seismic Hazard Estimation for South West India", Lecture Notes in Civil Engineering, Springer, India. (In press)

3. **C. Shreyasvi**, Badira Rahmath N, Katta Venkataramana (2019), "Influence of variability in input parameters on Site response analysis", Lecture Notes in Civil Engineering, Springer, India. (In press)

National/International Conferences

1. **C. Shreyasvi**, Katta Venkataramana (2019), "Mapping of Seismic Hazard Parameters for Karnataka – A Southern State of India", International Engineering Symposium – 2019, Kumamoto University, Kumamoto, Japan, K4-1– K4-7. (Keynote lecture)

2. **Shreyasvi, C.**, and Venkataramana, K. (2018), "Spatial Variation of Seismic Hazard for South Western India", Proceedings of 16th symposium on Earthquake Engineering, December 20th – 22nd ,2018, IIT Roorkee, India, Paper No. – 214.

3. **Shreyasvi, C**., and Venkataramana, K. (2018). "Probabilistic Seismic Hazard Analysis of Coastal Karnataka and Its Surrounding Area", Proceedings of 2nd

International Conference on Advances in Concrete, Structural and Geotechnical Engineering, February 26th – 28th, 2018, BITS Pilani, India, pp 693-697.

4. **Shreyasvi, C**., and Venkataramana, K. (2017). "A study on the seismicity of Coastal areas in Karnataka", Proceedings of International Conference on Global Civil Engineering Challenges in Sustainable Development and Climate Change, March 17th – 18th, 2018, MITE, Moodabidri, India, pp 115-121.

5. **Shreyasvi, C.,** and Venkataramana, K. (2017). "A review of Probabilistic Methods in Seismic Hazard Analysis". Proceedings of International Engineering Symposium, March 1st – 03rd, 2017, Kumamoto University, Japan, pp- C-251 – C257.

BIO-DATA

PERSONAL PROFILE

NAME   :   SHREYASVI C

DATE OF BIRTH   :   6th MAY, 1991

GENDER   :   FEMALE

NATIONALITY   :   INDIAN

ADDRESS   :   D/O N. CHANDRASEKHAR,
                       #1700/35/2, 5TH 'A' CROSS, B. S. K. 1ST STAGE,
                       2ND BLOCK, BANGALORE -560 050; INDIA.

E-MAIL ADDRESS   :   shreyasvic@gmail.com

CONTACT NO   :   +91-8971966906

EDUCATIONAL QUALIFICATION:

DEGREE	YEAR	BOARD / UNIVERSITY
M.Tech in **Structural Engineering**	2013-2015	Dr. Ambedkar Institute of Technology, Bangalore, India. (Visvesvaraya Technological University)
B.E. in **Civil Engineering**	2009-2013	B.M.S College of Engineering, Bangalore, India. (Autonomous college under Visvesvaraya Technological University)

PUBLICATIONS:

Journals   :   4

Book Chapters   :   3

National/International conferences   :   13

Journal Articles:

1. **C. Shreyasvi**, Katta Venkataramana, Sumer Chopra (2019). "Local site-effect incorporation in probabilistic seismic hazard analysis – A case study from southern peninsular India, an intraplate region", *Soil dynamics and earthquake engineering,*123(2019) 381-398. https://doi.org/10.1016/j.soildyn.2019.04.035

2. **C. Shreyasvi**, Katta Venkataramana, Sumer Chopra, Madan Mohan rout (2019). "Probabilistic Seismic Hazard Analysis for Mangalore city and its adjoining regions, a part of Indian Peninsular – An Intraplate region", *Pure and Applied Geophysics*, 176(6), 2263-2297. DOI: https://doi.org/10.1007/s00024-019-02110-w

3. Nagaraj H B, **C. Shreyasvi** (2017). "Compressed Stabilized Earth Blocks Using Iron Mine Spoil Waste - An Explorative Study". *Proceedia Engineering, Elsevier.* https://doi.org/10.1016/j.proeng.2017.04.281

4. **C. Shreyasvi**, B. Shivakumara Swamy, (2015) "A case study on the seismic response of buildings with re-entrant corners." *International Journal of Engineering Research and Technology (IJERT)*, Vol. 4, Issue 5, May 2015.

Book Chapters:

1. **C. Shreyasvi**, Katta Venkataramana (2018), "Seismic Hazard Estimation for South West India", *Lecture Notes in Civil Engineering, Springer*, India. (In press)

2. **C. Shreyasvi**, Badira Rahmath N, Katta Venkataramana (2018), "Influence of variability in input parameters on Site response analysis", *Lecture Notes in Civil Engineering, Springer*, India. (In press)

3. **C. Shreyasvi**, Katta Venkataramana (2017). "Quantification of Seismic Hazard for Mangalore Region". *Geotechnics for Natural and Engineered Sustainable Technologies, Springer.* (In press)

Conference Papers:

1. **C. Shreyasvi**, Katta Venkataramana (2019), "Site-Specific Design Spectrum Model for a Region of Moderate Seismicity", Recent Trends in Civil Engineering, Vimal Jyothi Engineering College, Kannur, India. (Keynote lecture)

2. **C. Shreyasvi**, Katta Venkataramana (2019), "Mapping of Seismic Hazard Parameters for Karnataka – A Southern State of India", International Engineering Symposium – 2019, Kumamoto University, Kumamoto, Japan, K4-1– K4-7. (Keynote lecture)

3. **C. Shreyasvi**, Venkataramana K (2018), "Spatial Variation of Seismic Hazard for South Western India", 16th symposium on Earthquake Engineering, IIT Roorkee, India. Paper No – 214

4. Pradeep Kumar Pandre, **C. Shreyasvi**, Katta Venkataramana (2018). "Seismic Performance Assessment of Buildings Located On a Sloping Ground", 17th International Symposium On New Technologies for Urban Safety of Mega Cities in Asia, IIIT Hyderabad, India, Paper No – 54.

5. Pradeep Kumar Pandre, **C. Shreyasvi,** Katta Venkataramana (2018). "Seismic Response Study on Buildings Based on a Sloping Ground", 34th National

Convention of Architectural Engineers and National Seminar, NITK Surathkal, India.

6. Badira Rahmath N, **C. Shreyasvi**, Katta Venkataramana (2018). "Seismic Site Response Analysis of Calicut Region", 34th National Convention of Architectural Engineers and National Seminar, NITK Surathkal, India.

7. Katta Venkataramana, **C. Shreyasvi** (2018), "Recent Advances in Earthquake Resistant Construction Practices", Second National Conference on Structural Engineering and Construction Management, SECON' 2018, Federal Institute of Science and Technology (FISAT), Angamaly, India, pp 1-12. (Keynote lecture)

8. **C. Shreyasvi**, Katta Venkataramana (2018). "Probabilistic Seismic Hazard Analysis of Coastal Karnataka and Its Surrounding Area". 2nd International Conference on Advances in Concrete, Structural and Geotechnical Engineering, BITS Pilani, India, pp 693-697.

9. **C. Shreyasvi**, Katta Venkataramana (2017). "Quantification of Seismic Hazard for Mangalore Region". Indian Geotechnical conference – 2017, IIT Guwahati. http://igs.org.in/portal/igc-proceedings/Theme12/Th12_502.pdf

10. **C. Shreyasvi**, Katta Venkataramana (2017). "A study on the seismicity of Coastal areas in Karnataka". International Conference on Global Civil Engineering Challenges in Sustainable Development and Climate Change, MITE, Moodabidri, pp 115-121.

11. **C. Shreyasvi**, Katta Venkataramana (2017). "A review of Probabilistic Methods in Seismic Hazard Analysis". International Engineering Symposium – 2017, Kumamoto University, Kumamoto, Japan, C-251 – C257.

12. **C. Shreyasvi**, B. Shivakumara Swamy, (2015). "Comparative Study of Regular and Irregular Building Plan Using Non-Linear Time History Analysis". Conference On Advances in Research & Development and Dissemination of Interdisciplinary Developments for Sustainability, R. V. College of Engineering, Bengaluru.

13. **C. Shreyasvi**, B. Shivakumara Swamy, (2015). "Seismic Response of Buildings withRe-Entrant Corners in Different Seismic Zones". Conference on Advances in Structural, Highway and CADD Engineering, Ghousia College of Engineering, Bengaluru.

Invited lectures:

1. A lecture on "*Seismic hazard assessment of Mangalore and its adjoining regions*" at the Institution of Engineers (Mangalore Chapter), India. (Feb 2019)

2. A lecture on "Estimation of Seismic Hazard considering local site effects" in the Dept. of Civil Engg. National Institute of Technology Calicut, Kerala, India.

(Jan 2018)

Certifications and Training:

1. International School on use of E-infrastructures in Seismology – "Operational definition of seismic risk and intervention techniques for strategic buildings: an integrated system on HPC platform", Institute of Seismological Research, Raysan, Gandhi Nagar, India.   (April 2018)
2. Short course on Design of Reinforced Concrete Structures for Earthquake and Fire, IIT Gandhinagar, India.   (May 2018)
3. Training in the area of "Site amplification studies and ground motion Simulation" at Institute of Seismological Research, Raysan, Gandhi Nagar, India.   (May-Jun, 2018)
4. Seminar on "Seismic Isolation" organized by Structural Engineers World Congress in association with the Japan Society of Seismic Isolation, held at Global Academy of Technology and Management, Bangalore.

     (Oct – Nov 2017)
5. Training in the area of Probabilistic Seismic Hazard Assessment and Site response analysis to seismic excitation at Institute of Seismological Research, Raysan, Gandhi Nagar, India.   (May – July 2017)
6. Spring Internship Program – 2017, Kumamoto University, Kumamoto, Japan

     (March 2017)

7. Advances in Seismic Hazard Analysis and Soil-Structure Interaction, GIAN course conducted by IIT Madras, India.   (July 2016)
8. Literature Survey Workshop conducted by NICEE, IIT Kanpur, India.

     (May 2016)
9. Dr. AIT Techno Exhibition, "Comparative Study on Concrete with Recycled Aggregate and Flyash with Conventional Concrete."   (April 2015)
10. Diploma in AutoCAD 2D & 3D.   (June 2011)

Teaching Experience:

Teaching Assistant   *National Institute of Technology Karnataka*
Earthquake Engineering, Software applications in Structural Analysis, Material Testing Lab, Concrete and Highway Materials Lab, Geotechnical Engineering Lab, Surveying lab.   (Dec 2015 – May 2019)

Assistant Professor   *Dayananda Sagar Academy of Technology and Management, India*
Subjects handled: Prestressed concrete design of structures, Detailing of RCC structures, Elements of Civil Engineering.   (July – Dec 2015)

Teaching Assistant   *Dr. Ambedkar Institute of Technology, India.*
Geotechnical Laboratory, Design and drawing of steel structures.

     (sept 2013 – jun 2015)